Chapter 2
Müller Cells in the Healthy Retina

2.1 Morphology and Cellular Properties of Müller Cells as Constituents of Retinal Tissue

2.1.1 Basic Morphology of Müller Cells

Müller cells (Figs. 1.17c, d, 2.1, 2.5, 2.9, 2.13, and 2.31) are radial glial cells that reside in a part of the adult CNS. As such, they share the basic bipolar morphology of radial glial cells (Figs. 1.1 and 1.4) and possess the complete set of principal glial cell processes/contact types (Fig. 1.3) (Reichenbach, 1989b). Originating from soma which generally is located in the inner nuclear layer (where the somata of all Müller cells may even constitute a sublayer) two stem processes extend into opposite directions. The outer stem process reaches to the subretinal space (i.e., the relict of the optic ventricle) into which it sends numerous microvilli. The inner stem process approaches the vitread surface of the neuroretina where it forms a so-called endfoot abutting the basal lamina between the vitreous body and the neuroretina (the "inner limiting membrane", ILM). Both processes and the soma extend side branches which contact and/or ensheath virtually all neuronal elements of the retina (as well as the blood vessels in vascularized retinas; see Section 2.1.4).

Basically, the functional structure and ultrastructure of these three types of Müller cells processes are very similar throughout the various vertebrate species (Figs. 2.1 and 2.9) (Uga and Smelser, 1973). This is probably due to the fact that these processes are locally adapted to the microenvironment which they contact (Reichenbach, 1989b; Reichenbach et al., 1989a). However, the Müller cell morphology undergoes considerable quantitative (and even qualitative) modifications throughout the variety of vertebrate species. This variability is largely dependent on the photopic vs. scotopic specialization of a retina (or retinal area) which, in turn, mainly determines the absolute and relative thickness of the retinal layers (cf. Figs. 1.13 and 2.16); another factor is the presence or absence of intraretinal blood vessels. The outer process is rather short and stout in diurnal animals with photopically specialized retinas, as it has to span a thin ONL consisting of only one (pure cone retinas) to about three (mixed but cone-dominant retinas) rows of photoreceptor cell nuclei. This is the typical situation for most reptilians and

A. Reichenbach, A. Bringmann, *Müller Cells in the Healthy and Diseased Retina*,
DOI 10.1007/978-1-4419-1672-3_2, © Springer Science+Business Media, LLC 2010

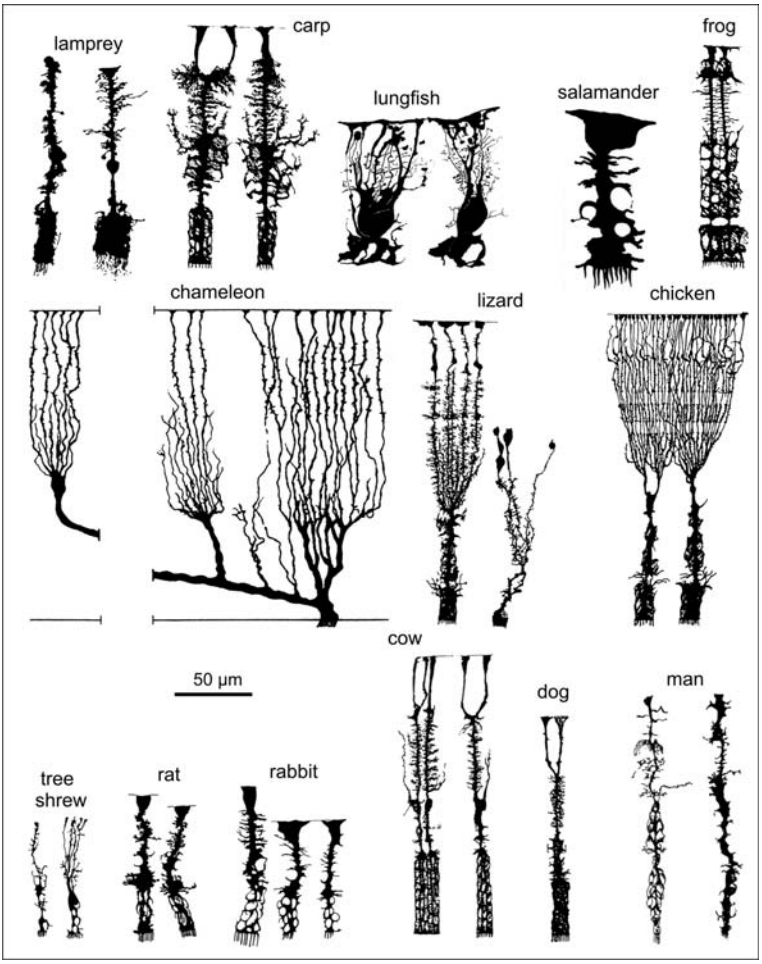

Fig. 2.1 Survey of the shape of Müller cells in various different vertebrate retinas. Most cells were drawn from Golgi-stained preparations, some are camera lucida-drawings of dye-filled cells. As far as possible, all cells are shown at the same magnification. The vitread endfeet of the cells are on top, their microvillous outer processes on bottom. Modified from Reichenbach and Wolburg (2005), where the references also can be found

birds but is the exception in mammals with the tree shrew as an extreme example (Figs. 1.13 and 2.1) (Müller and Peichl, 1989). Most mammalian and many fish retinas are rod-dominant which means that they possess a thick ONL with up to more than 12 rows of photoreceptor cell nuclei. Accordingly, the outer process of Müller cells in such retinas is rather long and displays an elaborated honey comb-like meshwork of velate sheaths enveloping the photoreceptor cell somata (Figs. 2.1, 2.2, and 2.3c). After enzymatic dissociation of the cells, it becomes obvious that the outer Müller cell process in such species may be split into several thin distal branches (Fig. 2.2b); the cytoplasmic tongues enveloping the photoreceptor somata

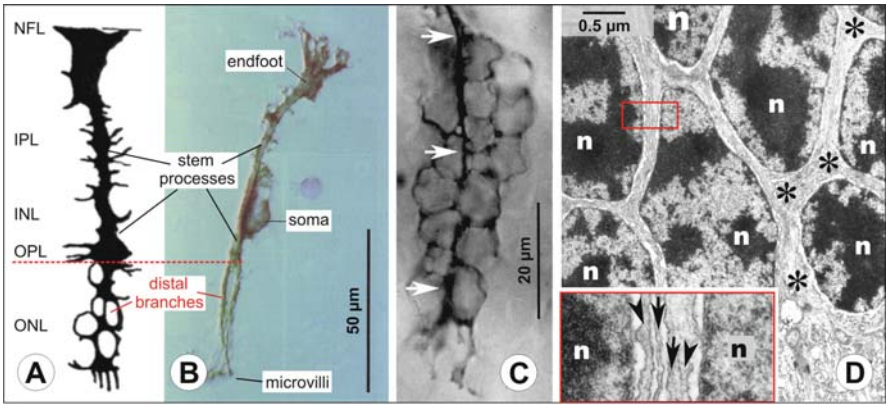

Fig. 2.2 Shape of the outer Müller cell processes; all images from rabbit retina/cells. (**a**) Camera lucida-drawing of a Golgi-stained Müller cell in the retinal periphery (about halfway between center and margin of the retina). (**b**) Enzymatically dissociated cell from similar retinal area. The border between OPL and ONL is indicated in (**a**) and (**b**); there, the outer stem process splits into several distal branches. (**c**) Microphotograph of the distal part of a Golgi-labeled Müller cell in the central retina (within the ONL); one of the distal branches is in focus along its entire length (*arrows*). It gives rise to several bubble-like sheaths enveloping photoreceptor cell somata. (**d**) Transmission electron microphotograph of the ONL. The nuclei of the rod photoreceptor cells (n) are surrounded by a very thin cytoplasmic rim (*arrowheads*) which, in turn, is enveloped by an even thinner cytoplasmic tongue (*arrows*) extending from the Müller cell branch (*asterisks*). NFL, nerve fiber layer; IPL, inner plexiform layer; INL, inner nuclear layer; OPL, outer plexiform layer; ONL, outer nuclear layer. Own data (AR); (**c**) and (**d**) modified after Reichenbach et al. (1988a, 1989a)

are extremely thin (Fig. 2.2d). Fine side branches are sent from the outer processes of all Müller cells also into the OPL where the synapses between the photoreceptor cells and the second-order neurons are ensheathed (Fig. 2.3a). Particularly in (diurnal) species with a thick INL, a minor part of the outer process is also located within the INL where it, together with the soma and with the proximal part of the inner process, forms velate sheaths around the neurons in the INL (Fig. 2.3b). The somata of Müller cells appear irregularly shaped in histological sections (particularly, in semithin sections after fixation in glutaraldehyde) such as if they were "intended" by their neuronal neighbour cells (Fig. 2.4). Indeed, it has been shown that Müller cells, including their somata, are softer than retinal neurons (Lu et al., 2006); isolated Müller cells (released from their tight neighbourhood) display a spherical or ovoid soma (Figs. 1.17 and c). The nuclei of Müller cells are displaced from the axis of Müller cells, apparently "piggybacked" by the two continuous stem processes (Figs. 1.17c, 2.2b, and 2.32e).

The inner process is singular and rather thick in rod-dominant retinas such as those of most mammals, amphibians, and fish (Fig. 2.1). On its course through the IPL, it gives rise to many fine, complex side branches ensheathing the synapses. As it enters the GCL/NFL, it becomes rather smooth; here, its shape is strongly determined by the (local) density of ganglion cell axons. When a high density of axons causes a thick NFL, rather large bundles of them are fasciculated by the inner Müller

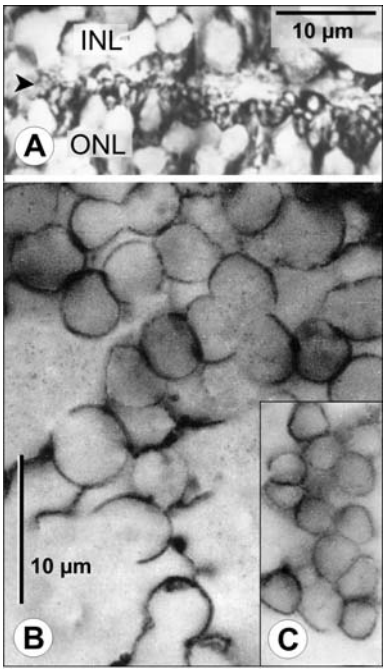

Fig. 2.3 Müller cell processes in the OPL (**a**), INL (**b**), and ONL (**c**). A, Immunohistochemical labeling of glutamine synthetase-positive Müller cell processes in the OPL (*arrowhead*) of a rat retina. Side branches of the Müller cell processes form "bouquets" ensheathing groups of rod spherules. Courtesy of A. Derouiche. (**b**), (**c**), Microphotographs of tangential sections through a Golgi-labeled rabbit retina; in this area, many adjacent Müller cells were labeled. The side branches of these cells together form a honey comb-like meshwork of bubble-like sheaths around the somata of neurons in the INL (**b**) similar as in the ONL (**c**); cf. also Fig. 2.2c. INL, inner nuclear layer; ONL, outer nuclear layer. (**b**) and (**c**) modified after Reichenbach et al. (1989a)

cell processes and their (relatively few) side branches. This may even cause a splitting of the inner processes into two or more branches which give space to the axon bundle(s) in between them; examples for this can be seen in the left carp Müller cell and the cow and dog Müller cells in Fig. 2.2 (cf. also Figs. 2.4 and 2.5). In a similar manner, the inner processes may "bypass" large blood vessels. Eventually, the inner stem process (or its branches) form(s) more or less funnel- or cone-shaped endfeet at the basal lamina (ILM). Rarely in species with retinas vascularized by very thick blood vessels such as the whale and the pig, some Müller cells form endfeet already at the outer surface of such vessels rather than at the ILM (Fig. 2.11a). Generally, the inner processes form so-called "en-passant endfeet" at intraretinal blood vessels if they come into contact with such vessels. The inner processes are strikingly different in diurnal animals with photopically specialized retinas, *viz* in most reptilians and birds, in the tree shrew as an exceptional mammal (Reichenbach et al., 1995d), and in the lungfish. In such retinas, the inner process splits into several branches as it enters the IPL (Figs. 1.17d, 2.1, and 2.31). In avian retinas, the

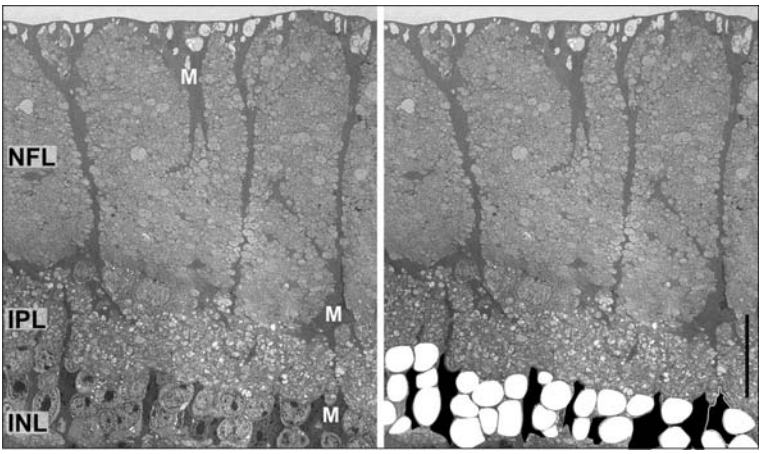

Fig. 2.4 Deformation of Müller cell somata by their neighboring neurons; transmission electron microphotograph of the center of a guinea-pig retina. Müller cell processes and somata (M) can be identified by their electron-dense (i.e., *dark*) cytoplasm. In the image at the right side, the somata of INL neurons are overlaid in white, those of Müller cells in *black*. Whereas the cross-sections of most neuronal somata appear as more or less regular *circles*, the Müller cell somata appear irregular, as if indented by their neighbors. Modified after Lu et al. (2006)

many branches may look as corn bound into sheaves (Fig. 2.1 and 2.31, chicken Müller cells). Each of the many thin branches forms an individual small endfoot at the ILM. It has been speculated that the splitting of Müller cell stem trunks into numerous filamentous processes represents a morphological adaptation to allow an effective spatial buffering of potassium ions in avascular avian retinas, and an effective absorption and distribution of nutrients leaking from the vitreally located supplemental nutritive organ, the pecten oculi (Dreher et al., 1994). As an alternative explanation, the splitting may be caused by developmental mechanics when the late-born Müller cells sent their growing inner processes through the already established dense network of synapses in the thick IPL of photopically specialized retinas.

At the end of this summary, a few peculiar specializations of Müller cells must be mentioned. First, in many urodeles (salamanders) and in lungfish all cells of the body are triploid or even tetraploid, i.e., they contain an enhanced amount of DNA. This causes a large size of the cell nuclei, and, indirectly, a large cytoplasmic volume of the cells. Consequently, the Müller cells of such species are very large (Fig. 2.1). Another peculiarity is found in the perifoveal Müller cells of the chameleon. These cells extend very long inner stem processes which run almost parallel to the retinal surface, and give rise to multiple secondary processes which run towards the ILM and split into the typical multiple branches of reptilian retinas when they enter the IPL (Fig. 2.1). Finally it appears to be noteworthy that in some fish retinas, the inner processes of Müller cells were described to form loose myelin sheaths around retinal ganglion cell axons (Yamada, 1989)

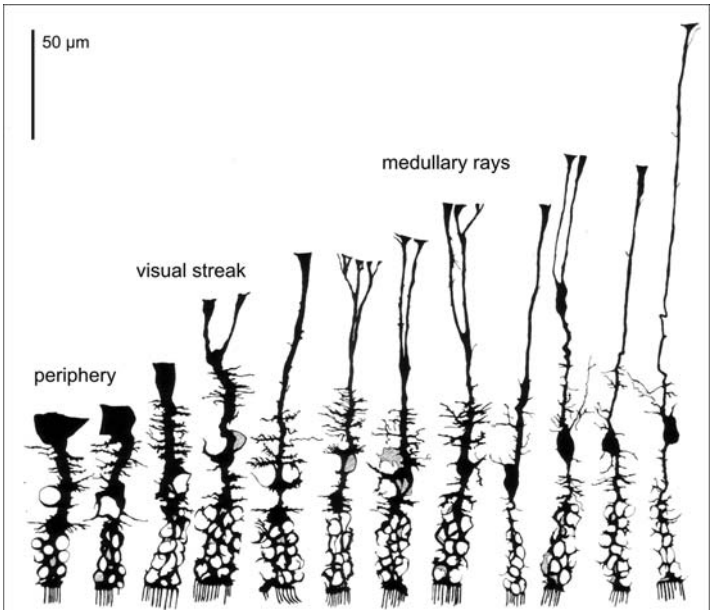

Fig. 2.5 The morphology of rabbit Müller cells varies in dependence on retinal topography; camera ludica-drawings of Golgi-stained cells. Cells from retinal periphery are short and thick; their *cobblestone-shaped* endfeet form a rather thick continuous layer at the inner retinal surface. By contrast, the inner processes of cells within the medullary rays are long and thin, and often even split into several branches to give space for the large axon bundles in the thick NFL. Modified after Reichenbach et al. (1989a)

2.1.2 Topographical Adaptations

The morphology of Müller cells varies not only among diverse species, but also within the same retina, in dependence on retinal topography. In the rabbit retina, for example, three main retinal areas can be discriminated, (i) the major part is the retinal periphery which is avascular, (ii) the horizontal equator contains the so-called "visual streak" which is characterized by an elevated cell density but is also avascular, and (iii) dorsal of this streak a thick NFL with myelinated axons forms the "medullary rays" (Fig. 1.16c); there, the inner retina is vascularized (for details, see Schnitzer, 1988b). Accordingly, the morphology of the Müller cells varies (Fig. 2.5) (Reichenbach, 1987; Reichenbach et al., 1989a). Peripheral rabbit Müller cells are short and stout, with a single large endfoot. In the visual streak, the Müller cells are longer and more slender, and their inner process may be split into two or more branches as it enters the thick NFL. Within the medullary rays, the inner processes are extremely long, thin, and smooth on their course through the very thick NFL (Fig. 2.5). In a similar manner, the complexity of the "sheaves" of the inner processes in avian Müller cells depends on the retinal topography (Anezary et al., 2001).

Strikingly, there is an inverse relationship between length and volume of the cells. The short (and thick) Müller cells of the retinal periphery have a larger volume than the long but thin cells of the central retina; moreover, the surface area of the vitread endfoot membrane of the peripheral cells is larger than that of the central cells (Pei and Smelser, 1968; Uga, 1974; Reichenbach and Wohlrab, 1986; Reichenbach et al., 1987, 1988a, 1989a, 1995c; Prada et al., 1989a, b; Distler and Dreher, 1996). If peripheral and central rabbit Müller cells are compared, the access of (the endfoot/endfeet of) a given cell to the ILM is even more reduced within the medullary rays because up to 50% of the inner retinal surface are occupied by the endfeet of astrocytes (Fig. 2.11e) (Richter et al., 1990) which are missing in the retinal periphery. However, the contribution of Müller cell volume to the total volume of the retina (in the rabbit for instance, about 7%) is remarkably constant, independent of the retinal topography (Reichenbach and Wohlrab, 1983; Reichenbach, 1987; Reichenbach et al., 1988a). This is achieved by a higher local density of Müller cells in the central retina. In the rabbit for example, the Müller cell density increases from about 8,000 cells/mm^2 in the periphery to about 15,000 cells/mm^2 in the retinal center (Reichenbach et al., 1991b; Dreher et al., 1992). Generally, Müller cells are rather regularly distributed within the retina (Figs. 2.17c, 2.24b, 2.25b, 2.33, 2.34c, d), and their mean densities vary not more than between some 7,000 and 15,000 cells/mm^2 throughout diverse specialized retinal areas in the retinas of various vertebrates studied so far (Chao et al., 1997; Dreher et al., 1992) (Fig. 2.6); for the exception of the primate fovea, see Sections 2.1.3 and 2.2.6.

2.1.3 Müller Cells in the Primate Fovea Centralis

The retinas of many predatory fish, reptilians, and birds contain one (or even two or three) retinal region(s) specialized for high acuity vision, a so-called fovea (Walls, 1963). Here, the densities of neurons are particularly high and the inner retina is deeply inclined in a funnel-shaped manner (Fig. 2.7a, b) (Walls, 1963; Collin et al., 2000). In the retinas of non-primate mammals such a structure is missing; instead, an area centralis (predators such as the cat) or visual streak (as in the rabbit, for instance) is developed with a high cellular density (cf. also Fig. 2.6) but without any inclination of the inner retinal surface (rather, the retina is thickened at such places). A fovea centralis was "re-invented" by the higher primates (Walls, 1963); however, its structure differs greatly from that of the non-mammalian foveas (Fig. 2.7) (Provis et al., 2005). The primate fovea constitutes a flat bowl rather than steep funnel. It is characterized by a complete lack of rod photoreceptors (i.e., 100% cones) and by the absence of inner retinal layers. This is despite of the fact that the foveal cones have even more secondary and tertiary neurons in their "private" pathways (cf. Fig. 1.13) than peripheral ones. These central-most inner retinal neurons, however, are displaced laterally such that the axons of the photoreceptor cells must first run centrifugally until they make synapses with their bipolar cells (cf. Fig. 2.7c, d). These laterally running cone axons form the Henle fiber layer; they are surrounded and bound together by the outer processes of Müller cells. Thus, the foveal cones

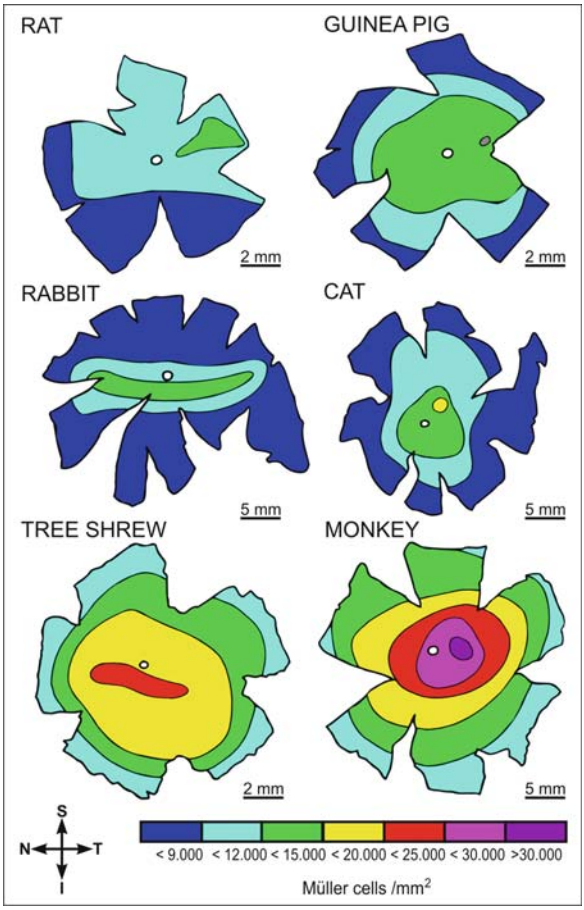

Fig. 2.6 The spatial density of Müller cells varies in dependence on retinal topography. Noteworthy, local specializations of the neural retinas such as a visual streak (rabbit, tree shrew) or the area (cat) or fovea centralis (monkey) are mirrored by the densities of Müller cells. Modified after Reichenbach and Robinson (1995), where the references also can be found

and the local Müller cell processes follow the same "Z course" (Fig. 2.7c, d). To span the "lateral shift" of up to 250 or 300 μm in the parafoveal region of the primate retina, the outer processes of Müller cells in the Henle fiber layer are very elongated (Distler and Dreher, 1996). Cone axons and Müller cell processes run in parallel; the ratio between Müller cell processes and cone axons may range between 1:1 and 1:2. In the macaque perifoveal OPL where the foveal cones make their synapses, the number of Müller cell processes and cone terminals was found to be equal (Burris et al., 2002). Every Müller cell process extends cytoplasmic tongues which ensheathe two to three terminals; in turn, each terminal is completely coated by side branches of two to three Müller cells (Burris et al., 2002). As the densities of foveal cones are high, high peak densities of >30,000 cells/mm^2 of Müller cells (counted at the level of their outer processes) were found in the parafoveal monkey retina (Distler and Dreher, 1996).

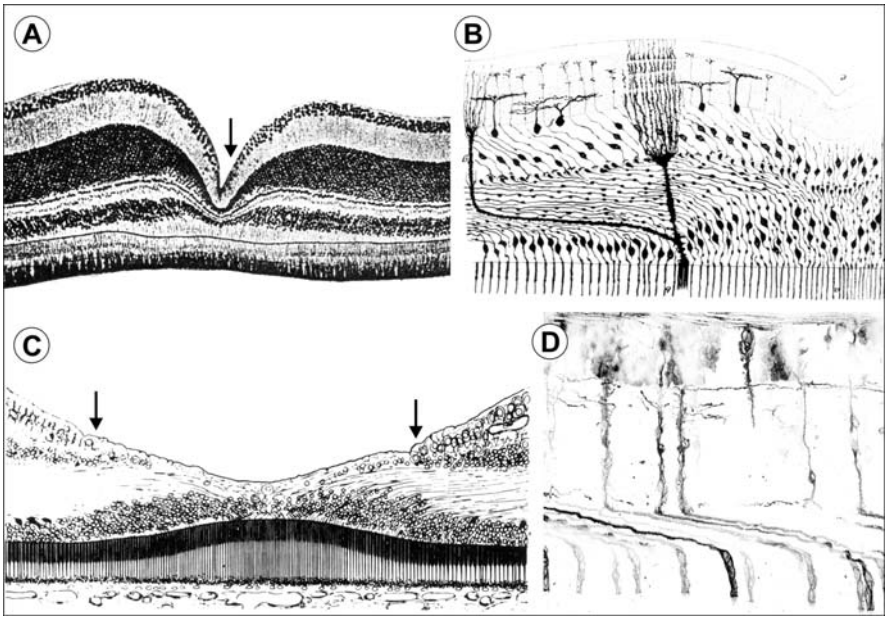

Fig. 2.7 Müller cells in the vicinity of the Fovea centralis of different vertebrates. (**a**) Deep, convexiclivate fovea of the European bank swallow; retinal ganglion cells are present up to the center of the pit (*arrow*). (**c**) Comparatively flat fovea of a human retina; there is a wide central area (the foveola) which is devoid of ganglion cells (*arrows*) (cf. also Fig. 2.29). (**b**) Camera lucida-drawing of Golgi-stained cells in the foveal region of a chameleon retina. In the center (*right side*) the neurites of the photoreceptor and bipolar cells run almost radially towards the inner retinal layers, similar as in the retinal periphery. A little distant from center, these neurites run obliquely or even transversally towards their synaptic partner cell which are shifted towards the periphery against their partnering photoreceptor cells. The Müller cell stem processes display a more or less radial course (as in the periphery); only some side branches follow the oblique course of the neurites for some distance before they turn towards the inner retinal surface. (**d**) Microphotograph of a Golgi-stained monkey retina, about 2 mm from foveal center. From foveal center to peripheral margin of the parafoveal region, photoreceptor (and bipolar) cell neurites and outer Müller cell processes run absolutely in parallel, in a Z-shaped course where at the outer margin of the OPL, the so-called Henle fiber layer, they span most of the central-peripheral shift between photoreceptor and ganglion cells. (**a**), (**c**), from Walls (1963); (**b**), from Ramón y Cajal (1972); (**d**), original microphotograph; Golgi-stained preparation, courtesy of H. Wässle and H. Boycott

Noteworthy, the Z-shaped morphology of the foveal and parafoveal Müller cells causes a particular problem. Their outer processes arise in the fovea but their endfeet abut the ILM at a distance of >100 μm from the foveal center, at the closest (Fig. 2.29b). This means that the endfeet of these cells cannot contribute to the inner tissue "sealing" along the ILM within the fovea proper. Instead, very atypical Müller cells are located there. Their outer processes fail to join the course of the cone axons into the Henle fiber layer; rather, they run more or less straight towards the inner retinal surface where their somata are located. The soma extends irregular "inner"

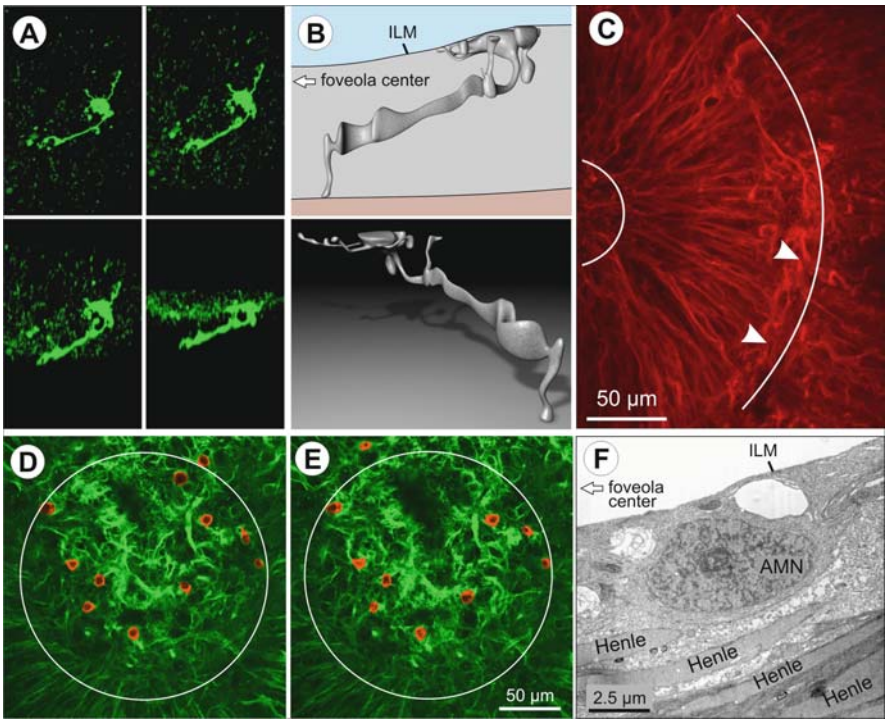

Fig. 2.8 Müller cells of the primate fovea and foveola. (**a**) Confocal images of an "atypical" Müller cell in the foveola of a macaque retina, filled by the fluorescent dye, Lucifer Yellow; *top row*: two microphotographs of the wholemount ("from vitreous"); *bottom row*: two reconstructions of the *Z*-axis ("side views"). (**b**) 3D-reconstruction of this "atypical" Müller cell. In contrast to those of the majority of central Müller cells (and the Henle fibers) the processes of this cell do not leave the foveola proper. ILM, inner limiting membrane. (**c**) Confocal image of the foveal area of a wholemounted macaque retina; Müller cells were labeled with an antibody directed against GFAP (*red*). At this level, many Müller cells are visible which run from the foveola (*small circle*) to the margin of the fovea (*large circle*) where they form endfeet at the inner limiting membrane (*arrowheads*). (**d**), (**e**) Two consecutive focus levels (more close to the inner surface of the foveola than the image in (**c**)) of another wholemounted macaque retina. Müller cell processes are labeled by an antibody directd against GFAP (*green*), their somata were encircled manually where they were cut by the optical section (*red*). Both the somata and the inner processes of these "atypical" Müller cells remain within the fovea where they form large, irregular endfeet (cf. (**a**)). (**f**) Transmission electron micrograph of a radial section of a macaque retina, 90 µm distant from foveolar center. The space between the parallel Henle fibers (and the processes of the "typical" Müller cells) and the inner retinal surface (ILM) is occupied by the soma and the inner process(es) of an "atypical" Müller cell (nucleus of this cell, AMN). Originals; (**a**), (**b**) courtesy of K. Rillich and J. Grosche; (**c**)–(**e**), courtesy of S. Syrbe

processes which spread along the ILM and thus form the innermost retinal tissue (Fig. 2.8). The nuclei of these cells are rather large and regularly rounded, perhaps because they are not intended by any neighboring neurons (cf. Fig. 2.4). Obviously, these cells do not develop any morphological interactions with neuronal elements

such as synapses, as such elements are missing along their course. It has been estimated that some 20–30 of these cells exist in a primate fovea, and are sufficient to cover the foveal ILM (Syrbe et al., unpublished data). For the developmental implications of these observations on foveal Müller cells, see Sections 2.2.4 and 2.2.6.

2.1.4 Ultrastructure of Müller Cells

Müller cells are strictly polarized cells; this includes the subcellular distribution of organelles (Fig. 2.9). The inner process with the endfoot is densely packed with smooth endoplasmic reticulum, intermediate filaments, and glycogen granula, whereas the outer process of the cells mainly contains the Golgi apparatus, multivesicular bodies, and microtubules.

(A) *The outer process* arises from the soma without any distinct border, and ends at the OLM from where it extends numerous microvilli into the subretinal space. It displays a very large surface-to-volume ratio (SVR; i.e., a large membrane area in relation to its cytoplasmic volume). This is due to the many thin bubble-like sheaths around the photoreceptor somata in the ONL (SVR = 20–25 μm^{-1}) and the long, thin microvilli (SVR = up to >50 μm^{-1} in rabbit) (Fig. 2.10) (Reichenbach et al., 1988a). Close to its origin from soma, it contains the stacks of the Golgi apparatus. Multivesicular bodies are present near the Golgi apparatus in the outer stem process, suggesting that Müller cells have a secretory function (Reichenbach et al., 1988a). Müller cells may exocytotically release glutamate (Fig. 2.75b) (Wurm et al., 2008) and other neuroactive factors such as growth factors, chemokines, and lipoproteins (Berka et al., 1995; Roesch et al., 2008), and mediate the transcytosis of retinoschisin (Reid and Farber, 2005). The presence of microtubules in the outer process may be related to intracellular transport processes.

Müller cells have a continuous subplasmalemmal layer of filamentous actin (Vaughan and Fisher, 1987) which extends into the outer process. At the level of the OLM, these processes contain rings of filamentous actin that surround the photoreceptors. These actin rings are associated with the adherens junctions between Müller and photoreceptor cells, and form a structural meshwork in which the processes of the photoreceptor cells are embedded when they leave the retina proper and enter the subretinal space (Fig. 2.10) (Del Priore et al., 1987). The cytoplasmic plaques of the adherens junctions between Müller and photoreceptor cells contain actin, myosin, α-actinin, and vinculin (Drenckhahn and Wagner, 1985; Williams et al., 1990). These junctions are extremely important for the development and maintenance of the layered retinal structure. Due to the presence of zonulae adherentes between Müller cells and photoreceptors, the outer limiting membrane is a diffusion barrier for subretinal space-derived proteins with a Stokes' radius greater than 36 Å (Bunt-Milam et al., 1985).

The Müller cell microvilli (Fig. 2.10) contain villin, ezrin and myosin I (Höfer and Drenckhahn, 1993). Their number and length may vary considerably among the various vertebrate species (Uga and Smelser, 1973). In diurnal mammals, they

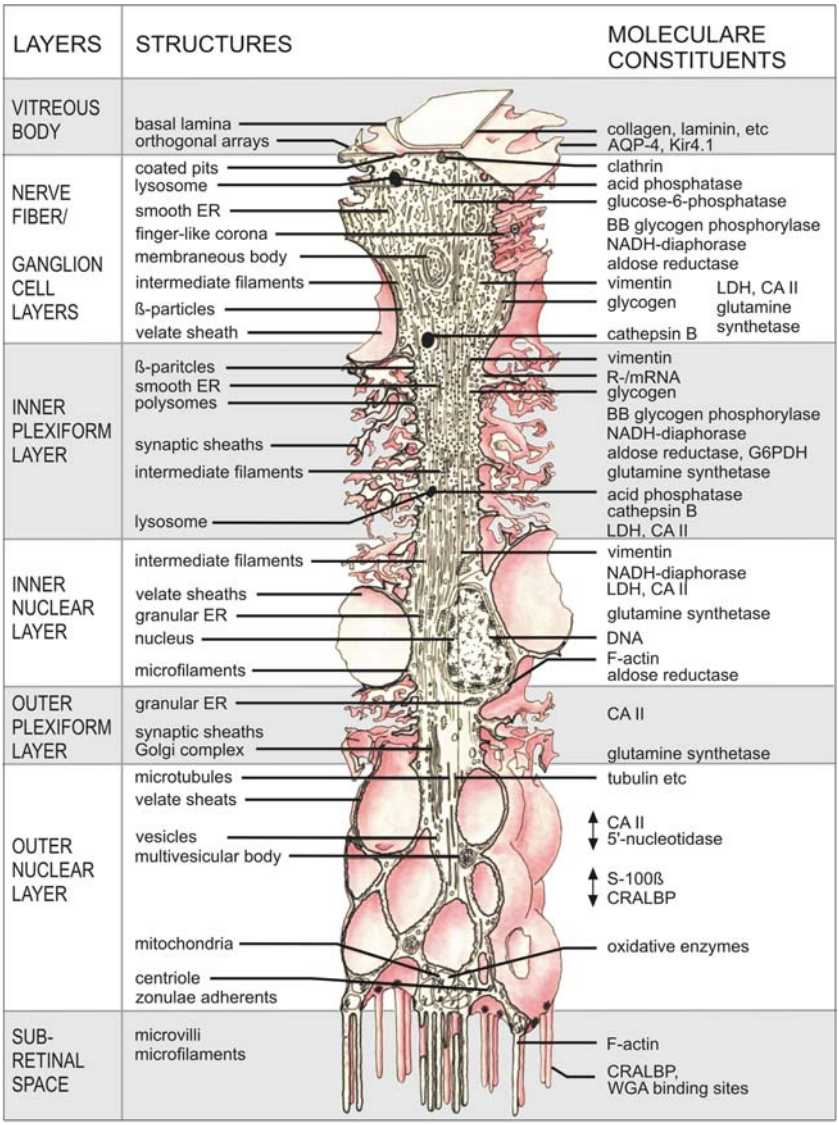

Fig. 2.9 Survey of the cytotopographical specializations of a rabbit Müller cell. ER, endoplasmic reticulum; AQP-4, aquaporin 4; Kir4.1, inwardly-rectifying K^+ channels; LDH, lactate dehydrogenase; CA II, carbonic anhydrase type II; CRALBP, Cellular Retinaldehyde-Binding Protein; WGA, wheat germ agglutinin. Modified after Reichenbach (1989b)

may form complex, multilayered "sheaths" around the cone inner segments which are interdigitating with the lateral "fins" arising from the latter (Fig. 2.10). In the elephant nose fish, *Gnathonemus petersii*, the microvilli are almost as long as the

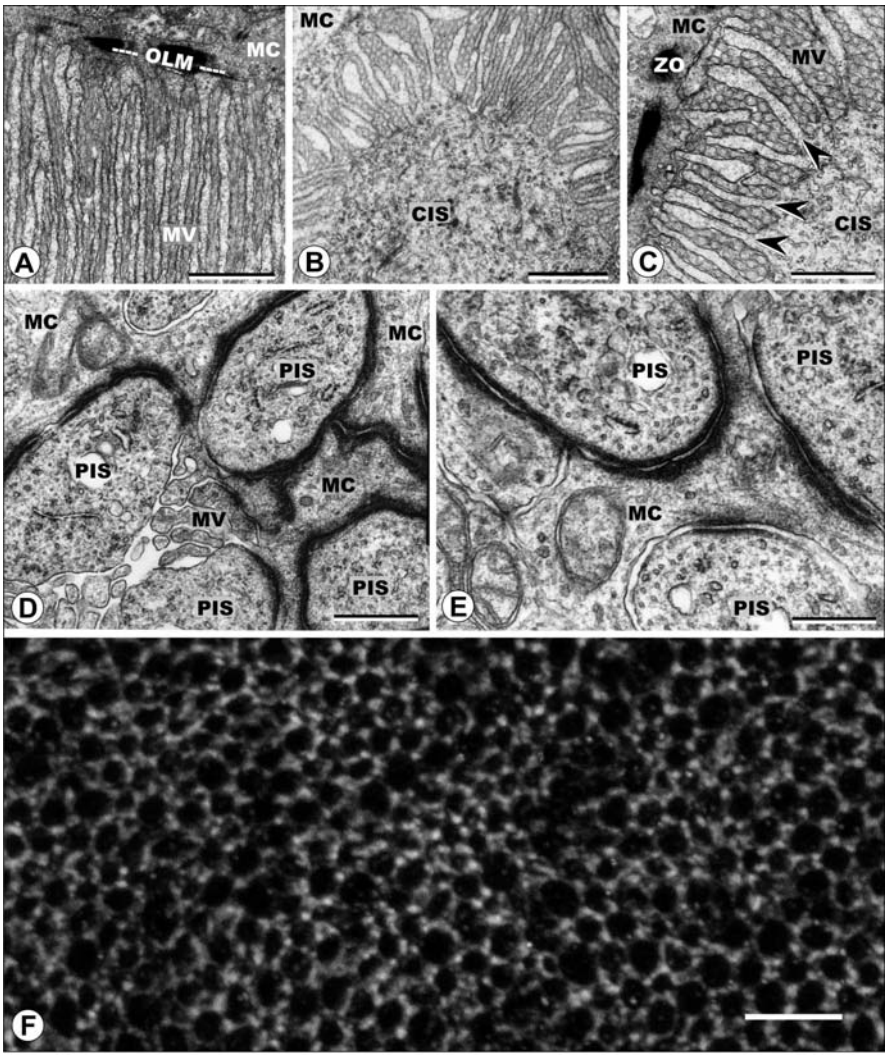

Fig. 2.10 Microvilli and Zonulae adherentes at the outer processes of Müller cells. (**a**)–(**c**) Transmission electron microphotographs from a tree shrew retina. (**a**) Radial section, showing the long, parallel microvilli (MV) extending from the Müller cells (MC) and a part of the "outer limiting membrane" (OLM). (**b**, **c**) Transversal sections at the level of the OLM; the cone inner segments (CIS) extend lateral "finches" (*arrowheads*) between which the Müller cell microvilli are located; zonulae adherentes (ZO) between adjacent Müller cells (and photoreceptors) constitute the OLM. (**d**, **e**) Transversal sections at the level of the OLM of a rabbit retina, demonstrating long, continuous strands of zonulae adherentes between the outer processs of Müller cells (MC) and the photoreceptor inner segments (PIS). (**f**) Immunohistochemical demonstration of the OLM-forming network of zonulae adherentes by an antibody against mpp5 (cf. Stöhr et al., 2005, for details) in a murine retina; confocal microscopy. Calibration bars, 1 μm (**c**, **e**), 2 μm (**a**, **b**, **d**), and 10 μm (**f**), respectively. (**a**)–(**c**), modified after Reichenbach et al. (1995d); (**d**), (**e**), courtesy of H. Wolburg, Tübingen; (**f**) courtesy of B. Biedermann, Leipzig

rest of the cell (about 65 vs. 85 μm). Each Müller cell sends up to 300 of these long, slightly tapering microvilli (their diameter decreases from some 170 to 120 nm) along with the elongated photoreceptor inner segments. This means that more than half the Müller cell volume is located in the microvilli (own unpublished data). It appears reasonable to speculate that the number and, even more, the total membrane surface of the micovilli is adjusted so as to meet the needs of molecule/nutrient exchange of the Müller cells with the subretinal space (Uga and Smelser, 1973); these may vary in dependence on the density/type of photoreceptors, the presence vs. lack of intraretinal vascularization, and other factors.

Close to the origin of the microvilli and to the OLM, the outer process of Müller cells (particularly, in avascular retinas) contains densely packed mitochondria; for more details, see below. As exceptional organelles, cilia have been observed to origin from the outer Müller cells processes in a fish retina (Ennis and Kunz, 1986).

(B) *The inner process* arises from the soma without any distinct border, and ends at the ILM where it forms an endfoot, or several endfeet. It displays a large surface-to-volume ratio on its course through the IPL where it extends many fine side branches towards the synapses (SVR = ca. 13 μm^{-1}). Where the inner process passes the NFL its surface is rather smooth (cf. Figs. 2.1 and 2.5) (SVR < 4 μm^{-1}). In typical mammalian retinas, the thick inner process (particularly, the big endfoot) contains the majority of the cytoplasmic volume of the cell (about 70%; Reichenbach et al., 1988a). The dominant organelles in the inner process are bundles of intermediate filaments (for their molecular composition and other details, see below). These filaments irradiate into the endfoot but barely reach into the proximity of the ILM. Rather, much of the endfoot is filled by densely packed smooth endoplasmic reticulum (Fig. 2.11b) (Uga and Smelser, 1973; Reichenbach et al., 1988a). Whereas in avascular retinas (e.g., rabbit, guinea pig) the inner process is virtually devoid of microtubules, in vascularized retinas (e.g. mouse, rat) it may contain almost as many microtunules as intermediate filaments.

The endfoot membrane of Müller cells shows several characteristic features where it abuts the basal lamina of the ILM. Generally, even the large endfeet of

Fig. 2.11 (continued) retinal periphery the Müller cell endfeet are larger, and less regularly arranged (**d**); cf. also Fig. 1.16a, b. (**e**, **f**) Electron microphotographs of freeze-fracture replicas of endfoot membranes in the central rabbit (**e**) and human retina (**f**). (**e**) The inner surface of the central rabbit retina is constituted by endfeet of both Müller cells (MC) and astrocytes. Where their "true" endfoot membrane adheres to the basal lamina, both types of macroglial cells express so-called orthogonal arrays of membrane particles (OAP; some are encircled). (**f**) Similar OAP are found in human Müller cell endfoot membranes (e.g., pf1) where they abut the basal lamina (BL) but not in membrane areas facing extracellular clefts (ECS) or other cells (e.g., pf2). (**g**) Transmission electron microphotograph of Müller cell endfeet (MC) in the perifoveal human retina. Here, the basal lamina (BL) is very thick (compare (**b**)) and shows irregular evaginations into the inner retina. The Müller cell endfeet extend numerous thin, irregular "fingers" which overlap with other "fingers" arising from the same cell or from adjacent Müller cells. Moreover, the occurrence of rather large, irregular extracellular spaces (ECS) complicates the structure of the inner retina in the parafoveal region. (**a**) courtesy of H. Kuhrt, Leipzig; (**b**) and (**c**) modified from Reichenbach et al. (1995d); (**e**) modified from Richter et al., 1990; (**f**) and (**g**) Reichenbach and Wolburg (2005)

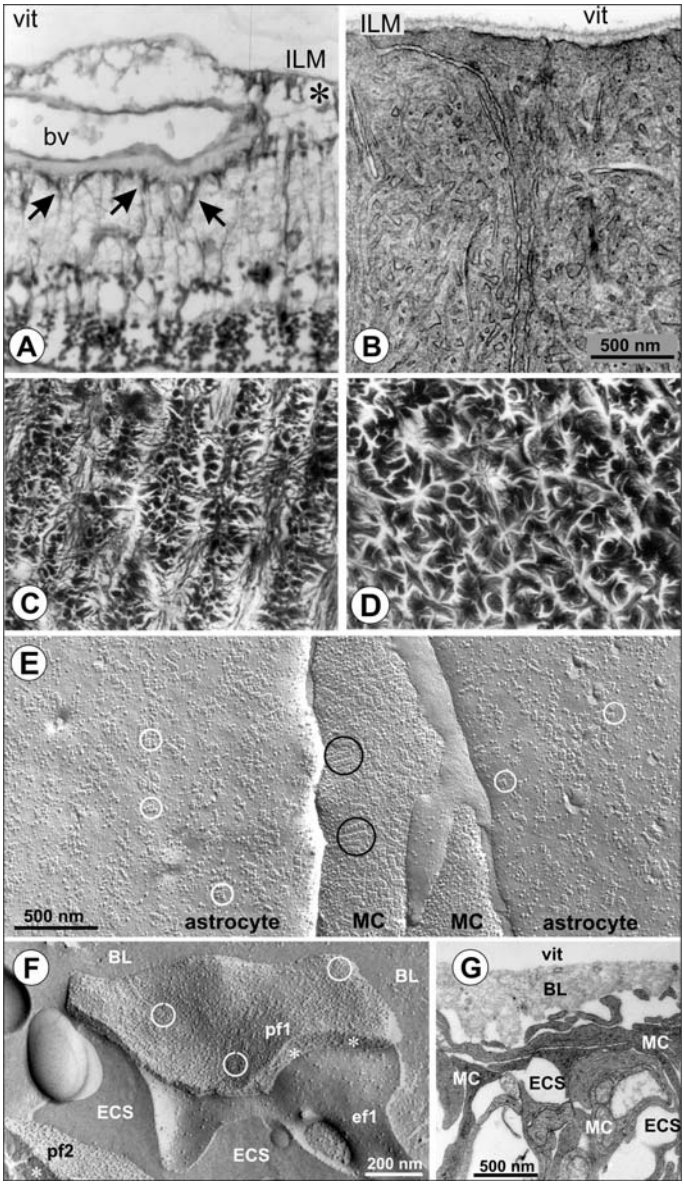

Fig. 2.11 Müller cell endfeet at the inner limiting membrane (ILM) and at intraretinal blood vessels (bv). (**a**) H-E stained paraffin section of a whale retina, labeling of Müller cells by vimentin immunohistochemistry (DAB); whereas most Müller cells abut the ILM by their endfeet (*asterisk*), some Müller cells end at large intraretinal blood vessels (*arrows*). (**b**) Transmission electron microphotograph of Müller cell endfeet in the peripheral rabbit retina. A thin basal lamina constitutes the ILM against the vitreous body (vit); much of the Müller cell endfoot cytoplasm is filled by smooth endoplasmic reticulum. (**c**, **d**) Immunohistochemical demonstration of Müller cell endfeet by vimentin-antibodies in a wholemounted tree shrew retina; due to the presence of axon bundles in the central retina (**c**) the local Müller cell endfeet are arranged in rows whereas in the

peripheral Müller cells (cf., e.g., Fig. 2.5) form several flat, overlapping extensions close to the ILM (Figs. 2.9, 2.11d, g) as if they would try to compete with their neighbours to occupy as much ILM surface area as possible. Only those membrane areas of these extensions which directly abut the basal lamina, represent a "true" endfoot membrane. In the Müller cells of most vertebrates studied so far, this "true" endfoot membrane can be reliably identified in electron optic freeze-fracture images by the expression of a high density of so-called "orthogonal arrays of particles"(OAPs) (Fig. 2.11e, f) (Wolburg and Berg, 1987, 1988); the only known exception are anuran (frog) Müller cells (Wolburg et al., 1992). As soon as the membrane deviates a few nanometers from basal lamina contact (e.g., due to an overlapping flat endfoot extension of the same or another cell), the density of OAPs decreases dramatically, and finally drops down to levels close to zero, at least in rabbit Müller cells (Wolburg and Berg, 1987). In vascularized (areas of) retinas, the Müller cell endfoot membranes are intermingled with those of astrocytes; these also express OAPs but their size and shape differs slightly (Fig. 2.11e) (Richter et al., 1990).The particles constituting the OAPs are thought to represent specific membrane proteins involved in the exchange of molecules between the Müller cell endfoot and the basal lamina and/or the vitreous body, respectively. The water channel protein, aquaporin4 (AQP4), has been identified as one of these molecules (Yang et al., 1996; Verbavatz et al., 1997). Other candidates are K^+ ion channels and integrin receptors, for example.

Another characteristic element of the endfoot membrane are coated pits of some 150 nm basal diameter; near these pits, the cytoplasm contains vesicles of 90–100 nm diameter (Reichenbach et al., 1988a). The function of these structures is unclear; the vesicles may be endocytotically engulfed (e.g., after activation of cell surface receptors), or alternatively may represent structures of exocytosis, for example for the synthesis of components of the basal lamina. Taken together, the (ultra-) structural data as well as physiological evidence (Karwoski et al., 1989) suggest that the Müller cell endfoot membrane is the site of a lively exchange of molecules and biological signals between the Müller cell and thus, the retina on the one hand, and the vitreous (and the basal lamina) on the other hand. The same applies to the perivascular "en passant"-endfeet. The basal lamina proper is composed of type IV collagen, laminin, heparan sulfate proteoglycan, nidogen, and fibronectin. The perivascular basal lamina of Müller cells forms a continuous membrane which completely surrounds the retinal capillaries, whereas the subendothelial basal lamina displays large fenestrations, allowing a direct contact between vascular endothelial cells and pericytes (Carlson, 1988; Carlson et al., 1988).

(C) *The lateral processes* or side branches are the contact sites with the neuronal elements. They arise from the outer and inner stem processes, particularly within the two plexiform (synaptic) layers. Generally these side branches are rather thin, and split into even thinner but very elaborated cytoplasmic tongues, similar to the PAPs of other macroglial cells (cf. Section 1.1.2, Fig. 1.6c). Thus, despite of their small volume they constitute a considerable portion of the total cell membrane area ($SVR > 14\ \mu m^{-1}$). Apparently both individual synapses (cone pedicles?) and groups

of them (rod spherules?) are ensheathed by glial side branches (Fig. 2.3a). The perineuronal membrane compartments of these fine processes are thought to express a wealth of proteins crucial for glia-neuron interactions, including ion and water channels, uptake carriers for neurotransmitter molecules, and others; however, they are virtually devoid of cytoplasmic organelles. Groups of polyribosomes are localized at the sites of origin of these lateral processes (as well as of the microvilli which extend into the subretinal space), suggesting that neuronal activity may stimulate the local synthesis of structural proteins and, thus, the growth of the perisynaptic processes and microvilli (Reichenbach et al., 1988a). The perisynaptic side branches grow also in adult animals (Reichenbach and Reichelt, 1986). It has been hypothesized that the underlying local protein synthesis may be stimulated by external potassium accumulation due to neuronal activity, as kind of a homeostatic mechanism (Reichelt et al., 1989). Indeed, light-evoked increases in extracellular potassium occur in the inner and outer plexiform layers, and (after cessation of illumination) in the subretinal space (Oakley and Green, 1976; Steinberg et al., 1980; Karwoski et al., 1985, 1989). However, the release of other molecules by active synapses, such as the neurotransmitters and metabolic waste products, may also contribute to the local shaping of glial sheaths (cf. Sections 2.4 and 2.5).

A particular structure is formed by thin side branches in the nerve fiber layer where the (thick) axons of the ganglion cells (even if unmyelinated as usual in vertebrate retinae) display "node-like specializations" with high densities of Na^+ channels, promoting saltatory conduction of action potentials towards the

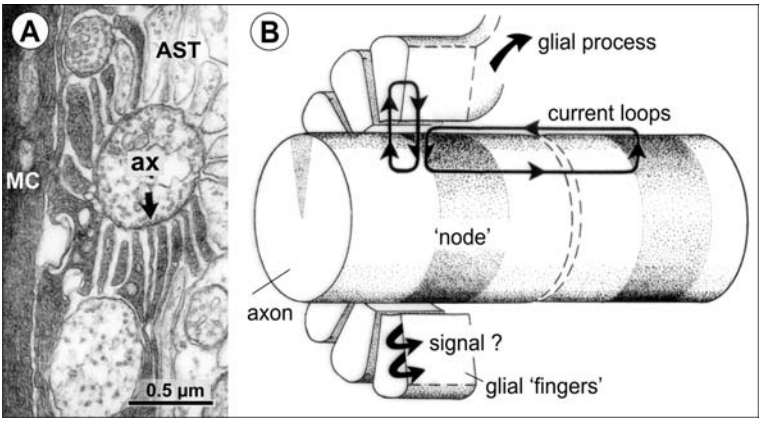

Fig. 2.12 Periaxonal processes extending from Müller cells. (**a**) Transmission electron microphotograph of a part of the nerve fiber layer of a cat retina. The axons of the retinal ganglion cells (ax) display local "node-like" specializations (*arrow*) probably representing sites of high Na^+ channel density, for saltatory action potential propagation. Both the astrocyte (AST) and the Müller cell (MC) extend fine, finger-like processes towards this axolemmal area; together they form a corona of such fine processes. (**b**) Semi-schematic view of such a corona of finger-like Müller cell processes at the "node" of a ganglion cell axon, together with the proposed flux of transmembraneous ion currents. (**a**) Modified from Holländer et al. (1991); (**b**) modified from Chao et al. (1994b)

(myelinated part of the same axons in the) optic nerve. Such node-like axonal specializations are abutted by coronae of finger-like glial processes arising from Müller cells (and astrocytes, if present) (Fig. 2.12a). These thin glial cytoplasmic tongues are devoid of cell organelles but come into close proximity of the axon; the extracellular clefts there are extremely narrow, about 6 nm (Hildebrand and Waxman, 1983; Hildebrand et al., 1993; Holländer et al., 1991; Reichenbach et al., 1988c). It has been speculated that "ephaptic" transmission of large currents may occur via this narrow cleft, from the node-like axonal membrane to the glial "finger" membrane, if an action potential is passing the axon. These currents would cause considerable alterations of the local glial membrane potential which, in turn, may trigger a variety of cellular responses. This has been proposed as a potential mechanism by which the glial cells can "sense" enhanced activity of the adjacent neurons, and respond with adequate feedback responses including an enhanced delivery of nutrients or other supportive molecules (Chao et al., 1994b).

The *localization of the mitochondria* within Müller cells (and in photoreceptor and pigment epithelial cells) depends on the oxygen supply of the retina. Paurangiotic and avascular retinas (e.g., from rabbits and guinea pigs) experience extremely low oxygen partial pressures (pO_2) proximal to the outer limiting membrane (Yu and Cringle, 2001). In Müller cells of these retinas, only a few mitochondria are located at the outer end of the cells, i.e. close to the choroidal blood supply, while the other parts of the cells are devoid of mitochondria (Fig. 2.9) (Sjöstrand and Nilsson, 1964; Magalhães and Coimbra, 1972; Uga and Smelser, 1973; Reichenbach et al., 1988a; Reichenbach, 1989a; Germer et al., 1998a, b; Stone et al., 2008). In vascularized retinas, by contrast, mitochondria are rather evenly distributed throughout the entire length of Müller cells (Germer et al., 1998a). When the avascular retina of guinea pigs is kept in organotypic cultures where high pO_2 levels are provided at the inner surface of the retina, the mitochondria migrate and re-arrange to an even distribution within Müller cells (Germer et al., 1998b). The retinas of various species such as frogs and carps are overlaid by supraretinal (intravitreal) blood vessels; this corresponds to an accumulation of mitochondria in the Müller cell endfeet (in addition to the above-mentioned accumulation at the outer limiting membrane) (Uga and Smelser, 1973). In Müller cells of avascular retinas (e.g. of rabbits), aerobic and anaerobic metabolism occurs in different cellular regions. Whereas the mitochondria are located at the outer margin of the cells, all enzymes for glycogen synthesis, glycogenolysis, and anaerobic glycolysis, as well as the stores of glycogen particles, are localized to the inner (vitread) part of the cells (Kuwabara and Cogan, 1961; Lessell and Kuwabara, 1964; Cameron and Cole, 1964; Matschinsky, 1970; Magalhães and Coimbra, 1970, 1972; Reichenbach et al., 1988a). The endfeet of rabbit Müller cells contain a huge apparatus for the production of freely diffusible glucose from glycogen, in the form of abundant smooth endoplasmic reticulum (Figs. 2.9 and 2.11b) (Reichenbach et al., 1988a) which are the site of glucose-6-phosphatase activity (Magalhães and Coimbra, 1972). In these cells, glucose is mainly taken up by the scleral microvilli (a certain amount of glucose may be also derived from the vitreous fluid), and is then either oxidatively metabolized by the mitochondria where it enters the cell, or transported into the

inner (vitread) part for glycogen storage and anaerobic metabolism. In contrast to those of Müller cells in avascular retinas, the glycogen stores are distributed uniformly in Müller cells of vascularized retinas (Rungger-Brändle et al., 1996). It has been concluded that the cytoplasmic localization of Müller cell mitochondria is not dependent on the local metabolic needs, but rather on the local availability of oxygen (Germer et al., 1998a, b). A similar rule has been postulated also for photoreceptor cells (Stone et al., 2008).

2.1.5 Müller Cell Markers

Under a series of circumstances, Müller cells can be easily identified by their characteristic morphology. This applies to enzymatically (or mechanically) dissociated single cells (Figs. 1.17b–d, 2.2b, 2.32e, 2.39c, 2.40a, and 2.46c) and even to certain histological preparations not specifically labeled for Müller cells (Figs. 2.1 and 2.4). To identify Müller cells in living retinal preparations (for example, to facilitate physiological investigations), acutely isolated retinal wholemounts or slices can be loaded for a few minutes with vital dyes such as Mitotracker Orange (Fig. 2.12a) or Celltracker Green. These vital dyes are almost selectively taken up by Müller cells (and by some photoreceptor segments), whereas the somata of the photoreceptor cells and of other neurons, astrocytes, and microglia remain unstained (Uckermann et al., 2004b). In such preparations, Müller cell nuclei were shown to be stained by ethidium bromide, diamidino yellow, or chromomycin A3, which selectively penetrate Müller cells and have a marked affinity for nucleic acid (Laties, 1983; Jeon and Masland, 1993).

Another innovative method to visualize Müller cells even in unstained vital preparations is the generation of transgenic animals in which a fluorescent reporter gene is coupled to the expression of a Müller cell-specific gene. Recently, a variety of such animals has been generated (Zhuo et al., 1997; Nolte et al., 2001; Bernardos and Raymond, 2006; Mori et al., 2006; Greenberg et al., 2007; Vazquez-Chona et al., 2009; Hirrlinger et al., 2009). Although it must be stated here that the degree and selectivity of Müller cell "labelling" cannot be easily predicted in such transgenic models, due to technical limitations of the genetic procedures (Caroni, 1997), it is obvious that they provide very versatile tools for a variety of studies. For instance, dependent on the aim of the given experiment, one may monitor (almost) the entire Müller cell population (Fig. 2.13b) or, alternatively, one or a few individual cells (Fig. 2.13a). Moreover, this technique allows not only to "label" Müller cell but also to introduce, or extinguish, the expression of distinct genes in Müller cells, and to study the effects of these changes on retinal function.

Despite of the above-mentioned techniques, however, in many cases it is necessary to identify the retinal glia including the Müller cells by means of immunohistochemical markers. There are various proteins which are restricted in their expression to astrocytes and Müller cells, or selectively to Müller cells,

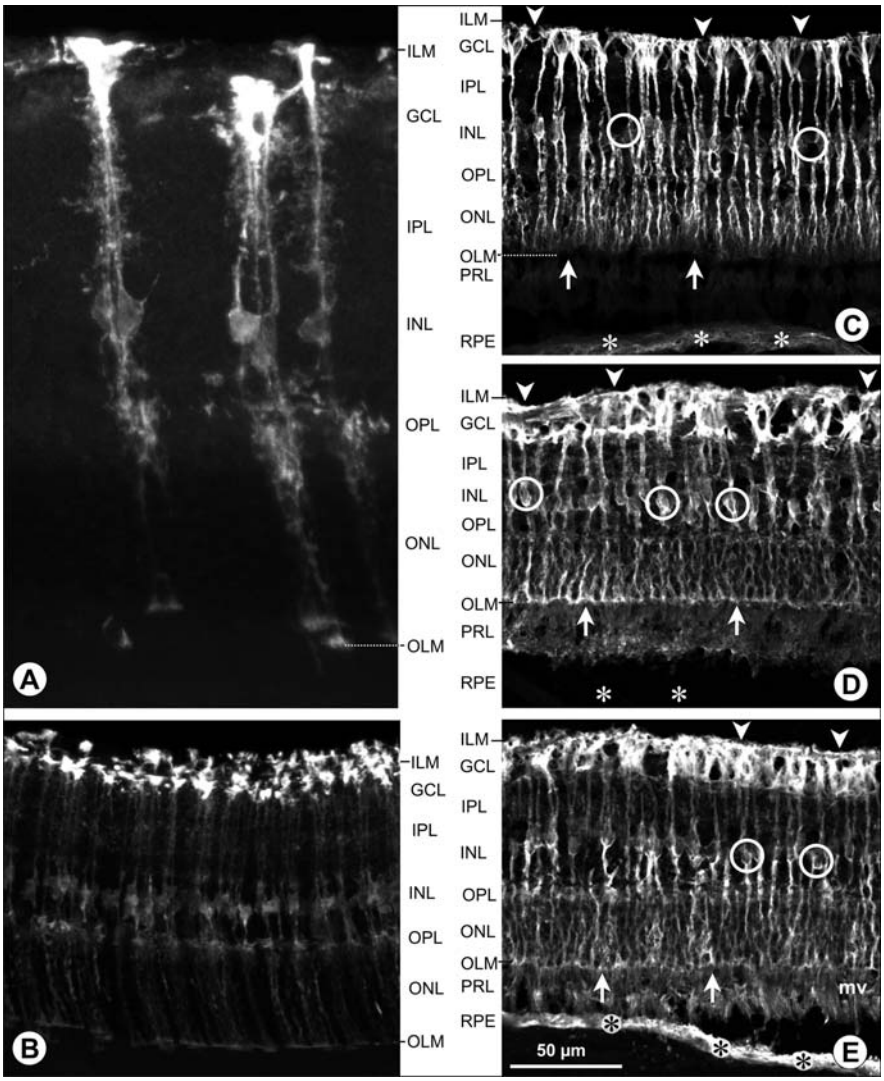

Fig. 2.13 Specific visualization of Müller cells by transgenic labeling (**a**, **b**) or immunohistochemistry (**c**–**e**). (**a**) 2-Photon-microphotograph of a radial slice of a vital, unstained retina of a MrgA1-EGFP mouse (Fiacco et al., 2007); only scattered individual cells are labeled but these can be studied in intriguing morphological detail. (**b**) 2-Photon-microphotograph of an unstained radial retina section of a GFAP-NCre x PLP-CCre EYFP mouse (Hirrlinger et al., 2009); virtually all Müller cells are labeled. (**c**), (**d**) Immunofluorescence in retinal sections of guinea-pig retinas stained for vimentin (**c**), glutamine synthetase (**d**), and CRALBP (**e**), respectively. All Müller cell stem processes are reliable labeled by the vimentin antibody (**c**) but some endfeet (*arrowheads*) and most somata (*circles*) cannot be visualized; likewise, the Müller cell processes at the OLM (*arrows*) are not labeled. Antibodies against glutamine synthetase label all Müller cell endfeet and somata, as well as their outer processes (**d**); identification (and counting) of the stem processes is a little more difficult because strong label in the fine (perisynaptic!) side branches

in the retina. This includes vimentin (Fig. 2.13c), glial fibrillary acidic protein (GFAP) (Figs. 3.1a, b and 3.13a), cellular retinaldehyde-binding protein (CRALBP) (Figs. 2.13e and 2.48), glutamate-aspartate transporter (GLAST), glutamine synthetase (Figs. 2.13d and 2.48), inwardly rectifying potassium channels of the Kir4.1 subtype (Figs. 2.43b, 2.46d, 2.48, 2.49, 3.8a, 2.13a, and 2.15a), aquaporin-4 (Figs. 2.48, 2.49, 2.57, 3.13a, 3.15a), pyruvate carboxylase, α-crystallin, the small GTP-binding protein RhoB, the glutamate carboxypeptidase II, carbonic anhydrase C, and microtubule-associated protein 4 (Linser and Moscona, 1981a; Bunt-Milam and Saari, 1983; Moscona et al., 1985; Parysek et al., 1985; Berger et al., 1999; Santos-Bredariol et al., 2006). In avascular retinas that lack astrocytes, these markers are only expressed by Müller cells. However, the expression of some of these markers varies in different vertebrate species and may also vary among glial cells of one retina. In the cat retina, CRALBP and glutamine synthetase are expressed by Müller cells but not by astrocytes, whereas carbonic anhydrase C, α-crystallin and GFAP are expressed by both Müller cells and astrocytes (Lewis et al., 1988). Noteworthy, astrocytes transiently express CRALBP during retinal development when they migrate into the retina from the optic nerve head (Johnson et al., 1997). It is noteworthy that the use of different immunohistochemical markers may reveal/highlight different aspects of the Müller cell morphology (Fig. 2.13c–e). For instance, antibodies directed against vimentin label both the filaments and the cytosolic (not-yet organized) protein; accordingly, almost the entire cells are labeled. However, the fine side branches, the somata, and the innermost parts of the endfeet are barely detectable (Fig. 2.13c). By contrast, antibodies against glutamine synthetase readily label the somata and the many fine side branches (which may even appear as a "background label") (Fig. 2.13d). The cellular structure is best revealed by antibodies directed against membrane (-bound) proteins such as CRALBP (Fig. 2.13e).

Genes that appear to be preferentially expressed by Müller cells in the adult retina include, for example, glutamine synthetase, clusterin, dickkopf homolog 3 (Dkk3), aquaporin-4, the tRNA ligase BING4, the transcription factor Sox2, the lipid transporter apolipoprotein E (ApoE), clusterin/ApoJ, the diazepam binding inhibitor, Abca8a (a transporter with ATPase activity), the isoprenoid binding protein Rlbp1, the receptors Gnai2 and Gpr37, caveolin 1 (which is important in nitric oxide metabolism and vesicle-mediated transport), Spbc25 (a component of the Ndc80 kinetochore complex), and other genes with unknown biological function (Blackshaw et al., 2004; Roesch et al., 2008).

The soluble cytoplasmic enzyme, carbonic anhydrase II, is expressed by Müller cells and by a subset of amacrine cells, whereas membrane-bound carbonic

Fig. 2.13 (continued) generated a high "background". A very good visualization of the Müller cells, including their microvilli (mv) is achieved by antibodies against CRALBP (**e**). Note, however, that these antibodies also label the retinal pigment epithelium (*asterisks*), even stronger than the antibodies against vimentin (**c**). (**a**) courtesy of P. Hirrlinger, Leipzig; (**b**) modified from Hirrlinger et al. (2009); (**c**)–(**e**), modified from Reichenbach and Wolburg (2005)

anhydrase XIV is localized to Müller cells, astrocytes, and vascular endothelium (Palatroni et al., 1990; Ridderstråle et al., 1994; Ochrietor et al., 2005; Nagelhus et al., 2005). Carbonic anhydrase II is expressed throughout the mammalian retina early in development. As the retina matures and the cell types differentiate, its expression becomes limited to Müller cells and a subset of amacrine cells (Linser and Moscona, 1981a; Linser et al., 1984; Vardimon et al., 1986). In addition to oligodendrocytes, carbonic anhydrase has also been localized to photoreceptors and horizontal cells in several vertebrate species (Linser and Moscona, 1984; Linser et al., 1985; Wistrand et al., 1986; Vaughan and Lasater, 1990; Terashima et al., 1996; Eichhorn et al., 1996).

There are also species variations in the distribution of the Ca^{2+}-binding protein, S-100 in the retina. In some species like rat, rabbit, guinea pig, and hamster, retinal S-100β is confined to Müller cells and astrocytes, whereas in other species (e.g., the chicken), S-100 is localized predominantly to neurons (Linser and Moscona, 1981b; Kondo et al., 1983; Terenghi et al., 1983; Molnar et al., 1985; Schnitzer, 1987a). In the human retina, Müller cells express S-100 under pathological but not under normal conditions (Molnar et al., 1985; BenEzra and Chan, 1987; Karim and Itoh, 1997).

As a peculiarity, Müller cells express myelin-associated glycoprotein, suggesting a relationship between Müller cells and oligodendrocytes, the myelin-forming cells of the central nervous system (Stefansson et al., 1984). In the retinas of rabbits and hares, bundles of ganglion cell axons in the nerve fiber layer are surrounded by myelin sheaths formed by oligodendrocytes. However, Müller cells of parakeets may form myelin lamellae that cover individual retinal ganglion cell axons (Yamada, 1989).

2.1.6 Intermediate Filaments

As mentioned above, several intermediate filament-forming proteins are characteristic for Müller cells. Generally, there is a heterogeneous group of proteins that form 10 nm-diameter filaments as a component of the cytoskeleton. In the course of retinal development, retinal progenitor cells and differentiating Müller cells express the intermediate filaments vimentin and nestin (Walcott and Provis, 2003; Fischer and Omar, 2005; Xue et al., 2006a). Nestin is a widely used cell-distinguishing marker of neural progenitors in the mammalian nervous system; it cannot form filaments on its own but requires vimentin as a polymerization partner. As maturation proceeds, Müller cells downregulate nestin, and mature Müller cells express predominantly vimentin, whereas retinal astrocytes express predominantly GFAP. (In some species, horizontal cells may also express vimentin and GFAP: Dräger, 1983; Shaw and Weber, 1984; Linser et al., 1985; Davidson et al., 1990; Vaughan and Lasater, 1990; Knabe and Kuhn, 2000) If Müller cells in a mature retina express GFAP, this expression is restricted to the endfeet and inner stem processes of the cells (Figs. 3.1a and 3.13a) (Erickson et al., 1987; Karim et al., 1996). In some species such as the mouse, there is no detectable GFAP in normal Müller cell

endfeet, and the only GFAP labeling occurs in astrocytes (with the exception of Müller cells at the ora serrata and around the optic nerve that may express GFAP) (Bromberg and Schachner, 1978; Sarthy and Fu, 1989; Sarthy et al., 1991; Chien and Liem, 1995; Verderber et al., 1995; Fisher et al., 2005). Vimentin is detected in Müller cell fibers throughout the entire retina, with more expression in inner than outer stem processes (Figs. 2.55c and 3.1a, b) (Nakazawa et al., 2007b). This corresponds well to the distribution of the filaments; in rabbit and guinea pig Müller cells, intermediate filaments are largely restricted to the inner part of the cells up to the level of the outer plexiform layer whereas the outer process contains microtubuli (Fig. 2.9) (Reichenbach et al., 1988a; Reichenbach, 1989b). It has been proposed that intermediate filaments provide resistance against mechanical stress of Müller cell endfeet and the inner retinal layers, such as caused by the growth of blood vessels (Lundkvist et al., 2004). Other causes of mechanical stress are pathological events (e.g., retinoschisis) and intense activity of glutamatergic neurotransmission which is associated with a thickening of the inner retinal tissue, at least in vitro (Fig. 2.58). Upregulation of GFAP in Müller cells is a hallmark of retinal gliosis (Bignami and Dahl, 1979) and correlates with an increasing biomechanical stiffness of the Müller cells (Lu et al., 2009). Thus, the intermediate filaments in Müller cells may be involved in their biomechanical responses to various injuries or physiological events. In this context it appears to be noteworthy that Müller cells express myosin VI which may play a role in retinomotor movements in response to changes in light conditions (Breckler et al., 2000).

2.1.7 Junctional Cell Coupling

Gap junctional coupling of cells creates a functional syncytium which is involved in the propagation of intercellular signals, and in other functions such as spatial potassium buffering. Fish, amphibian and reptilian Müller cells are coupled together via connexin 43 (Uga and Smelser, 1973; Conner et al., 1985; Mobbs et al., 1988; Giblin and Christensen, 1997). Amphibian Müller cells form a syncytium of thin processes surrounding every neuron from the outer limiting membrane to the inner limiting membrane (Ball and McReynolds, 1998). In contrast, avian Müller cells have no gap junctions; the lack of gap junctional coupling has been explained with the presence of the extremely elaborated "trees" of endfeet which may mediate the dissipation of locally elevated potassium (Ladewig et al., 1998). Mammalian Müller cells investigated so far are also not coupled together by gap junctions (Wolburg et al., 1990; Robinson et al., 1993), with the exception of rabbit Müller cells which may be coupled to at least one additional Müller cell (Nishizono et al., 1993; Zahs and Ceelen, 2006). In the cat and human retina, gap junctions are only present between processes of astrocytes (Holländer et al., 1991; Ramírez et al., 1996). Müller cells of other mammalian species with vascularized retinas (such as rat) can be coupled to astrocytes that lie at the inner surface of the retina (Robinson et al., 1993). In the rat retina, one astrocyte is coupled via gap junctions to 13–88 astrocytes, and to >100 Müller cells (Zahs and Newman, 1997). While the junctional

coupling between astrocytes is symmetric, the coupling between astrocytes and Müller cells is asymmetric, allowing only a unidirectional transfer of small intracellular molecules from astrocytes to Müller cells but not vice versa (Robinson et al., 1993; Zahs and Newman, 1997). Astrocytes and Müller cells express different connexins (Zahs et al., 2003; Zahs and Ceelen, 2006). Diffusion of internal messengers through gap junctions is implicated in the propagation of intercellular calcium waves between astrocytes (but not between astrocytes and Müller cells) (Newman and Zahs, 1997; Newman, 2001). Connexins which are located in the filamentous processes ensheathing the photoreceptor cells (Schütte et al., 1998) may have a functional role in the release of gliotransmitters from Müller cells, for example, by forming so-called "hemichannels".

Adherent junctions are present between astrocytes and Müller cells, and between adjacent astrocytes and Müller cells, but not between glial cells and neurons, or among neurons (with the exception of the junctional coupling between Müller and photoreceptor cells at the level of the outer limiting membrane; cf. Fig. 2.10) (Holländer et al., 1991; Ramírez et al., 1996). This suggests that the glial cell network contributes to the mechanical stability of the retina.

2.2 Retinal Columnar Units and Domains – Role(s) of Müller Cells in Retina Organization

2.2.1 The Müller Cell Population Forms a Regular but Locally Variable "Scaffold"

Considering the total Müller cell population rather than individual cells, it becomes apparent that the cells are rather regularly spaced (Figs. 2.17, 2.25b, 2.33b, c, 2.59, and 2.69) and thus form an arrangement of parallel "tubes" similar to the blades of grass in a meadow. For the rabbit retina it has been shown that this arrangement can be perfectly fitted by equations for a hexagonal pattern of cylinders with almost equal diameters and axis-to-axis distances (Reichenbach et al., 1991b). This rule seems to be valid for the local populations of Müller cells in all vertebrate species studied so far (e.g., Dreher et al., 1992; Mack et al., 1998; Chao et al., 1997; and own unpublished data). However, both the cell densities per mm^2 retinal surface area (i.e., the spacing distance between cells) (Fig. 2.6) and the diameters of the (inner) stem processes may vary across the retina topography; generally, Müller cells of the retinal periphery are more widely spaced (i.e., less densely arranged) and thicker than their counterparts in the retinal center (Fig. 2.14); although the thick peripheral cells are shorter than the central ones (Fig. 2.5) their cytoplasmic volume is bigger (cf. Section 2.1.2; Reichenbach et al., 1988a). It will be discussed later that this inverse relation between adult Müller cell densities and diameters largely results from late differential expansion ("growth") of retinal areas (Section 2.2.6).

In the context of functional retinal domains, it is of interest to know if and how the local variations in Müller cell densities (Fig. 2.6) correlate to local variations

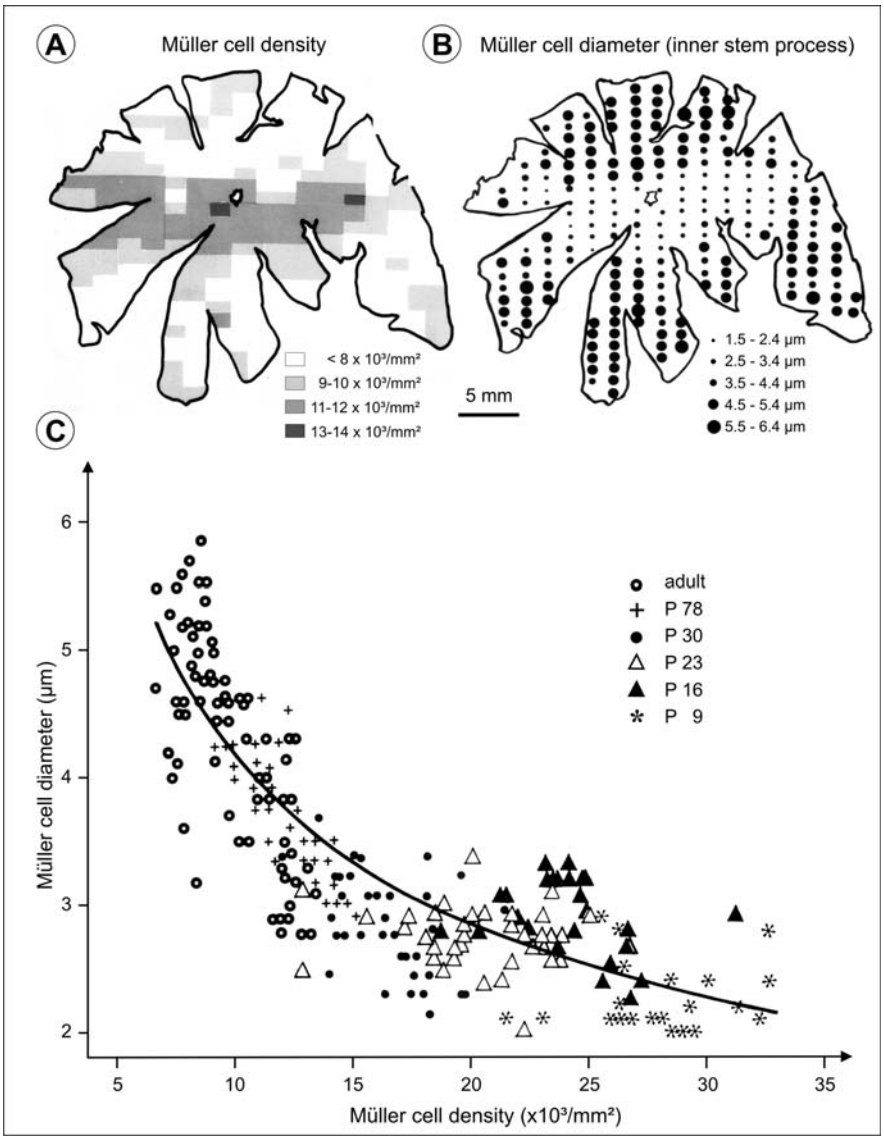

Fig. 2.14 Spatial density and stem process diameter of Müller cells vary inversely in dependence on retinal topography. (**a**, **b**) Topographical maps of spatial density (**a**) and process thickness (**b**) of Müller cells in adult rabbit retinas. (**c**) Correlation between Müller cell densities and diameters of Müller cell processes, measured at various developmental stages and different retinal sites (from center to periphery). Throughout all measurements, decreasing cell densities are accompanied by increasing process diameters; the correlation coefficient is very high (0.92). Compare also Figs. 2.5 and 2.6. Modified after Reichenbach et al. (1991b)

in photoreceptor/neuron cell densities. It is long known that retinal neurons display higher packing densities in the retinal center than in the periphery. Apparently, specialized areas of high cell densities (area centralis, visual streak) are easily recognizable also in the density maps of Müller cells (Fig. 2.6: rabbit, cat, three shrew). Quantitative comparative analysis of local cell densities on retinas from various mammalian species revealed strikingly constant ratios between many (but not all) types of retinal neurons and Müller cells (Reichenbach and Robinson, 1995, and references therein). In the rabbit retina for instance, a virtually perfect "constant set" of about 15 neurons – including 1 cone, 10 rods, 2 bipolar cells, and one amacrine cell – was observed throughout the retina, independent on local variations in absolute cell densities (Reichenbach et al., 1994). This, together with ontogenetic data from rabbit, and data from other species, had led to the concept that each Müller cell constitutes the core of a column of cells, as the smallest functional unit of the retina (Reichenbach et al., 1994; Reichenbach and Robinson, 1995).

2.2.2 Repetitive Retinal Columnar Units and Their Diversity Among Vertebrate Retina Types

As shown in Fig. 2.15, a distinct set of principal retinal neurons is aligned along each Müller cell, thus forming a so-called columnar unit (Reichenbach et al., 1994; Reichenbach and Robinson, 1995). Basically, a vertebrate retina can thus be considered as being composed of a large number (about 4,000,000 in the rabbit, almost 10,000,000 in the human eye) of such repetitive columnar units, each contributing its part to the visual information collected by the retina. As mentioned above, the

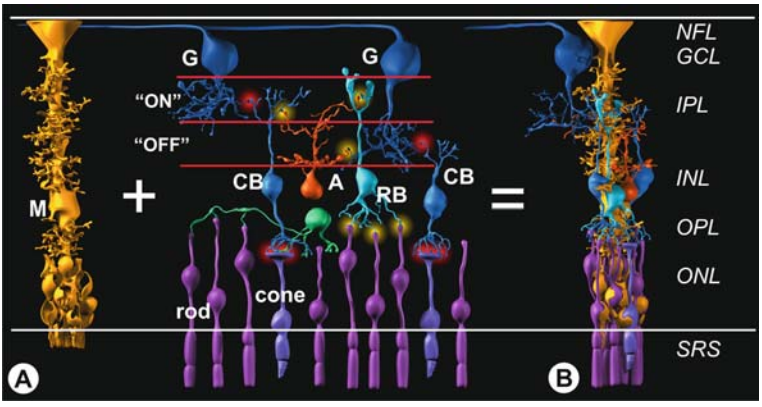

Fig. 2.15 The concept of columnar units in the vertebrate retina: I. artist's view of the constituents. Within the retina of a given species, the tissue is built up by a large number of repetitive groups of cells (**a**) arranged as columns (**b**). The center of each column is constituted by a Müller cell (M) which extends lateral side branches ensheathing the adjacent neurons of the unit. G, retinal ganglion cell; CB, cone-specific bipolar cells; A, amacrine cell; RB, rod bipolar cell. Each column spans all retinal layers (NFL, nerve fiber layer; GCL, ganglion cell layer; IPL, inner plexiform layer with "ON" and "OFF sublayers; INL, inner nuclear layer; OPL, outer plexiform layer; ONL, outer nuclear layer). The inner and outer segments of the photoreceptor cells, and the microvilli of the Müller cells, reach into the subretinal space (SRS). Original; courtesy of J. Grosche, Leipzig

constituents of a columnar unit are remarkably constant across a given retina, largely independent of local topographic specializations (for some exceptions, particularly, the primate fovea centralis, see Sections 2.2.4 and 2.2.6). However, the cellular composition of the columnar units differs considerably among the diverse vertebrates, even among mammalian species; this depends mainly on the diurnal vs. nocturnal lifestyle, i.e., the photopic vs. scotopic specialization of the retina (Fig. 2.16; cf. also Fig. 1.13).

To consider the putative functional impact of the columnar organization of the retina, some quantitative data are required (Tables 2.1 and 2.2). In all mammals studied so far, every unit contains, in addition to the "core Müller cell", (i) about

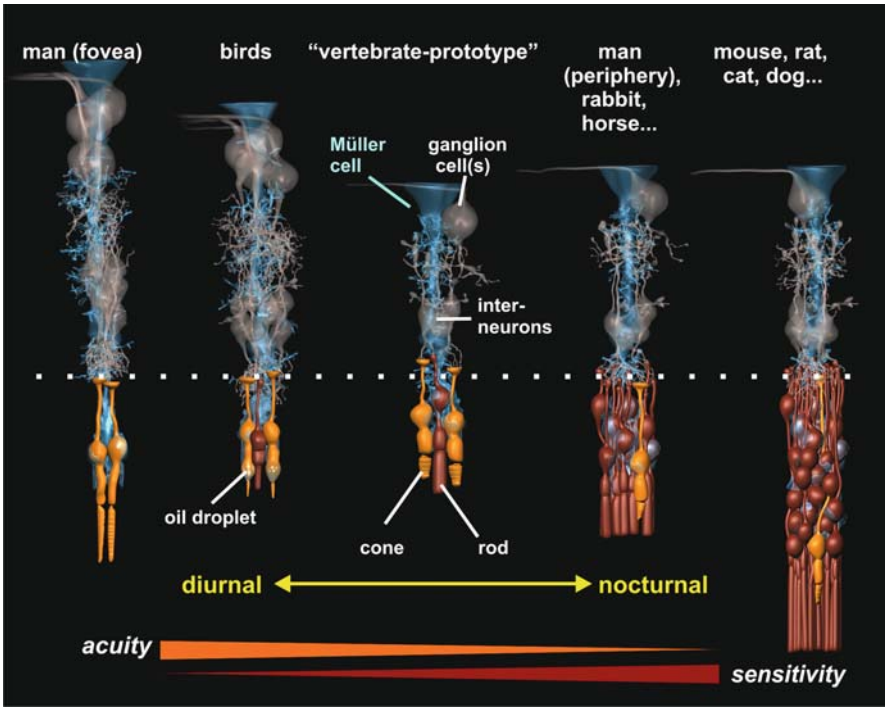

Fig. 2.16 The concept of columnar units in the vertebrate retina: II. artist's view of the different retinal specializations. It has been hypothesized that starting from a "vertebrate prototype" retina with a small "set" of neurons per column (up to two cones, one rod, a few interneurons and a ganglion cell), two opposite specializations have emerged by evolution. First (*towards left side*), photopic/diurnal specialization increased the number of interneurons and ganglion cells per column, a process which caused an increasing thickness of the inner plexiform layer where the enhanced number of synapses had to be arranged. At the extreme end of this type of specialization (in the primate fovea centralis), the rods are totally absent. Second (*towards right side*), scotopic/nocturnal specialization required the addition of more and more rods to each column. Because their signals are convergent, this process did not require much addition to the inner layers such as the IPL; compare also Fig. 1.13. Original; courtesy of J. Grosche, Leipzig

Table 2.1 Cellular composition of retinal columnar units of various vertebrates: survey

Species	Total cells/ MC	Photoreceptors/ MC	INL neurons/ MC	GCL neurons/ MC	Source
Tree shrew	7.00	1.70	4.30	1.05	1
Gray squirrel	8.19	2.82	4.64	0.73	2
Macaque (fovea)	8.76	1.36	4.80	2.60	3
Man (fovea)	9.04	0.93	5.73	2.38	3
Red squirrel	10.65	4.60	5.07	0.98	8
Mean photopic	8.73	2.28	4.91	1.55	
Capybara	12.52	9.35	2.82	0.35	8
Black rhinoceros	12.98	10.02	2.68	0.43	7,11
Bactrian camel	13.53	10.37	2.84	0.31	11
Common squirrel monkey	14.00	10.10	3.70	0.30	5
Orangutan	14.08	9.47	4.22	0.38	5,7
Lion tamarin	14.10	8.50	5.20	0.40	5
Madagascar sucker-footed bat	14.24	10.94	2.81	0.49	8
Zebra	14.29	10.90	3.08	0.30	2,8
Musk deer	14.33	11.66	2.40	0.21	11
Lama	14.54	10.86	3.37	0.30	7,8,9,11
Alpaca	14.66	11.38	2.98	0.32	7,11
Siamang	15.10	10.80	3.90	0.50	5
Hamadryas baboon	15.30	10.90	4.00	0.30	5
Man (periphery)	15.36	11.03	3.98	0.33	2,4,7
Rabbit	15.43	11.37	3.75	0.31	6
Guinea pig	15.72	11.60	3.45	0.67	2
Horse	15.81	13.44	2.22	0.15	2
Pig	15.82	12.15	3.24	0.43	2
Benett's tree kangaroo	15.94	12.35	3.26	0.33	8,11
Common degu	15.95	9.85	5.73	0.37	7
Barbarian sheep	16.25	12.97	3.25	0.30	2
Reindeer	16.45	12.76	3.34	0.36	7,11
Deer	16.60	12.13	2.88	0.90	2
Tufted capuchin	16.90	11.30	5.00	0.70	5
Red kangaroo	17.35	13.66	3.28	0.41	8,11
Yellow baboon	17.40	12.50	4.50	0.40	5
Eld's deer	17.86	14.43	3.15	0.28	7
Giraffe	17.91	13.73	3.86	0.32	7
Gibbon	18.40	12.50	5.10	0.70	5
Mara	18.38	14.23	3.94	0.21	7
Bison	19.08	15.56	2.95	0.57	8
Pygmy hippopotamus	19.91	15.34	3.73	0.84	11
Pudu	20.40	14.21	5.52	0.67	8
Porpoise	21.01	18.65	1.94	0.42	8
Nil rat	21.50	12.60	7.60	1.30	5
Mean mesopic	16.26	12.10	3.70	0.44	
Black-backed jackal	24.50	20.96	2.98	0.56	8
Grizzly bear	24.76	19.26	4.91	0.59	8
Whale	26.38	23.00	2.80	0.58	2

Table 2.1 (continued)

Species	Total cells/ MC	Photoreceptors/ MC	INL neurons/ MC	GCL neurons/ MC	Source
Siberian tiger	27.15	23.08	3.50	0.57	7,8,11
Black panther	27.22	23.02	3.57	0.63	7,8
Mink	29.10	22.68	5.88	0.54	2
Darwin's leaf eared mouse	29.12	21.76	6.94	0.42	7
Long-finned pilot whale	29.21	25.98	2.72	0.51	8
Ocelot	29.98	25.99	3.42	0.57	8
Cougar	30.26	25.29	4.64	0.33	7
Moon-toothed degu	30.26	22.72	7.00	0.54	7
Pallas's long-tongued bat	30.35	24.80	5.05	0.50	8
Sperm whale	30.70	25.54	4.30	0.86	8
Fitchew	31.50	25.58	5.26	0.67	2
Lion	32.00	28.23	3.27	0.50	8
Bridges's degu	32.25	24.23	7.49	0.53	7
Brown fur seal	32.26	28.66	3.18	0.42	8
Rat	32.38	25.45	6.37	0.56	2,7
Dog	32.62	26.12	5.95	0.55	2
Fox	32.66	26.77	5.40	0.50	2,8
Mouse	33.63	27.94	5.49	0.20	10
Clouded leopard	34.34	29.42	4.35	0.57	8
Cat	35.73	30.16	5.25	0.32	2
Giant rat	36.73	30.46	5.77	0.50	7
Mean scotopic	30.63	25.30	4.81	0.52	
Common marmoset	7.50	4.10	3.10	0.30	5
White-headed marmoset	7.80	4.10	3.30	0.40	5
Hedgehog	8.98	5.38	3.16	0.44	9
Mandrill	9.50	6.60	2.80	0.20	5
Mongolian gerbil	10.69	7.03	3.09	0.57	2
Meerkat	10.88	6.20	4.05	0.63	8
Pygmy marmoset	11.70	6.70	4.70	0.40	5
Asian palm civet	12.18	8.50	3.24	0.44	8
Elephant shrew	12.60	7.84	4.37	0.39	8
Photopic/mesopic intermediate	10.20	6.27	3.53	0.42	

[1]Reichenbach et al. (1995a, b), [2]Reichenbach (unpublished data), [3]Syrbe (2007), [4]Görner (2009), [5]Awißus (2007), [6]Reichenbach et al. (1994), [7]Schwarting (2004), [8]Kuhrt (unpublished data), [9]Gentsch (unpublished data), [10]Jeon et al. (1998), and [11]Nauck (unpublished data).

Preliminary definitions: scotopic (<5 photoreceptor cells, close to 1 ganglion cell per column); mesopic (<20 photoreceptor cells, «1 ganglion cell per column); scotopic (>20 photoreceptor cells/column); photopic/mesopic intermediate (~10 photoreceptor cells; «1 ganglion cell per column).

1 cone plus a variable number of rods, (ii) at least three interneurons of the INL (two bipolar cells and one to two amacrine cells), a number which may increase by one cell in cases of strong photopic (and scotopic?) specialization but is fairly similar in such different retinas as that of mouse, rabbit and monkey (Jeon et al.,

Table 2.2 Cellular composition of retinal columnar units of representative mammals, with the main neuronal cell types given (all numbers per one Müller cell)

Cell type	Tree shrew[a]	Rabbit[b]	Mouse[c]
ONL cells	1.7	11.37	27.94
Cones	1.6	*ca.*1	0.77
Rods	<0.1	*ca.*10	27.17
INL cells	4.3	3.75	5.49
Bipolar cells	~3	2.22	2.56
Amacrine cells	~1	1.49	2.74
Horizontal cells	0.03	[0.042]	0.19
GCL cells	1.05	0.31	0.20
Total neurons	7.0	15.43	33.63

[a]Reichenbach et al. (1995d).
[b]Reichenbach et al. (1994).
[c]Jeon et al. (1998).

1998, and references therein), and (iii) one (up to more than two) ganglion cell(s) in photopically specialized retinas, but less than one (as an average, about 0.5) ganglion cell in the other retinas. Thus, such a column is endowed with all elements necessary to constitute a functional unit for "forward transmission" of visual information (cf. Section 1.2.2) in photopic mammalian retinas (or retinal areas). In more scotopically specialized retinas or retinal areas, however, the concept seems to suffer from a "missing half ganglion cell" per unit (Tables 2.1 and 2.2). As will be detailed below (Sections 2.2.4 and 2.2.5), more ganglion cells are generated in ontogenesis than survive in the adult retina; in fact, >50% of all young ganglion cells are eliminated by "physiological cell death" (Farah, 2006, and references therein). This means that probably each columnar unit is primarily endowed with (at least) one ganglion cell; in scotopically specialized retinas where convergence is the dominant principle of wiring (cf. Fig. 1.13) it seems to be "acceptable" if later not every column retains "its own" ganglion cell. Apparently, the number of horizontal cells is much lower than that of the columnar units; in most species, there is only one horizontal cell available for about 25 columns (Table 2.2); this relation is further reduced by the fact that there are two or even three subtypes of horizontal cells which each constitute own mosaics. Likewise, even if one or two amacrine cells belong to each column, the existence of about 30 subtypes of amacrine cells (Masland, 2001, and references cited therein) clearly shows that not every column can contain a full set of amacrine cells. However, this is not in contradiction to the concept of columnar units which provide the forward signalling pathways; lateral (e.g., contrast) wiring by horizontal and amacrine cells makes only sense if performed between several of these units. Similarly, wide-field bipolar and ganglion cell types necessarily involve several or even many of these units, and thus are outnumbered by them by obvious reasons.

Much less quantitative data are available on non-mammalian retinas. As far as can be stated on the basis of the available data, however, the columnar principle

applies to all vertebrate retinas (Reichenbach and Robinson, 1995, and references therein). So it has been shown that proliferation of retinal progenitor cells in amphibians (Wetts and Fraser, 1988) and chick (Fekete et al., 1994) results in radially arranged, columnar clones of daughter cells. Repetitive cellular units have been identified in the fish retina (Mack, 2007). As far as has been studied, Müller cell densities are rather low in non-homeothermic vertebrates. Müller cell densities of 1,500 mm^{-2} (toad) (Gábriel et al., 1993), 1,600 mm^{-2} (turtle) (Gaur et al., 1988), and <5,000 mm^{-2} (cichlid fish) (Mack, 2007) have been counted. This seems to reflect a large number of neurons per columnar unit and, thus, per Müller cell. In the toad, >80 neurons per Müller cell can be calculated from the available data (Gábriel et al., 1993). In the cichlid fish retina, the lifelong addition of new rods to the columns (cf. Section 2.2.4) causes a continuous increase of this ratio, from about 54 neurons per Müller cell in young fish to >67 in older fish (Mack et al., 1998). It may be speculated that the metabolic activity of neurons in non-homeothermic vertebrates is lower than that in birds and mammals and that this lower metabolic "load" of the adjacent Müller cell may allow them to support larger units.

Generally in unspecialized, "prototype" retinas of early vertebrates, rather oligocellular columnar units might have been consisted of one Müller cell and one or two cones, one rod, about three interneurons, and (less than) one ganglion cell (Fig. 2.16). From this "starting point", the adaption of animals to diurnal vs. nocturnal lifestyles may have enforced retinal specialization towards photopic vs. scotopic performance, leading to either (i) enhanced numbers of cones (or cone subtypes), interneuron (subtypes), and ganglion cells per unit (photopic), or (ii) enhanced number of rods and rod-specific interneurons per unit (scotopic). Besides the primate fovea centralis, some reptilian and avian retinas show extreme photopic specialization, by displaying up to seven different types of cones (four different visual pigments plus various types of coloured oil droplets; 40–100% of the photoreceptor cells being cones) and up to 6–8 times more interneurons in the INL than photoreceptors in the ONL. At the opposite extreme, retinas of nocturnally specialized mammals as well as deep-sea fish are dominated by rods (98–100% of the photoreceptor cells) and contain up to 6–8 times less interneurons in the INL than photoreceptors in the ONL (Fig. 2.16; for reviews see Walls, 1963; Reichenbach and Robinson, 1995; Lamb et al., 2007).

These quantitative data support two conclusions. First, throughout the vertebrates every Müller cell forms the core of a columnar arrangement of retinal neurons which, in turn, forms the smallest functional unit of forward processing of visual information. This means that probably the Müller cell is responsible for all functional and metabolic interactions with this particular set of ("its") neurons. This means that the Müller cell population is essential for the function and integrity of the repetitive units. Moreover, labeled/stained Müller cells can be used to study the functional topography of the retina (see Fig. 2.6) as well as of developmental growth/expansion processes of the retinal tissue (Section 2.2.6; Fig. 2.25b). Second, the cellular composition of the columnar units may differ greatly among diverse species and even within, for instance, the primate retina (Fig. 2.16). This means

that different Müller cells may be subject of very different functional and metabolic tasks. It is conceivable that the metabolic load of a voluminous rabbit Müller cell, in charge of 15 neurons, is less than that of a thin, slender mouse Müller cell, in charge of >30 neurons. Such differences might be partially compensated by the presence of an intraretinal vascularization in the murine retina, for instance, but may play a role in determining the vulnerability of retinas under conditions of metabolic challenge including retinal diseases.

2.2.3 A Hierarchy of Retinal Domains

If compared to what is known about hierarchical domains elsewhere in the CNS (Section 1.1.3), the columnar neuronal units are interaction partners of one Müller cell, and thus represent cellular domains. Of course, subcellular domains can be defined, as well. For example, the periaxonal coronae of finger-like processes (Fig. 2.12), the perisynaptic sheaths (Fig. 2.3a) and even the perisomatic "honeycombs" (Fig. 2.3b, c) constitute sites of rather autonomous interactions between a part of the Müller cell and a distinct neuronal element. At the other end of the scale, the entire Müller cell population of a retina forms a large macrodomain, as it interacts with virtually all retinal neurons. If only a small local retinal area is activated by a light stimulus (or by a pathological damage), the Müller cells within this area form a distinct activated domain, due to (i) simultaneous signaling from the activated neurons (cf. Section 2.7) or from the common pathogenic stimulus, as well as (ii) glia-to-glia signaling via (hitherto unknown) extracellular signaling pathways (e.g., Humphrey et al., 1993; Francke et al., 2005) or, in some instances, via gap-junctional coupling (see Section 2.1.7). Thus, the retina is no exception to the general rule that CNS tissue consists of a wealth of hierarchically organized but functionally variable domains (see Fig. 2.17). The developmental mechanisms of this organization principle will be described in Sections 2.2.4, 2.2.5, 2.2.6, and 2.2.7, its physiological and pathological consequences will be subject of the subsequent chapters of this book.

2.2.4 Retina Development I: Cell Proliferation, Progenitor Cells, and Radial Glia

After neural induction and genetic determination of the future retina within the neural plate (cf. Section 1.2.1, Figs. 1.8, 1.9, and 1.10) (Reichenbach and Pritz-Hohmeier, 1995; Lamb et al., 2007) including specification of the retinal topography in respect to dorsal vs. ventral, nasal vs. temporal, and center vs. periphery (e.g., Peters and Cepko, 2002, and references therein), the identical replication of pluripotent retinal progenitor cells causes an increase in the area of the future retinal tissue (Fig. 2.18). As the duration of the cell cycles does not differ greatly between the species (at least, among homeothermic animals), it is mainly the number of consecutive cell cycles that determines the size of the future retina and eye. Roughly, this correlates with the duration of gestation and, thus, with body weight and size of the

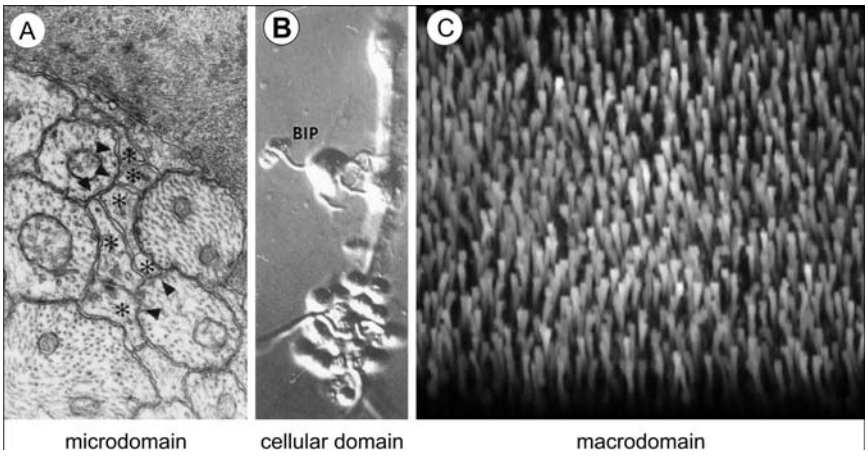

Fig. 2.17 Ascending hierarchic levels of glial domains involved in glia-neuron interactions. (**a**) example for a microdomain, consisting of a few finger-like end branches which interact with the node-like specialization of a ganglion cell axon; (**b**) cellular domain, consisting of an entire Müller cell interacting with the neurons of "its" columnar unit; and (**c**) a macrodomain, consisting of a large population of Müller cells, together interacting with the (light-stimulated) neurons and the intraretinal blood vessels of a given retinal area. (**a**) Transmission electron micrograph of a tree shrew retina; modified from Reichenbach et al. (1995d); (**b**) Group of unstained cells enzymatically dissociated from guinea-pig retina, Nomarski optics, BIP, bipolar cell; original (courtesy of J. Grosche, Leipzig); (**c**) 3D reconstruction of a series of confocal images of a guinea-pig retina, Müller cells visualized by vimentin immunohistochemistry, original (courtesy of J. Grosche, Leipzig)

species, in eutherian mammals. However, there is no constant relation between retinal area/eye size and body size, even among closely related primates (Finlay et al., 2005). Obviously, the number of the cell cycles of these pluripotent progenitor cells is under genetic control, generating the striking differences between the extremely small (but otherwise well-organized) eye and retina of the mole (Glösmann et al., 2008) and the large eye and retina of the giraffe (Schiviz et al., 2008), for example. Cell cycle mutants in zebrafish display small eyes (microphthalmia); the proto-oncogene, N-myc, has been shown to the involved in the control of retinal progenitor cell proliferation and eye size in the murine retina (Martins et al., 2008).

Once the future retina is determined in size, (the majority of) the proliferating cells restrict their potency to become so-called early retinal progenitor cells (Reichenbach, 1993; Reichenbach and Robinson, 1995). Like their precursors, these early retinal progenitor cells are elongated bipolar cells; their nucleus undergoes "interkinetic migration" (Baye and Link, 2007) within the elongated tubular cytoplasm that spans the thickness of the neuroepithelium between the reminder of the optic ventricle (which later becomes the subretinal space; the "ventricular zone") and the basal lamina bordering the future vitreous body. The nuclei spend the S-phase (DNA replication) distant from the ventricular zone but move to this zone

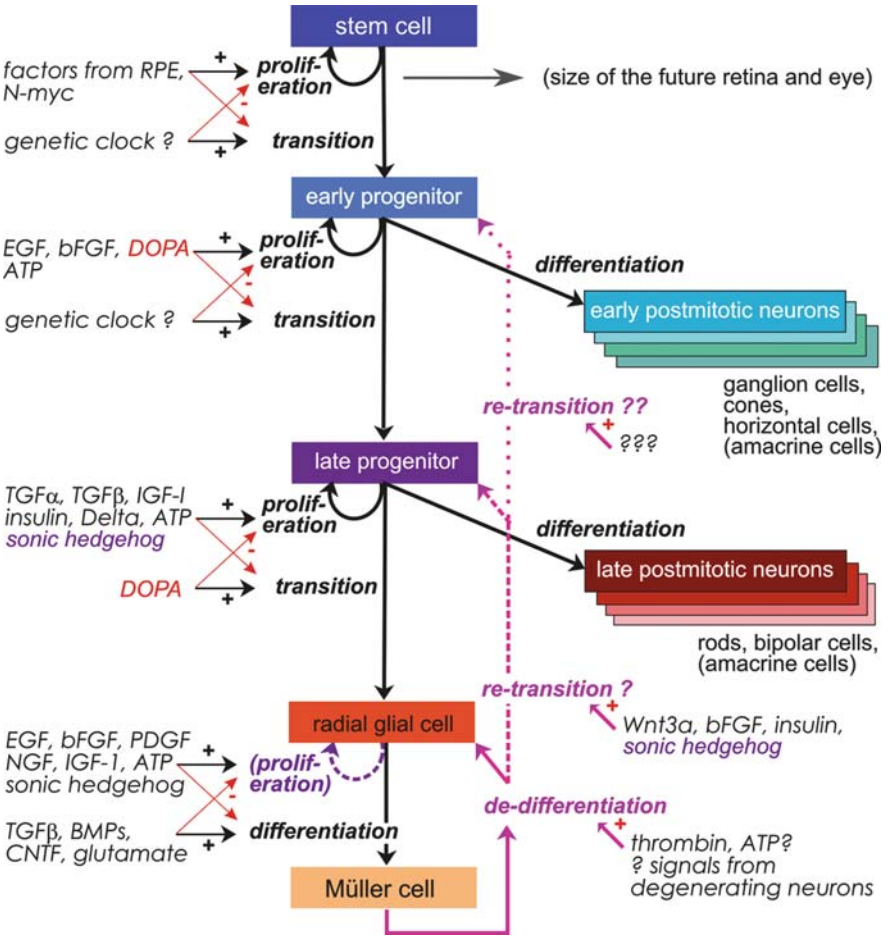

Fig. 2.18 Schematic flow-diagram of cytogenesis in the mammalian retina. After a phase of identical replication of retinal stem cells, a stepwise transition occurs via to early to late progenitor cells and, finally, radial glial cells which is accompanied by distinct restrictions/changes of potency (*thick black arrows*). The duration of each proliferation phase (i.e., the number of cell divisions) until transition to the next step is tightly controlled, in a species-specific manner, by a variety of factors (some of the hitherto-known factors are given at the left side). This allows a subsequent determination of (i) the size of the future retina and eye (stem cells; very variable), (ii) the contribution of primary photopic cells (early progenitors; not very variable), and (iii) the addition of complementary bipolar and amacrine cells (not very variable) and rod photoreceptor cells (very variable) by the late progenitors. There appear to be some key regulators that modulate the relation between early and late neuron production (e.g., DOPA and sonic hedgehog). One of the daughter cells of the late progenitor cells becomes a radial glial cell which normally differentiates as a Müller cell without further proliferation. Under pathological conditions (*thick red arrows*), however, Müller cell may de-differentiate into radial glial cells, and undergo proliferation. Under experimental conditions, even a re-transition to late progenitors has been induced whereas a re-transition into early progenitors was not yet achieved in mammals. Modified after Reichenbach et al. (1998); for further details, see Sections 2.2.4 and 3.1.4. Although not indicated in this figure, the cell type specification/ratio of the neuronal progenies of both early and late progenitors is also controled by signal molecules; the interested reader is referred to Reichenbach et al. (1998), Dyer and Cepko (2001b), Lamb et al. (2007), and others

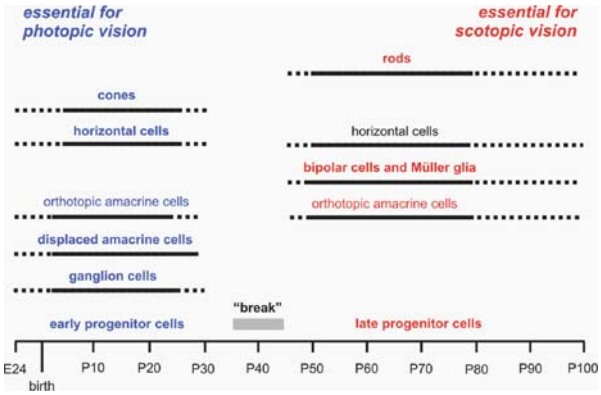

Fig. 2.19 "Birthdating" of the various cell types in the retina of the wallaby. Marsupials undergo an extremely slow ontogenetic development, such that the two subsequent phases of progenitor cell proliferation are even separated by a "break" of almost two weeks. This reveals that most cell types essential for photopic vision (e.g., cones, horizontal cells, and ganglion cells) are generated by early progenitor cells. By contrast, the rods (which are essential for scotopic vision) are generated by late progenitor cells, together with bipolar cells (and a few other cell types). Radial-glia-like cells are present during both phases of proliferation but postmitotic Müller cells result only from the late proliferation. The two phases of cytogenesis overlap considerably in rapidly developing laboratory rodents but the basic pattern appears to be very similar throughout all mammals; as an exception, the late generation of a sub-population of horizontal cells has not been described in eutherian mammals. Modified after Harman and Beazley (1989)

to divide in the M-phase (Hinds and Hinds, 1974, 1979). After commitment, one of the daughter cells becomes postmitotic, and starts differentiation into one of a distinct set of "early-born" retinal neuron types, including ganglion cells, horizontal cells, cones, and certain amacrine cells (Figs. 2.18 and 2.19). The other daughter cell retains the properties of an early progenitor cell, and continues to proliferate. This asymmetric division of the early progenitor cells lasts for a distinct period which (i) appears to be similar throughout the variety of mammals (see below) and (ii) ends by a distinct break in marsupials with their extremely prolonged ontogenesis (Fig. 2.19; Harman and Beazley, 1989); in large mammals with long gestation periods, this break is still indicated (LaVail et al., 1991) whereas in small laboratory rodents the first proliferation phase overlaps considerably with the subsequent proliferation of "late retinal progenitors" (Blanks and Bok, 1977; Young, 1985a, b).

These late retinal progenitor cells generate a different set of retinal cells, mainly rod photoreceptor cells, bipolar cells, (a) subset(s) of amacrine cells, and Müller cells (Figs. 2.18 and 2.19); the generation of some horizontal cells by these late progenitors in marsupials is an exception among mammals. Noteworthy, these asymmetrically dividing late progenitor cells are hardly discernible from the young postmitotic Müller (radial glial) cells which belong to their progeny; both cell types share the bipolar, elongated shape, as well as the expression of a series of proteins including vimentin, nestin, carbonic anhydrase II, and others (Reichenbach, 1993; Zahir et al., 2006, and references therein) (cf. also Section 3.1.4). This causes the

apparent paradoxon that radial glial-like cells are observable throughout most of retinal ontogenesis/cell proliferation but postmitotic Müller cells are (among) the latest cell type(s) to be generated (Morrow et al., 2008). To resolve this dilemma, it has been proposed that the last division of an early progenitor cell generates one young Müller cell plus one of the late-generated neuronal cells (e.g., a rod or a bipolar cell) (Reichenbach and Robinson, 1995) (Figs. 2.18 and 2.19). Indeed, clonal analysis has shown that the progeny of late progenitor cells often contains one (and never more than one) Müller cell, and that their last division may generate one Müller cell and one rod or one bipolar cell (Turner and Cepko, 1987; Reichenbach et al. 1994). Thus, the progeny of every late progenitor cell may constitute the major part of a columnar unit (Reichenbach and Robinson, 1995).

In contrast to the proliferation of the early progenitors which appears to be rather constant in duration, the late progenitor cells may undergo a variable number of cell divisions in different mammals. This appears to be a major mechanism to control the scotopic specialization of retinas in nocturnal mammals (Fig. 2.20) (Reichenbach and Robinson, 1995; Finlay et al., 2005); the more rods are required to guarantee high light sensitivity, the more rounds of division are performed by the late progenitor cells. By contrast, the proliferation of the late progenitors appears to be largely suppressed in the region of the future primate fovea, such that no rods are generated there (La Vail et al., 1991). If quantitative data from many adult mammalian retinas (Tables 2.1 and 2.2) are summarized diagrammatically (Fig. 2.21) it becomes apparent that despite of considerable species differences, the number of cells per

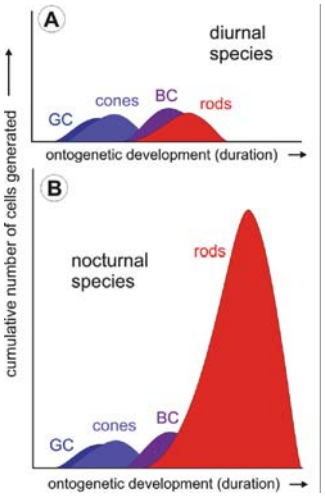

Fig. 2.20 Different retinal specializations (cf. Fig. 2.16) may be achieved by modifying the duration of the proliferation phases of late/early progenitor cells. In diurnal animals, both phases are rather short, which results in a small number of neurons per columnar unit, and a cone-to-rod ratio of one or more. In nocturnal animals, the proliferation of the late progenitors occurs over an elongated period which results in an enhanced number of rods per column. Modified from Finlay et al. (2005)

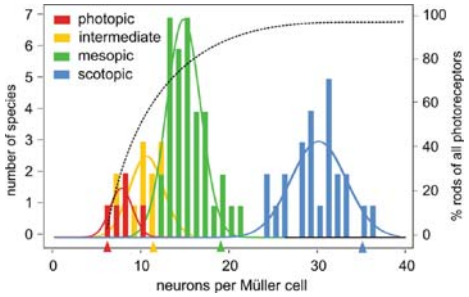

Fig. 2.21 The number of neurons per columnar unit (i.e., the neuron-to-Müller cell ratio) does not vary stochastically among various different mammalian retinas; rather, distinct groups can be identified. This is compatible with the hypothesis that every step towards more scotopic sensitivity (i.e., a higher proportion of rods) requires an additional round of cell divisions of the late progenitor cells (cf. also Table 2.1 and Fig. 2.22). With increasing neuron-to-Müller cells ratios, the percentage of rods increases concomitantly (*dotted line*). The arrowheads mark duplications of the cell numbers generated by the late progenitors, according to the hypothesis shown in Fig. 2.22. Noteworthy, the actually counted numbers of cells in the adult retinal columns must be smaller than the hypothetical number of cells generated during ontogenesis, since a considerable part of cells die by so-called "physiological cell death". Modified, by adding many new data, after Reichenbach and Robinson (1995)

columnar unit does not vary randomly. Rather, there occur distinct peaks at about 8–10, about 14, and ca. 30 neurons per Müller cell (Fig. 2.21). This fits well with the assumption that the two phases of retinal cytogenesis are differentially regulated, with an early constant phase, generating a "uniform" set of (photopic) neurons, and a late variable phase, generating the necessary bipolar (and amacrine) cells plus rod photoreceptors, the number of which latter roughly doubles with every additional round of cell divisions, and one Müller cell (if comparing the real peaks of cell numbers in Fig. 2.21 with the numbers expected by the theory – Figs. 2.21 and 2.22 – it must be kept in mind that "physiological" cell death causes a reduction in the number of surviving cells). After a few of these late divisions, the number of rods dominates the number of neurons per column (e.g., more than 80% of retinal cells are rods in nocturnal rodents; Tables 2.1 and 2.2) such that the number of neurons per column also almost doubles with the last divisions of the late progenitors (Tables 2.1 and 2.2; Figs. 2.21 and 2.22). Recently, several signalling molecules have been identified which can modify the number of cells and the balance between the cell types generated by the late progenitor cells (Dyer and Cepko, 2000b, 2001a, b; Dyer, 2003; Wallace, 2008; Ohsawa and Kageyama, 2008; Lamb et al., 2007; and references therein). It has long been known that in albinotic humans in whom the melanin/DOPA metabolism is impaired, the fovea centralis is missing and rods are generated in the central retinal area where the fovea would occur (Usher, 1920; Kinnear et al., 1985; and references therein). This fits with the observation that DOPA can inhibit the proliferation of late progenitor cells (Ilia and Jeffery, 2000) (Fig. 2.18).

In summary, (i) distinct, species- (and retinal area-) specific mechanisms of early and late progenitor cell proliferation determine the size and the composition of the

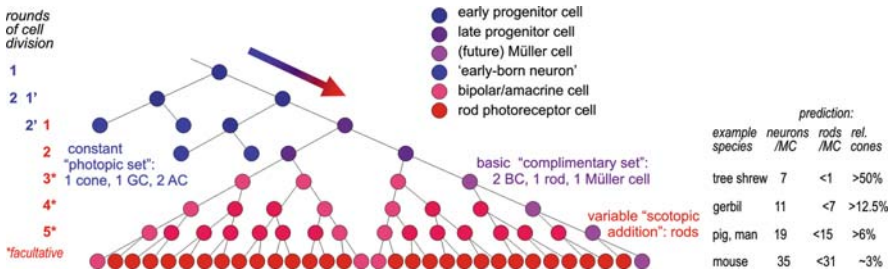

Fig. 2.22 Hypothetical sequence of cytogenesis in various mammalian retinas. A functional retina with all basic constituents is first achieved after each two rounds of cell division of the early and late progenitor cells. The early progenitor cells generate a constant set of neurons involved in photopic vision (1 cone, 1 ganglion cell = GC, about 2 amacrine cells = AC, and rarely an horizontal cell instead of an AC; on average some 0.04 horizontal cells per unit). The first two rounds of cell division of the late progenitor cells generate a "complementary" set of cells necessary to complete the basic retinal cell types, including on average 2 bipolar cells (BC), one rod (or one amacrine cell instead of a BC or rod), and one Müller cell. This results in a cone-dominant retina with small columnar units (about 7 neurons per Müller cell), similar as found in tree shrews and squirrels. Very probably, this sequence of cytogenesis is shared by all mammals. To increase the light sensitivity of a retina, cell division of the late progenitor cells continues for one, two, or three additional rounds. Whenever this late proliferation ceases, the postmitotic cells differentiate into the above-mentioned "complementary set" of cells (1 Müller cell, $\geq$ 2 bipolar cells, $\geq$ 1 amacrine cell) plus a number of rods which increases with each round of cell division. Thus, after three additional rounds of late progenitor cell division, a scotopically specialized retina is achieved, with large columnar units of about 35 neurons per Müller cell, such as in the mouse and other nocturnal species. Still each unit contains 1 cone, 1 GC, 2–3 amacrine cells, $\geq$ 2 bipolar cells, and an average of 0.04 horizontal cells (as any mammalian retina) but it is dominated by a large number of rods (up to 31). If these predicted numbers are compared to real cell counts in the retinas of various species (e.g., Table 2.1 and Fig. 2.21) it must be kept in mind that (i) "physiological" cell death may reduce the number of cells in the adult retina (by more than 50% in the case of ganglion cells!) and (ii) in the primate fovea, an additional round of division of the early progenitor cells cannot be excluded at the present state of knowledge. Modified after Reichenbach and Robinson (1995)

columnar units, (ii) Müller (radial glial) cells are closely related to (at least, late) progenitor cells, (iii) Müller cells are the "siblings" of the late-generated neurons in "their" columns, and (iv) radial glial (Müller) cell-like cells are present throughout most of the developmental stages of the retina.

2.2.5 Retina Development II: Cell Differentiation and Migration – Layers and Mosaics

It has already been mentioned that interkinetic cell nucleus migration occurs in both early and late progenitor cells, and that thus all cells are born at the ventricular surface of the retina. Ganglion cells which are the first cell type born in virtually all retinas studied so far, start their differentiation by extension of a radial process towards the inner basal lamina, and by the movement of their nucleus within this process up to an inner position close to their final destination (similar as the progenitors do to start the S-phase). However, eventually they withdraw their

external (ventricular) cell process, and start to grow an axon along the endfeet of the radial glia/progenitor cells, towards the future optic nerve (Hinds and Hinds, 1974). As the retinal neuroepithelium is rather thin during this early developmental stage, and merely consists of parallel tubular cells spanning the epithelium, the young ganglion cells do not need any specific aid or guidance for this translocation from outer to inner retina. Early-born horizontal cells translocate their somata in a similar way, but over a shorter distance (Hinds and Hinds, 1979). The cones, as another type of early-generated cells, just reside at the very ventricular surface where they were born, and do not need to migrate at all.

The later-born bipolar and amacrine cells are confronted with another situation; now, the retinal neuroepithelium became thicker, and is crowded with many proliferating as well as with early-differentiating cells which latter grow processes not in parallel to the radial "palisades". In order to achieve at their final destination, the (future) inner nuclear layer, they may need a "climbing guidance" provided by the progenitor/radial glial cells (Meller and Tetzlaff, 1976). Very probably, they use their "sibling" radial glial (Müller) cell as a climbing pole (Reichenbach et al., 1994) (Fig. 2.23); this may also apply to (some of) the young rod cells which need to move their soma by up to more than 150 μm. If such "sibling groups" of young neurons migrate together along the same radial glial/progenitor cell process, their leading and training processes will touch each other frequently, and may later form synapses among each other with high probability. This may support the formation of

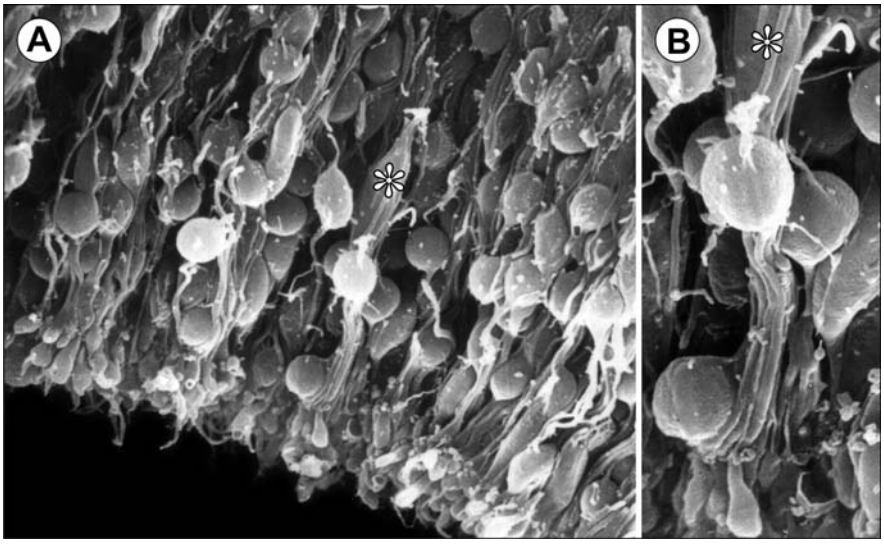

Fig. 2.23 Radial glial/early Müller cells in the developing retina. Scanning electron microphotographs of the ONL of a rabbit retina at postnatal day 4, magnification × 3,100 (**a**) and × 8,600 (**b**), respectively. The asterisk marks an elongated cell body probably belonging to a young Müller cell. It outer process and soma are surrounded by several processes of young (rod or bipolar?) neurons, suggesting that these migrating cells use the radial glial cell process as climbing pole and guide. Modified from Reichenbach et al. (1989a)

functional units by such columnar arrangements of cells. The radial glial cell processes may also be used as guides by early-born cells. For instance, horizontal cells perform a late "backward" migration towards the outer margin of the inner nuclear layer (Scheibe et al., 1995) for which they may use these processes as guidelines. As another example, the growth of ganglion cell dendrites into the inner plexiform layer is facilitated by Müller cell inner processes and somata (Bauch et al., 1998) similar as the extension (and retraction) of photoreceptor (Johnson et al., 1999) and bipolar cell axons may be guided by the radial glial cell processes.

Once all cell types arrived in their respective layers of destination, they form synapses with the appropriate partner cells, and the two main synaptic (plexiform) layers form between the three nuclear layers. This process contributes to the formation of retinal mosaics. The term "retinal mosaics" describes the regular arrangements of the populations of retinal cell types; the members of distinct types of ganglion cells, for instance, are regularly spaced such that every retinal area is "covered" by the dendritic tree of (at least) one of the cells; the so-called "coverage factor" may vary for individual cell types from close to 1 up to >4 (Wässle and Riemann, 1978; Cook and Becker, 1991; Scheibe et al., 1995). In some sense, the Müller cells and their accompanying late-generated neurons also form a mosaic; this is explained by the above-described processes of cell generation and migration. However, the early-generated neurons are born before the late progenitors form the "columns of siblings", and thus are not necessarily arranged in accordance with these (Reese et al., 1995, 1999; Reese and Tan, 1998; Fekete et al., 1994). Obviously, these neurons (i.e., cones, ganglion cells, and horizontal and amacrine cells) are spaced by (an)other mechanism(s), probably via contact- or near distance-inhibition of the generation and/or differentiation of the same cellular (sub-) type (Scheibe et al., 1995; Galli-Resta et al., 1999, 2008, and references therein). Thus, although not generated at the same time and not spaced by the same mechanism, densely arranged early-born neurons such as the cones basically display the same arrangement as the columns of late-generated cells (Fig. 2.24); it has been shown that there is roughly one cone per Müller cell throughout the mammalian retinal diversity (Reichenbach and Robinson, 1995) (Table 2.2). Similarly, there may be roughly one ganglion cell per Müller cell early in retinal development; later on, in scotopically specialized retinas (or retinal areas) more than half this population is extinguished by "physiological cell death" (Hughes and McLoon, 1979; Bähr, 2000). This mechanism seems to be much less dominant in other retinal cell types, such that the spatial density of horizontal cells, and of special subtypes of amacrine and ganglion cells, is much lower than that of the columnar units from the very beginning of retinal cell generation.

In summary, (i) radial glial (Müller) cell–like cells constitute guidance aids for migration and cell process growth of (particularly but not exclusively their "sibling") neurons (ii) "sibling groups" of late-generated neurons migrate together and preferentially form synapses in "their" columns, and (iii) spacing of regular mosaics of cells of a given cell type occurs independently in early- and late-born neurons but fit together when cellular densities are high enough; thus, (iv) Müller cells form the cores of functional units consisting of (several) late-generated and

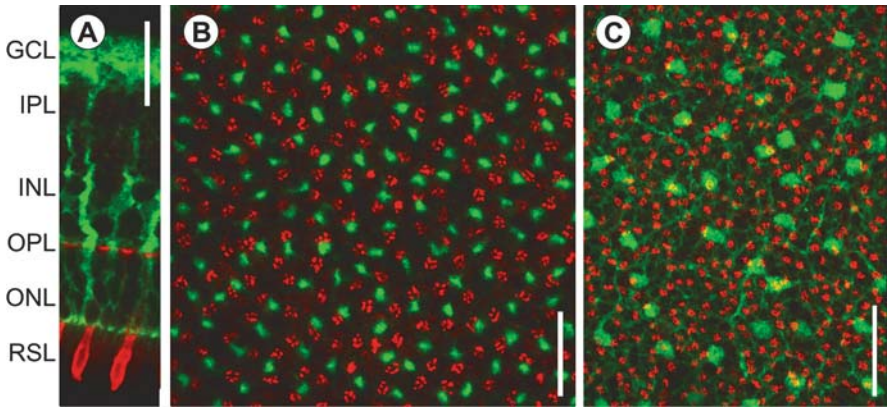

Fig. 2.24 Early- and late-born retinal cells join and (re-)arrange to form common mosaics. (**a**, **b**) The early-born cones adjust their final (micro-) topographical location such as to fit into the pattern of the late-born "columnar unit cells" (rods, bipolar, and some amacrine cells) along the central Müller cell. Images (**a**) and (**b**) were taken from a guinea-pig retina, by a confocal microscope. (**a**) Radial section; Müller cells were immunolabeled for vimentin (*green*), cones were labeled by peanut agglutinin (*red*). The red cone inner segments in the photoreceptor segment layer (RSL) appear as "continuous" with the outer processes of Müller cells in the outer nuclear layer (ONL) which envelop the cone cell somata. (**b**) Wholemount, focus on the outer plexiform layer (OPL). The number of cone pedicles (*red*) roughly equals that of Müller cell processes (*green*); often the two elements even appear as pairs. (**c**) The wide-field neurons arrange their dendritic fields in regular mosaics such that each cell covers and integrates a very similar number of "forward-processing" columnar units. Double-staining of cone pedicles (*red*: peanut agglutinin label) and horizontal cells (*green*: calbindin immunohistochemistry) in the wholemounted mouse retina. GCL, ganglion cell layer; IPL, inner plexiform layer; INL, inner nuclear layer. Calibration bars, 20 μm (**a**, **b**) and 50 μm (**c**), respectively. (**a**, **b**), Original (courtesy of E. Ulbricht, Leipzig); (**c**) modified from Wässle et al. (2009)

(a few) early-generated retinal neurons; (v) "lateral information processing" by horizontal and amacrine cells with their large dendritic fields computes the "forward signaling-information" of several (to many) columnar units.

2.2.6 Retina Development III: Late Shaping Processes – Retina Expansion and Foveation

Once cell proliferation ceased, and the retinal layers and mosaics are formed, the shaping of the retinal tissue continues. As a main mechanism, there occurs a considerable expansion of the retinal surface area, together with growth of the eyeball, *after* cessation of cell generation (Fig. 2.25a). As no new cells are generated, and as cell death is negligible during later postnatal development, constant populations of retinal cells become re-distributed within a larger surface area – which means that cellular densities must decrease. This is indeed the case; in the peripheral rabbit retina for example, cellular densities decrease between postnatal day 9 and adulthood by a factor of almost 4, i.e., for Müller cells from >30,000 to ca. 8,000 mm^{-2} and for A-type horizontal cells from ca. 350 to <100 mm^{-2} (Reichenbach et al.,

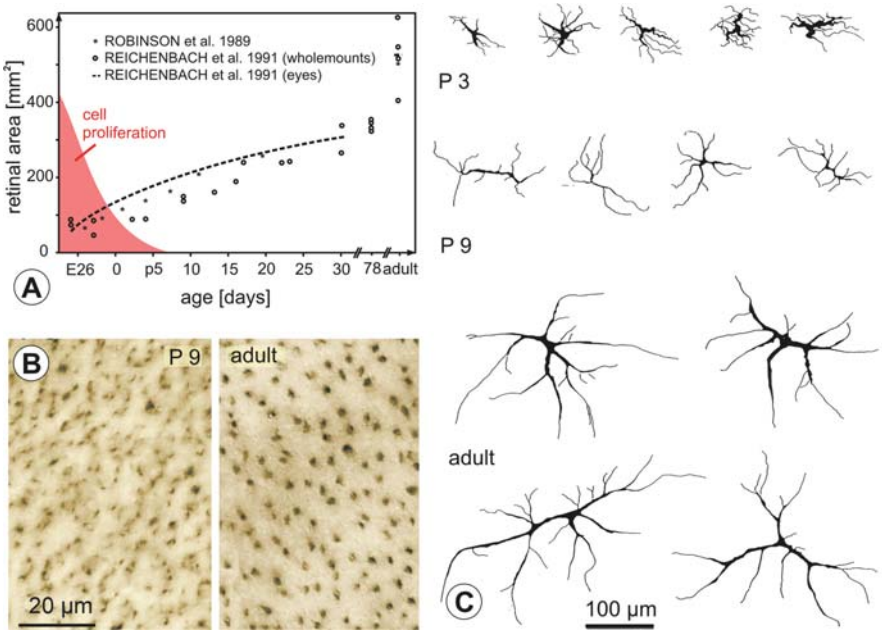

Fig. 2.25 "Active" and "passive" growth of the retina; all data from rabbit. (**a**) The surface area of the retina increases 4-fold even after cessation of cell proliferation which means that the existing cells are re-distributed within a larger area. (**b**) As Müller cells do not proliferate in the healthy retina, they constitute a constant population which is re-distributed (i.e., spatially separated) in the expanding retina. Accordingly, their spatial density decreases (vimentin immunohistochemistry of retinal wholemounts). (**c**) Much of the postnatal cell process elongation of horizontally-wired interneurons occurs parallel to the local expansion of the retinal area which allows the cells to maintain their synaptic contacts to other cells (e.g. photoreceptors) which become spatially separated by this tissue expansion. Camera-lucida drawings of horizontal cells in Golgi-stained wholemount preparations; the basic dendritic pattern and synaptic contacts of the cells are established shortly after postnatal day (P) 3; thereafter, the overlap factor of the dendritic fields of the cells remains constant because the length of their dendrites keeps space with the local tissue expansion. (**a**) modified after Reichenbach et al. (1991a); (**b**) modified from Reichenbach et al. (1991b); (**c**), modified from Scheibe et al. (1995)

1991b; Scheibe et al., 1995). Noteworthy, the degree of retinal expansion is not uniform across the retinal topography. Retinal areas which are responsible for high acuity-vision in the mature retina (area centralis, visual streak) expand less than the retinal periphery such that the neonatal high cell densities are (not maintained, but) reduced significantly less than in the periphery (cf. Fig. 2.6). As the Müller cells constitute a constant population after cessation of cell birth, and as they cannot move laterally within the tissue for obvious morphological reasons, labeled Müller cells in retinal wholemount preparations can be used as "markers" to study the local tissue expansion during postnatal development (Reichenbach et al., 1991a–c) (Fig. 2.25b).

The basic mechanism of this postnatal retina expansion has been described as a continuous series of stretching and "after-grow" processes, according to the balloon model of Mastronarde et al. (1984) (Fig. 2.26a). The driving force is the intraocular

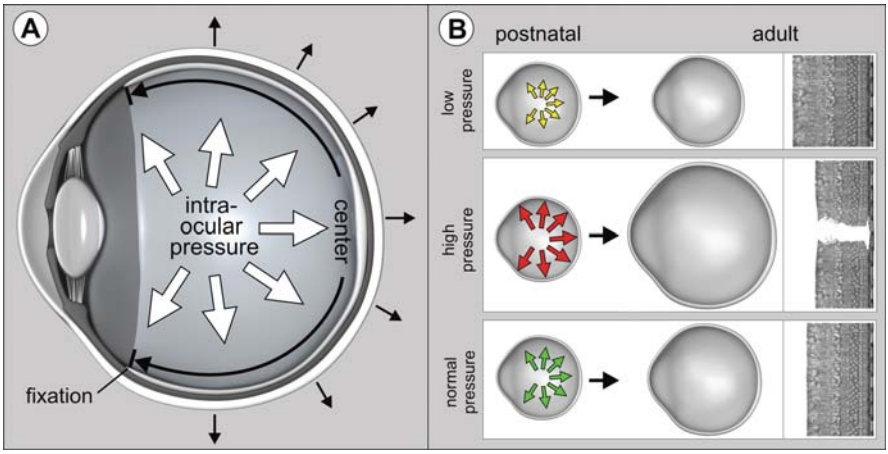

Fig. 2.26 "Passive" growth of the eye and the retina. (**a**) "Balloon model" of the growing eye where the intraocular pressure is the driving force, and the biomechanical resistance of the sclera is the limiting factor, of ocular enlargement. The retina is fixed to the underlying tissues only at its anterior margin, and becomes "passively" stressed – and stretched according to its local biomechanical resistivity – by the enlarging eyeball. (**b**) Semi-schematic depiction of the consequences of different intraocular pressure levels on ocular size and retinal thickness. Low pressure causes sub-normal eye and retina expansion, which allows the retina to remain rather thick. The same would result from elevated scleral stiffness. High intraocular pressure (or scleral weakness) causes supra-normal eye and retina expansion; the retina becomes thinner than normal, and may even be disrupted (for instance, in cases so-called buphthalmia/malign myopia). For normal development of retinal thickness, see Fig. 2.27. Originals (courtesy of J. Grosche, Leipzig)

pressure; if it is relaxed by inserting an open tube into the interior of the developing eye, growth of the eyeball is greatly reduced (Coulombre, 1956). By contrast, the eyeball grows excessively if the inner ocular pressure is elevated during early glaucoma (Link et al., 2004) (Fig. 2.26b). The resistance limiting ocular expansion is provided by the sclera. If the developing sclera follows the intraocular pressure and the ocular cavity thus enlarges, the retina (fixed to the underlying ocular wall only at its anterior margin where the transition into the RPE occurs; cf. Fig. 1.10) is passively stretched like a glove by the fist (Mastronarde et al., 1984). Local differences in retinal stretching correspond to local differences in retinal stiffness (Kelling et al., 1989; Reichenbach et al., 1991c). The future area centralis (or visual streak, respectively) represents a "developmentally advanced area" (Robinson, 1991) where the cells had been born and differentiated earlier, and thus the cell processes are more elaborated, interwoven, and synaptically interconnected than elsewhere in the retina. This may contribute to the enhanced resistance against mechanical stretching in these areas which causes less local tissue expansion after application of identical mechanical load (Reichenbach et al., 1991c).

It is noteworthy that local growth of the sclera and the eyeball is under control of retinal circuits. This is necessary in order to achieve and/or to maintain visual acuity, in a process called emmetropization (Wildsoet, 1997). If the optic apparatus of the growing eye fails to project a sharp image onto the retina, certain amacrine cells trigger a – hitherto widely unknown – signalling cascade towards the underlying sclera

which stimulates the expansion of the globe; in mammals this seems to involve a decrease of the mechanical resistance of the sclera against the inner ocular pressure whereas in the chicken active growth processes in the sclera seem to dominate. Excessive eye elongation due to this mechanism is called "form deprivation-induced axial myopia" (Wiesel and Raviola, 1977; Feldkämper and Schaeffel, 2003). Müller cells may potentially be involved in these regulatory mechanisms, for two reasons. First, there is a long distance between the inner retina (the site of the "sensoring" amacrine cells) and the sclera (the subject of regulation); Müller cells span at least a part of this distance – from inner to outer retina – and are principally well-suited to transport signals over this distance. Second, Müller cells can sense mechanical load of the retinal tissue, and respond to stretching by transient intracellular Ca^{2+} rises, expression of early immediate genes, and increased production of basic fibroblast growth factor (bFGF) (Lindqvist et al., 2009). bFGF has been shown to counter-act the development of form deprivation-induced axial myopia (Rohrer and Stell, 1994). Thus, Müller cells may prevent retinal over-stretching in the course of postnatal eye growth.

What are the consequences of differential retinal stretching for retinal tissue and cells, the columnar units, and the mosaics? First, the stretched retina becomes thinner (Fig. 2.26b). This is no simple mechanical effect like in a stretched rubber band; rather, the cells become re-arranged because there is more space now for them, and the "crowding" is relieved. Accordingly, the number of stacks in the nuclear layers is reduced, and these layers become thinner (Fig. 2.27). By contrast, the thickness of the plexiform layers remains unchanged, or even increases (particularly, in the central retinal areas) due to further elaboration of the synaptic circuits and increasing diameters of the cellular processes (Fig. 2.27). When the retinal thickness decreases (and the retinal area increases) the Müller cells become shorter and thicker (Figs. 2.5, 2.14c, 2.25b, and 2.27) while their cell volume increases. Simultaneously, the columnar units become shorter in the radial direction but increase in diameter; this is accompanied by a re-arrangement of the neurons around the "core Müller cell". Apparently, the somata/nuclei of all rods belonging to a columnar unit are first stacked over each other like the pearls in a chain. Then later during retina expansion, the innermost somata "sink down" along the Müller cell outer process such that the rod somata finally form two or more shorter chains around the central axis of the unit. Noteworthy, the constituents of a columnar unit do not change during this re-shaping (Reichenbach et al., 1994), i.e., "all siblings stay together".

The mosaics of many of the wide-field cells change accordingly (Fig. 2.25c). "Active" growth of their dendrites occurs during a fast, short "burst" during the perinatal period (e.g., in the rabbit retina the A-type horizontal cells between the 3rd and 9th postnatal day; Fig. 2.25c; Scheibe et al., 1995). Thereafter, the basic synaptic contacts to their appropriate partner cells are established, and further expansion of the dendritic fields occurs together with the locally expanding retinal tissue area, by the same factor of areal expansion – probably to very maintain these established synaptic contacts. A similar observation has been made for alpha-ganglion cells of the rabbit retina (Deich et al., 1994) although the periods of "active" and "passive" dendritic growth may greatly overlap in some types of retinal ganglion cells

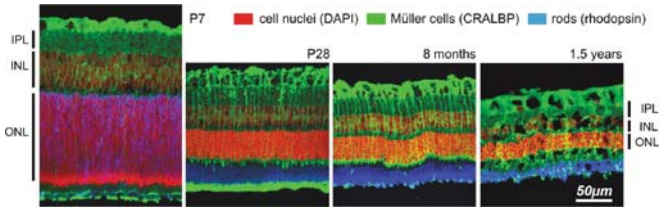

Fig. 2.27 "Passive" retinal expansion causes a thinning of the retina; immunohistochemical triple stainings of rabbit retinas at several developmental stages. While the cells become less restricted in space due to the tissue expansion, they re-arrange their stacking mode which reduces the thickness of the nuclear layers despite the cells slightly increase their size. At postnatal day (P) 7 for instance, all rods belonging to a columnar unit (about 10) are stacked on top of each other such that the outer nuclear layer (ONL) is 10 rows thick. Two weeks later, the retinal surface area has roughly doubled (cf. Fig. 2.25a) and the rod nuclei now are redistributed into two stacks per unit; consequently, the thickness of the ONL is now reduced to 5 rows. One and a half year later, another re-arrangement must have been enabled by further retinal expansion (cf. Fig. 2.25a); the thickness of the ONL is now at 2–3 rows which means that the rod nuclei of a unit now form three stacks around the outer process of "their" Müller cell. In a similar manner, the neuronal cell somata in the inner nuclear layer (INL) become re-arranged during this tissue expansion. Noteworthy, (i) the rod nuclei form straight radial chains throughout all these changes, and (ii) the synaptic layers (e.g., the IPL, inner plexiform layer) hardly become thinner (and may even increase their thickness in the central retina), probably due to continuous elaboration of the synaptic wiring; likewise, the photoreceptor inner and outer segments hardly change in length after they become mature in the second week of life. As a peculiarity in the rabbit retina, the nerve fiber layer within the area of the "medullary rays" increases much in thickness during postnatal development, due to myelination of the ganglion cell axons (not shown). Original (courtesy of M. Gryga, Leipzig)

(Dann et al., 1988; Wong, 1990). This means that in many instances the partnering columnar units of wide-field neurons are constant during retinal expansion but in other instances new partners are acquired, the receptive fields increase, and considerable synaptic plasticity is required even during normal postnatal development. It has been argued that the particular softness of the Müller cell processes within the two synaptic layers supports the (re-)growth of neuronal cell processes and, thus, synaptic plasticity (Lu et al., 2006) because growing neurites prefer soft substrates (Discher et al., 2005).

Noteworthy, the above considerations describe the situation in the retinas of mammals (as well as birds, and, probably, reptilians). In fish and amphibian retinas, there occurs a similar "passive" expansion of the eye and retina but in addition, new retinal cells are added at the retinal margin lifelong (Stenkamp, 2007). Thus, in these animals mainly the "old", central retina is "stretched" whereas the far periphery enlarges by proliferation of progenitor cells and differentiation of new retinal tissue. An even more peculiar case is found in fish retinas. Throughout the lifespan of these animals, new rod photoreceptor cells are inserted into the expanding "old" central retina, in order to keep the density of rods (and, thus, retinal light sensitivity) constant despite of retina expansion (Raymond Johns and Fernald, 1981; Fernald, 1989). This means that the number of rods per – otherwise unaltered – columnar unit increases lifelong, as does the total number of neurons per Müller

cell (Mack et al., 1998). The increased "functional load" of the ageing Müller cells is accompanied by an increased complexity of their morphology and by an increased expression of the enzyme, glutamine synthetase (Mack et al., 1998). This glia-specific enzyme is involved in the recycling of the neurotransmitter, glutamate (cf. Section 2.4.1), the major part of which is released by the rod photoreceptor cells (cf. Section 1.2.2). The new rod cells are generated by asymmetric divisions of so-called "rod progenitor cells" which recently where shown to be Müller cells (Bernardos et al., 2007).

To understand the formation of the *fovea centralis* in the primate retina is a particular challenge (Provis et al., 1998). The region of the future fovea appears to be determined from the beginning of retinogenesis, by the local expression of domain-specifying genes (Reichenbach and Pritz-Hohmeier, 1995; Lamb et al., 2007). It is characterized by (i) enhanced generation of ganglion cells (and other early-born neurons) by the early progenitor cells and/or by inhibition of their "physiological cell death" (i.e., an area of elevated ganglion cell density), (ii) inhibition of the generation of rod cells by the late progenitor cells (i.e., a rod-free area; probably, the late progenitors undergo only two rounds of mitosis to generate two cone bipolar cells, one amacrine cell, and a Müller cell; Fig. 2.22), (iii) expression of repellant activity against the growth of ganglion cells axons (which causes centrifugal growth of the foveal and perifoveal ganglion cell axons, and a missing nerve fiber layer in the foveal center), and (iv) the occurrence of atypical Müller cells not associated with columnar units of retinal neurons (cf. Section 2.1.3; Fig. 2.8). However, the characteristic shape of the fovea develops late, long after determination and after cessation of cell proliferation (Mann, 1950) (Fig. 2.28a). The two main events are a centripetal movement of the perifoveal photoreceptor cells and a centrifugal translocation of the inner retinal layers (accompanied by the formation of the pit or "fovea") (Fig. 2.28b) which together result in a Z-shaping of the local Müller cells (Fig. 2.7d, Fig. 2.28b) because these are embedded in the tissue and must follow its deformation. Likewise, the neuronal cells of the (peri-)foveal columnar units remain attached to "their" Müller cell, and thus (i) the constituents of the columns do not change during this re-shaping (Fig. 2.28b) but (ii) the secondary and tertiary neurons are displaced from the cones providing their sensory input, which requires that (iii) the axons of the cones must be elongated by "secondary, passive" growth from about 5 μm after synapse formation up to more than 250 μm in the adult primate retina, to maintain these synaptic contacts (Perry and Cowey, 1988). The accumulation of these transversally directed processes at the outer margin of the outer plexiform layer – which appears to act as a "sliding zone" between the centripetally moving outer, and the centrifugally moving inner retina – causes the formation of a distinct retinal layer, the so-called Henle fiber layer, between the OPL and the ONL (Fig. 2.29). This layer is formed by a mixture of photoreceptor axons and outer Müller cell processes, which continue to run in parallel during their re-shaping and elongation (Fig. 2.7d). Between the axons of cones in the fovea of macaque retina and the accompanying Müller cell processes, a 1:1 ratio has been counted (Burris et al., 2002). In fact, due to the absolutely parallel course of all cell processes in the Henle fiber layer, immunohistochemically labeled Müller cell

processes (Fig. 2.29) can be used to follow the course of the dislocation of neuronal wiring in the columnar units, and to count their constituents (Syrbe, 2007; Görner, 2009) (cf. Fig. 2.28b).

As already mentioned, the mechanics of foveation are poorly understood. The centripetal dislocation of photoreceptor cells can be explained best. The young cones within the future fovea are rather thick, short cells in a loosely arranged, one-row ONL over a long period (Fig. 2.28a) and have not yet developed outer segments (Hendrickson, 1992). When the inner segments of these cells contract to become more slender and elongated, they must move more closely together, because they are bound to each other – and to the outer Müller cell processes – by adherent junctions (Fig. 2.10). This process will then drag also the perifoveal cones, outer Müller cell processes, and rods towards the fovea. It has been shown that such a rather simple mechanism can account for the observed changes in photoreceptor cell densities in the foveal and perifoveal human retina (Diaz-Araya and Provis, 1992).

If the foveal cone inner segments become very thin (<2 μm in adults) and closely spaced, this must enforce a stacking of the cone somata because their diameter is larger (about 5 μm) (Borwein et al., 1980) and, thus, the formation of thick ONL with up to 5 rows of somata/nuclei (Fig. 2.30b) (Ahnelt et al., 2004). The outer

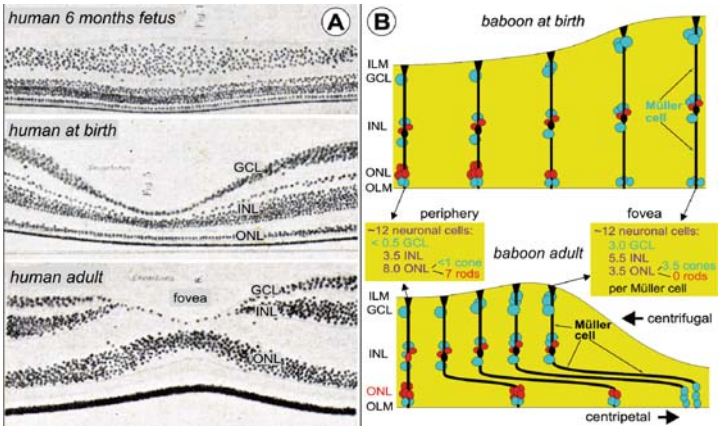

Fig. 2.28 Development of the primate fovea centralis. (**a**) The human fovea develops late and slowly, long after local cessation of cytogenesis. No fovea is visible in the 6 months-old fetus (*top*); rather, the retina is thicker at the place of the future fovea than elsewhere, due to a high density of ganglion cells (and interneurons). At birth, a foveal pit is visible but still all retinal layers can be identified, and the outer nuclear layer (ONL) is constituted by a single row of cone nuclei. It needs several years until the adult situation is established; the mature fovea is devoid of the ganglion (GCL) and inner nuclear layers (INL) but shows a thick ONL which consists of several rows of cone nuclei. (**b**) The process of foveation involves a counter-shift of the inner (centrifugal) vs. outer retinal layers (centripetal). Using vimentin-immunolabeled Müller cells as "markers" of the paths of the neurites (cf. Figs. 2.7d and 2.29) the neuronal elements within the columnar units were counted in retina sections from newborn and adult baboons. Despite of the striking Z-shaped deformation of the central columnar units, the constituents of the columns remained constant (i.e., the cells maintained their mutual interrelationships). Note that central and peripheral units contain a similar total number of neurons although the relative contribution of the cell types differs greatly. (**a**) Modified from Mann (1950); (**b**) Modified after Finlay et al. (2005)

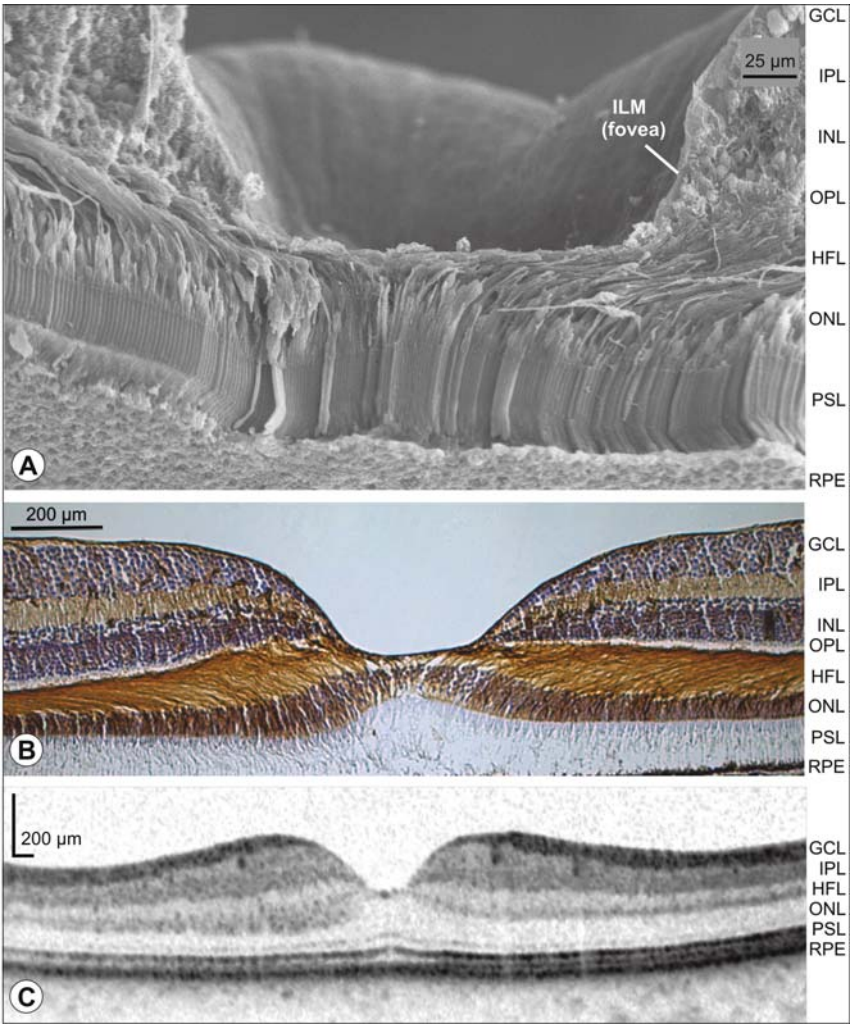

Fig. 2.29 Shape and cellular organization of the mature primate retina. (**a**) Scanning electron microphotograph of the fovea of a macaque monkey. The extremely high packing density of cone inner and outer segments in the photoreceptor segment layer (PSL), the complex centrifugal course of their axons crowded in the Henle fiber layer (HFL), and the absence of the ganglion cell (GCL), inner plexiform (IPL), inner nuclear (INL) and outer plexiform layers (OPL) are well illustrated. The outer processes of Müller cells run among the Henle fibers but cannot be reliably identified. (**b**) If the Müller cell processes are visualized by vimentin immunohistochemistry (counter-staining of cell nuclei by H-E; siamang [*Symphalangus syndactylus*] retina) they can be traced along their path from outer margin of the outer nuclear layer (ONL) up to their endfeet; it becomes obvious that they run in parallel to the Henle fibers. (**c**) Optical coherence tomographical (OCT) scan of an adult human (patient) retina in situ. Note that the radial extension of the retina ("thickness") is magnified more than the lateral one. The main retinal layers including the retinal pigment epithelium (RPE) can be identified, and the shape of the foveal pit is clearly depicted. Original images; (**a**) courtesy of J. Kacza and M. Francke, Leipzig; (**b**) courtesy of K. Görner, Leipzig; (**c**) courtesy of I. Iandiev, Leipzig

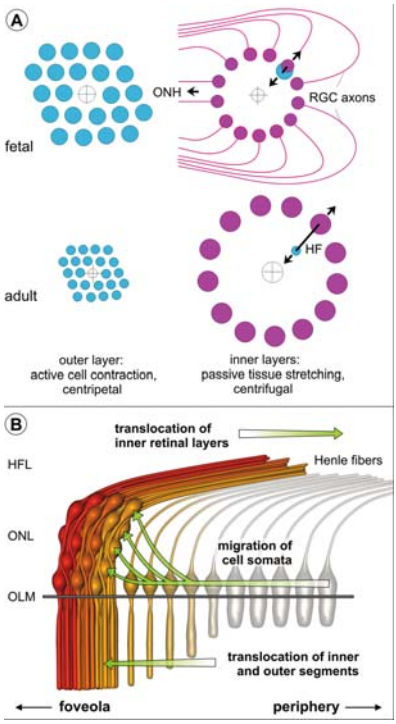

Fig. 2.30 Schematic view of the biomechanical processes involved in the development/shaping of the primate fovea. (**a**) The distributions of functionally related cones and retinal ganglion cells (RGC), respectively, are shown in a fetal (*top row*) and adult (*bottom row*) retina. While the cones become more slender, probably by contraction of their cytoskeletal elements, they move towards the center of the (future) fovea because they are adhering together by zonulae adherentes (cf. Fig. 2.10). Cones and rods outside the fovea proper are dragged centripetally, as well (not shown). By contrast, the ganglion cells move off the foveal area, perhaps dragged by their axons which are stressed (and must elongate) in the course of "passive" retinal expansion. In any case, this dislocates the ganglion cells (and the interneurons which undergo almost the same centrifugal shift) from the cones, i.e., from the input neurons of the columnar units; this causes the necessity of cone axon elongation as Henle fibers (HF). Note that the axons grow away from future foveal center from beginning; thus, the fibers of the "distal" ganglion cells need to assume a U-turn course on their way towards the optic nerve head (ONH). (**b**) Because the cone somata remain much thicker (about 5 μm) than their thinning – mature – inner and outer segments (1–2 μm), the close hexagonal packing of the latter enforces a stacking of the somata in several rows (cf. also Fig. 2.28a). Perhaps due to "waves" of cone segment contraction and dislocation, this leads to a peculiar roofing tile-like arrangement of the somata (as well as to deviations from hexagonal patterning of the inner and outer segment arrays; not shown). (**a**) Original; (**b**) re-drawn after Ahnelt et al. (2004)

processes of Müller cells remain attached to the OLM and must thus follow this thickening of the layer by their elongation.

It is much more difficult to understand how the inner retinal layers are displaced centrifugally. Most probably, the distribution of foveal ganglion cell axons plays a central role. It has already been mentioned that from the beginning of their growth, a repellant must be expressed in the future foveal tissue (perhaps, by the endfeet

and inner processes of the local Müller cells) which enforces a centrifugal course of these axons. Thus, most of the axons grow not towards the future optic nerve head, but even away from it (if extending from ganglion cells at the temporal side of the future fovea). At some distance, they appear to meet a similar (or the same?) repellant expressed by the radial glial cell endfeet in those more peripheral retinal areas in which cell proliferation still continues, and ganglion cell differentiation did not yet commence (Stuermer and Bastmeyer, 2000). This enforces them to turn their course away from these areas, towards the retinal center and eventually allows to approach the optic nerve head. Although these mechanisms need to be elucidated in more detail, it is clear that they have two effects. First, there is an axon-free area in the center of the future primate fovea, making the inner retinal zone thinner and less mechanically stiff than the adjacent areas. It has been hypothesized that this may lead to the formation of a primary foveal pit which then acts as a target of mechanical forces such as the intraocular pressure, displacing the inner retinal layers centrifugally (Springer and Hendrickson, 2004a, b; 2005). Alternatively, stress forces may by exerted from the centrifugally running axons onto the ganglion cell of their origin, drawing them away from foveal center like a dog is drawn by the dog leash. Such forces may arise by the expansion of the perifoveal retinal tissue (cf. Fig. 2.25). It should be kept in mind that this expansion must enforce an elongation of the curved perifoveal axons because they cannot straighten their course; they run between the Müller cell endfeet wich are shifted towards the periphery by the retinal expansion, and which are mechanically rather stiff (Lu et al., 2006) such that they probably cannot be cut by the stretched axons. This hypothesis is illustrated in Fig. 2.30a.

Finally it appears worth underlining that the counter-movement of inner and outer retinal layers (comparable to “tectonic plates”) requires an interposed “sliding zone”. This is obviously provided by the outer margin of the OPL, where both the photoreceptor cell axons and the outer Müller cell processes do not withstand the shifting forces but rather elongate to form the Henle fiber layer. It is not unusual throughout the CNS that axons that already established synaptic contact to their target undergo “secondary, passive” tractional elongation; this occurs in the growing brain as well as in the elongating spinal column (“cauda equine”) and in the peripheral nerves (van Essen, 1997; Pfister et al., 2004; Abe et al., 2004). Even in adult Müller cells, the outer (as well as the inner) process of Müller cells has been shown to be particularly soft (Lu et al., 2006). Thus, apparently two easily elongable structures meet in this sublayer, and make it a versatile sliding zone for the counter-dislocations of the other retinal layers.

In summary, (i) in later postnatal stages there occurs a considerable, topographically variable, and efficiently controled “passive” expansion of the retina; (ii) this process causes significant changes in both local cell densities and in retinal thickness and layering but (iii) the constituents of the columnar units remain unaltered, even during complex re-shaping in the course of foveation; whereas (iv) the wiring of wide-field neurons may be – but must not be – changed during these late stages; finally, (v) Müller cells are both important players in, and reliable indicators of, these late re-shaping processes.

2.2.7 *Functional Maturation of Efficient Glia-Neuron Interactions in the Retina*

In parallel to the developmental changes mentioned in Section 2.2.6, there occurs a gradual maturation of the glia-neuron interactions at all organization levels, from micro- to macrodomains. First, the Müller cells differentiate as such. Although, as stated above, the transition is all but distinct (Section 2.2.4, cf. also Section 3.4.1) the cells differentiate from late progenitor cells via several steps which may be characterized by the terms "radial glia", "immature Müller cells" and "mature Müller cells" (Table 2.3). Only the latter transition is accompanied by apparent morphological alterations, mostly consisting of the outgrowth and elaboration of fine side branches ensheathing the neuronal compartments, from the originally rather smooth tubular cells. These morphological changes are particularly impressive in chicken Müller cell which assume a very complex structure (Fig. 2.31) (Prada et al., 1989b) but occur as well in mammalian (e.g., Reichenbach and Reichelt, 1986) and fish Müller cells (Mack et al., 1998). Generally, the development of Müller cell side branches begins shortly after differentiation of the neuronal elements to be ensheathed; for instance, the fine side branches extend into the synaptic layers roughly one day after begin of synapse formation (Reichenbach and Reichelt, 1986). However, the morphological elaboration of these processes apparently continues lifelong, and the complexity of their shape increases over long periods beyond the establishment of synapses (cf. Fig. 2.31). As mentioned above (Section 2.2.6), the cytoplasmic volume of the Müller cells increases during later postnatal development due to the changes resulting from the passive retinal expansion. However, the dramatic increase in membrane surface area, caused by the development of the fine side branches, is by far not balanced by this volume increase, such that the surface-to-volume ratio of the cells increases considerably with their maturation.

The morphological changes are preceded, accompanied, or followed, respectively, by changes in a wealth of functional parameters (Table 2.3). Generally, there appear to be three different groups of features/expressed proteins, (i) some proteins appear to expressed virtually independent of late progenitor – radial glia – Müller cell differentiation, and thus probably are cell-fate specific (printed in black in Table 2.3); (ii) some features are developmentally down-regulated, and thus appear to be characteristic for progenitor cells (proliferative activity, nestin expression) or for (early) radial glia (e.g., Ca^{2+} responses to depolarization) and may be required for developmental plasticity (printed in blue in Table 2.3) and (iii) a series of features and/or proteins achieve full expression only in mature Müller cells, indicating that these are important for functional glia-neuron interactions during information processing in the retina (printed in red in Table 2.3). It is interesting to note that most of the early features are re-expressed in pathological states when the Müller cells become reactive, and de-differentiate; this will be discussed later (Section 3.1). The current section focuses upon the maturation of glia-neuron interactions. It has been suggested that the key event in the maturation of Müller cells (and probably of astrocytes, as well) is the rapid evolvement of a high density of inward currents through the membrane, mediated by specific K^+ ion channels (Kir4.1 in the case of

Table 2.3 Differentiation of Müller cells from late progenitor cells

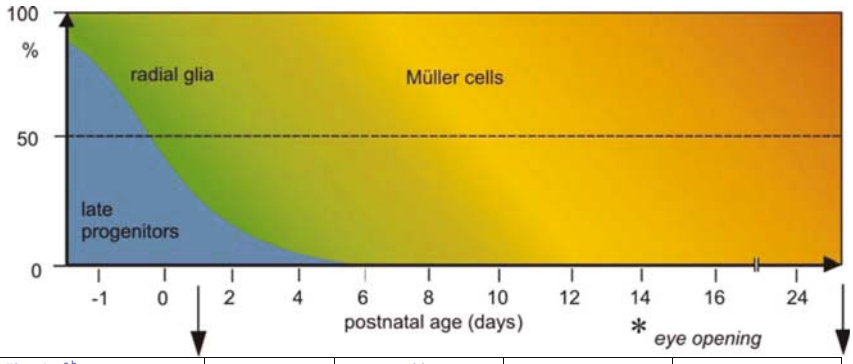

Proliferation[a,b]	+	(-)	–	–
Side branches[b]	–	(+)	+	++
Membrane capacitance / area[c]	17%[a] / 10%[b]	47%[a] / 20%[b]	70%[a] / 25%[b]	80%[a] / 60%[b]
Nestin[a]	+++	++	+	+
Vimentin, CA II[a,b]	+	+	+	+
CRALBP[a]	(+)	+	+	+
S100[a]	–	(+)	+	++
Glutamine synthetase[a,b]	–	(+)	+	++
pERK[a]	–	–	(+)	++
OAP density (endfeet)[b,c]	<3%	8%	33%	>50%
AQP4[a]	–	–	(+)	+
Kir4.1[a]	–	–	(+)	+
$P2Y_1$ receptor[a]	(+)	+	+	+
$P2Y_4$ receptor[a]	–	–	(+)	+
Membrane potential (mV)	–30[a] / –40[b]	–40[a] / –70[b]	–69[a] / –80[b]	–85[a] / –82[b]
Inward current density[c]	4%[a] / 10%[b]	4%[a] / 20%[b]	25%[a] / 40%[b]	60%[a] / 80%[b]
Outward current density[c]	26%[a] / 40%[b]	35%[a,b]	40%[a,b]	60%[a,b]
P_o BK channels[b]	0.7	0.7	<0.5	<0.1
A-type currents[d]	83%[a] / 100%[b]	80%[a] / 100%[b]	70%[a] / 80%[b]	15%[a] / 40%[b]
Na^+ currents[ad]	57%	57%	46%	7%
glut. uptake currents[a,b]	–	+	+	+
GABA uptake currents[b]	–	–	+	+
Ca^{2+} responses to ATP[d,e]	30%[a] / 84%[b]	60%[a] / 65%[b]	40%[a] / 50[b]	20%[a] / 7%[b]
Ca^{2+} responses to ATP soma/endfoot ratios[a]	0.9	0.4	0.4	0.4
Ca^{2+} responses to depolarization[b,d]	9%	34%	20%	8%
Volume regulation capability[a]	–	–	(+)	+
	Progenitors →	**Radial glia →**	**Immature Müller cells →**	**Mature Müller cells**
Synapse formation:				

[a]Rat.
[b]Rabbit.
[c]Percent of adult values.
[d]Percent of all cells. Blue: properties characteristic of progenitor cells/radial glial/immature Müller cells; red: properties characteristic of mature Müller cells ; black: cell fate-specific?
[e]Rat: measured at the soma, rabbit: measured at the endfoot.

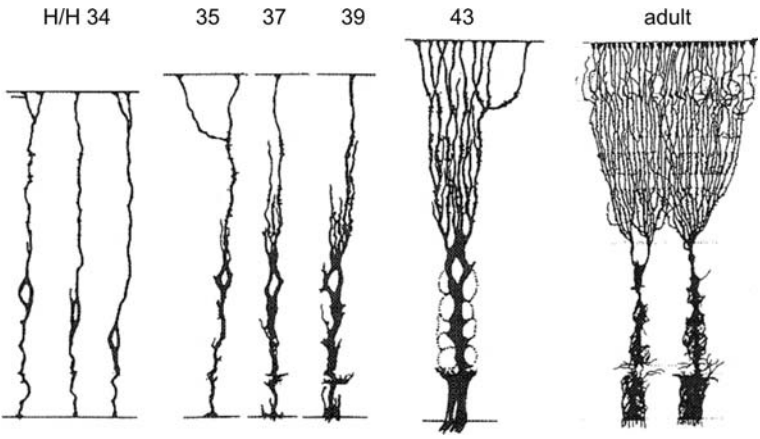

Fig. 2.31 The differentiation of Müller cells is accompanied by an increasing complexity of their shape, particularly by the outgrowth of side branches. Camera-lucida drawings of Golgi-stained chicken retinas from Hamburger/Hamilton stages (H/H) 34–43, and from an adult retina. Note that the split, sheaf-like shape of the inner processes of avian Müller cells develops gradually by the late outgrowth of additional branches through the densely arranged elements of the thick inner plexiform (and nerve fiber) layers (*on top*). Modified after Prada et al. (1989b)

Müller cells; cf. Section 2.4.2). This provides the cells with a low resistance against K^+ fluxes over their membrane, as well as with a very negative membrane potential (–80 mV and more). Both of these two "key features" of mature Müller cells constitute the precondition for a majority of their interactions with their environment, including the retinal neurons. This is obvious for functions such as K^+ and water clearance (Sections 2.4.2 and 2.4.3) but applies also to transmitter recycling (Section 2.4.1) because the uptake carriers for the neuronally released transmitter molecules are driven by the membrane potential. Other functions such as cell volume regulation (Section 2.4.4), gliotransmitter release (Section 2.7.2), and intracellular signaling after ligand receptor activation (Section 2.7.1) are also directly or indirectly dependent on a very negative membrane potential. Noteworthy, the key event in the reversal of Müller cell maturation, i.e. in Müller cell gliosis and de-differentiation, is the loss of the high K^+ ion conductance and thus of all these functions (cf. Section 3.1).

Table 2.3 shows that much of this Müller cell maturation occurs rapidly, within a few days around the eye opening of the animals when the retinal neurons become functionally active, but with a considerable delay (more than a week) after the structural formation of the synapses. This suggests that it is triggered by (specific) functional challenge rather than by the mere presence of the putative interacting elements (and/or by genetic programming). These functional challenges may consist of the release of certain molecules by the maturing, electrically active neurons. Among the candidates are K^+ ions (Reichelt et al., 1989) and excitatory neurotransmitters such as glutamate. For instance, it has been hypothesized that local protein synthesis in the Müller cell processes – required for the formation of glial sheaths with active potassium uptake capacity – may be stimulated by external potassium accumulation

due to neuronal activity, as kind of a homeostatic mechanism (Reichelt et al., 1989). Indeed, there are three layers within the retina where light-evoked increases in extracellular potassium occur, in the inner and outer plexiform layers, and (after cessation of illumination) in the subretinal space (Oakley and Green, 1976; Steinberg et al., 1980; Karwoski et al., 1985, 1989). Furthermore, it has been shown that elevated K^+ concentrations stimulate the protein synthesis of cultured Müller cells, as well as their Na^+,K^+-ATPase activity (Reichelt et al., 1989).

Moreover, the expression of glutamine synthetase by Müller cells was found to increase not only with the number (Mack et al., 1998) and maturation of rods as major glutamate sources in situ but also directly with the concentration of glutamate in the medium in vitro (Germer et al., 1997a). Moreover, the expression of the glutamate transport molecule, GLAST, by bullfrog Müller cells was found to increase transiently after switching the illumination conditions from light to dark (Xu et al., 2004), i.e. when elevated glutamate release by photoreceptor cells occurs (cf. Section 1.2.2). Taken together, there is evidence supporting the idea that the expression of homeostatic molecules and functions (which means, of glia-neuron interaction mechanisms) by the Müller cells is substrate-regulated. One may even speculate that Müller cells are stimulated to express uptake or clearance mechanisms for a given substance if its concentration in the adjacent extracellular space increases enough to challenge or even stress the Müller cells themselves, as, for example, high K^+-induced depolarization requires enhanced activity of the energy-consuming enzyme, Na^+,K^+-ATPase (Reichenbach et al., 1985). Whatever the regulatory mechanisms may be, they finally provide mature functional glia-neuron interactions, as a precondition for neuronal information processing (Section 1.1.1 and Chapters 2 and 3).

In summary, (i) (immature) Müller cells and/or their progenitors are crucial for the establishment (and maturation?) of retinal macrodomains and cellular domains (the "columnar units") early in retinal development, whereas (ii) maturing/mature Müller cells provide metabolic and functional support for the members of "its" unit and define and refine the functional microdomains of glia-to-neuron interactions; eventually, (iii) the functional adaptation of Müller cells to the challenges provided by their "sibling" neurons enables them to fulfil their "final physiological task", *viz* to enhance the signal-to-noise ratio of visual perception (cf. Section 1.1.1). Evidence supporting this statement will be provided in the following chapter.

2.3 Stimulus (Light) Transport to the Photoreceptor Cells – A Role for Müller Cells

2.3.1 Optical Properties of the Vertebrate Retina

Often the retina is considered as a transparent tissue through which light can pass without loss or scattering. However, this is not true; all cells and their processes and organelles are so-called phase objects from physical view which means that they must scatter the light (Zernike, 1955). In particular, the synapses in the two

plexiform layers have diameters close to 0.5 μm, i.e., within the wavelength range of visible light (ca. 400–700 nm = 0.4–0.7 μm) which clearly makes them light-scattering structures (Tuchin, 2000). Indeed, light scattering by the retinal tissue layers is evidenced by the mere fact that optical coherence tomography delivers images of these layers in the living eye (cf. Fig. 2.29c). Thus, the inverted design of the vertebrate retina (cf. Section 1.2.1) has been compared with "placing a thin scattering screen over the film in your camera" (Goldsmith, 1990). It has been discussed above (Section 1.2.1) that this inversion provides a series of (e.g., metabolic) advantages but there remains the question how it is possible that we see sharp, unblurred images at daylight, and can detect a few photons entering our eye (Pirenne, 1967), despite of the presence of light-scattering elements in front of our photoreceptor cells which should decrease both visual acuity and light sensitivity. A possible explanation would be that light-guiding fibers traverse the inner retinal layers, and directly transfer the light (and the image of the environment) towards the photoreceptor cells. It has long been accepted that the inner and outer segments of photoreceptor cells can be considered as light-guiding fibers (Enoch and Tobey, 1981, and references therein). However, these structures are placed at the end of the transretinal light path, and thus can only maintain but not improve the image quality arriving at the OLM, behind the light-scattering layers. Therefore, long, radially oriented elements such as the Müller cells are the only candidates for "living optical fibers" within the retina proper. This idea has been verified by a series of experiments (Franze et al., 2007) described in the following two sections.

2.3.2 Individual Müller Cells Are Light-Guiding Fibers

To prove whether individual enzymatically isolated, vital Müller cells display the properties of light-collecting and -guiding fibers, such cells were placed in the optical path of a modified "optical trap" (Guck et al., 2001) (Fig. 2.32). This device allows to capture, direct, and hold an elongated cell "swimming" in physiological solution in the optical axis of two opposite infrared laser beams (Fig. 2.32a). If then another laser with the wavelength of visible light is coupled into the path at one side, the amount of light arriving at the opposite side can be measured (Fig. 2.32c). If there is no light-guiding element in the path between the two glass fibers, the laser light beam will diverge, and only a part of the initial light intensity will arrive at the tip of the opposite fiber. However, when a Müller cell is placed into the path, with its endfoot directed towards the laser source (but not vice versa), much more light arrives in the opposite fiber (Fig. 2.32d). This clearly shows that (the endfeet of) Müller cells are light collectors and (their stem processes) light-guiding fibers (Franze et al., 2007).

This may be facilitated by the light-refracting properties of the cells (and their cytoplasm). The refractory index (RI) of isolated Müller cells was found to vary with the cellular topography (Franze et al., 2007). Along much of the two stem processes, RI levels of 1.38 were assessed; this is close to the high RI levels of photoreceptor outer segments (about 1.4) and higher than the average RI of the

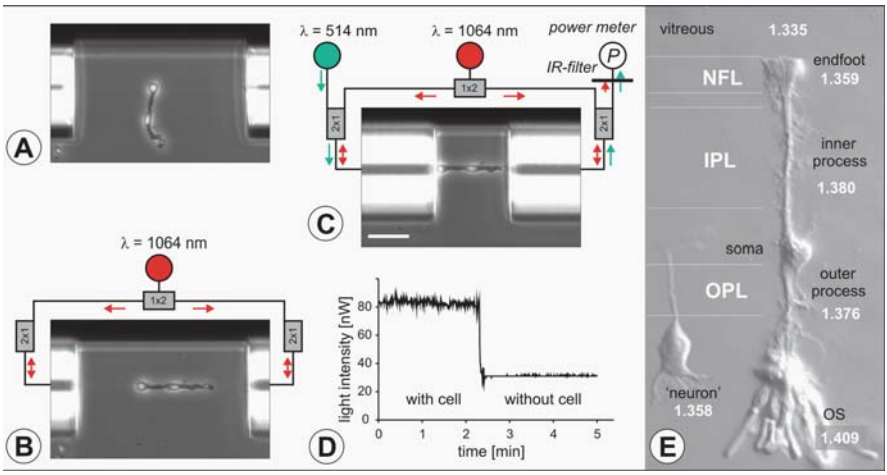

Fig. 2.32 Individual Müller cells as optical fibers. (**a**–**d**) Demonstration of light guiding properties of individual Müller cells measured in a modified dual-beam laser trap. (**a**) A cell is floating freely between the ends of two optical fibers, which are aligned against a backstop visible at top. (**b**) The Müller cell is trapped, aligned, and stretched out by two counter-propagating infrared (IR)-laser beams ($\lambda = 1{,}064$ nm; not visible in the image) diverging from optical fibers (Guck et al., 2001). (**c**) The fibers are brought in contact with the cell. Blue light ($\lambda = 514$ nm) emerges from the left optical (input) fiber, and is collected and guided by the cell to the right (output) fiber. The fraction of blue light re-entering the core of the output fiber is measured by a powermeter, while the IR light is blocked by an appropriate cut-off filter. Scale bar, 50 μm. (**d**) Typical time course of the power of the blue light measured. When the cell is removed from the trap, only a fraction of the blue light, which is no longer confined to the cell but diverges freely, is measured. The ratio P_{cell} /$P_{\text{no cell}}$ defines the relative guiding efficiency. (**e**) Nomarski image of a dissociated guinea pig Müller cell with several adhering photoreceptor cells including their outer segments (OS), and a dissociated retinal neuron (bipolar cell). The refractive index of the neuron and of the various Müller cell sections is noted in the image. Modified from Franze et al. (2007)

surrounding retinal tissue including the neurons (about 1.35–1.36) (Fig. 2.32e). As the nuclei of the Müller cells usually are "piggybacked" by – rather than embedded within – the stem processes (e.g., Figs. 2.2b and 2.32e), this is consistent with a role of the stem processes as light-guiding fibers. By contrast, the RI of the Müller cell endfeet was found to be rather low (about 1.35–1.36), about halfway between that of the stem processes and that of the vitreous body (1,335). This may allow for a "soft coupling" of the light path between the vitreous body and the retinal tissue, reducing light reflection (i.e., light loss) at the inner retinal surface. Furthermore, the particular paraboloid-like shape of the endfoot, together with its intermediate RI, make it together with the adjacent inner stem process an ideal "two-step light collector" with an acceptance angle of about 26° (Franze et al., unpublished data).

In more general terms, the so-called V parameter (a number depending on the diameters and RIs along a fiber-like structure) is commonly used to estimate the light-guiding capability of technical glass fibers; if it exceeds a level of about 2.0,

effective light guidance is taken as guaranteed (Snyder and Love, 1983). For guinea-pig Müller cells, an almost constant V parameter of about 2.8 has been calculated all along endfoot and both stem processes (Franze et al., 2007) which supports the experimental findings from a theoretical point of view. It remains to be elucidated how the high RI in the Müller cell stem processes is generated. Basically, a high concentration of any cytoplasmic protein(s) would be sufficient. It appears to be interesting in this context that the Müller cell parts where a high RI was measured (i.e., between the endfoot-inner stem process transition and the outer stem processes within the OPL) coincides with the sites where bundles of intermediate filaments are located (cf. Fig. 2.9); noteworthy, these filaments are arranged along the light path.

2.3.3 The Müller Cell Population Constitutes a Versatile "Fiberoptic Plate"

Whereas the above-mentioned data were obtained on enzymatically dissociated Müller cells, it could be shown that Müller cells act as light-guiding fibers also within the intact retinal tissue. Using the reflection mode of a confocal laser scanning microscope, light reflection from various layers of living, intact retinal wholemount preparations can be visualized (Fig. 2.33). This experiment reveals that many retinal elements (particularly, the ganglion axon bundles in the NFL and the

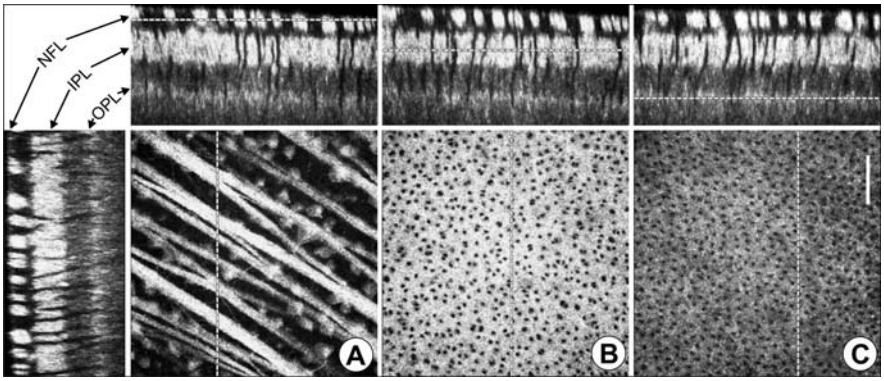

Fig. 2.33 Light back-scattering occurs in the retinal neuropil but not in the Müller cells. Confocal images in reflection-mode were taken of a living unstained guinea-pig retina oriented with the vitread side up. Three different retinal levels are shown, (**a**) nerve fiber layer (NFL), (**b**) inner plexiform layer (IPL), and (**c**) outer plexiform layer (OPL). At the top of (**a–c**), orthogonal *z*-axis-reconstructions (*side views*) of the confocal image stacks are shown; the dotted horizontal lines indicate the levels at which the images (**a–c**) were taken. A regular pattern of non-reflecting tubes is apparent that traverses the entire retina. Furthermore, large parts of the innermost retinal layers are non-reflecting. However, individual retinal ganglion cells and axon bundles in the NFL can be clearly seen by their strong reflection (**a**). In addition, both plexiform layers display a strong and uniform background reflection (**b**, **c**). Scale bar, 25 μm

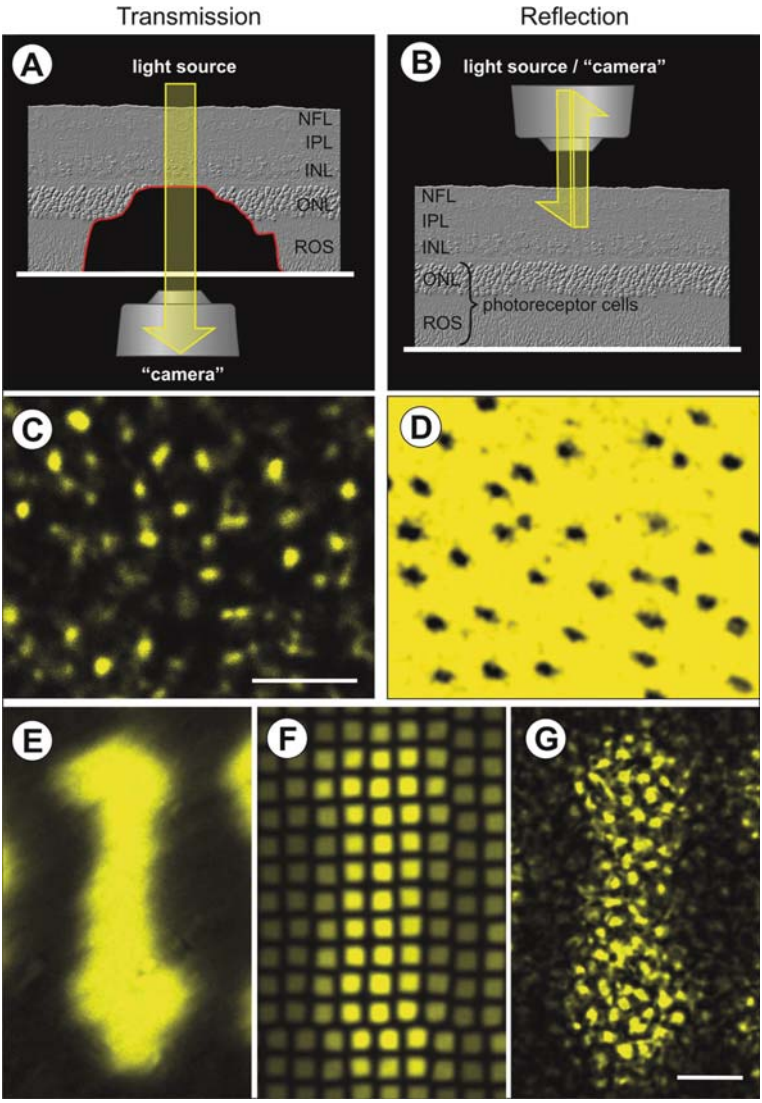

Fig. 2.34 (**a**–**d**) Light transmission (**a**, **c**) and light reflection (**b**, **d**) in the inner retina. (**a**) Semi-schematic of the confocal imaging of transmitted light. A laser beam ($\lambda = 543$ nm) passes through the inner retina of a freshly dissociated eye cup. The transmitted light is captured at the inner nuclear layer (INL; surgically exposed) with an objective and detected by the photomultiplier of an inverted confocal microscope (NFL, nerve fiber layer; IPL, inner plexiform layer; ONL, outer nuclear layer; ROS, receptor cell outer segments). (**b**) Semi-schematic of the imaging in reflection mode. Laser light is delivered via the microscope objective of an upright confocal microscope, and light scattered back from inner retinal layers is detected. (**c**) Confocal transmission image of the living unstained retina. Scale bar, 10 μm. (**d**) Confocal reflection image of the retina at the level of the IPL (cf. also Fig. 2.33); the scale bar in (**c**) is valid also for (**d**). (**e**–**g**) Comparison of

synaptic structures in the two plexiform layers; cf. Section 1.2.2) cause significant backscattering of light. However, there are "holes" in these backscattering layers where much less light is reflected. Serial reconstructions along the Z-axis demonstrate that these "holes" in fact are cross-sections through long tubes which display (almost) no light backscattering, and which traverse much of the retinal thickness. By applying a combination of vital staining and immunohistochemistry for vimentin it was unequivocally demonstrated that these "tubes" are constituted by the Müller cells (Franze et al., 2007).

Since the inner and outer segments of the photoreceptor cells were known to be efficient light-guiding fibers by their own, some experiments were carried out on retinas on which the photoreceptor layer was removed mechanically (Fig. 2.34a,c) or by experimental retinal detachment and subsequent photoreceptor cell degeneration (Fig. 2.34 g). These experiments demonstrated that indeed, the pattern of "dots" of reduced backscattering corresponds to a very similar pattern of "dots" of enhanced light transmission through the inner retina (Fig. 2.34b, d) confirming that Müller cells are efficient optical fibers also in the intact retinal tissue (Franze et al., 2007). Moreover, it was shown an image (the letter "i" in the text on a microfiche) was transferred through the retina as well as through a commercially available fiberoptic plate (Fig. 2.34e–g). Such fiberoptic plates, consisting of thousands of parallel optical glass fibers, are technically used to transfer images over a distance (the thickness of the plate) with minimal loss of light intensity and image information (for instance, if toxic or infectious material is to be observed). The Müller cell population thus constitutes a "natural fiberoptic plate", transferring the image from the inner (vitread) retinal surface through the light-scattering retinal layers, towards the photoreceptor cells (Franze et al., 2007). This generates a "transported" image which is resolved in "pixels" (corresponding to individual Müller cells as pendants of the glass fibers) but maintains the general shape and contrast of the "original" image (Fig. 2.34e–g).

This effect should significantly help to improve the optical properties of the inverted vertebrate retina. Together with the reduced light reflection at the retinal surface by the "soft coupling" of Müller cell endfeet (cf. Section 2.3.2), Müller cell-provided light guidance may significantly reduce a loss of light intensity by backscattering, and thus help to maintain a high sensitivity of scotopic vision. Moreover, Müller cell-provided light guidance may also improve the acuity of

Fig. 2.34 (continued) the inner retina with a commercial fiberoptic plate (FOP). (**e**) Non-confocal brightfield image of a letter on a microfiche as a test object. (**f**) The letter imaged through a commercial FOP built-up by an array of optical fibers (diameter 6 μm). The image is broken up into dots corresponding to light transmission through individual fibers. (**g**) The letter imaged through a guinea-pig inner retina preparation. The image-transferring dots display the same spatial distribution as the "bright" and "dark" dots in (**c**) and (**d**) representing the array of Müller cells. The photoreceptor cells had been eliminated by generating an experimental retinal detachment and subsequent photoreceptor degeneration. Scale bar, 20 μm. Modified from Franze et al. (2007)

photopic vision. It has already been pointed out that the local densities of cones and Müller cells are roughly equal (Section 2.2.5; Fig. 2.24). Thus, every cone may have "its personal" Müller cell as an optical fiber delivering "its personal" part of the image, different and independent of what its neighbor cone receives. In this context, it appears to be essential that a local high densitiy of cones is mirrored by the same local high density of Müller cells (cf. Fig. 2.6), in order to increase spatial resolution. It does not argue against this hypothesis that several (up to >20) rods are to be "illuminated" by the same Müller cell, as the scotopic system is characterized by a high degree of convergence, and spatial resolution does not matter (cf. Fig. 1.13).

2.3.4 A Possible Contribution of Rod Cell Nuclear "Chains" in the ONL

The above-mentioned data support the idea that image acquisition by (the outer ends of) the outer segments of photoreceptor cells is facilitated by the organization of the

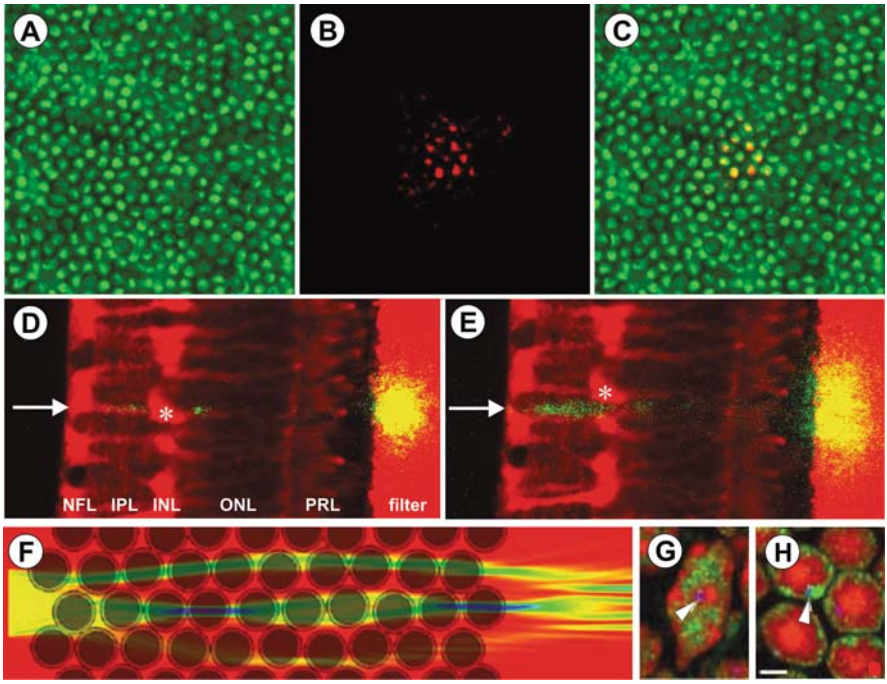

Fig. 2.35 Intraretinal light guidance. (**a**–**e**) Müller cells as optical fibers illuminating the photoreceptor cells of "their" columnar unit. If the endfoot of one Müller cell is selectively illuminated by a laser beam emerging from a thin glass fiber, light is transported to a distinct group of photoreceptor outer segments at the opposite surface of the retina. The number of photoreceptor cells is always 9–13, i.e., close to the average of 11.6 photoreceptor cells per Müller cell in the guinea-pig

retina in two consecutively arranged fiberoptic plates, the first one delivered by the Müller cells (Franze et al., 2007) and the second one by the inner and outer segments of the photoreceptors themselves (Enoch and Tobey, 1981). However, there is an apparent "gap" between these two "fiberoptic plates", *viz* the ONL. As mentioned earlier, the outer processes of Müller cells within this layer are very thin and irregularly shaped (cf. Fig. 2.2) such that they certainly are not suitable as optic fibers (a V parameter can hardly be estimated but would certainly be $=1$). Nonetheless, the illumination of one Müller cell endfoot/inner process is reliably propagated into an illumination of the photoreceptors of "its" column – for instance, in the guinea pig retina, of about 10 photoreceptors (Fig. 2.35a–e). This raises the question how the "ONL gap" is bridged.

Recently it has been hypothesized that the regular columnar arrangement of the photoreceptor cell somata/nuclei (cf. Section 2.2.6 and Fig. 2.27) may play an important role (Solovei et al., 2009). If these cell nuclei function as light-reflecting lenses, every column would provide a chain of lenses, transporting the light similar as a light fiber (Fig. 2.35f). The length of the gap – to be bridged by the "lens chain" – varies among the diverse vertebrate retinas; in nocturnal species

Fig. 2.35 (continued) retina (cf. Table 2.1). (**a**–**c**) A wholemounted guinea-pig retina (vitread surface up) is placed on an inverted-stage microscope; (**a**) brightfield illumination visualizes the regular arrangement of the photoreceptor outer segments. (**b**) When the thin (ca. 5 μm diameter) laser beam of a light fiber hits a Müller cell endfoot at the upper surface of the retina, a distinct group of bright dots appears at the level of the outer segments. (**c**) the overlay of (**a**) and (**b**) shows that light is transferred into the outer segments of about 10 photoreceptor cells. (**d**, **e**) A similar experiment on a guinea-pig retinal slice preparation. The slice is placed – together with the filter on which it was cut – in a movable chamber on the stage of a confocal microscope such that the retina and the filter are visible "from the cut side", and the retina can be moved perpendicular to its vitread surface. An optic fiber is placed close to this vitread surface, and illuminates small spots of it (diameter about 5 μm). Müller cells, photoreceptor cells, and the filter are filled with the vital dye, MitoTracker Orange, and thus display red fluorescence in the confocal mode. Laser light which is scattered from the tissue or from the filter, is green; an overlay of both images appears yellow if light is scattered by the dye-filled elements. (**d**) When the laser beam hits a Müller cell endfoot, light scatter within the retinal tissue is almost absent, and at the level of the filter (i.e., behind the photoreceptor outer segments) a narrow, bright light beam arrives. (**e**) When the slice is moved by a few micrometers and the laser beam cannot longer enter endfoot/inner process of this Müller cell (*asterisk*), considerable light scatter occurs within the retinal layers, and the arriving spot at the level of the filter is large and blurred, due to beam divergence within the tissue. NFL, nerve fiber layer; IPL, inner plexiform layer; INL, inner nuclear layer; ONL, outer nuclear layer; PRL, photoreceptor layer. (**f**–**h**) The linear rows of rod nuclei in the ONL may act as chains of lenses, allowing the light beam to pass the ONL. (**f**) Mathematical simulation of light transport through the nuclei of adult mouse rod photoreceptors. (**g**–**h**) postnatal re-modeling of the chromatin structure and the shape of rod nuclei in the mouse retina; (**g**) at early postnatal stages the nuclei are elongated and display a conventional chromatin pattern; (**h**) in the adult retina the rod nuclei are spherical and show an inverted pattern of hetero- (*red*) and euchromatin (*green*); the nucleoli (*blue*, *arrowheads*) moved towards the nuclear surface. This inversion of the nuclear architecture – which is unique, and occurs only in rods of nocturnal mammals – may be required to optimize the optical properties of these nuclei in the long "lens chains" of the thick outer nuclear layer in these species (cf., e.g., Figs. 1.13 and 2.16). (**a**–**e**) Courtesy of S. Agte, Leipzig, (**f**–**h**) modified from Solovei et al. (2009)

with scotopically specialized retinas, up to ≥11 stacks or rows of photoreceptor cell nuclei are found in the ONL whereas in diurnal species the ONL is much thinner (Figs. 1.13 and 2.16). This suggests that well-directed light propagation through the thick, multilayered ONL of nocturnal mammals requires better adapted optical properties of the rod nuclei than in the thin, oligolayered ONL of diurnal species. Indeed it has been found that nuclear chromatin becomes condensed and inversely arranged (heterochromatin localizes to the nuclear center whereas euchromatin lines the nuclear border, rather than vice versa as in "normal" nuclei) during postnatal development of rods in nocturnal species such as the mouse whereas this does not occur in diurnal species such as the pig (Fig. 2.35 g, h) (Solovei et al., 2009). This inversion of chromatin is, to the best of present knowledge, unique to mammalian rods photoreceptor cell nuclei (i.e., was not found in any other cell of our body, so far) and should generate severe problems in gene translation; thus, it is reasonable to assume that it is a necessary evolutionary adaptation to the particular optic requirements of the thick ONL in retinas of nocturnal animals (Solovei et al., 2009).

This scenery raises the question of how the light is transferred from the Müller cells to the "lens chains" of rod nuclei. It has already been pointed out that the outer stem processes of the Müller cells taper at the border between OPL and ONL, and split into thin branches (cf. Fig. 2.2). A similar tapering can be observed on the outer segments of cones in many species including the human retinal periphery; it has been argued that such tapered cylinders are efficient light radiators which, in the case of cone outer segments, are well suited to transfer the light (which has been guided but not absorbed in the outer segment) to the adjacent rod outer segments (Miller and Snyder, 1973). In analogy, the tapered outer processes of Müller cells may act as light radiators illuminating the chains of rod nuclei.

2.3.5 And What About the Optics of the Fovea(s)?

If considering the optics of retinal tissue, intuitively they should be best in the fovea centralis. Strikingly, however, the above-mentioned rules do neither apply to the non-mammalian fovea nor to that of primates. In both instances, the Müller cells are long and thin such that they hardly can achieve a V parameter sufficient for a function as optic fibers; moreover, their course is more or less bended or even Z-shaped, convergent towards the photorecpetor cells – which would cause an unwarranted diminution of the image (Fig. 2.7b, d). Moreover, it has been shown that in the primate fovea the cone nuclei are not arranged in vertical rows but rather are obliquely stacked, similar to roofing tiles (Fig. 2.30b) (Ahnelt et al., 2004); if these nuclei would act as lens chains, they would also cause a diminution of the image. How did the evolution solve this problem?

It has long been hypothesized that in the deep, "convexiclivate" fovea of some predatory birds (and fish) may function as a concave lens providing a local magnification of the image (Fig. 2.36a) (Walls, 1963, and references therein; Collin et al., 2000). This requires that the retinal tissue (particularly, its surface constituted by the Müller cell endfeet: Collin et al., 2000) displays a higher refractive index than the

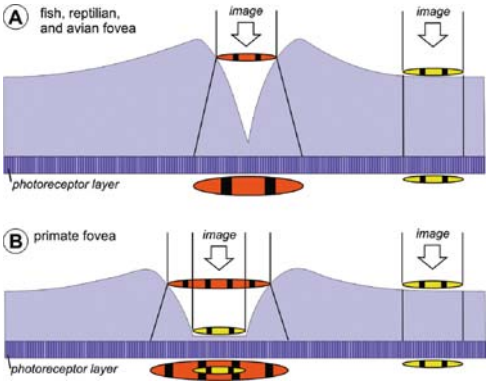

Fig. 2.36 Presumed optics of the non-primate (*top*) and primate (*bottom*) fovea centralis. (**a**) It has been hypothesized already by Walls (1963) that the steep, convexiclivate fovea in avian and lizard retinas constitutes a means to expand the image on its way through the retinal tissue and thus to generate a magnified image at the level of the photoreceptor cells. (**b**) Here it is hypothesized that a similar function may be carried out by the wall of the primate fovea (which is rather steep, too; cf. Fig. 2.29c) whereas the flat foveola proper allows a short, direct pathway of the image to the central cones, without many interposed tissue layers. See text for details. Original

vitreous body; indeed, this has been demonstrated unequivocally (Valentin, 1879) (cf. also Fig. 2.32e). This magnification would allow more (cone) photoreceptors to share the same (region of) the image, and thus to detect image details with enhanced spatial resolution.

By contrast, the primate fovea is generally considered as a rather flat "dish" (Fig. 2.7c) which cannot provide significant optical effects, with one exception: in its center, the foveola proper, the light arrives almost directly at the cones because the light-scattering inner retinal layers are shifted aside (→ Section 2.2.6). However, recent advancements in optical coherence tomography (OCT) allow to study the human retina in situ in more detail; this shows that the primate fovea may display a more complex shape, as also seen in many histological preparations (but usually considered there as a shrinkage artefact) (Fig. 2.29a–c). In this view, the primate fovea appears as a bowl with a flat bottom and steeply elevating walls. This suggests that two distinct parts exist in respect to optical function. First, the flat bottom provides a perfect, thin "glass window" in front of the central-most cones. Thus, these cones receive an almost un-blurred image; the few atypical Müller cells in this area (Fig. 2.8, Section 2.1.3) may contribute to the formation of such a smooth "glass window". The second optical compartment is constituted by the rather steep walls; very probably, these play a similar role as the convexiclivate fovea of the non-mammalian retina, i.e., they provide a magnification of the image for the cones in the neighborhood of the foveola (Fig. 2.36b). Such a mechanism would compensate for the optical problems in this region, where the retina is very thick (which means many light-scattering layers in front of the cones) and where the Müller cells are too thin and too long to act as optic fibers (and, furthermore, take a course which would result in a diminution rather than a magnification of the image if they would guide

the light); it should be kept in mind that this central area of the retina contributes much to our acute vision.

It may be finally mentioned that even outside the fovea, the reptilian and avian Müller cells with their many thin branches (Fig. 2.1) appear not to be suitable for light guidance. This might constitute a problem in respect to visual acuity despite of the clear photopic specialization of most avian retinas. It may be speculated that this is (one of) the reason(s) for the presence of up to three foveas in the same retina, in some birds (Walls, 1963).

2.4 Müller Cells Are Endowed with Tools to Control the Neuronal Microenvironment

Once the image has been transferred to the photoreceptor cells, retinal information processing is triggered (→ Section 1.2.2), and the homeostatic functions of glial cells become challenged (→ Section 1.1.1). In the following sections, it will be shown that Müller cells express suitable membrane proteins and enzymes for this purpose. Several homeostatic mechanisms will be presented under separate headlines but it should be kept in mind that a given membrane protein usually is involved in more than one of these mechanisms, and that most of their homeostatic functions depend on the characteristic very negative membrane potential of the cells (→ Section 2.4.2).

2.4.1 Carriers, Transporters, and Enzymes: Neurotransmitter Recycling

In the retina, both chemical and electrical synapses are essential to mediate the transmission of visual signaling triggered by the photoreceptors. Müller cells are involved in the synaptic signaling of the sensory retina, by rapid uptake of neurotransmitter molecules and by providing the precursor molecules of neuronal transmitter synthesis. Müller cells express uptake and exchange systems for the major excitatory neurotransmitter, glutamate, and may also express transporters for other neurotransmitters such as γ-aminobutyric acid (GABA), glycine, and adenosine. The glutamate and GABA uptake by Müller cells links neuronal excitation with the release of lactate and other molecules that nourish retinal neurons, as well as with the defense against oxidative stress. Any malfunction or even reversal of glial glutamate transporters under pathological conditions may contribute to neurotoxicity.

Generally, the driving force of the uni- or bidirectional substrate transport across membranes is the transmembrane gradient of the substrate itself and/or of ions which are co-transported with the substrate. The majority of neurotransmitter uptake by Müller cells is sodium-dependent (Sarthy et al., 2005; Biedermann et al., 2002) and allows uphill transport of substrates into the cells against a concentration gradient. The driving force for these transporters is the electrochemical gradient of

sodium ions over the plasma membrane that is generated by the energy-consumptive activity of the Na, K-ATPase. In the case of electrogenic sodium-dependent transporters, there is a net influx of positive charges into the cells, while in electroneutral transporters, the inward shift of positive charges is balanced by the co-transport of other ions.

2.4.1.1 Glutamate Removal and Metabolism

The principal amino acid neurotransmitters in the retina are L-glutamate, GABA, and L-glycine. Glutamate is the most prominent excitatory neurotransmitter in the retina (Thoreson and Witkovsky, 1999), and is used in the retinal forward transmission of visual signals by photoreceptors, bipolar, and ganglion cells (Massey and Miller, 1987, 1990) (cf. Section 1.2). In the outer retina, glutamate is released continuously from photoreceptor cells in darkness; this release is modulated by light. In the inner plexiform layer, ON-bipolar cells release glutamate in the light, and OFF-bipolar cells release glutamate in the dark. Photoreceptor and bipolar cells do not generate action potentials but respond to light with graded potentials that modulate the continuous release of glutamate. (Ganglion and amacrine cells are the only neurons in the retina that generate action potentials.)

2.4.1.2 Glutamate Removal

In the neural retina, photoreceptors, neurons, and macroglia express high-affinity glutamate transporters (Rauen and Wiessner, 2000). Generally in the CNS, glial glutamate transporters are responsible for the bulk of glutamate uptake, while neuronal glutamate transporters appear to have more specialized roles, ensuring a high signal-to-noise ratio of synaptic transmission (Beart and O'Shea, 2007). Müller cells and astrocytes remove the majority of glutamate from extracellular sites (Fig. 2.37) (Rauen et al., 1998; Rauen, 2000; Pow et al., 2000), at least in the inner retina (White and Neal, 1976; Ladanyi and Beaudet, 1986; Harada et al., 1998; Rauen et al., 1998; Pow et al., 2000; Holcombe et al., 2008). Under pathological conditions (when the amino acid transport into Müller cells is reduced), a larger amount of glutamate is also transported into inner retinal neurons (Barnett et al., 2001; Holcombe et al., 2008). Müller cells take up glutamate which is diffused out of the synaptic clefts, thereby preventing a lateral spread of the transmitter (Rauen et al., 1996). However, whether or not the glutamate binding to glial transporters (Wadiche et al., 1995) and the uptake of glutamate by retinal glial cells contribute to the termination and shaping of the time course of synaptic glutamate action is still unclear. The role of glial transporters in shaping the time course of excitatory transmission may vary in dependence on the type of synapses investigated. It has been suggested that the majority of glutamate released from photoreceptor terminals is removed by presynaptic transporters of photoreceptor cells (Hasegawa et al., 2006) and, likely, by postsynaptic transporters localized to horizontal and bipolar cells (Rauen et al., 1996). On the other hand, the rapid termination of the postsynaptic action of glutamate in nonspiking inner retinal neurons was suggested to be mediated (at least

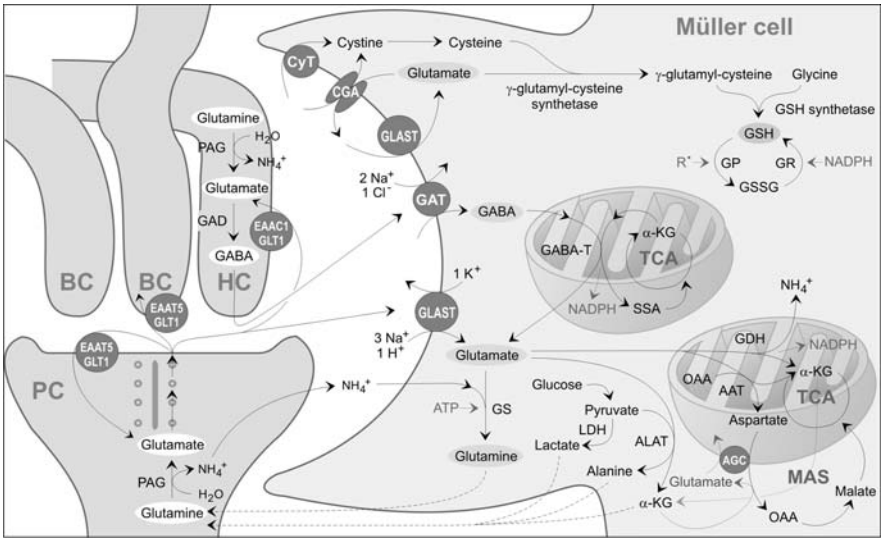

Fig. 2.37 Recycling of amino acid neurotransmitters in the outer plexiform (synaptic) layer of the mammalian retina. The ribbon synapse of a photoreceptor cell (PC) synthesizes glutamate which is continuously released during darkness. The postsynaptic elements are dendrites of bipolar (BC) and horizontal cells (HC). Horizontal cells release GABA which is formed from glutamate. The synaptic complexes are surrounded by Müller cell sheets; the right side shows neurotransmitter uptake systems and some metabolization ways of Müller cells. Glutamate, GABA and ammonia (NH_4^+) are transported into the Müller cell and transformed to glutamine, alanine, and α-ketoglutarate (α-KG). These products are released from Müller cells and taken up by neurons. Glutamine serves as precursor for the transmitter synthesis in neurons (glutamate-glutamine cycle). Lactate, alanine, α-ketoglutarate and glutamine are utilized by neurons as substrates for their energy metabolism. Another metabolic way is the production of glutathione (GSH) which is an intracellular antioxidant, released from Müller cells and taken up by neurons under oxidative stress conditions. ALAT, alanine aminotransferase; AAT, aspartate aminotransferase; CGA, cystine-glutamate antiporter; CyT, cystine transporter; EAAC1, excitatory amino acid carrier 1; EAAT5, excitatory amino acid transporter 5; GABA-T, GABA transaminase; GAD, glutamic acid decarboxylase; AGC, aspartate-glutamate carrier; GAT, GABA transporter; GDH, glutamate dehydrogenase; GLAST, glutamate-aspartate transporter; GLT-1, glutamate transporter-1; GlyT, glycine transporter; GP, glutathione peroxidase; GR, glutathione reductase; GS, glutamine synthetase; GSH, glutathione; GSSG, glutathione disulfide; LDH, lactate dehydrogenase; MAS, malate-aspartate shuttle; OAA, oxaloacetate; PAG, phosphate-activated glutaminase; R•, free radicals; SSA, succinate semialdehyde; TCA, tricarboxylic acid cycle

in part) by its uptake into Müller cells (Matsui et al., 1999). Müller cell glutamate transporters, rather than neuronal transporters, also shape the synaptic responses of retinal ganglion cells (Higgs and Lukasiewicz, 2002). When all glutamate transport in the retina is blocked by a competitive inhibitor, amplitude and duration of ganglion cell EPSCs increase dramatically; when only the neuronal transport is blocked, little change in synaptic current is observed (Higgs and Lukasiewicz, 2002). Diffusion of glutamate out of the synaptic cleft of photoreceptor cells proceeds with a time constant of less than 1 ms (Vandenbranden et al., 1996), which

is 10–100 times faster than the time constants of light-evoked responses in second-order neurons (Copenhagen et al., 1983). Müller cell processes are 1–3 μm away from the sites of glutamate release (Sarantis and Mobbs, 1992), and thus are located within diffusion times of a few milliseconds from the synaptic cleft.

There is further support for the assumption that Müller cell-mediated glutamate recycling is more directly involved in the regulation of the activity of inner retinal neurons than of photoreceptors. For example, this concerns the cellular distribution of glutamate-metabolizing enzymes; aspartate aminotransferase is predominantly localized to photoreceptors and some horizontal cells (Gebhardt, 1991), glutamate dehydrogenase to photoreceptor inner segments and Müller cells (Gebhardt, 1992), and glutamine synthetase to Müller cells (Riepe and Norenberg, 1977). The precursor molecule for glutamate synthesis in bipolar and ganglion cells (glutamine) is derived almost exclusively from Müller cells while photoreceptor cells synthesize only a part of their glutamate from Müller cell-derived glutamine (Pow and Robinson, 1994). (In addition, a significant amount of GABA in amacrine cells is synthesized from glutamate after uptake of Müller cell-derived glutamine; Pow and Robinson, 1994.)

The clearance of synaptic glutamate by Müller cells is required for the prevention of neurotoxicity; malfunction of the glutamate transport into Müller cells results in increased extracellular level of glutamate that can be toxic to neurons through over-stimulation of ionotropic glutamate receptors (Choi, 1988). After experimental inhibition of the glutamate uptake by Müller cells, even low concentrations of extracellular glutamate become neurotoxic (Kashii et al., 1996; Izumi et al., 1999, 2002).

Glial Glutamate Transporters

The removal of glutamate from extracellular sites in the retina involves at least five excitatory amino acid transporters (EAAT1-5) (Kanai and Hediger, 2004). The major glutamate transporter of Müller cells is the electrogenic, sodium-dependent glutamate-aspartate transporter (GLAST or EAAT1) (Otori et al., 1994; Derouiche and Rauen, 1995; Rauen et al., 1996, 1998; Lehre et al., 1997; Rauen, 2000). This carrier system transports, in addition to L-glutamate, also L- and D-aspartate (but not D-glutamate). GLAST transports also various sulphur-containing analogues of these amino acids such as cysteic acid and cysteinesulphinic acid (Bouvier et al., 1991). In Müller cells of the mouse, approximately 50% of glutamate is taken up via GLAST, another 40% through electroneutral, sodium-dependent (presently undefined) glutamate transporters, and 10% via sodium-independent transporters or exchangers (Sarthy et al., 2005). It has been shown that rat Müller cells express, in addition to normally spliced GLAST, the splice variants GLAST1a and 1b which lack exon 3 and 9, respectively (Macnab et al., 2006; Macnab and Pow, 2007). While GLAST is localized throughout the Müller cell bodies, GLAST1a is localized preferentially to the endfeet and inner stem processes of the cells, suggesting a selective regulation of GLAST function in different membrane domains of the cells (Macnab et al., 2006).

In addition to GLAST, the presence of other EAATs in Müller cells of various species has been described; this includes glutamate transporter-1 (GLT1 or EAAT2; goldfish, rat, man), excitatory amino acid carrier 1 (EAAC1 or EAAT3; carp, bullfrog, rat, man), EAAT4 (rat, cat), and EAAT5 (rat) (Vandenbranden et al., 2000a; Rauen, 2000; Zhao and Yang, 2001; Kugler and Beyer, 2003; Fyk-Kolodziej et al., 2004; Ward et al., 2005). Müller cells of the salamander express at least four distinct EAAT subtypes (Eliasof et al., 1998). Similarly to Müller cells, astrocytes express multiple glutamate transporters (GLAST, EAAC1, EAAT4) (Rauen et al., 1996; Lehre et al., 1997; Pow and Barnett, 1999; Rauen, 2000; Kang et al., 2000; Kugler and Beyer, 2003; Ward et al., 2004). Knockout or antisense knockdown of GLAST results in a marked suppression of the electroretinogram b-wave (which reflects the depolarization of glutamatergic ON-bipolar cells in response to activation by photoreceptor cells) and oscillatory potentials, whereas GLT1 knockout mice appear to exhibit minimal compromise of retinal function, suggesting that GLAST is essential for the maintenance of normal synaptic transmission (Harada et al., 1998; Barnett and Pow, 2000). In GLAST knockout mice, the retinal levels of glutamate and GABA (which is produced from glutamate: Fig. 2.37) is increased about twofold as compared to that in wild type animals (Sarthy et al., 2004). While retinas of GLAST and GLT1 knockout mice show a benign phenotype, retinal damage after ischemia is exacerbated, suggesting that both transporters play a neuroprotective role during ischemia in the retina (Harada et al., 1998).

Ion Dependency of Glutamate Uptake

The transport of glutamate by EAATs is well documented to involve the cotransport of three sodium ions and one proton, and the counter-transport of one potassium ion, with each glutamate anion (Barbour et al., 1988; Amato et al., 1994; Pannicke et al., 1994; Owe et al., 2006; Beart and O'Shea, 2007). The transport of an excess of (positively charged) sodium ions into the cell generates an inward current that can be recorded with electrophysiological methods (Fig. 2.38a, c) (Brew and Attwell, 1987; Barbour et al., 1988, 1991; Schwartz and Tachibana, 1990; Pannicke et al., 1994; Sarthy et al., 2005). Based on the average current generated by the electrogenic glutamate transport, it was calculated that the intracellular concentration of glutamate in Müller cells may rise at a rate of ~0.5 mM per second if no metabolization of glutamate occurs (Barbour et al., 1993). The influx of both glutamate and sodium ions may result in a swelling of Müller cells after prolonged (1 h) incubation of retinal slices with high glutamate (Izumi et al., 1996, 1999). The amplitude of the glutamate transporter currents in Müller cells is strongly voltage-dependent (Fig. 2.38b); a very negative membrane potential is essential for efficient uptake of glutamate (Brew and Attwell, 1987; Sarantis and Attwell, 1990; Barbour et al., 1991; Pannicke et al., 1994). Cell depolarization, for example by an increase in extracellular potassium or by activation of glial ionotropic receptors, decreases the uptake rate substantially (Fig. 2.71d) (Pannicke et al., 2000b). Close to the resting membrane potential of Müller cells (approximately –80 mV), the glutamate concentration that half-maximally activates the electrogenic transporters is 10–20

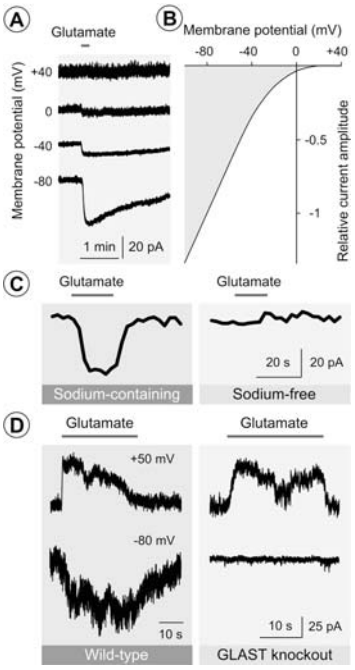

Fig. 2.38 Electrogenic glutamate transport in Müller cells. Whole-cell records of membrane currents were made in acutely isolated cells. (**a**) Administration of glutamate (1 mM) to a Müller cell of the rabbit retina evokes inward currents at negative membrane potentials. The increase in current noise at 0 and +40 mV is caused by activation of voltage-dependent potassium channels. (**b**) Current–voltage relation of the glutamate transporter currents in Müller cells of the guinea pig. (**c**) The electrogenic glutamate transport in Müller cells is dependent on extracellular sodium ions. Omission of sodium from the extracellular solution results in abolishment of the glutamate (100 μM)-evoked inward currents. The traces were recorded in a Müller cell of the rat at a potential of –80 mV. (**d**) Administration of glutamate (1 mM) to a Müller cell of a wild-type mouse evoked inward currents at –80 mV, and outward currents at +50 mV. The inward currents are mediated by the sodium-dependent glutamate uptake, while the outward currents are mediated by the chloride conductance of the glutamate transporter. (The amplitude of the anion conductance was increased by replacing of extracellular chloride by thiocyanate ions.) In a cell from a GLAST knockout mouse, glutamate does not evoke an inward current, whereas outward currents remain. The absence of inward currents suggests that at the resting membrane potential of murine Müller cells an electrogenic glutamate uptake is only mediated by GLAST. The presence of the chloride conductance may suggest that EAAT5 (which have a large chloride conductance and minimal glutamate transport capability) is also expressed in the cells. Modified from Pannicke et al. (2005a) and Sarthy et al. (2005)

μM in amphibian Müller cells, and 2.1 μM in rat Müller cells (Barbour et al., 1991; Rauen et al., 1998; Matsui et al., 1999). EAATs subserve (at least) dual functions, both as glutamate transporter and chloride channel (Ryan et al., 2004). In electrophysiological recordings, the glutamate-elicited chloride conductance is recognizable as an outward current at positive membrane potentials (Fig. 2.38d) (Eliasof and Jahr, 1996; Sarthy et al., 2005). While glutamate can be transported in the absence of a change in chloride conductance, the latter cannot occur without

activation of the transporter (Grewer and Rauen, 2005). However, the chloride conductance of GLAST is relatively low when compared to that of EAAT4/5 (Grewer and Rauen, 2005); the glutamate-evoked anion conductance observed in GLAST knockout mice (Fig. 1.2d) might be mediated by EAAT5 (Sarthy et al., 2005).

Reversal of Glial Glutamate Transport

The electrogenic glutamate uptake carriers transport potassium out of Müller cells (Amato et al., 1994). Light-evoked suppression of the glutamate release from photoreceptor cells will reduce the efflux of potassium from Müller cells in the outer retina; this may contribute to the light-evoked decrease in the extracellular potassium concentration in the outer retina (Amato et al., 1994). Since the electrogenic glutamate transport is activated by intracellular potassium and inhibited by extracellular potassium, pathological rises in extracellular potassium (occuring during ischemia, epilepsy, and glaucoma, for example) will inhibit the glutamate uptake by depolarizing Müller cells and by preventing the efflux of potassium ions from the glutamate carrier (Barbour et al., 1988). This will facilitate a rise in the extracellular glutamate concentration to neurotoxic levels. Pathological rises in extracellular potassium, and depolarization of the cells by opening of cation channels, for example, may even reverse the direction of the glutamate transport (Szatkowski et al., 1990; Billups and Attwell, 1996; Marcaggi et al., 2005). A non-vesicular, voltage-dependent release of glutamate from glial cells via reversed operation of the glutamate transporters was suggested to contribute to the excitotoxic damage of retinal ganglion cells (Maguire et al., 1998). The release of aspartate (which activates *N*-methyl-*D*-aspartate [NMDA] receptors) by reversal of glial glutamate transporters may underlie (at least in part) the increase in aspartate and activation of NMDA receptors during ischemia (Marcaggi et al., 2005). However, also under normal conditions, some glutamate which was taken up by Müller cells might be transported back to the neurons by reversal of the direction of the glial glutamate transport (Pow et al., 2000).

Cystine-Glutamate Antiport

In Müller cells (but not neurons) of the rat retina, and in Müller cells of the carp, the presence of the electroneutral, sodium-independent and chloride-dependent cystine-glutamate antiporter (system X_c^-) was described (Kato et al., 1993; Pow, 2001a; Tomi et al., 2003). This antiporter normally mediates an uptake of cystine in exchange with glutamate; cystine is used for the production of glutathione (Fig. 2.37). Since this antiporter transports cystine using the transmembrane gradient of glutamate as the driving force (Bannai and Tateishi, 1986), the exchanger can also mediate a sodium-independent uptake of glutamate when the extracellular concentration of glutamate is high. This antiporter might contribute to a release of glutamate from Müller cells under oxidative stress conditions such as ischemia-reperfusion when an elevated production of glutathione (and, therefore, an increased uptake of cystine) is required (Kato et al., 1993; Pow, 2001a).

Uptake of Ammonia

Intracellular alkalinization stimulates the glutamate uptake through GLAST (via an increase in the driving force for the transporter-mediated uptake of protons). Ammonia (which is generated in neurons during the synthesis of glutamate from glutamine: Fig. 2.37) speeds the glutamate uptake in Müller cells by two mechanisms: via an increase in the intracellular pH and by a separate, likely direct, effect on the glutamate transporter (Mort et al., 2001). Ammonia is released from glutamatergic neurons, and is taken up by glial cells (Coles et al., 1996; Tsacopoulos et al., 1997). The mechanism of this uptake is unclear. At physiologic pH values close to 7.4, the vast majority of ammonia is charged (NH_4^+), and only a small fraction (less than 2%) is uncharged (NH_3) and can passively penetrate the plasma membrane. It has been suggested that glial cells take up ammonia through potassium channels (Allert et al., 1998). However, results of own unpublished investigations make it rather unlikely that the potassium channels of Müller cells are permeable for ammonium ions (Pannicke, 2007). Ammonia is not transported by electrogenic glutamate transporters (Mort et al., 2001); the presence of ammonia-transporting systems in Müller cells of vertebrate species remains to be established. Glial cells of the bee retina take up ammonia via a chloride cotransporter selective for ammonia over potassium (Marcaggi and Coles, 2001; Marcaggi et al., 2004). Another possibility is a diffusion of ammonia through aquaporins (Wu and Beitz, 2007).

Regulation of GLAST

The expression and activity of GLAST in Müller cells is regulated by the availability of the substrate, likely mediated by intracellular signaling pathways. Extracellular glutamate increases the expression of GLAST in cultured Müller cells (Taylor et al., 2003; Imasawa et al., 2005) while extended exposure to high concentrations of glutamate induces a time-dependent internalization of transporter proteins (Gadea et al., 2004). Glutamate receptor activation in Müller cells results in an increase in the cytosolic free calcium and in activation of protein kinase C (Lopez-Colome et al., 1993). Activation of the protein kinase C increases glutamate uptake by phosphorylation and increased expression of transporter protein (Gonzalez et al., 1999; Bull and Barnett, 2002), suggesting that the enhanced expression or activity of GLAST by activated Müller cells observed under certain pathological conditions (Reichelt et al., 1997a) such as ischemia (Otori et al., 1994) may be caused by this mechanism. In addition to protein kinase C, cyclic adenosine 5′-monophosphate (cAMP) increases GLAST expression and glutamate uptake in retinal glial cells (Sakai et al., 2006). Neuroprotective factors such as glial cell line-derived neurotrophic factor also cause an upregulation of GLAST (Naskar et al., 2000).

Retinal Development

In the human fetal retina, Müller cells express GLAST after cessation of the proliferation of late progenitor cells, shortly before synaptogenesis commences at 10

weeks of gestation (Walcott and Provis, 2003; Diaz et al., 2007). In the rat retina, weak immunoreactivity for GLAST in presumptive Müller cells is already seen at postnatal day 0, and a rapid increase occurs between postnatal days 7 and 10 (Pow and Barnett, 1999) in correlation with a rise in the expression of glutamine synthetase (Fig. 2.48) (Wurm et al., 2006a). In the course of the development of the rat retina, there is a gradual reduction in the numbers of cells that take up glutamate; uptake is initially associated with a wide variety of cells including neuroblasts, presumptive Müller cells and astrocytes while in adult tissues, uptake is restricted mainly to Müller cells and astrocytes (Pow and Barnett, 1999). In the developing mammalian retina, up to 50% of the retinal ganglion cells die by programmed cell death. The transient release of glutamate from dying cells is not associated with a significant elevation in extracellular glutamate, suggesting that normally functioning transporters can rapidly restore homeostatic levels (Pow and Barnett, 1999).

Pathology

Elevated levels of extracellular glutamate have been implicated in the pathophysiology of neuronal loss during ophthalmic disorders such as glaucoma, ischemia, diabetes, and inherited photoreceptor degeneration (Ambati et al., 1997; Brooks et al., 1997; Lieth et al., 1998; Dkhissi et al., 1999; Kowluru and Kennedy, 2001; Martin et al., 2002; Delyfer et al., 2005b). A malfunction of the glutamate transport into Müller cells will contribute to the increase in extracellular glutamate towards excitotoxic levels. Transient retinal ischemia or diabetes do not significantly alter the expression of GLAST, nor the amplitude of GLAST-evoked membrane currents (Barnett et al., 2001; Ward et al., 2005; Pannicke et al., 2005a, 2006) but reduce the efficiency of the glutamate transport into Müller cells (Barnett et al., 2001; Li and Puro, 2002); under these conditions, a large amount of glutamate is transported into photoreceptor, bipolar and ganglion cells (Barnett et al., 2001). In retinas of patients with glaucoma, a downregulation of GLAST (but not GLT1) was described (Naskar et al., 2000). Elevation of the intraocular pressure in experimental glaucoma above a distinct level causes a failure of GLAST activity, resulting in a decreased accumulation of glutamate in Müller cells and in a significant glutamate uptake by retinal ganglion cells; the failure of GLAST coincides with excitotoxic damage to the retina (Holcombe et al., 2008). An increase in the intraocular pressure causes inner retinal hypoxia (via compression of blood vessels) resulting in elevated formation of free radicals in the mitochondria and lipid peroxidation that disrupts the glutamate transport in Müller cells. A dysfunctional electrogenic glutamate transport in Müller cells, caused by free radicals, has been also described in experimental diabetes (Li and Puro, 2002). A similar mechanism (malfunction of the glutamate transport into Müller cells caused by free radicals formed in the mitochondria) may explain the retinal ganglion cell death in Leber hereditary optic neuropathy (Beretta et al., 2006). Human Müller cells from patients with various retinopathies such as retinal detachment, proliferative vitreoretinopathy, and glaucoma, display

an increase in the density of the glutamate transporter currents as compared to cells from healthy donors (Reichelt et al., 1997a). An increase in GLAST labeling was also observed in experimental retinal detachment (Sakai et al., 2001). However, under these conditions, Müller cells depolarize as consequence of a functional inactivation or downregulation of Kir channels (Reichelt et al., 1997a; Bringmann et al., 1999b). An inactivation of Kir channels and depolarization of Müller cells was observed in animal models of various retinopathies such as ischemia-reperfusion (Fig. 3.5a, b), ocular inflammation, diabetic retinopathy (Fig. 3.13b), retinal detachment (Fig. 2.8b, c) and proliferative vitreoretinopathy (Figs. 2.40b and 3.2) (Francke et al., 2001, 2002; Uhlmann et al., 2003; Pannicke et al., 2004, 2005a, b, 2006; Iandiev et al., 2006b; Wurm et al., 2006b). As the electrogenic glutamate transport is strongly voltage-dependent (Fig. 2.38a, b), depolarization of Müller cells will decrease the efficiency of the glutamate uptake by Müller cells (Napper et al., 1999). An age-dependent decrease in Kir currents of human Müller cells (Fig. 2.63c) (Bringmann et al., 2003a) will lower the threshold for membrane depolarization in cells of elderly people. Depolarization of Müller cells can be also evoked by inflammatory lipid mediators such as arachidonic acid and prostaglandins which are produced under oxidative stress conditions or after activation of NMDA receptors (Asano et al., 1987; Birkle and Bazan, 1989; Davidge et al., 1995; Lambert et al., 2006; Balboa and Balsinde, 2006) and which potently inhibit the Na, K-ATPase activity resulting in intracellular sodium overload (Lees, 1991; Staub et al., 1994). Arachidonic acid also directly inhibits the glutamate transporters (Barbour et al., 1989). Furthermore, a reduction in extracellular pH as occurring in ischemia, as well as zinc ions which are released from photoreceptors inhibit the forward and reversed glutamate transport in Müller cells (Billups and Attwell, 1996; Spiridon et al., 1998; Vandenberg et al., 1998). All these factors may contribute to a reduction of the glutamate transport into Müller cells under pathological conditions. A counterregulation of the decrease in electrogenic glutamate uptake in Müller cells under pathological conditions may be caused also in an indirect fashion, through an increase in the membrane localization of the Na, K-ATPase which is required for the transmembraneous sodium-gradient. It has been shown that interleukin-1 activates the p38 mitogen-activated protein kinase (MAPK)/caspase 11 pathway in Müller cells, which destabilizes the actin cytoskeleton, allowing a Na, K-ATPase redistribution in the membrane (Namekata et al., 2008). Thus, interleukin-1 may act as a neuroprotective factor by stimulating the glutamate uptake in Müller cells (Namekata et al., 2008).

Various retinal diseases are associated with a breakdown of the blood-retinal barriers, resulting in a leakage of serum into the retina. Glutamate is a normal constituent of the blood and is present in plasma at concentrations between $\sim$100 and 300 μM (Castillo et al., 1997). Administration of plasma or glutamate activates electrogenic glutamate transporters in bovine and human Müller cells but also inhibits Kir channels and induces a membrane depolarization (Kusaka et al., 1999). A decrease in Kir currents and a depolarization of Müller cells is induced also by other blood-derived molecules such as thrombin (Puro and Stuenkel, 1995). A reduced efficiency of glutamate transport into Müller cells may explain in

part the clinical observation that the presence of hemorrhages at sites of vascular leakage is associated with an increased reduction in retinal function (Gass, 1997).

2.4.1.3 Removal of NAAG

Müller cells may modify glutamatergic neurotransmission also through extracellular hydrolysis of the neuropeptide N-acetylaspartylglutamate (NAAG) by the membrane-bound glutamate carboxypeptidase II which results in a liberation of glutamate (Berger et al., 1999), or through the uptake of NAAG by means of the peptide transporter PEPT2 (Berger and Hediger, 1999). NAAG is an agonist at metabotropic glutamate receptors and an antagonist at NMDA receptors (Coyle, 1997), and is present in retinal ganglion and amacrine cells (Tieman and Tieman, 1996). Glutamate carboxypeptidase II-mediated liberation of glutamate may be implicated in excitotoxicity under pathological conditions such as ischemia (Harada et al., 2000a).

2.4.1.4 Glutamate Metabolism – Production of Glutamine

After being taken up by Müller cells, glutamate is (i) rapidly converted to glutamine by the enzyme, glutamine synthetase, or (ii) utilized for the production of glutathione or (iii) used as substrate in further biochemical pathways that produce fuel for the oxidative metabolism of retinal neurons (Fig. 2.37). The activity of the glutamine synthetase strongly controls the rate of glutamate uptake by Müller cells (Rauen et al., 1998). The rapid metabolization of glutamate to glutamine causes a stronger driving force for the glutamate uptake in Müller cells than in neurons which have intracellular free glutamate concentrations two orders of magnitude higher than Müller cells (Marc et al., 1995). Semi-quantification of immunohistochemically stained retinal slices revealed a glutamate concentration in Müller cells of $\sim$50 μM or less, and a glutamine concentration of 1–3 mM (Marc et al., 1990, 1998a; Pow and Robinson, 1994). The amino acid signature of Müller cells of all vertebrate classes is dominated by glutamine and taurine (Kalloniatis et al., 1994, 1996; Marc et al., 1995, 1998b; Marc and Cameron, 2001), with the exception of the lungfish retina where taurine is abundant in photoreceptors (Pow, 1994). Glutamine is released from Müller cells and taken up by neurons as a precursor for the synthesis of glutamate and GABA (glutamate-glutamine cycle) (Pow and Crook, 1996); glutamate and GABA are then sequestered into synaptic vesicles, and exocytotically released into the extracellular space upon neuronal activation (or, as in the case of GABA, released via reversal of its transporters: Duarte et al., 1998; Andrade da Costa et al., 2000; Calaza et al., 2006). Alternatively, glutamine in Müller cells can be transported into the mitochondria where it might be hydrolyzed to glutamate and ammonia by the phosphate-activated glutaminase (Takatsuna et al., 1994).

In the neural retina, glutamine synthetase is localized in astrocytes and Müller cells (Riepe and Norenburg, 1977; Linser and Moscona, 1979), and is distributed throughout the cytosol of Müller cells (Fig. 2.48) (Derouiche and Rauen, 1995).

Due to the high efficiency of the glutamine synthetase, endogenous glutamate in Müller cells can be demonstrated immunohistochemically only when the glutamine synthetase activity is inhibited pharmacologically or under pathological conditions (Pow and Robinson, 1994; Marc et al., 1998b; Rauen, 2000; Takeo-Goto et al., 2002). When the glutamine synthetase in Müller cells is pharmacologically blocked, bipolar and ganglion cells lose their glutamate content, and the animals become rapidly (within 2 min) functionally blind (Pow and Robinson, 1994; Barnett et al., 2000). This is accompanied by a considerable reduction of the electroretinogram b-wave (Barnett et al., 2000). The lack of immunohistochemically detectable glutamate in bipolar and ganglion cells after inhibition of glutamine synthetase suggests that these neurons do not synthesize significant amounts of glutamate from other substrates than glutamine (Pow and Robinson, 1994). By comparison, inhibition of glutamine synthesis decreases but not abolishes the level of detectable glutamate in photoreceptor cells, suggesting that these cells take up significant amounts of glutamate from the synaptic cleft (Hasegawa et al., 2006), and are able to synthesize glutamate by transamination of α-ketoglutarate (Pow and Robinson, 1994).

Not only photoreceptor cells but also Müller cells possess enzymes that are involved in de novo synthesis of glutamate from pyruvate: pyruvate carboxylase, that catalyzes the carboxylation of pyruvate to oxaloacetate as substrate of the Krebs cycle, and glutamate dehydrogenase, which converts α-ketoglutarate to glutamate; both enzymes are preferentially localized to glial cells (Gebhard, 1992; Hertz et al., 1992). The activity of the malate-aspartate shuttle (Fig. 2.37) in Müller cells is low (LaNoue et al., 2001) due to the low expression level of aspartate aminotransferase (Gebhard, 1991) and of glutamate-aspartate exchangers (Xu et al., 2007). Thus, the vast majority of glutamate is converted to glutamine, and only a small fraction of glutamate is transported into the mitochondria (Poitry et al., 2000). Hydrocortisone increases the expression of glutamine synthetase in Müller cells, and decreases the level of glutamate-aspartate exchangers (Ola et al., 2005). The low activity of the malate-aspartate shuttle may be the molecular basis for the high rate of aerobic glycolysis in Müller cells (LaNoue et al., 2001) (cf. Section 2.5).

Glutamine Transport

A bidirectional transport of glutamine across plasma membranes can be mediated by various neutral amino acid carriers known as systems A and L, and the sodium-dependent amino acid exchanger ASCT2 (Varoqui et al., 2000; Kanai and Hediger, 2004). The principal transporters for glutamine in a rat Müller cell line and in primary cultures of mouse Müller cells are amino acid transporters of the system N: SN1/SNAT3 (system N1 or sodium-coupled neutral amino acid transporter 3) and SN2/SNAT5 (system N2 or sodium-coupled neutral amino acid transporter 5); these transporters are responsible for about 70% of the glutamine transfer across the plasma membrane (Umapathy et al., 2005). The sodium-dependent system A (ATA1/SNAT1, ATA2/SNAT2) and the sodium-independent system L (LAT1, LAT2) contribute to a lesser extent to the glutamine transport across Müller cell membranes (Umapathy et al., 2005). The presence of SN1 in Müller cells in the intact retina was shown by immunohistochemical techniques (Boulland et al., 2002).

Regulation of Glutamine Synthetase

The gene transcription of both GLAST and glutamine synthetase is stimulated by glucocorticoids (Vardimon et al., 1988; Gorovits et al., 1996; Rauen and Wiessner, 2000). The upstream region of the glutamine synthetase gene contains a glucocorticoid response element (GRE) that can bind the glucocorticoid receptor protein (Zhang and Young, 1991). There is an inverse relation between the expression of glutamine synthetase and Müller cell proliferation in the developing retina, in the mature retina (under pathological conditions), as well as cultured cells (Gorovits et al., 1996; Kruchkova et al., 2001). At early developmental stages, the c-Jun protein (which is one component of the activator protein-1 (AP-1) complex of transcription factors that is involved in the regulation of cell proliferation) is abundant in proliferating retinal cells. This protein renders the glucocorticoid receptor moclecules transcriptionally inactive, and glucocorticoids cannot induce the expression of glutamine synthetase (Ben-Dror et al., 1993; Berko-Flint et al., 1994). Concomitant with a decline in cell proliferation and c-Jun expression, the developing retina acquires the cabability to express glutamine synthetase in response to glucocorticoids. This capability can be suppressed by introduction of the oncogene v-src, which stimulates retinal cell proliferation (Vardimon et al., 1991), or by dissociation of the retinal tissue into separated cells (Linser and Moscona, 1979; Vardimon et al., 1988; Reisfeld and Vardimon, 1994). Cell dissociation results in a rapid increase in c-Jun expression, stimulation of glial cell proliferation, and inactivation of the glucocorticoid receptor. Under these conditions, glutamine synthetase expression cannot be induced. In the developing retina of the rat, Müller cells express glutamine synthetase when the glutamatergic synapses mature; first expression of glutamine synthetase occurs around postnatal day 6 (Fletcher and Kalloniatis, 1997), before the expression of other Müller cell-specific proteins such as Kir4.1 and aquaporin-4 is apparent (Wurm et al., 2006a). It has been shown that the expression of glutamine synthetase by cultured Müller cells is stimulated by elevation of the levels of extracellular glutamate (Germer et al., 1997); likewise, it increases if the number of (glutamate-releasing) photoreceptor cells per Müller cell increases during growth of the fish retina (Mack et al., 1998). Thus, there seems to exist a – hitherto unknown – mechanism of substrate regulation of the enzyme (see below; cf. also section “ammonia-mediated regulation”).

Pathology

The expression of glutamine synthetase is regulated by glutamate (Shen et al., 2004). When the major glutamate-releasing neuronal population, the photoreceptors, degenerate (for example in inherited photoreceptor degeneration, retinal light injury or detachment), the expression of glutamine synthetase in Müller cells is reduced (Lewis et al., 1989; Härtig et al., 1995; Grosche et al., 1995; Germer et al., 1997a; Reichenbach et al., 1999). A decline in glutamine synthetase expression and activity was also observed under ischemic, inflammatory, and traumatic conditions, and in the glaucomatous retina (Nishiyama et al., 2000; Kruchkova et al., 2001; Moreno et al., 2005; Hauck et al., 2007; Chen et al., 2008). In Müller cells

of rats with inherited photoreceptor degeneration, the degradation of glutamate is prolonged; this dysfunction of Müller cells is obvious before apparent histological and functional changes of the retina occur (Fletcher and Kalloniatis, 1996). In experimental retinal detachment, retinal neurons display a depletion of glutamate beginning within 5 min of detachment, which is followed by an increase in the glutamine content of Müller cells, suggesting that an acute efflux of neuronal glutamate contributes to excitotoxicity in the detached retina (Sherry and Townes-Anderson, 2000). Within three days of retinal detachment, the expression of the glutamine synthetase in Müller cells declines, resulting in a depletion in glutamine in the retina and in an increased Müller cell glutamate content, up to supramillimolar levels (Lewis et al., 1989; Marc et al., 1998b). The failure of Müller cells to metabolize glutamate persists as long as the retina remains detached (Marc et al., 1998b). No alterations, or even a slight enhancement, in the glutamine synthetase expression in Müller cells was observed in diabetic retinopathy and after optic nerve crush (Mizutani et al., 1998; Lo et al., 2001; Chen and Weber, 2002; Gerhardinger et al., 2005). After optic nerve crush a translocation of the glutamine synthetase protein within the Müller cells was observed towards their endfeet in the ganglion cell layer, where the injured ganglion cells likely release excess glutamate (Chen and Weber, 2002). Whether the reduction in glial glutamate transport is responsible for the reduced ability to convert glutamate into glutamine in retinas of diabetic animals (Lieth et al., 2000) remains to be determined.

Growth Factor-Mediated Regulation

The decline in glutamine synthetase expression in Müller cells under various pathological conditions is mediated (at least in part) by growth factors such as the basic fibroblast growth factor (bFGF) (Kruchkova et al., 2001). In avian Müller cells, bFGF increases the c-Jun protein expression and inhibits the glucocorticoid-induced expression of glutamine synthetase (Kruchkova et al., 2001). bFGF is rapidly released in the retina after detachment (Geller et al., 2001), and increasingly expressed under ischemic conditions, after light injury, and in response to inherited photoreceptor degeneration and mechanical injury (Miyashiro et al., 1988; Gao and Hollyfield, 1995a, b, 1996; Matsushima et al., 1997; Cao et al., 1997a, b; Kruchkova et al., 2001). Though bFGF is one of the major neurotrophic factors which support neuronal survival in the retina (Faktorovich et al., 1990, 1992), the bFGF-evoked downregulation of glutamine synthetase and a potential rise in glutamate might rather aggravate the process of neuronal degeneration. The decrease in glutamine synthetase expression after retinal detachment is likely also a result of the separation of Müller cells from the pigment epithelium and a subsequent interruption of the supply with pigment epithelium-derived factor (Jablonski et al., 2001).

Ammonia-Mediated Regulation

The expression of glutamine synthetase appears to be also regulated by the availability of ammonia. Exposure to elevated levels of ammonia (as occurring in cases of liver failure) causes an upregulation of glutamine synthetase expression in Müller

cells (Reichenbach et al., 1995a, b, c, d; Germer et al., 1997a; Albrecht et al., 1998; Bringmann et al., 1998a, b). As the glutamine synthethase of Müller cells is the most important enzyme available for ammonia detoxification in the retina (in addition to the glutamate dehydrogenase), this is an important additional function of neurotransmitter recycling. Because the glutamine synthetase reaction requires energy, and the K_m of glutamine synthetase for ATP is high (2.5 mM: Meister, 1974), a chronic exposure to high ammonia may cause a metabolic overload of Müller cells and, finally, retinal damage by hepatic retinopathy (cf. Section 3.2.8).

Glutamine synthetase is evenly distributed in the cytosol (Fig. 2.48) while mitochondria are unevenly distributed in Müller cells from avascular retinas such as of the salamander and guinea pig (Figs. 2.9 and 2.39) (Germer et al., 1998; Poitry et al., 2000; Biedermann et al., 2002); thus a major part of ATP used by glutamine synthetase is suggested to be produced through the cytosolic glycolytic pathway. Glutamate and ammonia cause a large increase in lactate (and glutamine) production and release from Müller cells; in addition, adenosine 5′-diphosphate (ADP) and P_i produced by the glutamine synthetase reaction stimulate mitochondrial respiration (Poitry et al., 2000). Lactate and pyruvate are preferentially utilized by photoreceptor neurons as fuel for their oxidative metabolism (Poitry-Yamate et al., 1995; Xu et al., 2007) (cf. Section 2.5).

Glutamate Metabolism – Production of Glutathione

Glutamate taken up by Müller cells is also utilized for the production of glutathione, a tripeptide synthesized from glutamate, cysteine and glycine (Fig. 2.37) (Pow and Crook, 1995; Reichelt et al., 1997c). Glutathione is a major antioxidant that protects cells against oxidative and nitrosative stress by scavenging free radicals. There are various enzymes that use glutathione as substrate to remove toxic peroxides, to control the redox state of the cells, and to regulate protein function through thiolation and dethiolation, e.g. glutathione peroxidase, reductase, transferase, and glutaredoxin. More than other tissues, the retina has a high need for antioxidant protection; this results from constant exposure to irradiation which is exacerbated by high oxygen consumption, and from the presence of high polyunsaturated fatty acid levels (particularly, in the photoreceptor outer segments). Under normal conditions, retinal glutathione is almost exclusively confined to Müller cells, astrocytes, and horizontal cells (Pow and Crook, 1995; Schütte and Werner, 1998; Huster et al., 1998; Marc and Cameron, 2001). It has been estimated that the intracellular glutathione concentration in Müller cells is 3–5 mM, and that glutathione constitutes about 2% of their total protein (Paasche et al., 1998). Under conditions associated with oxidative and nitrosative stress, e.g. ischemia, reduced glutathione is rapidly released from Müller cells and provided to neurons (Schütte and Werner, 1998). Müller cells possess sodium-dependent and -independent transport systems for glutathione (Kannan et al., 1999). Glutathione acts as a cofactor for glutathione peroxidase. This enzyme reduces peroxides to water or alcohol. During this process, glutathione peroxidase is oxidized and must subsequently be regenerated by oxidizing two molecules of

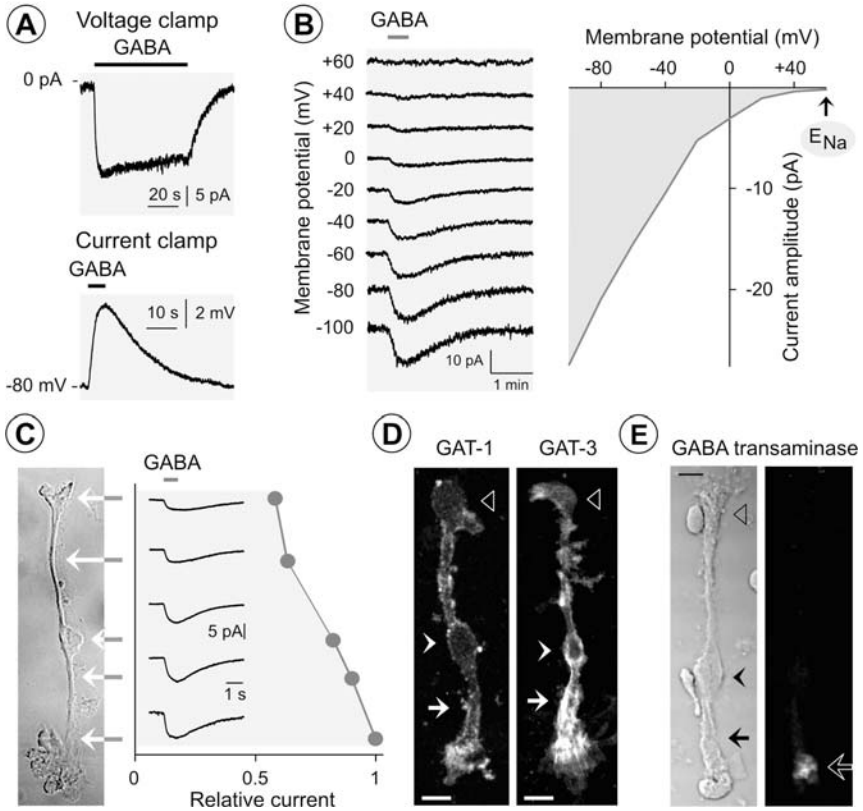

Fig. 2.39 Electrogenic GABA transport in Müller cells of the guinea pig. The membrane currents evoked by activation of the transporters were recorded in single, acutely isolated cells. (**a**) Extracellular administration of GABA (1 mM) evokes an inwardly directed membrane current (*above*) and a depolarization of the cell by ~5 mV (*below*). The voltage-clamp record was done at a membrane potential of –80 mV. (**b**) The GABA transporter currents are voltage-dependent. The *left side* shows an example of current records at different membrane potentials in one cell; the *right side* displays the current–voltage curve of the GABA transporter currents. The amplitude of the transporter currents is zero near the equilibrium potential of sodium ions (E_{Na}) (with symmetrical chloride concentration at both sides of the membrane). GABA was administered at a concentration of 100 μM. (**c**) Subcellular distribution of the GABA transporter currents. The distribution of the currents was determined by focal ejections of GABA (1 mM) onto the following membrane domains of isolated Müller cells: endfoot, inner stem process, soma, inner and outer parts of the outer stem process. (**d**) Distribution of GAT-1 and GAT-3 immunoreactivities in isolated Müller cells. Filled arrows point to the outer stem processes, filled arrowheads indicate the cell somata, and unfilled arrowheads the cell endfeet. (**e**) Localization of the immunoreactivity for the mitochondrial enzyme GABA transaminase (*unfilled arrow*) within a single Müller cell. Bars, 10 μm. Modified from Biedermann et al. (2002)

glutathione to glutathione disulfide (GSSG). GSSG is recycled by glutathione reductase, which utilizes NADPH as the reducing agent. Glutathione released in the extracellular space may also act as neuromodulator and neurotransmitter; via its

γ-glutamyl moiety, it binds to ionotropic glutamate receptors (at micromolar concentrations), and via its free cysteinyl thiol group, it modulates the redox site of NMDA receptors (at millimolar concentrations) which has been shown to increase NMDA receptor channel currents (Janaky et al., 1999).

The formation of glutathione in Müller cells is critically dependent on the availability of extracellular glutamate and cystine (Reichelt et al., 1997c). Pharmacological blockade of glutamate transporters or knockout of GLAST result in a decrease in the glutathione level of Müller cells (Reichelt et al., 1997c; Harada et al., 2007). Cysteine is formed by reduction of cystine that is taken up from the extracellular space via the cystine-glutamate antiporter (Fig. 2.37); inhibition of the antiporter results in a large decrease in retinal glutathione level (Kato et al., 1993). Inhibition of the antiporter can also result from an increase in the extracellular glutamate concentration. Under oxidative stress conditions, e.g. ischemia-reperfusion, the need for glutathione increases. An enhanced uptake of cystine causes an increase in the release of glutamate from Müller cells through the cystine-glutamate antiporter (Kato et al., 1993). It has been suggested that a significant proportion of the glutamate released from Müller cells during reperfusion after ischemia is mediated via the cystine-glutamate antiporter (Pow and Barnett, 2000) which might contribute to the excitotoxic damage of retinal neurons (in addition to the direct effects of glutathione on ionotropic glutamate receptors) (Pow, 2001a).

Pathology

A decrease in the glutathione level might contribute to retinal degeneration under oxidative stress conditions. During hypoxia and hypoglycemia, the glutathione levels in Müller cells decrease dramatically (Huster et al., 2000), and under nitrosative stress conditions, the glutathione content of Müller cells drops to 50% within 2 h (Frenzel et al., 2005). In the retina, the concentration of glutathione normally exceeds that of GSSG by a factor of 7–9 (Kern et al., 1994). In experimental diabetes, the retinal content of glutathione decreases while the GSSG level increases (Kern et al., 1994), reflecting the oxidative stress conditions in diabetic retinopathy. Müller cells from aged animals contain less glutathione than cells from young animals (Paasche et al., 1998). The age-dependent glutathione deficiency is accompanied by mitochondrial damage and reduced membrane potential and vitality of Müller cells (Paasche et al., 2000), suggesting that aging Müller cell mitochondria are impaired by accumulating oxidative damage. Externally applied radical scavengers enhance the intrinsic glutathione content of aged Müller cells and protect the mitochondria from the damaging actions of free radicals (Paasche et al., 1998, 2000). An age-dependent decrease in the Müller cell-mediated defense against free radicals may accelerate the pathogenesis of retinopathies in elderly.

Energy Metabolism

The metabolization of glutamate in Müller cells is tightly coupled to the nutritive function of glia. Müller cells produce various substrates for the oxidative metabolism of photoreceptors such as glutamine, lactate, alanine, and α-ketoglutarate (Poitry-Yamate et al., 1995; Kapetanios et al., 1998; Tsacopoulos

et al., 1998; Poitry et al., 2000) (cf. Section 2.5). The production of lactate in Müller cells is stimulated by glutamate and ammonia (Poitry-Yamate et al., 1995; Poitry et al., 2000; Marcaggi and Coles, 2001; Voutsinos-Porche et al., 2003). In addition to the glutamine synthetase reaction, energy substrates are formed from glutamate in various other biochemical reactions such as transamination of pyruvate with glutamate to alanine and α-ketoglutarate, transamination of oxalacetate with glutamate to α-ketoglutarate and aspartate, and deamination of glutamate to α-ketoglutarate and ammonia (Fig. 2.37) (Poitry et al., 2000). Via conversion to α-ketoglutarate, glutamate functions as a substrate for the tricarboxylic acid cycle (Kalloniatis and Napper, 2002).

The availability of ammonia is a major factor that determines the metabolic fate of glutamate. When enough ammonia is available, the vast majority of glutamate in Müller cells is metabolized to glutamine (Poitry et al., 2000), as indicated by the observation that blockade of glutamine synthetase results in a dramatic increase in the glutamate level of Müller cells (Pow and Robinson, 1994). When the concentration of ammonia decreases, more glutamate enters the mitochondria (Poitry et al., 2000). Inhibition of the glutamine synthetase suppresses the stimulatory effect of both agents on glycolysis, and induces a massive entry of glutamate into the mitochondria (Poitry et al., 2000). The rate of glutamine production also determines the amount of pyruvate transaminated by glutamate to alanine and α-ketoglutarate.

2.4.1.5 GABA Uptake and Metabolism

GABA is the major inhibitory neurotransmitter in the vertebrate retina. Subclasses of horizontal, amacrine, ganglion, bipolar, and interplexiform cells utilize GABA as transmitter. Termination of the synaptic action of GABA is achieved by uptake into presynaptic neuronal terminals and surrounding glial cells. In addition to neurons such as amacrine and interplexiform cells (Moran et al., 1986; Pow et al., 1996; Johnson et al., 1996), Müller cells may take up GABA from the extracellular space (Sarthy, 1982). Generally, it is assumed that in retinas of most lower vertebrates and birds, GABA removal is almost exclusively mediated by neuronal cells, while in the mammalian retina, both neurons and Müller cells remove GABA from the extracellular space (Yazulla, 1986).

GABA Uptake

The uptake of GABA is mainly mediated by sodium- and chloride-dependent high-affinity GABA transporters (GATs); per transport step, two sodium and one chloride ions are co-transported with one GABA molecule (Qian et al., 1993; Biedermann et al., 2002). Omission of sodium (Fig. 2.74b) or chloride ions from the extracellular solution fully inhibits the transport of GABA. Since GABA is electrically neutral at physiological pH, the transport process causes inwardly directed membrane currents that can be recorded with electrophysiological methods (Fig. 2.39a). The shift of one positive charge from the extra- to the intracellular side of the plasma membrane results in a depolarization of the cells (Fig. 2.39a). The electrogenic transport of GABA is concentration-dependent, with near-maximal currents at 100 μM GABA.

At a membrane potential of –80 mV (which is close to the resting membrane potential of Müller cells), the GABA concentration that half-maximally activates the electrogenic transporters is 5.7 and 7.9 μM in Müller cells of guinea pigs and man, respectively (Biedermann et al., 2002). The GABA transporter currents are voltage-dependent; when the plasma membranes are more hyperpolarized, the amplitude of the currents increases (Fig. 2.39b) while the affinity of GABA to the transporter molecules decreases (Biedermann et al., 2002). In Müller cells of the guinea pig, a depolarization of the plasma membrane from –120 to 0 mV decreases the current amplitude from 37 to 5 pA, and the affinity constant from 17 to 2 μM (Biedermann et al., 2002). The GABA transporter currents are unevenly distributed over the plasma membranes of Müller cells, with the largest currents at the end of the outer stem processes (Fig. 2.39c). The time dependence of the GABA clearance from the extracellular space surrounding one Müller cell has been estimated; when the cells display a membrane potential of –80 mV, a pulse of 100 μM extracellular GABA is fully cleared after 70 ms (Biedermann et al., 2002). Due to this high efficiency of the GABA uptake, Müller cells are suggested to be involved in the rapid termination of the GABAergic transmission in the mammalian retina. It has been shown that cultured Müller cells of the chick do not release GABA upon membrane depolarization, suggesting that (different from neurons) transporter-mediated GABA release is not a common mechanism operating in these cells (de Sampaio Schitine et al., 2007). On the other hand, Müller cells have been suggested to release GABA after treatment with kainate, high-potassium, or a GABA mimetic in tissue preparations of rat and primate retinas (Neal and Bowery, 1979; Sarthy, 1983; Andrade da Costa et al., 2000).

To date four GABA transporters have been described (GAT1-4) in addition to the vesicular transporter VGAT, with GAT-3 being the predominant glial form (Schousboe, 2003). The expression of GAT subtypes in Müller cells varies among the species. Müller cells of the guinea pig display immunoreactivities for GAT-1 and GAT-3 (but not GAT-2) (Biedermann et al., 2002). The transporter proteins are located in the plasma membranes along the whole cells, and show an elevated expression level in the outer stem processes (Fig. 2.39d). The localization of the GAT proteins (Fig. 2.39d), and the distribution of the GABA transporter currents (Fig. 2.39c), correspond well with the observations that GABA is taken up by both amacrine and Müller cells in the inner retina, and exclusively by Müller cells in the outer retina of mammalian species (Marc, 1992). Müller cells of the chick and rat also express GAT-1 and -3 (Brecha and Weigmann, 1994; Honda et al., 1995; Johnson et al., 1996; Kim et al., 2003; de Sampaio Schitine et al., 2007) while Müller cells of the rabbit express GAT-3 but not GAT-1 (Hu et al., 1999). On the other hand, Müller cells of the bullfrog retina express GAT-1 and GAT-2 but not GAT-3 (Zhao et al., 2000), and Müller cells from other non-mammalian vertebrate species such as tiger salamander (Yang et al., 1997) and salmon (Ekström and Anzelius, 1998) apparently do not express GAT proteins. Cultured avian Müller cells, but not avian Müller cells in situ, accumulate GABA (Marshall and Voaden, 1974; Pow et al., 1996; Calaza et al., 2001; de Sampaio Schitine et al., 2007). However, a failure in demonstrable GABA uptake in Müller cells of non-mammalian vertebrates should be considered with caution. It can not be ruled out that GABA is

rapidly converted by the GABA transaminase in Müller cells but not in neurons, resulting in a failure of detectable GABA in Müller cells. This assumption is supported by a study of Sarthy and Lam (1978) that showed very little apparent GABA transport activity but high levels of GABA transaminase in Müller cells from turtle. A failure in the immunohistochemical detection of GAT proteins in non-mammalian Müller cells may be due to poor cross reactivity of antibodies directed against rodent sequences.

GABA Metabolism

When GABA enters the cell interior, it is readily converted to glutamate by the GABA transaminase via a NAD(P)-dependent process (Fig. 2.37). Due to the efficiency of the GABA transaminase reaction as the primary mechanism of GABA turnover, Müller cells display a very low level (<100 μM) of intracellular GABA which is hardly detectable with immunohistochemical methods (Davanger et al., 1991; Marc et al., 1998a). GABA immunoreactivity in Müller cells is only detectable under pathological conditions or after pharmacological inhibition of the GABA transaminase (Cubells et al., 1988; Neal et al., 1989; Barnett and Osborne, 1995; Perlman et al., 1996; Ishikawa et al., 1996b; Yazulla et al., 1997; Takeo-Goto et al., 2002). The GABA transaminase is localized in the mitochondria (Schousboe et al., 1977). In the avascular retina of the guinea pig, the mitochondria (and thus the immunoreactivity for the GABA transaminase: Fig. 2.39e) are solely located within the outer end of the outer stem processes, i.e. near to the choroidal blood supply in situ (Germer et al., 1998a, b). Extracellular administration of GABA evokes a NAD(P)H fluorescence signal (caused by the reduction of NAD(P) to NAD(P)H) selectively in the mitochondria of Müller cells (Biedermann et al., 2002). In diabetic and ischemic retinas of the rat, GABA rapidly accumulates in Müller cells (Barnett and Osborne, 1995; Ishikawa et al., 1996a; Napper et al., 2001) due to a decrease in the GABA transaminase activity (Ishikawa et al., 1996b; Kobayashi et al., 1999). During ischemia, Müller cell energy levels are sufficient to allow the active uptake of released GABA, but insufficient to metabolize it to glutamine (Barnett and Osborne, 1995). Such an intracellular GABA accumulation will impair the efficiency of GABA uptake into Müller cells due to a decrease in the transmembrane driving force. Though the enzyme glutamic acid decarboxylase (GAD), which synthesizes GABA from glutamate, has been reported to exist in cultured Müller cells (Kubrusly et al., 2005), it remains to be determined whether or not it is catalytically active in Müller cells in situ.

2.4.1.6 Uptake of Glycine and D-Serine

In the vertebrate CNS, glycine acts both as an inhibitory neurotransmitter and as a coagonist at postsynaptic NMDA receptors. In the retina, populations of amacrine, bipolar, and interplexiform cells utilize glycine as a transmitter (Davanger et al., 1991; Pow, 2001b). The termination of the synaptic action of glycine is thought to be mediated exclusively by re-uptake. In retinas of a variety of mammalian and non-mammalian species, Müller cells apparently do not take up glycine, and the

expression of glycine transporters is restricted to neurons (reviewed by Pow, 2001b). However, in amphibian retinas, both neurons and Müller cells express glycine transporters (GlyTs). GlyT1-like transporters are expressed in Müller cells while GlyT2-like transporters are present in neurons such as amacrine and horizontal cells (Du et al., 2002a; Lee et al., 2005; Jiang et al., 2007). GlyTs are electrogenic, sodium-dependent transporters; thus, extracellular glycine evokes inward currents in amphibian Müller cells (Du et al., 2002a). In human Müller cells which do not express glycine transporters, extracellular glycine does not evoke alterations in the membrane conductance (Bringmann et al., 2002a). The species-dependent expression of glycine transporters suggests that Müller cells participate in the termination of glycinergic neurotransmission in retinas of "lower" vertebrates, and do not play a significant role in removal of glycine in mammalian retinas. In retinas of amphibians and other "lower" vertebrates, a regulation of the glycine transport in Müller cells may contribute to the modulation of the NMDA receptor activity at glutamatergic synapses.

Whereas Müller cells of "higher" vertebrates, e.g. chicken and man, do not express glycine transporters in situ (Pow and Hendrickson, 1999; Bringmann et al., 2002a) they have the capacity to express GlyT1 when placed into culture (Gadea et al., 1999; Reye et al., 2001). These data underline the assumptions that results obtained in cultured cells do not necessarily reflect the *in-situ* siuation, and that Müller cells in pathological tissues may exhibit different patterns of transporter expression than in normal tissues (Pow, 2001b). Chicken Müller cells in culture express two transport systems for glycine, one with low affinity ($K_m = 1.7$ mM) which is sodium-dependent and ascribed to the transport system A, and another with high affinity ($K_m = 27$ μM) which is sodium- and chloride-dependent and identified as GlyT1 (Gadea et al., 1999). The glycine transport in cultured Müller cells is stimulated by intracellular calcium, calmodulin, and calmodulin kinase II (Gadea et al., 2002). Extracellular ATP evokes a release of calcium from intracellular stores, resulting in a stimulation of the glycine transport. Destabilization of actin inhibits the uptake of glycine (Gadea et al., 2002), suggesting that the membrane expression of the transporters is regulated by the actin cytoskeleton.

Another endogenous ligand of the glycine modulatory binding site of the NMDA receptor is D-serine. In the frog retina, the D-serine degrading enzyme D-amino acid oxidase is localized to Müller cells and rods (Beard et al., 1988). The uptake of D-serine from Müller cells is likely mediated by the sodium-dependent neutral amino acid exchanger ASCT2 (O'Brien et al., 2005; Dun et al., 2007), coupled to a counter-movement of L-serine or L-glutamine (Ribeiro et al., 2002). The coupling of glutamine efflux to D-serine uptake might regulate the extracellular D-serine concentration in dependence on the strength of neuronal activity (Ribeiro et al., 2002).

2.4.1.7 Uptake of Dopamine/Serotonin

Dopamine is the predominant biogenic amine in the retina. It has been shown that cultured chicken Müller cells express dopamine D_1 receptors, tyrosine hydroxylase, L-DOPA decarboxylase (two of the enzymes that synthesize dopamine), but not the

dopamine transporter DAT (Kubrusly et al., 2005). Though acutely isolated mammalian Müller cells may express functional D_2 receptors (Biedermann et al., 1995), it remains to be determined whether Müller cells in situ also express these enzymes and transporters. In slices of control and ischemic retinas of the rat, only catecholaminergic amacrine cells display immunoreactivity for tyrosine hydroxylase (Iandiev et al., 2006e). In the carp retina, Müller cells (in addition to retinal neurons) may take up serotonin (Negishi and Teranishi, 1990). In the retina, tryptophan is present in Müller cells and photoreceptors, suggesting that serotonergic neurons are dependent upon the transfer of tryptophan from Müller cells to manufacture serotonin (Pow and Cook, 1997).

2.4.1.8 Uptake of Cannabinoids

Cannabinoid ligands have electrophysiological effects on cones and bipolar cells. Müller cells and cone inner segments in the goldfish retina express the fatty acid amide hydrolase (Glaser et al., 2005) which hydrolyzes the endocannabinoid anandamide. Müller cells and cone photoreceptors take up anandamide; it was suggested that the bulk clearance of anandamide in the retina occurs as a consequence of a concentration gradient created by the fatty acid amide hydrolase activity (Glaser et al., 2005).

2.4.1.9 Degradation of Purinergic Receptor Agonists

Extracellular ATP acts as transmittter in the retina (Perez et al., 1988) being involved in early retinal development (Sugioka et al., 1996, 1999) and in the neuronal information processing of the mature retina. Upon illumination of the retina or administration of a depolarizing high-potassium solution, neurons release ATP via a calcium-dependent mechanism (Perez et al., 1986; Santos et al., 1999; Newman, 2005). ATP is suggested to be co-released from cholinergic neurons, resulting in activation of an inhibitory glycinergic feedback loop (Neal and Cunningham, 1994). Furthermore, ATP modulates the uptake of GABA in the rat retina (Neal et al., 1998). In addition to neuronal release, ATP is released from Müller cells when calcium transients are evoked in the glial cell network of the retina by electrical or mechanical stimuli or by receptor agonists such as dopamine and thrombin (Newman, 2001, 2003b); administration of other receptor agonists such as glutamate, heparin-binding epidermal growth factor-like growth factor (HB-EGF), atrial natriuretic peptide (ANP), and vascular endothelial growth factor (VEGF) also evokes a release of ATP from Müller cells which is implicated in the autocrine regulation of Müller cell volume (Fig. 2.75b) (Uckermann et al., 2006; Weuste et al., 2006; Kalisch et al., 2006; Wurm et al., 2008). In addition to ATP, adenosine is involved in reciprocal signaling between retinal neurons and glial cells. Adenosine is released in the retina upon stimulation with a high-potassium solution (Perez et al., 1986), and glia-derived adenosine (after release of ATP and extracellular degradation to adenosine) causes suppression of neuronal activity (Newman, 2003b) (cf. Section 2.7).

In the retina, extracellular nucleotides are degraded by ecto-enzymes while adenosine is taken up through nucleoside transporters. Nucleoside transporters in Müller cells of the rat retina have been shown to be involved in the regulation of the Müller cell volume under varying osmotic conditions (Uckermann et al., 2006). Müller cells express ecto-5′-nucleotidase (CD73) (Kreutzberg and Hussain, 1982; Hussain and Baydoun, 1985; Braun et al., 1995; Lutty et al., 2000; Iandiev et al., 2007c). Ecto-5′-nucleotidase hydrolyzes nucleoside monophosphates such as adenosine 5′-monophosphate (AMP) to the respective nucleosides (Zimmermann, 1992). Ecto-enzymes that degrade extracellular ATP are located in synaptic and Müller cell membranes of the rat retina (Puthussery and Fletcher, 2007). Müller cells express at least one ectoenzyme that degrades extracellular ATP, the nucleoside triphosphate diphosphohydrolase 2 (NTPDase2, CD39L1, ecto-ATPase) (Iandiev et al., 2007c). Another ATP-degrading ectoenzyme, NTPDase1 (CD39, ecto-apyrase, ecto-ADPase), is solely localized to vascular endothelial cells in the rodent retina, while a significant expression of NTPDases 3 and 8 and an activity of alkaline phosphatase are absent at physiological pH (Lutty and McLeod, 1992; McLeod et al., 2006; Iandiev et al., 2007c). NTPDase1 hydrolyzes ATP and ADP equally well, whereas NTPDase2 preferentially degrades ATP to ADP, with a delayed and very slow hydrolysis of ADP to AMP (ATP to ADP hydrolysis ratio of ∼10:1: Failer et al., 2003). Thus, within the retinal parenchyma, ATP can be rapidly hydrolyzed to ADP by NTPDase2 (expressed by neuronal and Müller cell membranes) while ADP will be degraded to AMP with a considerable delay (due to the very low ADPase activity of NTPDase2). Enzyme histochemistry in slices of the murine retina revealed a degradation of ATP throughout the retinal parenchyma, whereas ADP is rapidly hydrolyzed solely in the blood vessels (Iandiev et al., 2007c).

2.4.2 Potassium Channels of Müller Cells: Retinal Potassium Homeostasis

Neuronal activity is associated with rapid ion shifts between intra- and extracellular spaces. Sodium and calcium ions flow into activated neurons while potassium ions are released from neurons. Neuronal activity evoked by the onset of light stimuli causes increases in the extracellular potassium level (by ∼1 mM) in the plexiform (synaptic) layers, and a decrease in the potassium concentration (by 2–3 mM) in the subretinal space surrounding the photoreceptors (which hyperpolarize in response to light stimulation) (Oakley and Green, 1976; Steinberg et al., 1980; Karwoski et al., 1985, 1989). The end of light stimuli causes an increase in the potassium level of the subretinal space. If uncorrected, increases in extracellular potassium will cause neuronal depolarization and hyperexcitability. Thus, homeostasis of the extracellular potassium concentration is a precondition of regular neuronal information processing. A major functional role of glial cells in the CNS including the sensory retina is to buffer the activity-dependent variations in the extracellular potassium level via permission of transcellular potassium currents, a process termed “spatial

potassium buffering" or "potassium siphoning" (Orkand et al., 1966; Newman et al., 1984; Karwoski et al., 1989; Reichenbach et al., 1992; Newman and Reichenbach, 1996). Müller cells take up excess potassium ions from the extracellular space (particularly, in the plexiform layers), and release equal amounts of potassium into fluid-filled spaces outside of the neural retina where the potassium concentration is constant (blood, vitreal fluid) or decreased (subretinal space) during light stimulation (Fig. 2.43c) (Newman et al., 1984; Karwoski et al., 1989; Reichenbach et al., 1992). The light-evoked potassium efflux from Müller cells into the subretinal space (in association with the potassium influx into the inner end of the cells) establishs a dipole, with a positive field potential in the outer retina (underlying the slow PIII response of the electroretinogram) (Witkovsky et al., 1975; Newman and Odette, 1984; Yanagida and Tomita, 1984; Reichenbach and Wohlrab, 1985; Dmitriev et al., 1985; Xu and Karwoski, 1997; Kofuji et al., 2000). The spatial buffering potassium currents through Müller cells limit the lateral spread of excitation beyond the borders of light-stimulated retinal columns, and thus help to maintain visual acuity (Reichenbach et al., 1993a, b).

As a consequence of the strong expression of a variety of potassium channels, the plasma membranes of Müller cells are highly permeable to potassium ions (Newman, 1984, 1985a). In Müller cells of the frog, the potassium-to-sodium membrane permeability ratio is approximately 490:1, while the chloride permeability is very low (Newman, 1985a). The high potassium permeability of the plasma membrane is the basis of the very negative resting membrane potential of the cells (approximately –80 mV) close to the equilibrium potential of potassium ions (Witkovsky et al., 1985). Recordings of the whole-cell currents of isolated Müller cells (Fig. 2.40a) reveal different types of potassium currents (Fig. 2.40b, c) (Newman, 1985b; Chao et al., 1994a). Around the resting membrane potential and upon membrane hyperpolarization, inwardly rectifying potassium (Kir) currents can be recorded which are mediated by Kir channels (Fig. 2.40d). These channels are characterized by their capability to mediate larger inward potassium currents (into the cell) than outward currents (out of the cell). Depolarization of the plasma membrane of Müller cells may activate various types of voltage-gated outwardly rectifying potassium currents including fast transient (A-type) potassium (K_A) currents, delayed rectifying potassium (K_{DR}) currents, and currents through calcium-activated potassium channels of big conductance (BK currents) (Fig. 2.40c). The glial Na, K-pump or Na, K-ATPase is localized mainly in glial membranes in the plexiform layers and in the microvilli (Ueno et al., 1981; Stirling and Sarthy, 1985; Reichenbach et al., 1988b); its activity is particularly stimulated by elevated external potassium concentrations (Reichenbach et al., 1985; Reichelt et al., 1989). It contributes, together with certain transporter molecules (e.g. the K/Na/2Cl cotransporter) to the Müller cell-mediated potassium homeostasis (Reichenbach et al., 1986, 1992). However, passive currents through Kir channels play the major role in the clearance of the retinal tissue from excess potassium. Kir channels are the only potassium channels that display a high open-state probability at the very negative resting membrane potential characteristic for Müller cells (Brew et al., 1986; Newman, 1993). The fact that a blockade of the Kir channels

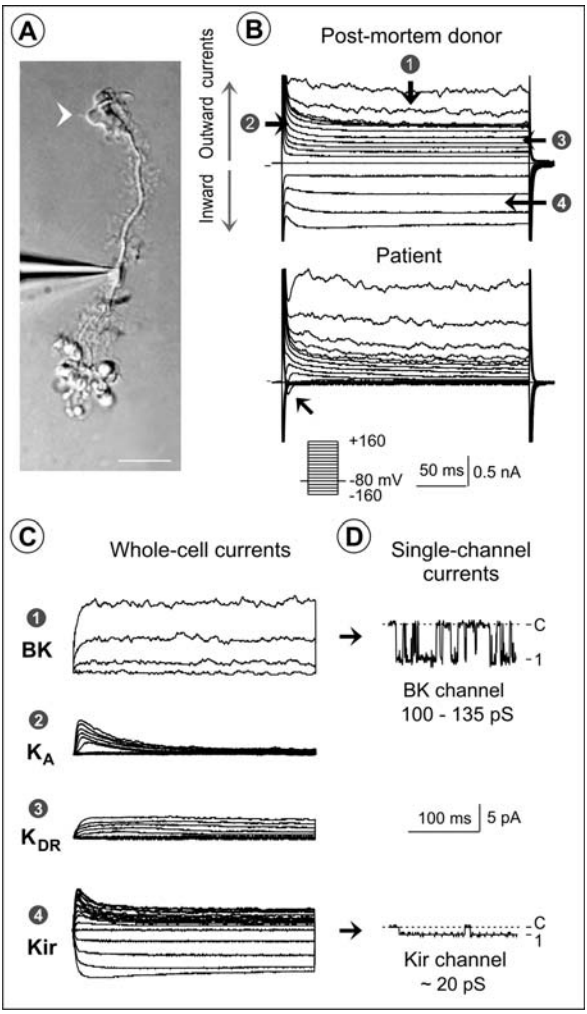

Fig. 2.40 Potassium currents of Müller cells. (**a**) A patch pipette is attached on the soma of a Müller cell isolated from a rabbit retina. When the plasma membrane is ruptured at the tip of the pipette, the whole-cell currents of the cell can be recorded. When the pipette is attached to the cell without rupturing the membrane, the activity of single channels in the membrane patch enclosed by the pipette tip can be recorded (cell-attached mode of patch clamping). *Arrowhead*, cell end-foot. Bar, 15 μm. (**b**) Potassium currents in human Müller cells. The currents were evoked in a cell from a post-mortem donor without apparent eye diseases (*above*) and a cell from a patient with proliferative vitreoretinopathy (*below*). Outward currents (upwardly depicted) were evoked with step-wise depolarization up to +160 mV from a holding potential of –80 mV. Inward currents (downwardly depicted) were evoked by hyperpolarizing voltage steps up to –160 mV. Note the absence of inward potassium currents in the trace of the patient's Müller cell. The arrow indicates transient inward currents evoked by depolarizing voltage steps which are mediated by voltage-gated sodium channels. (**c**) The whole-cell currents of Müller cells are composed of at least four different kinds of potassium currents: inwardly rectifying potassium (Kir) currents, and three

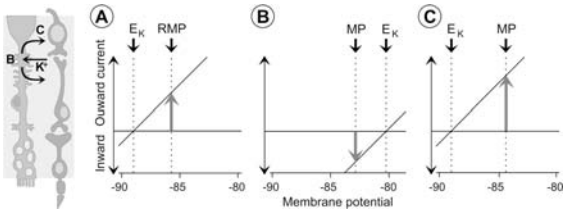

Fig. 2.41 Classical view of passive potassium currents through glial cells that counterbalance local imbalances in the extracellular potassium concentration. Potassium currents through open Kir channels are inwardly directed at membranes potentials (MPs) more negative than the equilibrium potential for potassium ions (E_K), and outwardly directed at MPs more positive than E_K. (**a**) Under resting conditions, the resting membrane potential (RMP) of glial cells is more positive than E_K. This causes an electrochemical driving force for an efflux of potassium ions resulting in leak currents out of the cells which are counterbalanced by the activity of the Na, K-ATPase. (**b**) At sites of a local accumulation of extracellular potassium ions, E_K shifts towards more positive voltages whereas the MP of the whole cell is shifted only slightly (since it is clamped by the surrounding membrane; light-evoked depolarizations of Müller cells are small in amplitude, ~0.5–2 mV: Karwoski and Proenza, 1977). The MP negative to E_K causes a driving force for an influx of potassium into the glial cells. (**c**) At sites distant from the localized increase in extracellular potassium, E_K is similar as under resting conditions whereas the membrane is slightly depolarized. The slight depolarization increases the driving force for an efflux of potassium from the cells

with barium ions results in a strong enhancement of the light-evoked alterations in the extracellular potassium level underlines the importance of glial Kir channels for retinal potassium homeostasis (Oakley et al., 1992; Frishman et al., 1992).

The classical view of the mechanism how glial cells buffer imbalances in the extracellular potassium concentration suggests that a local increase in extracellular potassium causes the driving force for passive potassium currents through the glial cells (Fig. 2.41) (Orkand et al., 1966). An increase in extracellular potassium shifts the equilibrium potential for potassium ions towards more positive voltages. When this increase is localized to a small site (around few synapses, for example), the equilibrium potential of potassium becomes more positive than the resting membrane potential of the cell (which is only slightly shifted towards more positive voltages since the surrounding non-affected membrane "clamps" the potential at a high value). As a result, potassium moves down its electrochemical gradient and enters the glial cells (Fig. 2.41b). At sites distant from the local increase in extracellular potassium, the slight depolarization of the membrane enhances the

Fig. 2.40 (continued) kinds of outwardly rectifying currents: BK, currents through calcium-activated potassium channels of big conductance; K_A, transient (A-type) potassium currents; and K_{DR}, delayed rectifying potassium currents. (**d**) The currents through single potassium channels recorded in cell-attached membrane patches display the different conductance of BK and Kir channels. **c**, closed state; 1, open state current levels. Modified from Francke et al. (2001a, b) and Bringmann et al. (1999a, b)

electrogenic driving force for the efflux of potassium from the cells (Fig. 2.41c). Thus, potassium enters the Müller cell where the extracellular potassium concentration is elevated and exits where the extracellular potassium level is unchanged. Such a spatial buffering mechanism is estimated to clear excess potassium from the retina up to ~4 times faster than extracellular diffusion (Newman et al., 1984; Eberhardt and Reichenbach, 1987; Reichenbach et al., 1992). However, this classical view needs a supplement since it would imply that potassium can be released from Müller cells also at sites near the local increase in extracellular potassium, e.g. into spaces around non-activated synapses. To avoid affection of neuronal activity due to Müller cell-derived potassium, Müller cells release potassium only through membrane domains which have contact to fluid spaces outside of the neuroretina; such membranes are characterized by a large (outward) conductance for potassium ions. By contrast, potassium efflux from other, intraretinal membrane domains is prevented by a high resistance against potassium outward currents. Thus, the direction of potassium efflux from the neuroretina is determined by the subcellular localization of different subtypes of Kir channels.

2.4.2.1 Kir Channels

Single Kir channels (Fig. 2.42a) of Müller cells from various vertebrate species display conductances between 17 and 28 pS (Fig. 2.42b), in dependence on the

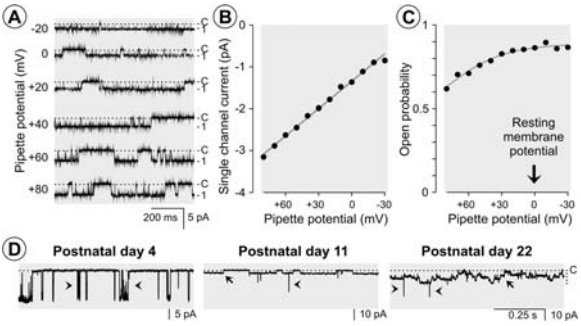

Fig. 2.42 Single Kir channels of Müller cells. (**a**) Activity of one Kir channel in a membrane patch which was recorded at the soma of a human cell. Downward deflections reflect channel openings. **c**, closed state. (**b**) Mean current–voltage relation of single Kir channels of human Müller cells, with a slope conductance of 21 pS. (**c**) Mean open-state probability of Kir channels of human Müller cells in dependence on the pipette potential (which is inversely related to the membrane potential of the cells). A pipette potential of 0 mV means that the patch potential is near the resting membrane potential of the cells. (**d**) The density of single Kir channels in membrane patches increases during the postnatal maturation of Müller cells. Examples of channel records in soma membrane patches of Müller cells from rabbits of various postnatal stages (pipette potential +80 mV). The patch of the cell from the postnatal 4 (P4) cell contained no Kir channel but one BK channel (*arrowheads*). The patch of the P11 cell contained one Kir channel (*arrow*) and a BK channel, while the patch of the P22 cell contained at least four Kir channels together with a BK channel. The recordings were made in the cell-attached mode with 130 and 3 mM potassium in the pipette and bathing solution, respectively. Modified from Bringmann et al. (1999a, b)

recording conditions (Newman, 1993; Ishii et al., 1997; Kusaka and Puro, 1997; Rojas and Orkand, 1999; Bringmann et al., 1999a, 2000f). The conductance of Kir channels increases when the extracellular potassium concentration rises (Newman, 1993). Kir channels have a high open-state probability (>0.8) over a wide voltage range around the resting membrane potential (Fig. 2.42c) (Kusaka and Puro, 1997; Bringmann et al., 1999b). This high open-state probability of Kir channels is a precondition for the mediation of prompt potassium currents across the plasma membrane when the local level of extracellular potassium is altered.

Among the various subtypes of Kir channels expressed by Müller cells (Raap et al., 2002), especially the Kir4.1 and Kir2.1 subtypes are implicated in mediating the potassium buffering currents (Ishii et al., 1997; Kofuji et al., 2000, 2002).

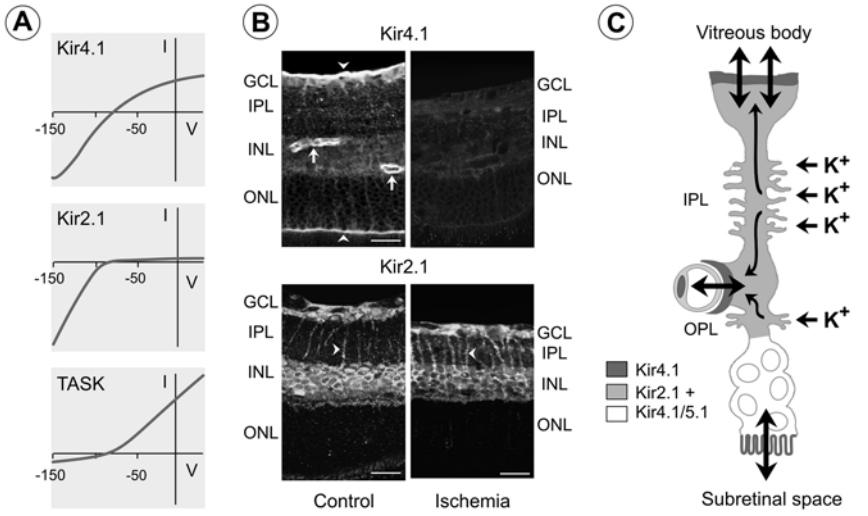

Fig. 2.43 The subcellular localization of different Kir channel subtypes determines the direction of spatial buffering potassium currents through Müller cells. (**a**) Current–voltage (I–V) relations of various glial potassium channels. The Kir4.1 channels mediate inward and outward currents with similar amplitudes, whereas the Kir2.1 channels mediate inward currents, and two-pore domain (TASK) channels mediate outward potassium currents. (**b**) Immunolocalization of glial Kir channels in the normal and postischemic rat retina. The Kir4.1 protein is predominantly localized at the limiting membranes of the neuroretina (*arrowheads*) and around the blood vessels (*arrows*). The Kir2.1 protein is localized in the inner retina in membrane domains of Müller cells that abut on neuron compartments, e.g. in the processes that traverse the inner plexiform layer (IPL) (*arrowheads*). Seven days after a 1-h transient retinal ischemia, the expression of Kir4.1 protein is largely downregulated whereas the localization of the Kir2.1 protein is unaltered. Note the decrease in the thickness of the inner retina which is a characteristic feature of retinal ischemia-reperfusion injury. (**c**) Scheme of the potassium buffering currents that flow through Müller cells during neuronal activation. Activated neurons release potassium ions which are absorbed by Müller cells through Kir2.1 and Kir5.1/4.1 channels, and distributed into the blood vessels, the vitreous, and the subretinal space through Kir4.1 channels. Kir4.1 channels mediate in- and outward currents and, thus, contribute to the osmohomeostasis between the neuroretina and extra-retinal fluid-filled spaces. GCL, ganglion cell layer; INL, inner nuclear layer; ONL, outer nuclear layer; OPL, outer plexiform layer. Bars, 20 μm. Modified from Iandiev et al. (2006a)

Kir4.1 channels are weakly rectifying channels, i.e. they mediate inward and outward potassium currents with similar amplitudes (Fig. 2.43a) (Takumi et al., 1995; Kubo et al., 1996; Shuck et al., 1997). Kir2.1 channels are strongly rectifying channels and mediate predominantly inward potassium currents but almost no outward currents (Fig. 2.43a) (Kubo et al., 1993). The channel proteins of both subtypes are expressed in a polarized fashion in the plasma membrane of Müller cells. The Kir4.1 channel protein is prominently located in such membrane domains across which the cells extrude potassium into spaces outside the neural retina, i.e. in perivascular membranes, in membranes of the endfeet which have contact to the vitreous chamber, and in the microvilli that extend into the subretinal space (Figs. 2.43b) (Nagelhus et al., 1999; Kofuji et al., 2000; Poopalasundaram et al., 2000). (In avascular retinas such as that of the guinea pig, the Kir4.1 protein is localized predominantly at the inner limiting membrane and, at a lower level, at the outer limiting membrane: Fig. 2.46d; Francke et al., 2005.) Kir2.1 channels are localized in membrane domains of Müller cells that face retinal neurons (Fig. 2.43b) (Kofuji et al., 2002; Iandiev et al., 2006a; Ulbricht et al., 2008). Thus, the polarized expression of different subtypes of Kir channels (together with the local transmembraneous potassium gradients) determines the direction of the transglial potassium currents: excess potassium is absorbed by Müller cells from the interstitial spaces around excited neurons, and is distributed into the blood, the vitreous fluid, and the subretinal space (Fig. 2.43c).

Single spots of Kir5.1 immunoreactivity have been found to be distributed diffusely at the cell body and the outer portions of rat Müller cells (Ishii et al., 2003b); other studies did not find expression of Kir5.1 in Müller cells of frogs, mice, and guinea pigs (Skatchkov et al., 2001; Kofuji et al., 2002; Raap et al., 2002). Kir5.1 subunits are not functional by themselves, but are capable to coassemble with Kir4.1. This results in an alteration of the gating properties of Kir4.1, i.e. in a steeper inward rectification (Pessia et al., 1996). Thus, heterotetrameric Kir4.1/5.1 channels may be expressed at low density in Müller cell membranes across which excess potassium is taken up from the interstitium, while homomeric Kir4.1 channels are clustered in the vitreal endfeet and in perivascular membranes (Fig. 2.43c) (Ishii et al., 2003b).

Kir4.1 and Kir2.1 are ATP-dependent channels (Takumi et al., 1995; Fakler et al., 1994). Opening of the channels requires the generation of ATP by local glycolysis near the channel proteins, and subsequent hydrolysis of ATP by an ATPase (Fakler et al., 1994; Kusaka and Puro, 1997). In addition, the activity of Kir2.1 channels is regulated by protein kinases; phosphorylation of the channel protein by the cAMP-dependent protein kinase (protein kinase A) stimulates the opening of the channels whereas phosphorylation by the calcium-dependent protein kinase (protein kinase C) reduces the channel activity (Fakler et al., 1994).

Whole-Cell Kir Currents

The membrane conductance of whole Müller cells is dominated by large potassium (Kir) currents which are inwardly directed when the membranes are hyperpolarized,

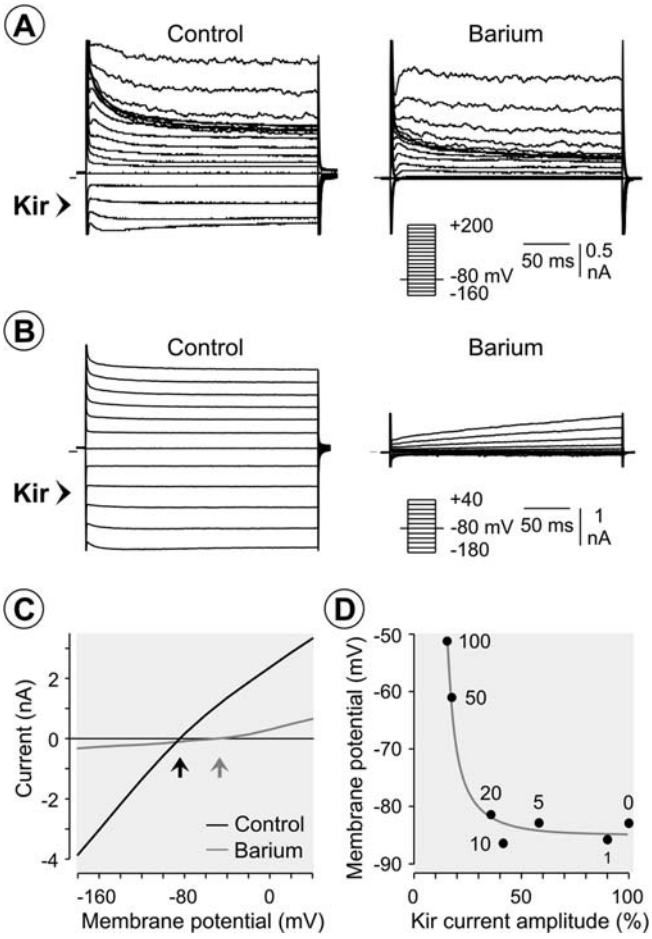

Fig. 2.44 The whole-cell Kir currents of Müller cells are blocked by extracellular barium ions. (**a**) Currents recorded in a human Müller cell. Barium chloride (1 mM) blocks the inward potassium currents (*arrowhead*). The currents were evoked by stepwise depolarization (up to +200 mV) and hyperpolarization (up to –160 mV) from a holding potential of –80 mV. (**b**) Blocking effect of barium ions (100 μM) on the potassium currents of a rat Müller cell. (**c**) Mean current–voltage relations of the whole-cell currents of rat Müller cells. Note the weak inward rectification of the currents under control conditions, and the positive shift of the zero-current (0 nA) potential of the currents (*arrows*) in the presence of barium that reflects the depolarization of the cells. (**d**) Dependence of the membrane potential of rat Müller cells upon the Kir current amplitude. The data were measured in the presence of different concentrations of extracellular barium (in μM; given besides the data points). Modified from Bringmann et al. (1999b) and Pannicke et al. (2005a)

and outwardly directed at potentials positive to the resting membrane potential of approximately –80 mV (Fig. 2.44a, b). The current–voltage relation of the whole-cell currents reveals weak inward rectification of the potassium currents

around the resting membrane potential (Fig. 2.44c) (Felmy et al., 2001), suggesting that a large portion of the currents is mediated by the weakly rectifying Kir4.1 channels. However, the rectification degree of the whole-cell currents differs in Müller cells from different species, e.g. from man (Fig. 2.44a) and rat (Fig. 2.44b), reflecting a species-dependent variation in the expression of distinct Kir channels. The Kir currents are blocked by extracellular barium ions (Fig. 2.44a, b) (Newman, 1989; Reichelt and Pannicke, 1993; Chao et al., 1994a) with an IC_{50} of ~7 μM in rat cells (Fig. 2.44d) (Pannicke et al., 2005a).

Kir4.1 channels mediate ~90% of the potassium conductance of Müller cells at the resting membrane potential (Kofuji et al., 2000). Müller cells of Kir4.1 knockout mice display a depolarization of their membranes (Kofuji et al., 2000), suggesting that the Kir4.1 channel is the major determinant of the very negative membrane potential of approximately –80 mV. A full blockade of the Kir channels with barium ions results in a depolarization of the cells to values between –50 and –40 mV (Fig. 2.44c) which is the activation threshold of outwardly rectifying K_A and K_{DR} currents (Pannicke et al., 2000a). However, there is a non-linear relation between the Kir current amplitude and the membrane potential of Müller cells, i.e. Müller cells display a membrane depolarization only when the Kir currents are depressed to values lower than ~40% of control (Fig. 2.44d) (Bringmann et al., 2000a; Pannicke et al., 2005a). This non-linear relation is also reflected in the physiological properties of developing Müller cells where the membrane potential increases faster than the Kir currents (Figs. 2.45a and 2.47d). Apparently, Müller cells express more Kir channels in their membranes than required to maintain a negative membrane potential; this provides a distinct safety against membrane depolarization when the expression of Kir channels decreases, e. g., under pathological conditions (Fig. 2.45a).

Subcellular Distribution of Kir Channels

Müller cells display a non-uniform distribution of the potassium conductance across their plasma membranes. Cells of animal species with avascular retinas (fish, amphibians, rabbit, guinea pig) have the highest potassium conductance in the membranes of their endfeet facing the vitreous cavity; the outer (photoreceptor) end of the cells display also a relatively high potassium conductance (Fig. 2.46c) (Newman, 1984, 1985a, 1987; Francke et al., 2005). In dogfish, amphibian and rabbit Müller cells, 80–95% of the total membrane conductance is localized in the endfoot (Newman, 1984, 1985a, 1988; Reichenbach and Eberhardt, 1988; Skatchkov et al., 1995). The non-uniform distribution of the potassium conductance corresponds with the density of single Kir channels that is far higher in the endfoot membrane than in other cell regions (one salamander Müller cell possess ~54,000 Kir channels; ~90% of the channels are located in the cell endfoot), and with the distribution of the Kir4.1 channel protein which is predominantly located in endfoot membranes (Fig. 2.46d) (Brew et al., 1986; Newman, 1993; Rojas and Orkand, 1999; Francke et al., 2005). Müller cells of some species with vascularized retinas (man, *Macaca*, pig) also display the highest potassium conductance in their endfeet membranes (Fig. 3.8c) (Pannicke et al., 2005c; Iandiev et al., 2006b), while cells of other species

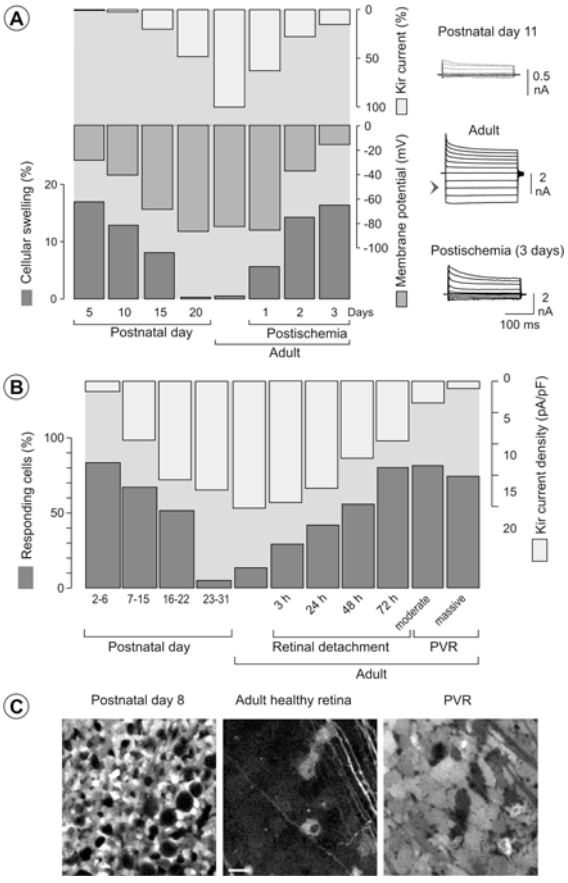

Fig. 2.45 The expression level of Kir channels is related to different physiological properties of Müller cells. (**a**) In Müller cells of the rat, the amplitude of the Kir currents (*above*) is positively related to the resting membrane potential (*middle*) and inversely related to the extent of the osmotic cell swelling recorded under hypoosmotic conditions (*below*). These relations were observed during the ontogenetic development (*left side*) and during retinal ischemia-reperfusion (*right side*) which was induced by a 1-h elevation of the intraocular pressure above the systolic blood pressure. The images shown at right display examples of potassium current records in individual Müller cells. Kir currents are depicted downwardly (*arrowhead*). (**b**) In Müller cells of the rabbit, the density of Kir currents (*above*) is inversely related to the incidence of Müller cells that respond to administration of ATP (200 μM) with a rise in the cytosolic calcium level (*below*). This relation was observed during the postnatal development (*left side*), as well as during experimental retinal detachment and proliferative vitreoretinopathy (PVR; *right side*). PVR is a common complication of retinal detachment in human subjects that is associated with a massive proliferation of Müller cells. Note that the developmental increase in Kir currents occurs earlier in rabbit cells (**b**) compared to rat cells (**a**) that is in accordance with the different time points of eye opening (rabbit: around the postnatal day 10; rat: around the postnatal day 15). (**c**) Examples of peak calcium responses (*bright areas*) to ATP (200 μM) on the inner retinal surface of rabbit retinas. Whereas nearly all Müller cell endfeet display a calcium response in the retina of the postnatal day-8 rabbit and of the rabbit with PVR, only some Müller cell endfeet respond in the retina of the adult control animal. Modified from Bringmann et al. (1999a), Francke et al. (2001a, b), Uckermann et al. (2002), Uhlmann et al. (2003), Pannicke et al. (2004, 2005a), and Wurm et al. (2006a)

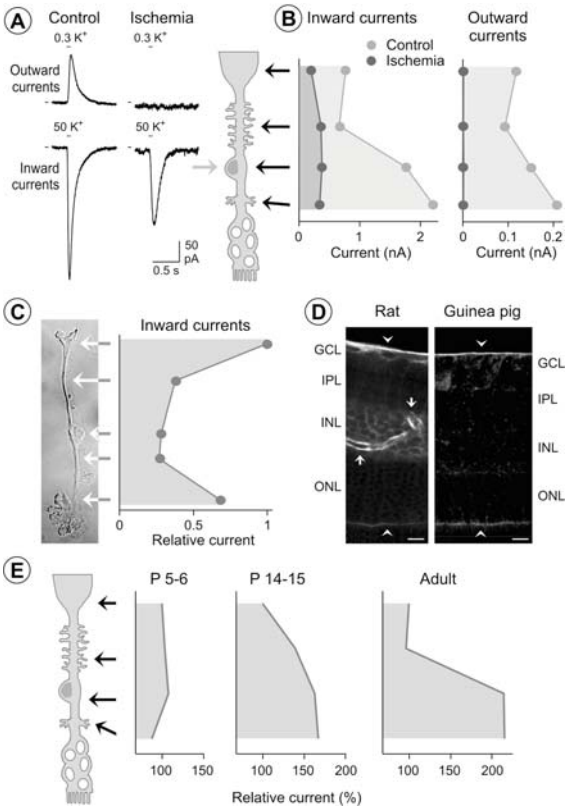

Fig. 2.46 The potassium conductance displays a non-uniform distribution across the surface of Müller cells and decreases under pathological conditions. The subcellular distribution of the potassium conductance was determined by focal ejections of a high- (10 or 50 mM) and a low-potassium (0.3 mM) solution, respectively, onto different membrane domains of isolated Müller cells (endfoot, inner stem process, soma, inner part and end of the outer stem process). The solutions evoke inward and outward potassium currents, respectively. The control potassium concentration was 3 mM. (**a**) Current traces evoked in the soma membrane of rat Müller cells. The cells were isolated from a control retina and a retina obtained three days after transient ischemia. Retinal ischemia-reperfusion was induced by a 1-h elevation of the intraocular pressure above the systolic blood pressure. Note the decrease in the amplitude of the inward current and the almost complete absence of outward currents in the cell of the postischemic retina in comparison to the control cell. (**b**) Subcellular distribution of the inward and outward potassium conductance in rat Müller cells from control and postischemic retinas. (**c**) Subcellular distribution of the inward potassium conductance in Müller cells of the guinea pig. (**d**) Distribution of the Kir4.1 protein in slices of a vascularized (rat) and an avascular retina (guinea pig). In the rat retina, the Kir4.1 protein is prominently located around the vessels within the inner nuclear (INL; *arrows*) and at the limiting membranes of the retina (*arrowheads*). In the guinea pig retina, the Kir4.1 protein is located predominantly at the limiting membranes (*arrowheads*). GCL, ganglion cell layer; IPL, inner plexiform layer; ONL, outer nuclear layer. Bars, 10 μm. (**e**) Developmental alteration in the subcellular distribution of the inward potassium conductance in Müller cells of the rat. The prominent inward conductance in the middle portion of the cells develops relatively late. Relative currents (normalized to the currents at the endfoot region, 100%) are shown. P, postnatal day Modified from Biedermann et al. (2002), Pannicke et al. (2004), and Wurm et al. (2006a)

with vascularized retinas (rat, mouse, *Aotus*) have the highest conductance in the middle portion of the cells, i.e. at the soma and the inner part of the distal cell process (Fig. 2.46b) (Newman, 1987; Connors and Kofuji, 2002; Pannicke et al., 2004). These cell portions are located in the inner nuclear layer in situ where retinal blood vessels form a sheath-like network, and where Kir4.1 channels are located in perivascular membranes of Müller cells (Fig. 2.46d). In Müller cells of the cat (vascularized retina), the highest potassium conductance is localized at the outer (photoreceptor) end of the cells that has contact to the subretinal space (Newman, 1987). The distribution of the potassium conductance (mainly reflecting the distribution of currents through Kir4.1 channels) suggests that Müller cells of avascular retinas extrude the vast majority of excess potassium into the vitreous fluid (some release also occurs into the subretinal space) whereas Müller cells of most species with vascularized retinas dissipate excess potassium ions predominantly into retinal capillaries (and, to a lower degree, into the vitreous fluid) (Newman, 1987). In cats, excess potassium from the inner retina is predominantly redistributed towards the subretinal space (Frishman and Steinberg, 1989). Potassium deposited by Müller cells on the ablumenal walls of retinal capillaries would not diffuse passively into the blood because vascular endothelial cells in the central nervous system are largely impermeable to potassium (Hansen et al., 1977). Rather, such potassium ions could be actively transported into the blood by the Na, K-ATPase located on the ablumenal face of vascular endothelial cells (Betz et al., 1980). Potassium released into the subretinal space may buffer the large light-evoked decrease in extracellular potassium produced by photoreceptors (Steinberg et al., 1980), and may be transferred across the retinal pigment epithelium by spatial buffering currents (Immel and Steinberg, 1986).

The efficiency of potassium buffering currents is also dependent on the morphology of Müller cells. In Müller cells of non-vascularized retinas, the resistance for intracellular potassium currents through the inner process of the cells depends on the distance between the sites of potassium influx (plexiform layers) and efflux (endfoot and subretinal microvilli), as well as on the diameter of the inner process (Reichenbach and Wohlrab, 1983, 1986). Müller cells of the retinal center are longer and thinner than cells from the retinal periphery (Fig. 2.5) and thus have a higher resistance against intracellular potassium currents. In addition, the small area of the vitreal endfoot membrane increases the output resistance of the central cells (Reichenbach and Wohlrab, 1986). It has been calculated that rabbit Müller cells are unable to mediate spatial buffering potassium currents through the whole cell bodies when they are longer than $\sim$150 μm (Reichenbach and Wohlrab, 1986; Eberhardt and Reichenbach, 1987). Thus, the potassium clearance function of Müller cells may be a limiting factor for their maximal length in (and thereby for the thickness of) avascular retinas (Dreher et al., 1992); avascular retinas are thinner than vascularized retinas (Chase, 1982). Very probably, there are two potassium current loops in Müller cells of central regions of vascularized retinas; the outer loop redistributes potassium from the outer plexiform layer and the outer part of the inner plexiform layer into the blood vessels, and the inner loop removes the potassium from the inner part of the inner plexiform layer and from the ganglion cell layer into the vitreous.

Increase in Kir Currents During Development of Müller Cells

A high expression level of Kir channels (especially of Kir4.1 channels) is the precondition for a stable negative membrane potential (Fig. 2.44d), and is required for various fundamental functions of Müller cells such as the maintenance of the retinal potassium homeostasis, the effective clearance of neurotransmitters through electrogenic transporters, and cell volume homeostasis. Therefore, a high expression level of functional Kir channels is a major criterion of differentiated Müller cells (Bringmann et al., 2000a) (cf. Section 2.2.7). In the course of the ontogenetic development of the retina, Müller cells differentiate from mitotically active late progenitor cells. In the developing rabbit retina, late progenitors proliferate up to postnatal days 4 (central retina) and 10 (peripheral retina), respectively (Reichenbach et al., 1991a). In the course of the maturation of rabbit Müller cells from progenitor cells after the postnatal day 5, the profile of the membrane conductances alters from a current pattern with prominent K_A and BK currents into a pattern with large Kir, K_{DR}, and BK currents (Fig. 2.47a). Müller cell maturation is associated with an increase in the density of single Kir channels in membrane patches (Fig. 2.42d) (Bringmann et al., 1999a). The resting membrane potential is increased to values negative to –80 mV (around postnatal day 12) when the amplitude of the Kir currents is increased to ~40% of the adult level (Fig. 2.47d). The developmental increase in Kir currents between postnatal days 6 and 20 occurs along with the the light-evoked ganglion cell activity and the increase in the density of retinal synapses (Fig. 2.47d).

In developing Müller cells of the rat, the Kir currents increase after the postnatal day 11 (Fig. 2.45a) which is associated with the emergence of Kir4.1 protein in the retina (Fig. 2.48) (Wurm et al., 2006a). The developmental expession of the Kir4.1 protein occurs in two phases. Around the postnatal day 15, the Kir4.1 protein is distributed relatively uniformly along the Müller cell fibers; thereafter, the Kir4.1 protein is redistributed towards a prominent localization in Müller cell membranes that surround the blood vessels and at the limiting membranes of the retina (Fig. 2.48). The redistribution of the Kir4.1 protein is reflected by the developmental alteration of the potassium conductance of Müller cells. The potassium conductance displays a relatively uniform distribution in Müller cells around the postnatal day 15, before the development of a prominent conductance in the middle portion of the cells (Fig. 2.46e) (Wurm et al., 2006a). The developmental increase in Kir currents and the decrease in K_A currents are delayed by visual deprivation (Wurm et al., 2006a), suggesting that light-driven neuronal activity accelerates the maturation of Müller cells.

Kir Currents in Gliotic Müller Cells

Under various pathological conditions, there is a downregulation and/or dislocation of Kir4.1 channels which is accompanied by a decrease in the potassium conductance of Müller cells indicating a functional inactivation of Kir channels (cf.

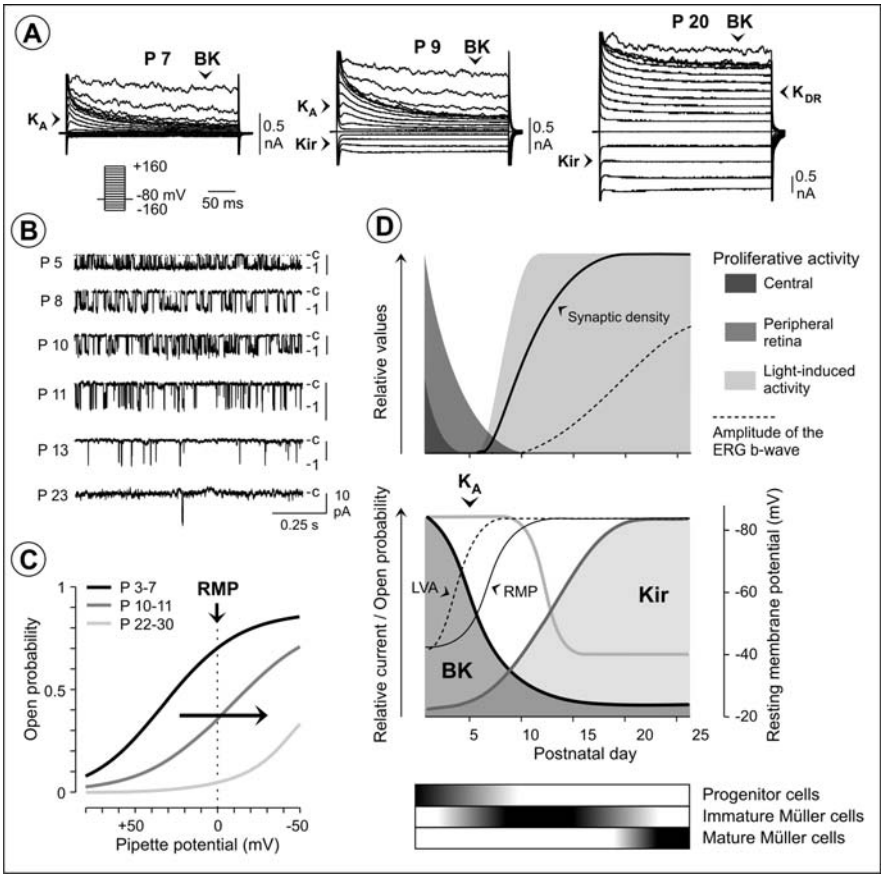

Fig. 2.47 Developmental alterations in the potassium conductance of rabbit Müller cells. (**a**) In the course of the postnatal development, the amplitude of the Kir currents increases. Examples of whole-cell potassium currents of three cells from postnatal day (P) 7, 9, and 20 rabbits. Note the different current scalings. (**b**) The activity of single BK channels recorded in cell-attached membrane patches with a pipette potential of 0 mV (i.e. near the resting membrane potential) decreases with the postnatal age. **c**, closed state; 1, open state current level. (**c**) The activation curve of BK channels (i.e. the relation between the open-state probability of the channels and the pipette potential which is inversely related to the membrane potential of the cells) displays a developmental shift towards more positive membrane potentials. The activity of the channels near the resting membrane potential (RMP) decreases strongly. (**d**) The potassium conductance of Müller cells alters along the maturation of the retina. *Above*: Markers of retinal development: proliferative activity in the retina (Reichenbach et al., 1991a); percentage of light-responsive ganglion cells (Masland, 1977); density of ribbon synapses (McArdle et al., 1977); and the amplitude of the electroretinogram (ERG) b-wave (Noell, 1958). *Middle*: Mean alterations in the open-state probability of BK channels at the resting membrane potential, in the amplitudes of Kir and K_A currents, in the amplitude of currents through low voltage-activated (LVA) calcium channels, and in the resting membrane potential in dependence on the postnatal age. *Below*: Schedule of Müller cell development from mitotically active late progenitor cells. Modified from Bringmann et al. (1999a, 2000c)

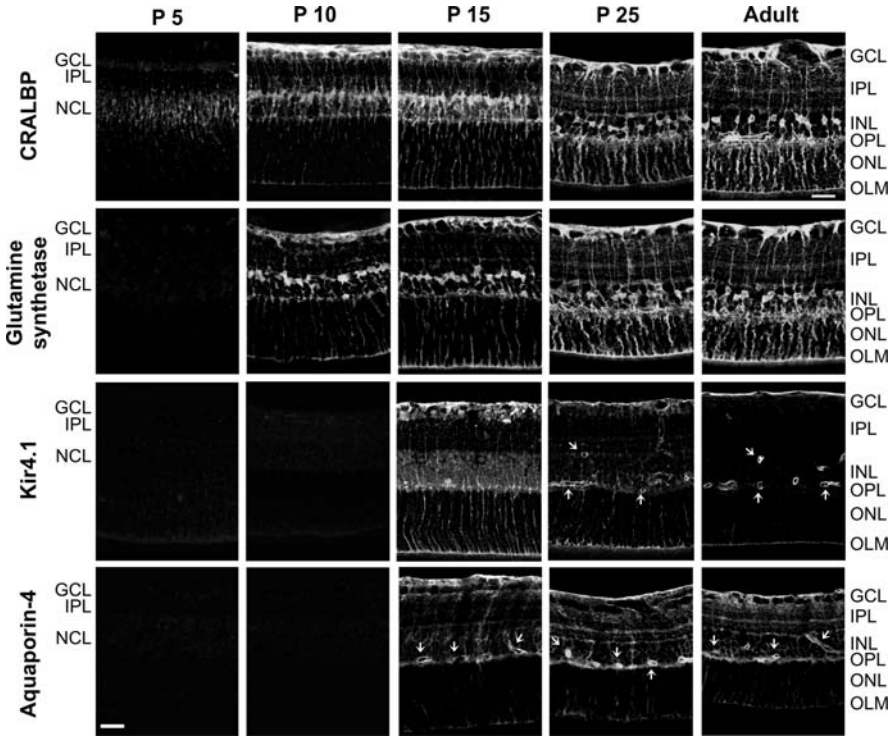

Fig. 2.48 Expression of Müller cell proteins in the developing rat retina. Retinal slices from animals of different postnatal days (P), and of adult animals, were immunostained against CRALBP, glutamine synthetase, Kir4.1, and aquaporin-4 proteins. The Kir4.1 protein displays a relatively uniform distribution across the whole length of Müller cell fibers at P 15, and redistributes towards a prominent localization around the retinal vessels (*arrows*) and at the limiting membranes of the retina in the further course of development. On the other hand, aquaporin-4 protein displays a distribution similar to adult tissues from the very beginning of developmental expression. GCL, ganglion cell layer; INL, inner nuclear layer; IPL, inner plexiform layer; NCL, neuroblastic cell layer; OLM, outer limiting membrane; ONL, outer nuclear layer; OPL, outer plexiform layer. Bar, 20 μm (for all images). Modified from Wurm et al. (2006a)

Sections 3.1 and 3.1.2). Such a decrease in the Kir current amplitude, and a redistribution of the Kir4.1 protein from the prominent expression sites around the vessels and at the limiting membranes of the retina, were observed in experimental models of retinal ischemia-reperfusion (Figs. 2.43b and 2.45a), ocular inflammation, diabetic retinopathy (Fig. 3.13b), retinal detachment and proliferative retinopathy (Fig. 2.45b), and blue light-evoked retinal degeneration (Fig. 3.15b) (Francke et al., 2001a, b, 2002; Uhlmann et al., 2003; Pannicke et al., 2004, 2005a, b, 2006; Uckermann et al., 2005a; Iandiev et al., 2006a, b, 2008a; Wurm et al., 2006b). After transient retinal ischemia, there is a decrease in Kir4.1 (but not Kir2.1) gene and protein expression (Fig. 2.43b) (Pannicke et al., 2004; Iandiev et al., 2006a). A strong decrease in Kir currents, and a decrease in the gene expression of Kir4.1,

were also observed in human Müller cells from patients with proliferative retinopathy (Fig. 2.40b) (Francke et al., 1997; Bringmann et al., 1999b, 2001, 2002b; Tenckhoff et al., 2005). Under these conditions, the Kir4.1 protein is distributed relatively uniformly across the Müller cell membranes. The current pattern with small Kir currents, as well as the uniform distribution of the Kir4.1 protein in Müller cells, resemble the characteristics of developing Müller cells in the postnatal period, before they differentiate into mature cells (Fig. 2.45a, b) (Bringmann et al., 1999a; Pannicke et al., 2002; Wurm et al., 2006a); these alterations reflect the dedifferentiation of adult Müller cells under pathological conditions (see also Section 3.1.4).

However, Müller cell gliosis is not necessarily associated with a reduction in Kir currents, i.e. Müller cells respond in a different fashion to various pathological stimuli. Severe pathological conditions may occur without any significant decrease in the Kir conductance of Müller cells. Examples for such an "atypical" Müller cell gliosis are the Borna disease virus-induced retinitis, inherited photoreceptor degeneration in Royal College of Surgeons (RCS) rats, destruction of the optic tract, or bright white light-induced retinal degeneration; in these cases, other signs of gliosis (such as increased immunoreactivity for GFAP and cellular hypertrophy) were obvious (Pannicke et al., 2001; Felmy et al., 2001; Iandiev et al., 2008b; and own unpublished results). In *rds* mice that display a slow degeneration of photoreceptor cells, only a slight transient decrease in the Kir current density (but no alteration in the Kir4.1 protein) was found; this was explained by a transient hypertrophy of the cells (Iandiev et al., 2006d).

A decrease in functional Kir channels is associated with a depolarization of the Müller cells when the Kir currents are decreased to values lower than ~40% of control (Fig. 2.45a) (Pannicke et al., 2005a). Though other types of potassium channels such as K_{DR}, BK, or TASK-like channels may maintain a less negative membrane potential between –50 and –40 mV (Pannicke et al., 2000a; Skatchkov et al., 2006), the potassium siphoning by Müller cells must be severely impaired under such conditions since membrane hyperpolarization is a precondition for the passive transglial potassium currents. Moreover, BK (and probably TASK) channels are not continuously open (like Kir channels) but activate only after receptor stimulation. When the potassium fluxes through Kir channels are impaired, Müller cells are stimulated to remove excess potassium by an active uptake via their Na, K-ATPase (Reichenbach et al., 1986, 1992). Elevations in extracellular potassium increase the activity of Na, K-ATPases in cultured Müller cells (Reichelt et al., 1989) which lack functional Kir channels (Kuhrt et al., 2008). This activation may finally cause functional overload and metabolic exhaustion of the cells. The depolarization of Müller cells after functional inactivation of the Kir channels will also result in an impairment of the electrogenic neurotransmitter uptake by the cells (Napper et al., 1999). Since the Kir conductance of Müller cells is involved in potassium homeostasis, neurotransmitter recycling, and water homeostasis, the dysfunction of Müller cells represents one major factor that causes neuronal hyperexcitation, glutamate toxicity, and the development of tissue edema under pathological conditions. Human Müller cells display an age-dependent decrease in the Kir current amplitude, on average by

approximately 50% between the ages of 40 and 80 years (Fig. 2.63c) (Bringmann et al., 2003a) which is near the threshold for a decrease in the resting membrane potential of Müller cells (Fig. 2.44d). The age-dependent decrease in Kir currents is associated with other gliotic signs such as an upregulation of GFAP expression (Wu et al., 2003), and may contribute to neuronal degeneration and to the development of tissue edema when additional pathological complications such as diabetic alterations of the blood vessels occur. Glutamate and blood plasma (which contains glutamate) decrease the Kir (and K_A) currents in Müller cells, suggesting that a leakage of blood serum compromises the potassium homeostasis of Müller cells (Kusaka et al., 1999).

The mechanism of the decrease in Kir currents under distinct pathological conditions is unclear. In experimental ocular inflammation, a transient downregulation of Kir4.1 was shown at the mRNA and protein level (Liu et al., 2007). A decrease in the retinal content of Kir4.1 mRNA and protein was also shown in retinal ischemia-reperfusion and in tissues from patients with a proliferative retinopathy (Pannicke et al., 2004; Tenckhoff et al., 2005; Iandiev et al., 2006a), whereas in an animal model of proliferative retinopathy, a dislocation and functional inactivation of Kir4.1 was not accompanied by a decrease in the Kir4.1 mRNA and protein content of Müller cells (Ulbricht et al., 2008). Extracellular matrices are involved in the distribution of Kir4.1 protein. In cultured Müller cells, the membrane anchoring and the clustered distribution of Kir4.1 channels, as well as the amplitude of Kir currents, depend on the presence of the extracellular matrix molecule, laminin (Ishii et al., 1997). Channel clustering enhances the activity of Kir4.1 (Horio et al., 1997). The clustering activity of laminin is translated into a subcellular localization signal for Kir4.1 in a PDZ-ligand domain-mediated fashion by dystroglycan, a central element of the dystrophin-associated protein complex (Noel et al., 2005). At its core, this complex includes α-syntrophin, the short dystrophin isoform Dp71, the transmembrane protein ß-dystroglycan, and the extracellular matrix receptor α-dystroglycan (Claudepierre et al., 2000). After transient ischemia of the rat retina, which causes a dislocation of the Kir4.1 protein (Fig. 2.49), the immunolabelings of laminin and type IV collagen remain unaltered, whereas dystrophin shows a redistribution similar to that of Kir4.1 protein (Fig. 2.49), suggesting that the downregulation of Kir4.1 occurs secondary to a disruption of the dystrophin complex. A similar disrupted distribution of the Kir4.1 protein (but no decrease in the potassium currents) has been observed in retinas of mdx^{3Cv} mice that fail to express dystrophin (Connors and Kofuji, 2002), and of mice with a genetic inactivation of Dp71 (Dalloz et al., 2003; Fort et al., 2008) which is involved in the clustering (but not membrane insertion) of Kir4.1 channels (Connors and Kofuji, 2002; Noel et al., 2005). The more diffuse distribution of Kir4.1 protein in Dp71-null mice is associated with an enhanced vulnerability of retinal ganglion cells to ischemia-reperfusion injury (Dalloz et al., 2003) which is known to be (at least in part) mediated by the toxicity of excess glutamate (Osborne et al., 2004). Very likely, a dysregulation of the glutamate uptake by Müller cells after alterations in Kir channel expression/localization contributes to the elevation in extracellular glutamate in ischemic retinas.

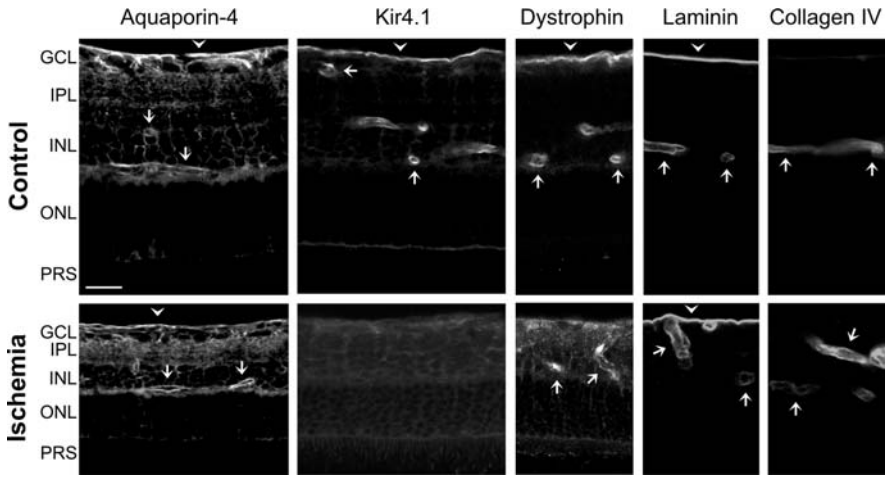

Fig. 2.49 The mislocation of the Kir4.1 channel protein induced by ischemia-reperfusion of the retina is accompanied by a more diffuse location of the dystrophin protein which is implicated in the membrane clustering of Kir4.1 channels. The proteins were immunostained in retinal slices of a control rat (*above*) and in slices obtained seven days after a 1-h transient retinal ischemia (*below*). The distribution of the aquaporin-4 protein, and of the basement membrane proteins laminin and type IV collagen was not altered after ischemia. The arrows indicate protein enrichment around the vessels, and the arrowheads point to the inner limiting membrane. Note the decreased thickness especially of the inner plexiform layer (IPL) which is a characteristic of retinal ischemia-reperfusion injury. GCL, ganglion cell layer; INL, inner nuclear layer; ONL, outer nuclear layer; PRS, photoreceptor segments. Bar, 20 μm (for all images). Modified from Pannicke et al. (2004)

2.4.2.2 BK Channels

In addition to Kir channels, BK channels may be involved in the activity-dependent buffering of extracellular potassium (Puro et al., 1996a; Ishii et al., 1997). This assumption can be drawn from the observation that extracellular nucleotides stimulate the activity of single BK channels at the resting membrane potential of Müller cells (Fig. 2.50) (Bringmann et al., 2002a). In addition to nucleotides, extracellular glutamate stimulates the opening of BK channels (Fig. 2.51) (Bringmann and Reichenbach, 1997), suggesting that BK channels of Müller cells are a target of neuron-derived signaling molecules. BK channels are potassium channels of big conductance between 100 and 135 pS in cell-attached membrane patches with high potassium (130 mM) in the pipette solution (Bringmann et al., 1998a, b, 1999a, b; Schopf et al., 1999). These channels are frequently found (in addition to Kir channels) in membrane patches of Müller cells from various species (Figs. 2.42d and 2.52a) (Bringmann et al., 1999a). Single Kir and BK channels are well discernible due to their different channel conductance (Fig. 2.40d), the different voltage dependence of channel opening, as well as the different gating properties with the presence (BK) vs. absence (Kir) of flickery closures during the opening of the channels.

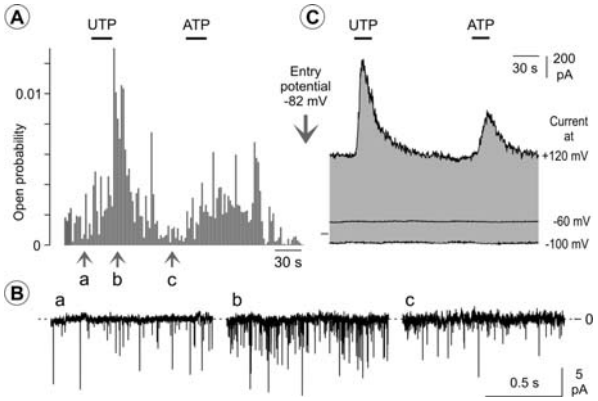

Fig. 2.50 Extracellular nucleotides stimulate the activity of BK channels at the resting membrane potential of a human Müller cell. (**a**) Time dependency of the open-state probability of single BK channels recorded in cell-attached patches of the soma membrane of an isolated cell from a post-mortem human donor without eye diseases. The pipette potential was held at 0 mV, i.e. the channel activity was recorded near the resting membrane potential of the cell. Extracellular administration of UTP (100 μM) and ATP (100 μM) resulted in a transient increase in the open-state probability of the channels. (**b**) Examples of channel records at the three time points indicated in (**a**). The downward deflections represent potassium fluxes from the extra- to the intracellular side of the membrane through single BK channels. 0, closed state current level. (**c**) After the end of the cell-attached records, the whole-cell mode was established and the agonists were tested again to verify that they induce an increase in the whole-cell BK currents. The whole-cell currents were recorded at three potentials. Shortly after the rupture of the cell membrane, the membrane potential of the cell was measured in the current clamp mode and was found at –82 mV. Modified from Bringmann et al. (2002a)

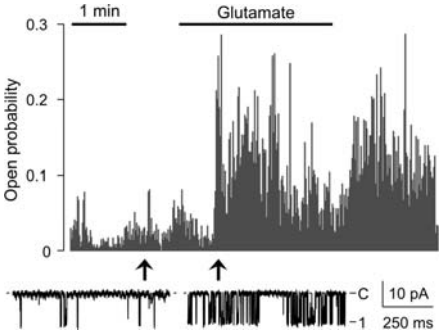

Fig. 2.51 Extracellular glutamate (200 μM) increases the activity of a single BK channel that was recorded in the cell-attached mode in a soma membrane patch of a human Müller cell. *Above*: Time dependency of the open-state probability. *Below*: Original records of the channel activity. The pipette potential was 0 mV (i.e. the recording was made near the resting membrane potential of the cell). **c**, closed state; 1, open state current levels

The regulation of the BK channel activity in Müller cells has been extensively investigated. These channels are mainly activated by membrane depolarization (Fig. 2.52a) and by an increase in the free calcium level at the intracellular side of the plasma membrane (Fig. 2.52b) (Bringmann et al., 1997, 1999a, b). The sigmoid activation curve of the channel (reflecting the increase in channel openings in

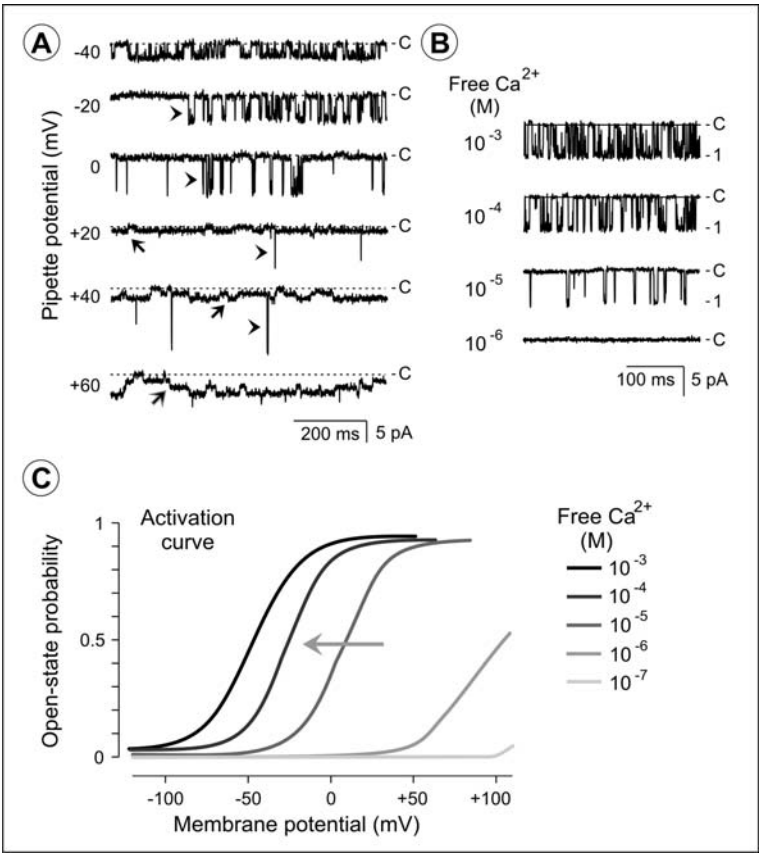

Fig. 2.52 Membrane depolarization and intracellular calcium activate BK channels in Müller cells. (**a**) Voltage dependency of a BK channel in a cell-attached membrane patch of a human Müller cell. The records display the activity of one BK channel (*arrowheads*) and at least three Kir channels (*arrows*) at different pipette potentials (that is inversely related to the membrane potential of the cell). A pipette potential of 0 mV is near the resting membrane potential of the cell. Note that the activity of the BK channel increases with membrane depolarization (negative pipette potentials). **c**, closed state current level. (**b**) Elevation of the calcium concentration at the cytosolic side of an excised membrane patch from a rabbit Müller cell increases the activity of a BK channel. (**c**) The activation curve of BK channels (recorded in excised membrane patches of human Müller cells) is shifted towards more negative membrane potentials when the calcium concentration at the cytosolic side of the patches increases. Modified from Bringmann et al. (1997, 1999b)

response to membrane depolarization) shifts towards more negative (i.e. physiologically relevant) potentials when the intracellular calcium level increases (Fig. 2.52c). The calcium-dependent open-state probability of human BK channels indicates a Hill coefficient of 1.7 (Bringmann et al., 1997), suggesting that two calcium binding sites are involved in channel opening. BK channels in excised membrane patches of Müller cells from various mammalian species display a half-maximal activation between 0 and +10 mV when the cytosolic calcium concentration is 10 μM (Bringmann et al., 1997, 1998b, 1999a; Schopf et al., 1999). This low calcium sensitivity suggests that Müller cells express the pore-forming α-subunit but not the regulatory ß-subunit of BK channels (Wallner et al., 1996). On the other hand, cultured human Müller cells express the ß2-subunit of BK channels after treatment with 17ß-estradiol; the ß-subunit-evoked shift of channel gating towards more negative membrane potentials may be implicated in the apoptosis-preventing effect of this sex steroid (Li et al., 2006).

There are several coactivating factors of BK channels in Müller cells. Intracellular magnesium ions increase the activity of BK channels (shift of the activation curve of the channel towards more negative potentials) but inhibit the potassium currents through the channel pore (resulting in a decrease in the amplitude of the channel currents) (Bringmann et al., 1997). The channel activity is also regulated by the cytosolic pH; an increase in the proton concentration decreases the channel opening probability (Bringmann et al., 1997), likely via interaction of the protons with the calcium binding sites of the channel protein. Arachidonic acid, which may be produced (for example) in response to neurotransmitters via a G protein and/or calcium-mediated stimulation of phospholipase A_2, strongly activates the BK channel activity in Müller cells (Bringmann et al., 1998a). In addition to arachidonic acid, various other polyunsaturated fatty acids (such as docosahexaenoic acid) stimulate the activity of BK channels. Membrane stretch increases the activity of BK channels, likely after opening of stretch-activated calcium-permeable cation channels (Puro, 1991b). The BK channel protein is a target of protein kinases. Whereas phosphorylation of the channel protein by protein kinase A increases the channel activity, phosphorylation by protein kinase C reduces the activity of the channels (Bringmann et al., 1997; Schopf et al., 1999). The inhibitory action of protein kinase C may limit the time period of channel activation when receptor agonists cause an increase in cytosolic calcium. The activation of BK channels by the action of protein kinase A is a further indication for a lack of a regulatory ß-subunit in BK channels of Müller cells (Dworetzky et al., 1996).

There are various inhibitors and activators of BK channels in Müller cells that can be used in electrophysiological investigations. The flavoid phloretin is a BK channel opener (Bringmann and Reichenbach, 1997) thought to act directly at the fatty acid binding sites of the pore-forming α-subunits of the channels (Gribkoff et al., 1997). Tetraethylammonium (TEA) at a concentration of 1 mM is a selective blocker of BK channels in Müller cells, exerting essentially no effects onto currents through Kir, K_A or K_{DR} channels (Bringmann et al., 1997, 2007). TEA is an open channel blocker, and the binding site is localized at the outer (but not inner) side of the pore region of the channel. A further selective blocker of open BK channels is iberiotoxin

(Latorre, 1994). Barium ions, when applied to the cytosolic (but not to the extracellular) side of membrane patches, inhibits the channel activity (Bringmann et al., 1997), likely via competition with calcium ions for the calcium binding sites of the channel protein. The inhibitory effect of barium on the BK channels at the cytosolic side of the membrane makes it sometimes difficult to explore the activity of BK channels in whole-cell current records when extracellular barium (administered to block the Kir currents) enters the cell interior through calcium channels.

The diverse possibilities of regulation of the channel activity (Fig. 2.53) together with the large conductance of the channel (resulting in a strong hyperpolarization of the membrane around the channels) suggest that BK channels provide an important link between various intracellular second messenger systems and the membrane conductance of Müller cells. Extracellular signaling molecules that induce an increase in cytosolic calcium or cAMP, a stimulation of the production of arachidonic acid, or a depolarization by activation of electrogenic uptake carriers (e.g. glutamate: Fig. 2.51), may cause an opening of BK channels. An increase in extracellular potassium concentration is associated with intracellular alkalinization (Newman, 1996). An intracellular alkalinization increases the opening probability of BK channels that will support the uptake of excess potassium released from activated neurons and, via membrane hyperpolarization, the electrogenic uptake of neurotransmitter molecules.

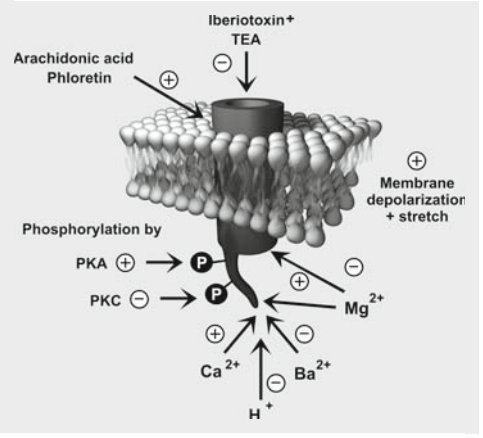

Fig. 2.53 Summary of factors that display stimulatory (+) and inhibitory (–) effects on the BK channel activity and conductance, respectively

Decrease in BK Channel Activity During the Development of Müller Cells

The ontogenetic development of Müller cells from mitotically active late progenitor cells is characterized by an increase in the expression of Kir channels that causes a negative shift in the resting membrane potential from values around –40 mV to approximately –80 mV (Figs. 2.45a and 2.47d). The developmental membrane hyperpolarization causes a strong decrease in the BK channel activity at the resting membrane potential (Fig. 2.47c) (Bringmann et al., 1999a). BK channels in Müller cells from young postnatal rabbits display a high open-state probability at the

resting membrane potential; in the course of development, the activity of the channels decreases (Fig. 2.47b). Since the calcium sensitivity of the channels does not change in the course of ontogenetic development, it is suggested that the decrease in the BK channel activity is predominantly caused by the increase in the resting membrane potential (Bringmann et al., 1999a). The activity of BK channels and the expression level of Kir channels are inversely related in developing Müller cells (Fig. 2.47d) and in gliotic Müller cells under pathological conditions (Fig. 2.54). It is suggested that a high activity of BK channels supports the proliferation of progenitor cells in the developing retina, and of gliotic Müller cells in the adult retina (Bringmann et al., 2000a).

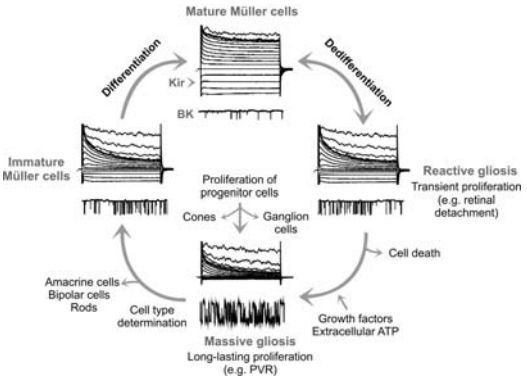

Fig. 2.54 The amplitude of Kir currents and the activity of BK channels alter inversely in dependence on the differentiation degree of Müller cells. Mature Müller cells display Kir currents with large amplitude and a small activity of BK channels at the resting membrane potential. A dedifferentiation of Müller cells under pathological conditions is associated with a decrease in the amplitude of Kir currents and an increase in the activity of BK channels. During the early development of the retina, progenitor cells do not display Kir currents while the proliferation of the cells is supported by a high activity of BK channels. In the course of the maturation of Müller cells from progenitor cells, the amplitude of the Kir currents increases and the activity of BK channels decreases. Modified from Bringmann et al. (2000a)

Whole-Cell BK Currents

In records of the whole-cell currents, the selective BK channel blockers TEA (at a concentration of 1 mM) and iberiotoxin can be used to identify the currents mediated by BK channels. Since both agents are open channel blockers, it may be helpful to activate the BK channels (for example by phloretin: Fig. 2.55a) before administration of the blocking agents, to enhance the probability of binding of the blocking substances within the channel pores. In whole-cell records, BK currents are activated at positive membrane potentials (Newman, 1985b; Bringmann et al., 2002a). Activation of whole-cell BK channels at positive potentials was also found in glioma cells (Ransom and Sontheimer, 2001) and is assumed to be a recording artifact since

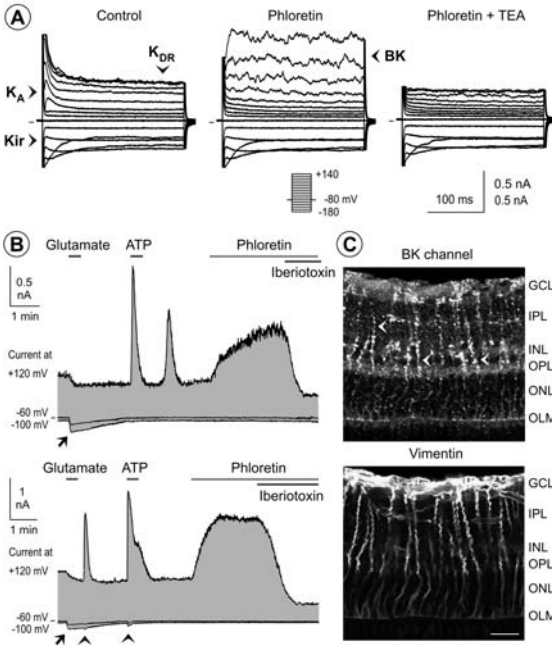

Fig. 2.55 Identification of BK channel-mediated currents in whole-cell records of the potassium currents of Müller cells. (**a**) Current traces of a Müller cell isolated from an experimentally detached porcine retina. The BK channel opener phloretin (200 μM) evokes an increase in the outward currents which is reversed by co-administration of the BK channel blocker TEA (1 mM). Note that phloretin decreases the amplitude of K_A and K_{DR} currents. (**b**) Time-dependent records of the whole-cell currents in two human Müller cells. The currents at +120 mV are mainly mediated by BK channels, as indicated by the effects of the BK channel opener phloretin (200 μM) and the selective BK channel inhibitor iberiotoxin (100 nM). The BK currents are transiently inreased in response to extracellular ATP (500 μM). Extracellular glutamate (500 μM) evokes a delayed transient increase in BK currents in a subpopulation of human Müller cells. The increase in the currents at –60 and –100 mV during the exposure of glutamate (*arrows*) reflects the activation of electrogenic (sodium-dependent) glutamate uptake carriers. The glutamate-evoked decrease of the currents at +120 mV likely reflects an inhibition of potassium channels by sodium ions which are transported from the extracellular space to the cell interior through electrogenic (sodium-dependent) glutamate transporters. The arrowheads indicate transient activation of calcium-evoked cation currents. (**c**) Immunoreactivities for the α-subunit of BK channels and vimentin in a slice of a porcine retina. The *arrowheads* mark Müller cell fibers that display BK channel protein. GCL, ganglion cell layer; INL, inner nuclear layer; IPL, inner plexiform layer; OLM, inner limiting membrane; ONL, outer nuclear layer; OPL, outer plexiform layer. Bar, 20 μm. Modified from Bringmann et al. (2002a, 2007)

in fact the channels activate at the resting (or slightly depolarized) potentials when the recordings are made in the cell-attached mode just before the rupture of the plasma membrane (Fig. 2.50). It is suggested that the positive shift of the activation threshold is caused by the loss of essential cytoplasmic components that coactivate the channels (such as activators of the protein kinase A) when the cell interior is filled with the pipette solution.

There is a conspicuous species dependency in the expression of BK channels. Whereas all Müller cells from toads, rabbits, and man investigated so far displayed BK currents in whole-cell currents records (Bringmann et al., 1998a, b, 1999a, b, 2000f), only about 50% of porcine Müller cells displayed such currents (Bringmann and Reichenbach, 1997), and no BK currents could be recorded in Müller cells from rats, mice, guinea pigs, sheeps, horses, and monkeys (Pannicke et al., 2005a, c, and unpublished data). (However, cultured guinea pig Müller cells possess BK channels [Kodal et al., 2000], suggesting that the expression level of the channels depends on the differentiation state of the cells.) In porcine Müller cells, the immunoreactivity of BK channels is localized in a clustered fashion, especially in the inner processes (Fig. 2.55c) (Bringmann et al., 2007), suggesting a role of these channels in the interaction between Müller cells and second- and third-order neurons of the retina. This interaction may be mediated by activation of the channels by neuron-derived transmitters such as glutamate (Figs. 2.51 and 2.55b) and nucleotides (Figs. 2.50 and 2.55b).

2.4.2.3 K_A Currents

The presence of fast transient K_A currents was firstly described in Müller cells of the tiger salamander (Newman, 1985b). As in the case of BK channels, there is a variation in the expression of K_A currents among Müller cells of various mammalian species. Approximately 75% of human Müller cells, 60% of monkey Müller cells, and 35% of rabbit Müller cells investigated express K_A currents (Bringmann et al., 1999a, b; Pannicke et al., 2005c) whereas almost no Müller cells of the rat and mouse express such currents (Pannicke et al., 2002, 2005a). However, the expression of K_A currents is dependent on the differentiation state of Müller cells. Both the incidence of cells displaying K_A currents and the amplitude of these currents (Fig. 2.47d) decrease in the course of ontogenetic maturation of Müller cells (Bringmann et al., 1999a; Wurm et al., 2006a). Under various pathological conditions in the retina of adult rats, a decrease in the Kir channel-mediated potassium currents of Müller cells is accompanied by an emergence of K_A currents (Pannicke et al., 2005a, b, 2006). While Müller cells of the mature retina of the rat normally do not express such currents (Fig. 3.5a), the incidence of cells displaying K_A currents strongly increases after transient ischemia (Fig. 3.5b), for example (Pannicke et al., 2005a). In Müller cells of the rat, an increase in the incidence of K_A currents is an early sign of gliosis, even when the Kir channels are not (yet) downregulated (Pannicke et al., 2001). The functional role of the increase in K_A currents under pathological conditions is unclear. K_A channels are implicated in rapid fluctuations of the membrane potential, likely together with voltage-dependent sodium channels (Wurm et al., 2006a). Rapid fluctuations of the membrane potential are necessary for the activation of voltage-dependent calcium channels, for example. Currents through voltage-dependent calcium channels mediate the mitogen-evoked calcium entry implicated in the proliferation of Müller cells, and it can be speculated that an increase in the activity of K_A channels support the proliferation of retinal progenitor cells and Müller cells under pathological conditions.

2.4.2.4 Other Potassium Channels in Müller Cells

Under distinct pathological conditions, when the Kir channels are downregulated or inactivated, other types of potassium channels (in addition to BK channels) may contribute to the potassium clearance by Müller cells. Müller cells of several amphibian and mammalian species express two pore-domain (TASK-like) channels (Eaton et al., 2004; Skatchkov et al., 2006). Currents through these outwardly rectifying potassium channels (Fig. 2.43a) contribute to the K_{DR} currents, and are implicated in the maintenance of the resting membrane potential when the Kir channels are inactivated. These channels may have also functional importance in the neuron-abutting membrane domains of Müller cells which are poorly equipped with Kir4.1 channels but express strongly rectifying Kir2.1 channels (Fig. 2.43b). Here, these channels may help to stabilize the very negative membrane potential of Müller cells that is necessary to reach the opening threshold of Kir2.1 channels. TASK-like channels are also implicated in the agonist-mediated regulation of the cellular volume under osmotic stress conditions when the Kir4.1 channels are inactivated or downregulated (Skatchkov et al., 2006).

Another type of potassium channels expressed by Müller cells are K_{ATP} channels which are inhibited in their activity by intracellular ATP. The pore-forming subunit of K_{ATP} channels (Kir6.1) is expressed in Müller cells of various vertebrate species (Skatchkov et al., 2001, 2002; Eaton et al., 2002). In frog Müller cells, the Kir6.1 protein is enriched in the endfoot membranes of the cells, and displays a colocalization with the Kir4.1 protein. Under conditions of ATP depletion, e.g. ischemia, spatial buffering potassium currents through K_{ATP} channels may help to protect the neurons from excitotoxic cell death.

2.4.3 Potassium and Water Channels: Retinal Water Homeostasis

2.4.3.1 Water Fluxes Through the Retina

Under normal conditions, water accumulates in the retinal tissue due to various processes (Fig. 2.56), including (i) an influx of water from the blood into the retinal parenchyma coupled to the uptake of metabolic substrates such as glucose, (ii) an endogenous production of water due to the aerobic energy production (the oxidative breakdown of one molecule of glucose results in the formation of 42 molecules of water), and (iii) an influx of water into the retina caused by the intraocular pressure (Marmor, 1999; Bringmann et al., 2004). The accumulation of metabolic water is especially abundant in the macular tissue because of the high densities of cone photoreceptors and second- and third-order neurons, and the high metabolic activity of photoreceptor cells. Photoreceptor cells need 3–4 times more oxygen than other neurons in CNS including retina, and are probably the cells of the body with the highest rate of oxidative metabolism (Alder et al., 1990; Linsenmeier et al., 1998). This generates the necessity of a substantial constitutive efflux of water out of the neural retina into the blood. In addition to the flux of metabolic water, there are rapid transmembrane ion and water shifts associated with neuronal activity (in particular,

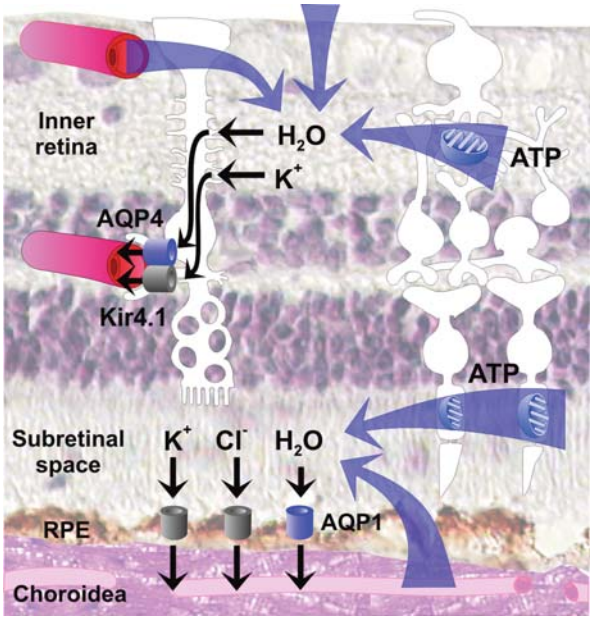

Fig. 2.56 Water fluxes through the retina. Under normal conditions, water accumulates in the neural retina and subretinal space due to an influx from the blood (coupled to the uptake of nutrients such as glucose) and vitreous chamber (due to the intraocular pressure), and the oxidative synthesis of adenosine 5′-triphosphate (ATP) in the mitochondria that generates carbon dioxide and water. The excess water is redistributed into the blood by a transcellular water transport through Müller cells and the retinal pigment epithelium (RPE). The water transport across cell membranes is facilitated by aquaporin (AQP) water channels. RPE cells express aquaporin-1, while Müller cells express aquaporin-4. The transcellular water transport is osmotically coupled to the transport of osmolytes, especially of potassium and chloride ions. The ion fluxes across the cell membranes are facilitated by transporter molecules and ion channels. In Müller cells, the Kir4.1 potassium channel is co-localized with AQP4 in membranes that surround the vessels, and at both limiting membranes of the retina. Modified from Bringmann et al. (2006)

with glutamatergic signaling) which should be buffered to avoid osmotic imbalances in the tissue.

The redistribution of excess water from the retinal tissue into the blood is carried out by pigment epithelial and Müller cells. The pigment epithelium dehydrates the subretinal space (Pederson, 1994) while Müller cells dehydrate the tissue of the neural retina (Bringmann et al., 2004). Water clearance from the retinal tissue is mediated by an osmotically driven transcellular water transport that is coupled to a transport of osmolytes, in particular, of potassium and chloride ions (Bialek and Miller, 1994; Pederson, 1994; Nagelhus et al., 1999). The water fluxes through the membranes of Müller and pigment epithelial cells are facilitated and directed by water-selective channels, the aquaporins.

2.4.3.2 Aquaporins in the Retina

Aquaporins are critically involved in the maintenance of the ionic and osmotic balance in the CNS (Verkman, 2003). There are at least 13 members of the aquaporin protein family (Verkman and Mitra, 2000) that faciliate bidirectional movement of water across membranes in response to osmotic gradients and differences in hydrostatic pressure. Though neural retinas express gene transcripts for numerous aquaporins (Tenckhoff et al., 2005), the presence of immunoreactivities of only four aquaporins have hitherto been demonstrated in the retina. Aquaporin-0 is expressed by bipolar, amacrine, and ganglion cells (Iandiev et al., 2007b); aquaporin-1 is expressed by photoreceptor cells (Fig. 2.57), pigment epithelial and distinct amacrine cells (Kim et al., 1998b, 2002; Stamer et al., 2003; Iandiev et al., 2005a, 2008b); aquaporin-4 is expressed by astrocytes, Müller cells, and vascular endothelial cells (Nagelhus et al., 1998); and aquaporin-9 is present in putative dopaminergic amacrine cells (Iandiev et al., 2006e). Under distinct pathological conditions (ischemia, diabetes), astrocytes and Müller cells express also aquaporin-1 (Fig. 3.13a) (Gerhardinger et al., 2005; Iandiev et al., 2006c, 2007a).

Aquaporin-4 water channels are expressed by Müller cell membranes especially within the inner retinal tissue and the outer plexiform layer, whereas the expression

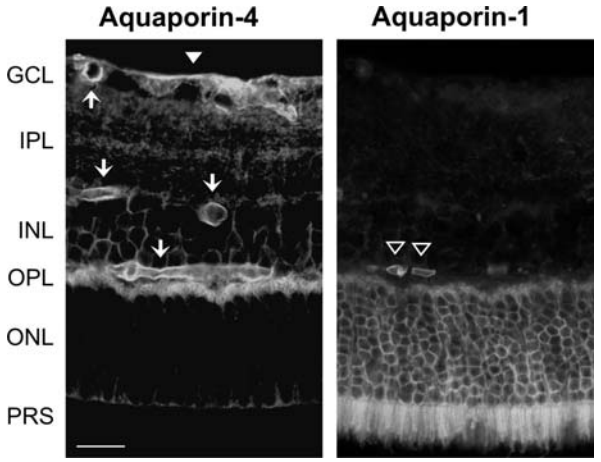

Fig. 2.57 Müller cells mediate the osmohomeostasis predominantly in the inner retina, as suggested by the distribution of the glial water channel protein, aquaporin-4. A retinal slice of the rat was immunostained against aquaporin-1 and -4. The aquaporin-4 protein is strongly expressed by Müller cells in the inner retina and the outer plexiform layer (OPL), whereas the expression of the protein in the outer nuclear layer (ONL) is faint. The aquaporin-4 protein is enriched in Müller cell membranes that surround the vessels (*arrows*), and in the vitreous-abutting endfeet membranes (*filled arrowhead*). Photoreceptor cells express aquaporin-1 protein. The unfilled arrowheads point to aquaporin-1-expressing erythrocytes within the retinal vessels. GCL, ganglion cell layer; INL, inner nuclear layer; IPL, innner plexiform layer; PRS, photoreceptor segments. Bar, 20 μm. Modified from Iandiev et al. (2006c)

in the outer nuclear layer is faint (Fig. 2.57). Kir4.1 and aquaporin-4 proteins are colocalized around blood vessels and at the limiting membranes of the retina, suggesting that the water transport through Müller cells is coupled to the transcellular spatial buffering potassium currents (Nagelhus et al., 1999). The Müller cell-mediated clearance of the retinal tissue from excess potassium will simultaneously redistribute metabolic water out of the neural retina (Bringmann et al., 2004). The colocalization of aquaporin-4 and Kir4.1 proteins also suggests that osmotic gradients between the retinal tissue and the blood and vitreous fluid are compensated by bidirectional potassium and water fluxes through Müller cell membranes. Aquaporin-4 expressed by vascular endothelial cells may be involved in the transcapillary water transfer (Nagelhus et al., 1998). In addition, aquaporin-4 is expressed by Müller cells in perisynaptic membranes in the plexiform and ganglion cell layers; thus, aquaporin-4 is expressed in all membrane domains through which Müller cells take up and release excess potassium. Aquaporin-4 knockout mice display reduced electroretinogram b-waves, suggesting that Müller cell-mediated water fluxes facilitate neural signal transduction (Li et al., 2002a). At the ultrastructural level, aquaporin-4 form the orthogonal arrays of intramembrane particles which are predominantly localized to Müller cell and astrocyte endfeet (Raviola, 1977; Wolburg and Berg, 1987, 1988; Gotow and Hashimoto, 1989; Richter et al., 1990; Wolburg, 1995; Yang et al., 1996; Verbavatz et al., 1997) (cf. Fig. 2.11e, f). Whereas endfoot membranes of frog Müller cells lack these particles, Müller cell endfoot membranes express these particles in all other vertebrates investigated, including urodeles (Wolburg et al., 1992; Wolburg, 1995). The density of these particles varies with the size of vitreal endfoot membranes; it is higher in Müller cells of the central retina than in cells from the retinal periphery (Wolburg and Berg, 1987).

2.4.3.3 Glutamate-Evoked Swelling of Retinal Neurons

As suggested by the retinal distribution of aquaporin-4 (Fig. 2.57) and Kir channel proteins (Fig. 2.43b), Müller cells are responsible for the ion and water homeostasis especially in the inner retina and outer plexiform layer. The particular importance of an efficient osmohomeostasis of the inner retina is mainly justified by the activity-dependent ion and water fluxes which are associated with glutamatergic signaling. Glutamate evokes a swelling of the inner (but not outer) retinal tissue (Fig. 2.58a) (Uckermann et al., 2004a). The thickening of the inner retinal tissue is caused by a swelling of retinal neurons and synapses (Fig. 2.59b, c). The swelling of neurons and synapses induces also morphological alterations of Müller cells, i.e. an elongation (Fig. 2.58b) and a decrease in the thickness (Fig. 2.59d) of the inner stem processes. A similar swelling of retinal neurons (and associated morphological alterations of Müller cells) is observed during stimulation of retinal tissues with a high-potassium solution or with VEGF (Fig. 2.76) (both interventions cause a release of endogenous glutamate), and shortly after a retinal ischemia (Fig. 2.59e) (Uckermann et al., 2004a; Wurm et al., 2008). Metabolic stress and ischemia cause an excessive release of glutamate from overstimulated neurons, resulting in neuronal cell swelling (Zeevalk and Nicklas, 1997; Izumi et al., 2003; Osborne et al.,

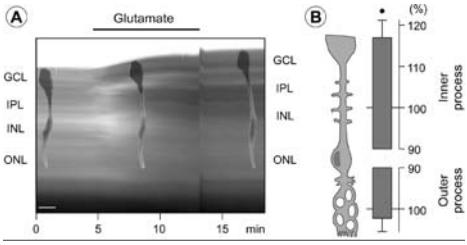

Fig. 2.58 Glutamate evokes a swelling of the inner but not outer retina, underlining the necessity for a Müller cell-mediated osmohomeostasis especially in the inner retina. (**a**) Time-dependent recording of a retinal slice from the guinea pig. Exposure of glutamate (1 mM) is indicated by the bar. A single fluorescence dye-loaded Müller cell is shown at different time periods. There is an artifact at the time of the removal of glutamate. (**b**) Lengths of the inner and outer stem processes of Müller cells in retinal slices from the guinea pig. The data were measured after 10 min of glutamate exposure, and are expressed in percent of control (100%). A swelling of the inner retina is also a characteristic of ischemia-reperfusion injury known to be evoked (at least in part) by excessive release of endogenous glutamate. GCL, ganglion cell layer; INL, inner nuclear layer; IPL, inner plexiform layer; ONL, outer nuclear layer. $P < 0.05$. Bar, 20 μm. Modified from Uckermann et al. (2004a)

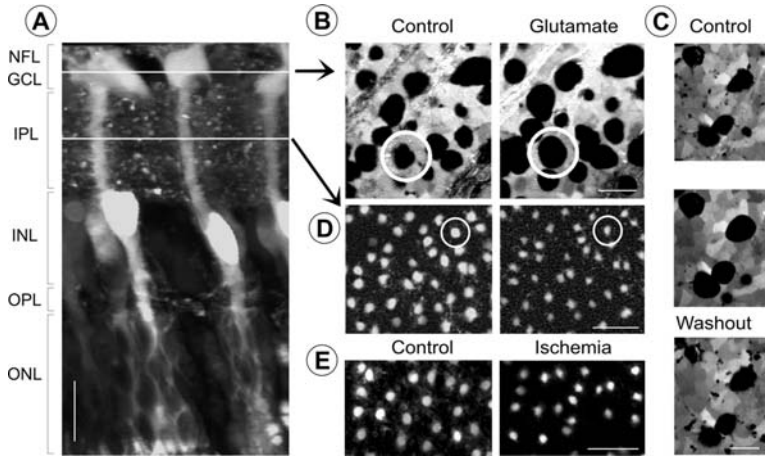

Fig. 2.59 Glutamate evokes morphological alterations of neurons and Müller cells in the guinea pig retina. (**a**) The retinal slice displays bright Müller cells and the optical planes within the ganglion cell/nerve fiber layers (GCL/NFL) and the inner plexiform layer (IPL) which were used to record the morphological alterations of the cells. The Müller cells were selectively stained with a vital dye, while neuronal structures remained dark. (**b**) The images were taken from an acutely isolated retinal wholemount. The tissue was exposed to glutamate (1 mM) for 10 min, resulting in a swelling of the neuronal cell bodies in the GCL. The elongated structures are nerve fiber bundles. (**c**) The swelling of neuronal cell bodies in the GCL is reversible after washout of glutamate. (**d**) Glutamate causes a reduction in the thickness of Müller cell stem processes that traverse the IPL, due to a swelling of the synapses between the Müller cell processes. (**e**) A decrease in the thickness of Müller cell processes (and an increase in the size of neuronal cell bodies; not shown) can be also observed shortly after a 1-h ischemia of the retina. INL, inner nuclear layer; ONL, outer nuclear layer; OPL, outer plexiform layer; PRS, photoreceptor segments. Bars, 20 μm. Modified from Uckermann et al. (2004a)

2004). The glutamate-evoked swelling of retinal neurons is primarily mediated by a sodium influx through α-amino-3-hydroxy-5-methyl-4-isoxazolepropionic acid (AMPA)/kainate receptor channels which is associated with a chloride influx into the cells. The ion movements cause an osmotic drag of water from the extracellular space into the cells, resulting in neuronal cell swelling. Metabolic poisoning of Müller cells with iodoacetate prevents the VEGF-evoked swelling of ganglion cell bodies, suggesting that glutamate released from Müller cells contributes to the swelling of retinal neurons (Fig. 2.76b) (Wurm et al., 2008).

The plexiform (synaptic) layers of the retina are high-resistance barriers for paracellular fluid movement (Antcliff et al., 2001). Since the synapses are closely ensheathed by Müller cell membranes, any water flowing into the neurons during activation of AMPA/kainate receptors will be delivered predominantly from the Müller cell interior through aquaporin-4 water channels (Fig. 2.60b, c). For osmotical reasons, a simultaneous water influx from the blood into the Müller cells will occur. Thus, aquaporin-4 water channels expressed by Müller cells facilitate the constitutive redistribution of metabolic water out of the retinal parenchyma into the blood as well as the activity-dependent water fluxes necessary for neuronal activation and synaptic transmission.

Cellular swelling results in a decrease of the extracellular space volume which must cause neuronal hyperexcitability (Dudek et al., 1990; Chebabo et al., 1995). The morphological alterations of Müller cells limit the glutamate-evoked decrease in the extracellular space volume, i.e. this decrease is smaller than expected when only the neuronal swelling is considered (Uckermann et al., 2004a). Thus, the compensatory reshaping of Müller cells is a homeostatic response to prevent deleterious decreases in the extracellular space volume. The morphological alterations of Müller cells are supported by the viscoelastic properties of the cells. Müller cells are softer than their neighboring neurons (Lu et al., 2006), enabling them to flexibly alter their morphology in dependence on the activity-dependent swelling of neurons and synapses. The two stem processes are particularly soft; in situ, these processes are located in the plexiform (synaptic) layers which display the largest glutamate-evoked morphological alterations due to the high density of synapses. Under conditions when the osmotic balance in the tissue is disturbed, a receptor-mediated mechanism of cell volume regulation (Fig. 2.75b) may contribute to the volume homeostasis of the extracellular space.

2.4.3.4 Disturbance of the Water Homeostasis Under Pathological Conditions

Various pathological conditions, especially ischemia-hypoxia, oxidative stress and inflammation, are associated with the formation of retinal edema (Stefánsson et al., 1987; Szabo et al., 1991; Marmor, 1999; Guex-Crosier, 1999). It has been shown that the water content of the rat retina displays a biphasic elevation in the course of experimental ischemia-reperfusion: during ischemic episodes, the water content progressively increases and falls to near-control level within hours after reperfusion; then, a second increase occurs after two days of reperfusion (Stefánsson et al., 1987). The increase in the retinal water content during the ischemic episode is accompanied

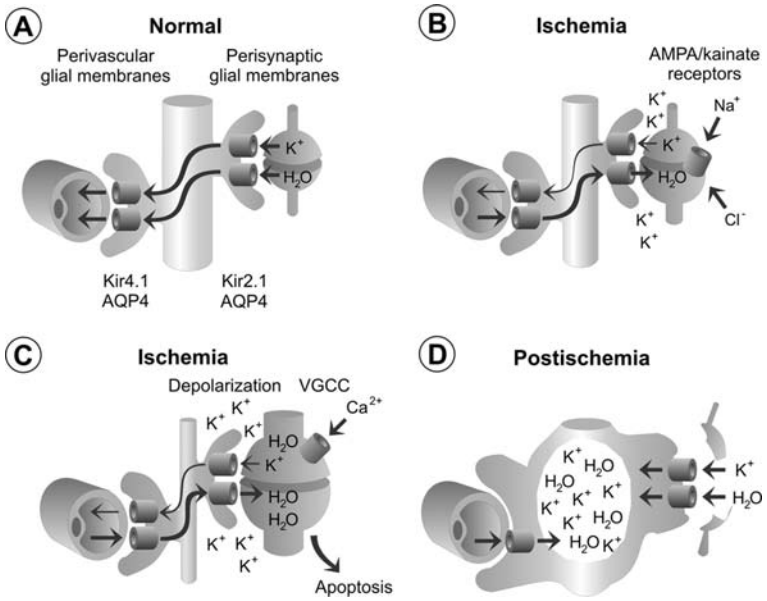

Fig. 2.60 Possible contribution of water fluxes through Müller cell's aquaporin-4 channels to the ischemic injury of the inner retina. (**a**) Under normal conditions, Müller cells (*middle*) mediate the constitutive dehydration of the inner retina. The water transport from the retinal interstitium through the Müller cell bodies into the blood vessels is facilitated by aquaporin-4 (AQP4) water channels expressed at high amount in the membrane domains of Müller cells that ensheath the vessels and synapses. The water transport is osmotically driven by the clearance currents of neuron-derived potassium that flows through the Kir2.1 and Kir4.1 channels expressed in the plasma membrane of Müller cells. (**b**) In the ischemic retina, over-excited neurons release a huge amount of potassium and glutamate that opens AMPA/kainate receptor channels. The flow of sodium ions through the receptor channels is accompanied by a flow of chloride ions, and the ion fluxes draw water into the synapses resulting in swelling of retinal neurons. The water that flows into the synapses is released from the Müller cell interior; this is followed by a water movement from the vessels into the Müller cells. (**c**) The strong activation of AMPA/kainate receptors, as well as the high extracellular potassium level, cause (in addition to synapse swelling) a long-lasting depolarization of the neurons resulting in activation of voltage-gated calcium channels (VGCCs). The intracellular calcium overload activates the apoptosis machinery of the cells. In this model, closure of aquaporin-4 will inhibit the water movement from the blood into the Müller cells and subsequently into the synapses. Since for all ion currents simultaneous water movements are necessary, this will hinder the rapid flux of sodium and calcium ions into the synapses, resulting in a reduced extent of neuronal cell swelling and apoptosis. (**d**) Within days after reperfusion, Müller cells downregulate the expression of Kir4.1 channels in the perivascular membranes while the Kir2.1 channels in the perisynaptic sheets are largely unaltered. This results in an accumulation of potassium ions within the Müller cell bodies that causes an osmotical driving force for water movement from the blood into the cells, resulting in Müller cell swelling. Modified from Bringmann et al. (2005)

by a progressive thickening of the inner retina while the photoreceptor layer remains unaffected (Stefánsson et al., 1987; Szabo et al., 1991), suggesting that it is caused by an overexcitation of glutamatergic synapses, resulting in swelling of inner retinal neurons. However, the biphasic elevation of the retinal water content during

ischemia-reperfusion (Stefánsson et al., 1987) indicates that different mechanisms may be involved in edema formation during early and late phases after reperfusion. It was suggested that the early phase of retinal water accumulation is caused by glutamate-evoked swelling of retinal neurons, whereas the late phase of water accumulation is caused by a disturbance of the Müller cell-mediated water homeostasis (Bringmann et al., 2005). This assumption is supported by various experimental and clinical observations. During ischemic episodes of the rabbit retina, both plexiform layers and the cytoplasm of neuronal cells become edematous while the Müller cells appear to be unaffected, whereas in the postischemic tissue, the neural elements degenerate and the Müller cells become edematous (Johnson, 1974). During diabetic retinopathy, swelling of ganglion cell bodies and their processes precedes the loss of these cells and the gliosis of the inner retinal layers (Duke-Elder and Dobree, 1967). In retinas of hypoxic rats, hypertrophy of astrocytes and Müller cells is observed as early as 3 h after hypoxia, swollen Müller cell processes (with loss of cytoplasmic organelles resulting in vacuolated appearance) are first found at three days after hypoxic exposure (Kaur et al., 2007).

Over-stimulation of ionotropic glutamate receptors during an ischemic episode results in long-term depolarization of retinal neurons. This causes an opening of voltage-gated calcium channels leading to neuronal calcium overload (Fig. 2.60c). The long-lasting intracellular calcium overload activates the apoptosis machinery of the cells, resulting in neuronal cell death. The swelling of retinal neurons is mediated by a sodium flux through ionotropic glutamate receptors associated with a water flux. Since the water is delivered by Müller cells through their aquaporin-4 channels, an inhibition of the rapid transglial water transport (from the blood and vitreous through the Müller cells into synapses) should delay the excessive ion movements through the open ionotropic glutamate receptors, resulting in lower levels of neuronal cell swelling and apoptosis. Indeed, retinas of aquaporin-4 knockout mice display significantly less neuronal degeneration after retinal ischemia than retinas of control mice (Da and Verkman, 2004). Thus, neuronal cell swelling and apoptosis in the ischemic retina is suggested to be supported by the Müller cell-mediated water transport. In retinas of hypoxic rats, an increase in gene and protein expression of aquaporin-4 is observed as early as 3 h after hypoxic exposure (Kaur et al., 2007).

The resolution of the ischemic edema within hours after reperfusion of the rat retina (Stefánsson et al., 1987) indicates that the water clearance function of Müller cells is not disturbed early after transient ischemia. However, the increase in the retinal water content within days after reperfusion suggests that there occurs a slowly developing disturbance of the water transport through Müller cells in the postischemic retina (Bringmann et al., 2005). Since the water transport through Müller cells is suggested to be coupled to the potassium clearance currents through the cells (Nagelhus et al., 1999), a functional inactivation of Kir channels must disturb the water absorption from the retinal tissue and the export of water into the blood. It has been shown in experimental models of various retinopathies (including retinal ischemia-reperfusion, inflammation, diabetic retinopathy, retinal detachment, and blue light-evoked retinal degeneration) that the Kir4.1 protein is dislocated in the

retina (Figs. 2.43b, 2.49, 3.13a, and 3.15a). The dislocation of the Kir4.1 protein is accompanied by a decrease in the Kir channel-mediated currents across Müller cell membranes (Figs. 2.45a, b, 2.46b, c, 3.5a, b, 3.13b, and 3.15b), suggesting a functional inactivation of the channels (Pannicke et al., 2004, 2005a, b, 2006; Francke et al., 2001a, b; Iandiev et al., 2008a). In all these animal models, an alteration in the osmotic swelling properties of Müller cells was observed. While Müller cell bodies in slices of adult healthy retinas held their volume constant (up to ~20 min: Hirrlinger et al., 2008) when the osmolarity of the extracellular medium is decreased, Müller cell bodies in slices of diseased retinas promptly swell upon hypoosmotic challenge (Figs. 2.75a, 3.5c, 3.8d, and 3.15c). There is a negative relation between the amplitude of the Kir currents and the extent of osmotic cell swelling, both in Müller cells of control retinas (when the Kir channels are blocked by barium ions: Fig. 2.61a, b) and under pathological conditions (Fig. 2.45a and 3.8e). (In addition, there is a correlation between the degree of osmotic Müller cell swelling and other signs of gliosis such as cellular hypertrophy: Pannicke et al., 2005b.) The swelling of Müller cells reflects an alteration in the rapid osmotically driven water movement across Müller cell membranes after functional inactivation of Kir4.1 channels. The downregulation and/or functional inactivation of Kir4.1 channels results in an almost total absence of passive outward potassium currents from Müller cells whereas a significant amount of inward currents remains present (Fig. 2.46a, b). The absence of outward currents through Kir4.1 channels will interrupt the spatial buffering potassium currents through Müller cells and, thus, the

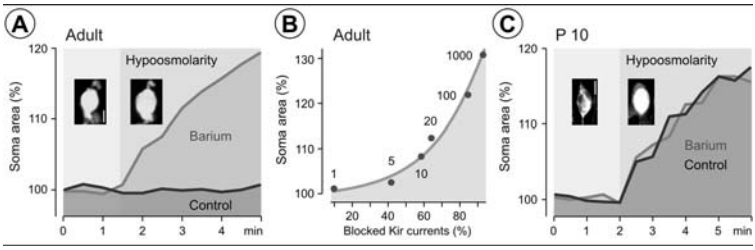

Fig. 2.61 Potassium currents through Kir channels are involved in the regulation of the Müller cell volume under hypoosmotic stress. The size of Müller cell bodies was recorded in retinal slices of adult rats (**a**, **b**) and of a postnatal day (P) 10 animal (**c**). (**a**) Under hypoosmotic conditions, a blockade of Kir channels by barium chloride (1 mM) results in a swelling of Müller cell bodies which is not observed in the absence of barium. The time-dependent alteration in the cross-sectional area of Müller cell somata is shown. The images display a Müller cell soma recorded in the presence of barium before (*left*) and after (*right*) hypoosmotic challenge. (**b**) There is a positive relation between the amplitude of the Kir channel-mediated outward potassium currents which are blocked by barium chloride, and the extent of Müller cell swelling under hypoosmotic stress. The data were measured in the presence of different concentrations of extracellular barium (in μM; given besides the data points). (**c**) In the retinal slice from the young rat, hypoosmotic challenge evoked a swelling of Müller cell bodies in the absence of barium chloride which is similar in the amplitude to the swelling under barium-containing conditions. The swelling is explained with the absence of Kir4.1 channels in Müller cells of this developmental stage. Bars, 5 μm. Modified from Pannicke et al. (2004), Wurm et al. (2006a), and Iandiev et al. (2007c)

export of potassium into the blood and vitreous. The disruption of the transglial potassium currents will also disturb the transport of water through Müller cells, resulting in an impairment of the water absorption from the retinal tissue. Moreover, since Müller cells are still capable to take up excess potassium from the extracellular space (through the Kir2.1 channels which are not altered in their expression after ischemia: Fig. 2.43b), the impairment in the release of potassium from Müller cells will result in an accumulation of potassium ions within the cells and, thus, in an increase in the intracellular osmotic pressure. The increase in the osmotic pressure will draw water from fluid-filled spaces outside of the neural retina (blood, vitreous) into the perivascular and endfoot regions of Müller cells, resulting in Müller cell swelling (Fig. 2.60d). The water influx from the blood and vitreous is supported by aquaporin-4 water channels which are not altered (Fig. 2.49) or even increased in their expression (Kaur et al., 2007). A disturbance in the Müller cell-mediated water absorption from the retinal tissue, and a swelling of Müller cells under distinct conditions associated with osmotic imbalances between retinal and extra-retinal tissues, may underlie the edema formation in the ischemic retina within days after reperfusion (Bringmann et al., 2005; Reichenbach et al., 2007). The proposed mechanism of glial cell swelling may have impact not only for the retina but also for the brain since similar changes of glial membrane conductance, i.e. a decrease of Kir currents in reactive cells of the injured or diseased tissue, have been described for brain astrocytes (Schröder et al., 1999; D'Ambrosio et al., 1999; Köller et al., 2000; Hinterkeuser et al., 2000). Swelling of perivascular astrocytic endfeet may occur under pathological conditions in situ when the osmotic pressure of the neural tissue increases due to neuronal hyperexcitation while the osmotic pressure of the blood remains constant, causing an osmotic gradient across the glio-vascular interface. Endocytosis of serum-derived proteins extravasated across the walls of leaky vessels may contribute to a swelling of Müller cells. In addition, an increase in aquaporin-4 expression has been related to a swelling of glial cells (Rama Rao et al., 2003).

It is unclear whether the activity of Kir channels in Müller cells (which depends on intracellular ATP: Fakler et al., 1994; Takumi et al., 1995; Kusaka and Puro, 1997) is also reduced during acute ischemia since Müller cells may produce their energy by anaerob mechanisms. When the ATP level falls within the Müller cells during ischemia, a closure of Kir channels will result in an accumulation of potassium ions in the retinal interstitium and within the Müller cells. This will enhance the neuronal excitation level and the release of glutamate from neurons, as well as the osmotic gradient that draws water from the blood and vitreous into the Müller cells. Serum-derived molecules such as thrombin, that are extravasated after ischemia-induced breakdown of the blood-retinal barriers, may also close Kir channels of Müller cells (Puro and Stuenkel, 1995).

2.4.3.5 Regulation of Aquaporin-4 and Kir4.1

Under various pathological conditions such as retinal inflammation, ischemia, detachment, and diabetes, the expression of Kir4.1 and aquaporin-4 proteins is differently regulated (Pannicke et al., 2004, 2006; Iandiev et al., 2006b; Liu et al.,

2007). Whereas the Kir4.1 protein is redistributed from the prominent expression sites around the blood vessels and at the limiting membranes of the retina, the localization of the aquaporin-4 protein remains unaltered (with the exception of Müller cell membranes that surround the superficial retinal vessels) (Figs. 2.49 and 3.13). The downregulation of perivascular Kir4.1 protein will cause an uncoupling of the aquaporin-4-mediated water transport from the potassium currents, resulting in an alteration of the water movements across the interface between Müller cells and retinal vessels. The reason for the different regulation of aquaporin-4 and Kir4.1 proteins under pathological conditions is unclear. A differential regulation of both proteins is also indicated by the fact that deletion of aquaporin-4 does not alter the retinal expression of Kir4.1 (Da and Verkman, 2004; Ruiz-Ederra et al., 2007). It has been shown in a study using knockout mice that α-syntrophin (a protein of the dystrophin-associated protein complex) is necessary for the membrane anchoring of approximately 70% of the aquaporin-4 protein in Müller cells while deletion of this protein has no effect on the membrane anchoring of Kir4.1 (Puwarawuttipanit et al., 2006). Deletion of the dystrophin gene product Dp71 in mice markedly reduces the retinal aquaporin-4 level and has no effect on the level of Kir4.1, while both proteins display a dislocation in Müller cells; these alterations are associated with an enhanced vulnerability of retinal ganglion cells to ischemia-reperfusion injury (Dalloz et al., 2003; Fort et al., 2008). Differences in the PDZ domain-binding C-termini of Kir4.1 and aquaporin-4 may facilitate the preferential binding of the two proteins to different syntrophin isoforms. In addition to differences in membrane anchoring, a different gene expression regulation of aquaporin-4 and Kir4.1 (with a downregulation of Kir4.1 and no alteration, or even an increase in aquaporin-4: Liu et al., 2007; Kaur et al., 2007) may contribute to the different regulation of both proteins under pathological conditions. On the other hand, under conditions of massive glial proliferation, the gene expression of both Kir4.1 and aquaporin-4 was shown to be downregulated (Tenckhoff et al., 2005).

2.4.3.6 Decrease in Osmotic Müller Cell Swelling During Ontogenetic Development

Glutamate-evoked rapid ion and water shifts between intra- and extracellular spaces will affect the osmohomeostasis of the tissue; for example, the intracellular osmolarity of Müller cells will increase due to the uptake of potassium ions and neurotransmitter molecules (which is associated with an influx of sodium ions via electrogenic uptake carriers). Under normal conditions, an increase in the intracellular osmolarity is balanced by the efflux of potassium ions through Kir4.1 channels into the blood and vitreous fluid. Therefore, functional Kir4.1 channels are one prerequisite for the capability of Müller cells to hold their volume constant despite of variations in the extra- and intracellular osmolarity (Pannicke et al., 2004).

The osmotic cell volume homeostasis of rat Müller cells develops during the first two postnatal weeks (Wurm et al., 2006a). Exposure of retinal slices from young postnatal animals to a hypoosmolar solution results in a swelling of Müller cell bodies (Fig. 2.61c) which is not observed in retinal slices of adult animals (Fig. 2.61a).

The osmotic swelling of Müller cells in retinas of young postnatal animals was explained with the absence of Kir4.1 channels which emerges (simultaneously with the aquaporin-4 protein) in the rat retina between the postnatal days 10 and 15 (Fig. 2.48). There is a negative relation between the amplitude of the Kir currents and the extent of osmotic Müller cell swelling in the course of the developmental maturation of Müller cells (Fig. 2.45a). The postnatal development of aquaporin-4 expression is also reflected by a postnatal increase in the size and number of orthogonal arrays of particles in the endfoot membranes of Müller cells (Richter et al., 1990).

2.4.3.7 Mechanisms of Osmotic Müller Cell Swelling

Passive potassium currents through Kir (particularly Kir4.1) channels are crucially involved in the homeostasis of the Müller cell volume under varying osmotic conditions. Prompt transmembraneous potassium fluxes through Kir4.1 channels compensate osmotic gradients across the Müller cell membrane and, therefore, prevent cellular swelling. (Another way for the extrusion of osmolytes is a transporter-mediated release of amino acid osmolytes such as taurine: Adler, 1983; Faff-Michalak et al., 1994; Faff et al., 1996, 1997; El-Sherbeny et al., 2004). Under conditions when the Kir4.1 channels are missing, downregulated, or functionally inactive (both in immature Müller cells and under pathological conditions in the adult retina), the hypoosmotic swelling of Müller cells is mediated by at least two further factors, oxidative stress and activation of enzymes that produce inflammatory lipid mediators (Fig. 2.62b) (Uckermann et al., 2005b; Pannicke et al., 2006; Wurm et al., 2006a, b; Iandiev et al., 2008a). The osmotic swelling of Müller cells is prevented when the activity of the phospholipase A_2 (which generates arachidonic acid) or the cyclooxygenase (which forms prostaglandins) is pharmacologically blocked, suggesting the involvement of inflammatory lipid mediators in the induction of cellular swelling. In addition, inhibition of oxidative stress by application of a reducing agent prevents the swelling of Müller cells. Conversely, acute administration of arachidonic acid, prostaglandin E_2, or hydrogen peroxide causes osmotic swelling of Müller cells in retinas from healthy adult animals. Arachidonic acid and its metabolites, especially prostaglandin E_2, are major mediators of retinal edema (Guex-Crosier, 1999; Miyake and Ibaraki, 2002). It is known that the activity of the phospholipase A_2 is increased in response to osmotic challenge and oxidative stress, resulting in peroxidation of membrane phospholipids and the release of arachidonic acid (Birkle and Bazan, 1989; Davidge et al., 1995; Lambert et al., 2006; Balboa and Balsinde, 2006). Free radicals and hydroperoxides also stimulate the activity of the lipoxygenase and cyclooxygenase (Asano et al., 1987). Müller cells increase the expression of cyclooxygenase-2 under various pathological conditions (Nakamichi et al., 2003; Wurm et al., 2006b). Arachidonic acid and prostaglandins potently inhibit the Na, K-ATPase activity; this leads to intracellular sodium overload and cellular swelling (Lees, 1991; Staub et al., 1994). Furthermore, arachidonic acid blocks membrane channels such as volume-regulated anion and (in Müller cells) outwardly rectifying K_A and K_{DR} channels (Lambert,

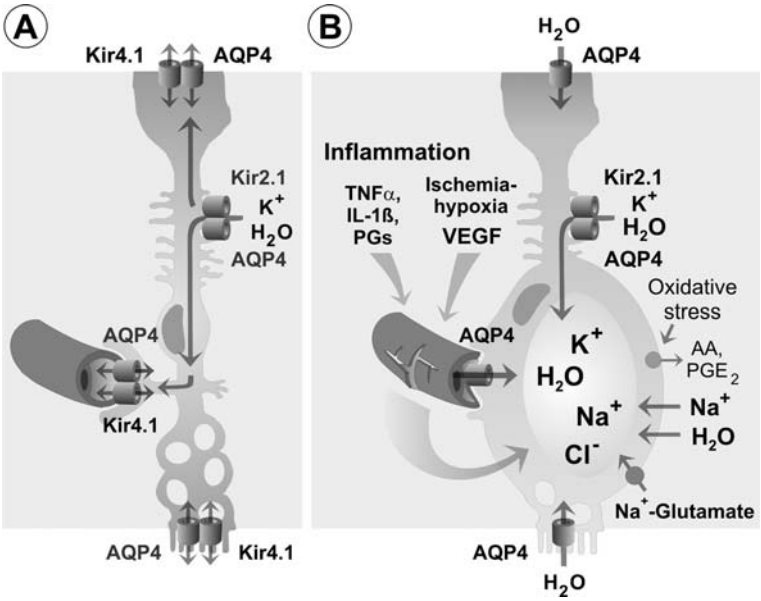

Fig. 2.62 Mechanisms of osmotic Müller cell swelling. (**a**) Under normal conditions, Müller cells mediate the fluid absorption from the retinal tissue into the blood by a co-transport of water (facilitated by aquaporin-4 water channels) and osmolytes, especially potassium ions (facilitated by Kir4.1 and Kir2.1 channels). (**b**) Under ischemic-hypoxic and inflammatory conditions, vascular leakage occurs due to the action of inflammatory factors and VEGF. Müller cells downregulate the expression of functional Kir4.1 channels. This downregulation impairs the release of potassium ions from Müller cells into the blood, and results in an accumulation of potassium ions within the cells (since the cells are still capable to take up ions from the interstitial spaces through other potassium channels such as Kir2.1). The increase in the intracellular osmotic pressure results in an osmotic gradient across the plasma membrane that draws water into the Müller cells facilitated by aquaporin-4 water channels. An influx of sodium ions into the cells, evoked by inflammatory mediators such as arachidonic acid (AA) and prostaglandins (PGs) which are formed in response to oxidative stress, and via electrogenic glutamate uptake carriers, contributes to the increase in the intracellular osmotic pressure. The uptake of extravasated serum proteins by Müller cells may further enhance the osmotic pressure of the cell interior. Modified from Reichenbach et al. (2007)

1991; Bringmann et al., 1998a) which mediate a compensatory efflux of osmolytes including amino acids and chloride and potassium ions. It is likely that the intracellular sodium overload evoked by arachidonic acid and prostaglandins is one major cause of Müller cell swelling, since an extracellular sodium-free solution prevents the swelling (Uckermann et al., 2006). A long-lasting influx of sodium ions driven by sodium-dependent glutamate transporters (Casper et al., 1982; Izumi et al., 1996) and an uptake of extravasated serum proteins may also contribute to the enhancement of the intracellular osmotic pressure and cellular swelling (Fig. 2.62b). In cultured brain astrocytes, overexpression of aquaporin-4 increases the water permeability of the plasma membranes (Solenov et al., 2004) and is associated with cellular swelling (Rama Rao et al., 2003). Further investigations are necessary to determine the intracellular pathways involved in osmotic Müller cell swelling.

2.4.4 Regulation of Müller Cell Volume – Retinal Volume Homeostasis

The above-described water fluxes around and through Müller cells are not constant in time and space; rather, fast local changes may occur. Within a certain range of osmotic challenges, the use of the given homeostatic capacity of Müller cells may just vary but under many circumstances, an (up-)regulation of homeostatic "tools" may be required. This chapter is devoted to the description of such regulatory mechanisms, as far as hitherto known.

It has already been mentioned that neuronal activity is associated with changes in the cellular and extracellular space volumes. There are two compartments where volume changes occur: the neural tissue and the blood vessels. Activation of neuronal ionotropic glutamate receptors causes (i) a net uptake of sodium chloride, swelling of neuronal cell bodies and synapses (Fig. 2.59) (Uckermann et al., 2004a), (ii) decreases in extracellular space osmolarity and volume, and (iii) vasodilation. By mediating transcellular ion and water transport, and by regulation of their cell volume, Müller cells are implicated in the homeostasis of the local extracellular space volume. To avoid deleterious decreases in the perisynaptic and perivascular spaces during neuronal activation (that will result in neuronal hyperexcitability: Dudek et al., 1990; Chebabo et al., 1995), Müller cells should avoid cellular swelling, or should even decrease their volume, when the neurons swell and the vessels dilate. Indeed, the decrease in the thickness of Müller cell processes during glutamate-evoked neuronal swelling (Fig. 2.59d) results in a reduced decrease in the extracellular space volume (Uckermann et al., 2004a). The Müller cell volume should be maintained or even decreased despite of alterations in the osmotic conditions that favor cellular swelling. First, the light-evoked changes in the ionic composition of the extracellular space fluid causes a decrease in the extracellular space osmolarity since the decrease in sodium chloride is about twice as large as the increase in potassium concentration (Dietzel et al., 1989; Dmitriev et al., 1999). Second, the uptake of neuron-derived osmolytes such as potassium, sodium-glutamate, and sodium-GABA increases the intracellular osmotic pressure of Müller cells. Thus, neuronal activity leads to an osmotic gradient that favors water flux from the extracellular to the intracellular space. Osmotic swelling of Müller cells should be inhibited under conditions when the extracellular fluid is hypoosmotic relative to the cell interior. It is conceivable that excited neurons release factors which inhibit glial cell swelling in areas of intense neuronal activity, and synaptically released glutamate and ATP may represent candidate factors involved in volume-regulatory neuron-to-glia signaling.

Kir Channel-Mediated Homeostasis of the Müller Cell Volume

Under normal conditions, Müller cell bodies do not increase their size when the osmotic conditions are changed during perfusion of retinal slices or isolated cells with a hypoosmolar solution (Figs. 2.45a, 2.61a, 2.75a, 3.5c, 3.8d, and 3.15c) (Pannicke et al., 2004; Wurm et al., 2006a). Apparently, Müller cells have a highly

efficient cell volume regulation which compensates for changes in the osmotic conditions. This cell volume homeostasis depends largely on the activity of Kir4.1 potassium channels; a release of potassium ions through Kir4.1 channels compensates for the osmotic gradient across the plasma membrane and thus prevents cellular swelling. Osmotic imbalances are exacerbated under pathological conditions when Müller cells are incapable to release excess potassium through Kir4.1 channels that will result in an accumulation of potassium within the cells (Fig. 2.62). Under such conditions, Müller cells swell in the presence of a hypoosmotic environment (Figs. 2.45a, 2.75a, 3.5c, 3.8d, and 3.15c). The impaired water and ion clearance capability of Müller cells after downregulation of Kir4.1 contributes to osmotic disturbances in the retina in situ. Cell volume homeostasis is also important in the normal tissue in such Müller cell compartments that face the neuropile, and that are largely devoid of Kir4.1 channels (Fig. 2.43b, c) (Kofuji et al., 2000, 2002). Since inflammatory lipid mediators evoke Müller cell swelling under hypoosmotic conditions also in the presence of Kir4.1 (Uckermann et al., 2005b; Pannicke et al., 2006; Wurm et al., 2006a, 2006b; Iandiev et al., 2008a), restriction of cellular swelling is important also at sites where such mediators are formed, e.g. around blood vessels where glial cell-derived arachidonic acid metabolites mediate vasodilation and constriction (Metea and Newman, 2006). Under conditions of osmotic imbalance, e.g., during intense neuronal activation, receptor-dependent and -independent mechanisms of cell volume regulation support the homeostasis of the Müller cell volume and thus of the extracellular space volume.

Receptor-Dependent Regulation of Müller Cell Volume

The osmotic swelling of Müller glial cells in acutely isolated slices of the rat retina (Figs. 2.75a, 3.5c, 3.8d, and 3.15c) or of acutely dissociated cells is inhibited by activation of an autocrine glutamatergic-purinergic signaling cascade (Fig. 2.75b) (Uckermann et al., 2006; Wurm et al., 2008). This cascade also reduces the volume of already swollen Müller cells (Uckermann et al., 2006). The first step of this cascade is the release of endogenous glutamate either from retinal neurons or from Müller cells themselves. In both cases, the release of glutamate is mediated by a calcium-dependent exocytotic release of glutamate-containing vesicles. This glutamatergic-purinergic signaling cascade can be evoked by various receptor agonists that induce a release of glutamate from neurons or Müller cells: VEGF (Fig. 2.75), NPY (via activation of Y1 receptors), and agonists of EGF and NP receptors (Uckermann et al., 2006; Weuste et al., 2006; Kalisch et al., 2006; Wurm et al., 2008).

Glutamate then activates group I/II mGluRs expressed by Müller cells resulting in a calcium-independent release of ATP from Müller cells. ATP is extracellularly catabolized to ADP by the action of the ecto-ATPase; the extracellularly formed ADP activates $P2Y_1$ receptors. Activation of these receptors, in turn, triggers a release of adenosine from Müller cells via nucleoside transporters. Finally, this adenosine stimulates A1 receptors. Activation of these receptors causes an opening of barium- and arachidonic acid-insensitive potassium channels (likely, two

pore-domain channels: Skatchkov et al., 2006), as well as of chloride channels, in the Müller cell membrane. The action of adenosine on ion channels does not require intracellular calcium but is mediated by the activation of the adenylyl cyclase, protein kinase A, and PI3K. The extrusion of ions through potassium and chloride channels compensates the transmembrane osmotic gradient and thus prevents water influx and cellular swelling under hypoosmotic stress conditions (Uckermann et al., 2006; Wurm et al., 2006a, 2008). In swollen Müller cells, the ion efflux is associated with a water efflux from the cells, resulting in a reduction of the cell volume. Two pore-domain channels may function as an osmolyte extrusion pathway that helps to maintain proper glial cell volume under conditions when Kir4.1 channels are downregulated in the injured retina. In species with Müller cells that express BK channels, these channels may be implicated in the cell volume regulation, as well (Puro, 1991a). The presence of NTPDase2 (the ecto-ATPase that preferentially degrades ATP to ADP) in Müller cells, and the absence of NTPDase1 (the ecto-apyrase that hydrolyzes ATP and ADP about equally well), may explain why in the purinergic signaling cascade of cell volume regulation, ATP is converted extracellularly to ADP whereas ADP is not further catabolized extracellularly to AMP and adenosine (Iandiev et al., 2007c).

Glutamate and purinergic receptor agonists mediate an activity-dependent regulation of the Müller cell volume. Glutamate evokes a swelling of neuronal cells in the retina (Fig. 2.59b, c) (Uckermann et al., 2004a) and simultaneously an inhibition of osmotic swelling of Müller cells or even a decrease in the Müller cell volume. However, it should be keep in mind that a prolonged administration of glutamate (for 1 h or longer) results in a swelling of Müller cells via the uptake of glutamate which is associated with a sodium and water transport into the cells (Izumi et al., 1996).

The glutamatergic-purinergic cell volume regulation may be particularly important under pathological conditions which are associated with ionic and osmotic imbalances in the retinal tissue and with an impaired volume regulation of Müller cells after downregulation of Kir4.1 channels. Under these conditions, Müller cells increase their calcium responsiveness to P2Y receptor activation (Figs. 2.45b, c, 2.73a, and 3.8f). NPY is known to be released in the retina in response to light (Bruun and Ehinger, 1993) and to be increasingly expressed under hypoxic and oxidative stress conditions (Yoon et al., 2002). The retinal expression of ANP and HB-EGF is increased after transient ischemia-reperfusion (Kalisch et al., 2006; Weuste et al., 2006). Likewise, VEGF is increased in the retina under ischemic-hypoxic and oxidative stress conditions (Hata et al., 1995; Pe'er et al., 1995; Kuroki et al., 1996; Vinores et al., 1997). Thus, it seems likely that the cell volume-regulatory neuron-to-glia signaling in the retina is increasingly effective under pathological conditions when Müller cells decrease their expression of Kir4.1 channels. Mechanical stress evokes a release of ATP from Müller cells (Newman, 2001, 2003b); this may be functionally important for the volume regulation of Müller cells both under normal (swelling of retinal neurons during intense activation) and pathological conditions (when tractional forces mechanically deform the retinal tissue in cases of retinal detachment and proliferative retinopathies). It has been shown

that the rapid changes of cell shape associated with cellular migration are mediated by transmembranous ion and water fluxes through potassium and chloride channels, and through aquaporins (Eder, 2005; Saadoun et al., 2005; Wu et al., 2007). The increase in calcium responsiveness to purinergic receptor activation found in Müller cells from pathologically altered retinas (Bringmann et al., 2001; Francke et al., 2002; Uhlmann et al., 2003; Iandiev et al., 2006b) may facilitate osmotic cell shape alterations implicated in proliferation and migration of reactive Müller cells (cf. Section 3.1).

Receptor-Independent Regulation of Müller Cell Volume

Cultured Müller cells (which lack functional Kir channels) possess a receptor-independent mechanism of osmoregulation, via the transmembrane transport of amino acid osmolytes such as taurine, homotaurine, and myo-inositol. Extracellular ammonia, high extracellular potassium, and hypoosmolar media evoke a swelling of cultured Müller cells and a subsequent (cAMP-dependent and -independent) release of taurine from the cells (Faff-Michalak et al., 1994; Faff et al., 1996, 1997). In the rat retina, taurine and homotaurine are localized mainly to Müller cells (Schulze and Neuhoff, 1983). In addition to retinal neurons, pigment epithelial, and vascular cells, Müller cells express the sodium- and chloride-dependent taurine transporter (Adler, 1983; El-Sherbeny et al., 2004). Receptor agonists may modulate the taurine transport through protein kinase A- and -C-mediated regulation of the number of transporters in the plasma membrane (Loo et al., 1996).

2.4.5 Contribution(s) of Other Ion Channels

In addition to potassium channels, Müller cells express other types of voltage- and second messenger-gated ion channels in their plasma membranes.

2.4.5.1 Voltage-Dependent Calcium Channels

Müller cells from all species investigated so far (e.g. salamander, toad, rat, rabbit, guinea pig, man) express voltage-gated calcium channels (Newman, 1985b; Puro and Mano, 1991; Puro, 1994; Puro et al., 1996a; Bringmann et al., 2000b–e; Xu et al., 2002; Welch et al., 2005). In whole-cell records of cells from many species, however, the calcium channel-mediated currents are very small when calcium or barium ions are used as charge carriers (even when the dominating potassium conductance is completely suppressed by a removal of potassium ions from the recording solutions). The detection of calcium channel-mediated currents can be improved when the extracellular solution does not contain divalent cations; under these conditions, sodium ions flow through the channels, and the amplitude of the currents is strongly increased (Fig. 2.63a) (Bringmann et al., 2000b, c, d, e). The reason for the small amplitude of calcium currents is unclear. It has been hypothesized that, simultaneous to the membrane depolarization, the

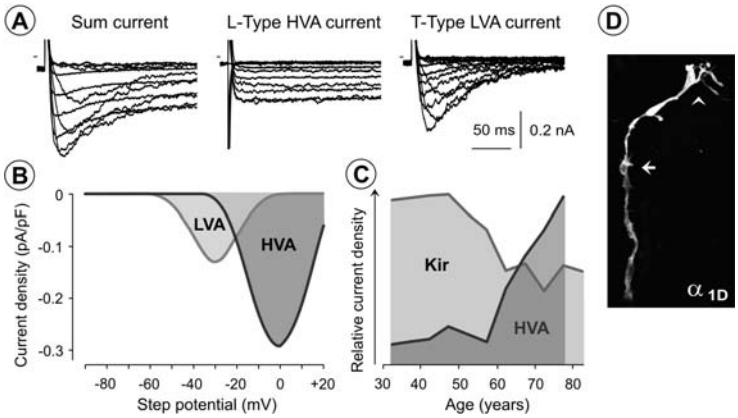

Fig. 2.63 Voltage-gated calcium channels of human Müller cells. (**a**, **b**) Acutely isolated Müller cells display transient (T-type) calcium currents through low voltage-activated (LVA) channels, and long-lasting (L-type) calcium currents through high voltage-activated (HVA) channels. (**a**) Example of sodium currents through voltage-gated calcium channels in one cell. The sum currents were evoked by depolarizing voltage steps (increment, 10 mV) from pre-pulses to –120 mV. The non-inactivating HVA currents were evoked by depolarizing voltage steps from pre-pulses to –70 mV. The difference between both records revealed the presence of a transient LVA current. Sodium ions were used as charge carrier to increase the amplitude of the currents through the calcium channels. (**b**) Mean peak current density-voltage relationships of calcium currents through LVA and HVA channels. LVA channels activate at potentials positive to –60 mV, while HVA channels activate at voltages positive to –40 mV. (**c**) Age-dependent alterations in the densities of Kir and HVA calcium currents in human Müller cells. Whereas the Kir currents display an age-dependent decrease, the currents through HVA channels increase in the course af aging. (**d**) An acutely isolated Müller cell displays immunoreactivity for the α_{1D} subunit of L-type calcium channels. Arrow, cell soma. Arrowhead, cell endfoot. Modified from Bringmann et al. (2000b, e, 2003a)

action of certain second messengers (formed after activation of growth factor or neurotransmitter receptors) is necessary to open the channels (Bringmann et al., 2000b). This assumption corresponds to findings in cultured astrocytes where calcium currents are usually undetectable but recordable after addition of neurotransmitters or agents that increase the intracellular level of cAMP (MacVicar, 1984; Barres et al., 1989). Sodium currents through voltage-gated calcium channels may not be physiological. On the other hand, there are indications that under certain pathophysiological conditions, e.g. after lipid peroxidation, voltage-gated calcium channels of retinal cells may indeed become permeable to sodium ions (Agostinho et al., 1997).

In salamander Müller cells, depolarizing current pulses evoke regenerative calcium spikes via activation of voltage-gated calcium channels (Newman, 1985b). High potassium-evoked depolarization of these cells triggers a verapamil-sensitive rapid increase in intracellular calcium throughout the length of the cells (Keirstead and Miller, 1995). In contrast, depolarization of dissociated Müller cells of the guinea pig with a high-potassium solution does not induce calcium responses in

the cells (though the cells express voltage-gated calcium channels as observed in electrophysiological recordings). Instead, a membrane hyperpolarization by a low-potassium solution evokes calcium responses in these cells. Such cytosolic calcium transients upon lowering of the extracellular potassium concentration to 2 mM or below were also found in brain astrocytes, and were suggested to be mediated by calcium influx through Kir4.1 potassium channels (Dallwig et al., 2000; Härtel et al., 2007).

In whole-cell records, Müller cells display both transient (T-type) and long-lasting (L-type) calcium channel currents (Fig. 2.63a). T-type currents are low threshold voltage-activated (LVA) currents, i.e. the threshold of activation of these currents with a depolarizing pulse is low. Calcium currents through LVA channels activate at potentials positive to –60 mV, and maximal currents are observed at –30 mV (Fig. 2.63b). L-type currents are high threshold voltage-activated (HVA) currents; these currents activate at potentials positive to –40 mV and have their maximal amplitude at 0 mV (Fig. 2.63b). Müller cells of the human retina express regularly both LVA and HVA currents, whereas Müller cells from adult rabbits express regularly LVA currents, but only a subpopulation of the cells (~25%) display HVA currents in addition (Bringmann et al., 2000c). Cultured human Müller cells possess L-type calcium channels composed of a_{1D}, a_2 and ß$_3$ subunits (Puro et al., 1996a). Activation of the channels results in an opening of calcium-activated potassium (BK) channels (Puro et al., 1996a). Acutely isolated Müller cells of the human retina display immunoreactivities for different types of the pore-forming subunits of L-type channels, e.g. for α_{1D} (Fig. 2.63d) and (at lower level) α_{1C}. Müller cells of the rat express α_{1D} subunits (Xu et al., 2002), and chicken Müller cells α_{1C} and perhaps α_{1D} (Firth et al., 2001). Müller cells of the tiger salamander have HVA channels which are distributed over the entire membrane of the cells, and express $\alpha_{1A,B,C,D}$ subunits (Welch et al., 2005).

The expression of voltage-gated calcium channels in rabbit Müller cells changes in the course of the ontogenetic development. In the rabbit retina, proliferation of late progenitor cells occurs up to postnatal days 4 (central retina) and 10 (peripheral retina), respectively (Reichenbach et al., 1991a–c). The differentiation of immature radial glial cells into mature Müller cells occurs between the postnatal days 6 and 20, as indicated by the developmental increase in Kir currents (Fig. 2.47d) (Bringmann et al., 1999a). Immature radial glial/Müller cells of the rabbit express only LVA channels; HVA currents are observed only in mature Müller cells after postnatal day 20 (Bringmann et al., 2000c). The amplitude of LVA currents increases during the first postnatal week and remains constant after postnatal day 6 (when the light-evoked ganglion cell activity begins: Fig. 2.47d). This means that immature and mature rabbit Müller cells have similar numbers of LVA channels. The early and sole expression of LVA calcium channels suggests that these channels are involved in the regulation of the proliferation of late progenitor cells as well as in the differentiation of Müller cells, e.g., in the outgrowth of glial side branches and perisynaptic membrane sheaths. The different expression patterns of LVA and HVA channels in developing and mature rabbit Müller cells suggest that the two channel types have different functional roles.

The expression of voltage-gated calcium channels in human Müller cells changes in the course of aging and under pathological conditions. In correlation with the age of human donors, the density of the HVA currents increases while the Kir currents decrease (Fig. 2.63c) (Bringmann et al., 2000b, 2003a). In Müller cells from patients with proliferative vitreoretinopathy (PVR), both LVA and HVA currents display a substantial reduction in their amplitudes (Bringmann et al., 2000b). The membrane conductance of Müller cells from patients with PVR is characterized by an almost total absence of Kir currents (Fig. 2.40b), a substantial increase in voltage-dependent sodium currents, and an enhanced activity of BK channels (Fig. 2.11b) (Francke et al., 1996, 1997; Bringmann et al., 1999b). All these alterations favor rapid fluctuations of the membrane potential that result in an enhanced activity of voltage-gated calcium channels. The downregulation of voltage-dependent calcium channels during proliferative gliosis may protect the cells from cytotoxic calcium overload.

Voltage-gated calcium channels play a role in Müller cell proliferation which commonly occurs in response to retinal injury. The growth factor- and nucleotide-evoked proliferation of cultured Müller cells from guinea pigs is inhibited in the presence of blockers of T- and L-type calcium channels (Kodal et al., 2000). bFGF, but not the platelet-derived growth factor (PDGF), increases the amplitude of L-type calcium currents in cultured human Müller cells; the bFGF-evoked proliferation of the cells depends on the activity of L-type calcium channels (Puro and Mano, 1991; Uchihori and Puro, 1991). The proliferation-inducing effect of calcium channel activation may occur at various levels. Elevations of cytosolic calcium are required for various steps of the cell cycle, and activation of voltage-gated calcium channels may result in a higher transcription rate and exocytotic release of growth factors which stimulate the proliferation of Müller cells via autocrine and/or paracrine pathways. In cultured Müller cells of the guinea pig, the release of growth factors from the cells, and the activation of matrix metalloproteinases (MMPs) that induce a release of membrane-bound growth factors, occur downstream of the calcium responses (Fig. 3.3) (Milenkovic et al., 2003). It has been shown that electrical stimulation of cultured Müller cells enhances the transcription of neurotrophic factors such as insulin-like growth factor (IGF)-1; this effect is mediated by a calcium influx through L-type calcium channels (Sato et al., 2008). IGF-1 stimulates the proliferation of cultured Müller cells (Ikeda and Puro, 1995; Ikeda et al., 1995). It is likely that voltage-gated calcium and BK channels co-operate to enhance the calcium entry from the extracellular space after receptor activation.

In Müller cells of the adult healthy retina, activation of voltage-gated calcium channels is implicated in the exocytotic release of glutamate; this release is stimulated by VEGF, for example, and is implicated in the autocrine regulation of cellular volume (Fig. 2.75b) (Wurm et al., 2008). Apparently, voltage-gated calcium channels have similar roles in differentiated and proliferating Müller cells: they mediate the calcium influx into the cells necessary for the exocytotic release of gliotransmittes such as glutamate and the secretion of growth factors, respectively, from Müller cells. In addition, activation of voltage-gated calcium channels is implicated in the phagocytotic activity of Müller cells (Mano and Puro, 1990).

2.4.5.2 Voltage-Dependent Sodium Channels

Müller cells of a variety of vertebrate species express neuron-type voltage-dependent sodium channels that generate, upon depolarizing voltage steps, fast transient, inwardly directed sodium currents which are sensitive to tetrodotoxin and saxitoxin (Fig. 2.64a). In human cells, the currents activate at voltages positive to –60 mV, peak at –20 mV, and reverse close to the equilibrium potential of sodium ions (Fig. 2.64b). Müller cells from tiger salamanders and guinea pigs do not have such currents, independent of age and retinal pathology (Newman, 1985b; Chao et al., 1994a, b). Müller cells of the cat, dog, horse, zebra, and baboon, and a subpopulation of macaque Müller cells, display voltage-dependent

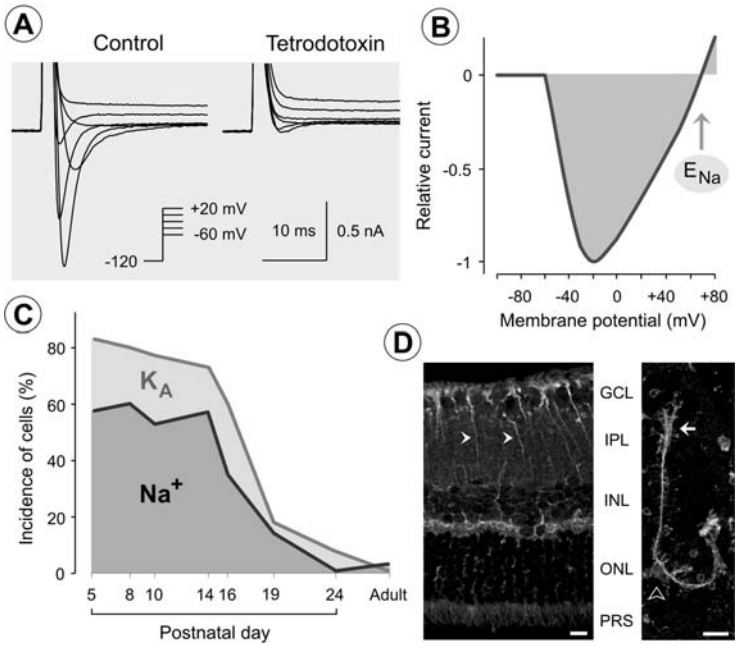

Fig. 2.64 Voltage-gated sodium channels of Müller cells. (**a**) The transient inward sodium currents of a human Müller cell derived from a patient with proliferative diabetic retinopathy are blocked by tetrodotoxin (1 μM). (**b**) Current–voltage relation of the sodium currents of human Müller cells. The currents activate beyond –60 mV, peak at –20 mV and reverse the direction close to the reversal potential of sodium ions (E_{Na}). (**c**) Incidence of Müller cells isolated from the developing retina of the rat which display tetrodotoxin-sensitive, voltage-gated sodium (Na^+) and K_A potassium currents in whole-cell records. (**d**) Müller cells of the adult rat retina display immunoreactivity for voltage-gated sodium channels. A retinal slice (*left*) and an acutely isolated Müller cell (*right*) were stained against the $Na_v1.6$ channel. *Filled arrowheads*, Müller cell fibers that traverse the inner plexiform layer (IPL). *Unfilled arrowhead*, cell soma. *Arrow*, cell endfoot. GCL, ganglion cell layer; INL, inner nuclear layer; NFL, nerve fiber layer; ONL, outer nuclear layer. PRS, photoreceptor segments. *Bars*, 10 μm. Modified from Bringmann et al. (2002b) and Wurm et al. (2006a)

sodium currents (Chao et al., 1993, 1994b, 1997; Reichelt et al., 1997b; Han et al., 2000). Rabbit Müller cells may express such currents under pathological conditions. Only a small fraction (∼3%) of Müller cells of the adult rat retina displays small tetrodotoxin-sensitive sodium currents when recorded in the whole-cell mode of the patch-clamp technique (Wurm et al., 2006a), while approximately 50% of Müller cells from the adult murine retina have such currents (Pannicke et al., 2002). One third of Müller cells from the healthy human retina display voltage-gated sodium currents; the incidence of cells with these currents increases up to ∼90% under pathological conditions (Francke et al., 1996; Reichelt et al., 1997a). In addition, the amplitude of the currents in human Müller cells increases under pathological conditions; Müller cells derived from patients with proliferative retinopathies show action potential-like discharges upon injection of depolarizing currents (Fig. 3.11c) (Francke et al., 1996). This capability may reflect the transdifferentiation of Müller cells into progenitor/neuron-like cells in the course of proliferative gliosis. The activity of voltage-gated sodium channels causes rapid fluctuations of the membrane potential that support the opening of voltage-dependent calcium channels; the calcium influx is required for the Müller cell proliferation and for the exocytotic release of growth factors and gliotransmitters such as glutamate from Müller cells (Fig. 2.75b).

The presence of voltage-dependent sodium currents is differently regulated in the course of the ontogenetic development of Müller cells from different species. While the incidence of murine Müller cells that display such currents increases in the course of retinal development (Pannicke et al., 2002), the incidence of rat Müller cells with such currents rapidly decreases (Fig. 2.64c) when the Kir currents display a steep developmental increase after postnatal day 14 (Fig. 2.45a) (Wurm et al., 2006a). The reason for this species difference is unclear. Interestingly, Müller cells of the adult rat retina display immunoreactivity for $Na_v1.6$ (Fig. 2.64d), and tetrodotoxin prevents the VEGF-evoked inhibition of osmotic swelling of Müller cells isolated from the adult rat retina which is mediated by the exocytotic release of glutamate (Fig. 2.75b). (Rodent Müller cells may also express the tetrodotoxin-resistant channel $Na_v1.9$: O'Brien et al., 2008.) These data suggest that Müller cells of the mature rat retina express voltage-gated sodium channels which are implicated in the agonist-evoked exocytosis of glutamate; however, these channels are not activable by membrane depolarization alone; instead, additional intracellular messengers (which are formed after receptor activation) are necessary to activate the channels. These second messengers are absent during whole-cell recordings. On the other hand, in immature Müller cells of the rat, these channels may be activable solely by membrane depolarization, and likely mediate (in association with other channels such as K_A channels: Fig. 2.64c) rapid fluctuations of the membrane potential which enhance the open probability of voltage-gated calcium channels. Thus, the decrease in the incidence of Müller cells in the developing rat retina that display voltage-gated sodium currents (Fig. 2.64c) may reflect an alteration in channel gating rather than a downregulation of channel protein. However, the functional significance and activation parameters of voltage-dependent sodium channels in Müller cells remain to be further elucidated.

2.4.5.3 Epithelial Sodium Channels

In the rabbit retina, Müller cells have α-epithelial sodium channels (ENaCs) (Brockway et al., 2002). The expression of α-ENaCs in cultured Müller cells of the rat is increased by activation of mineralocorticoid receptors with aldosterone (Golestaneh et al., 2001). ENaCs may play a role in the regulation of the extracellular sodium concentration and in the regulation of cell volume under varying osmotic conditions.

2.4.5.4 Cation Channels

Müller cells may express several types of non-selective cation channels. In bovine and human Müller cells, blood serum (but not plasma) activates calcium-permeable cation channels; this activation is followed by a delayed activation of an outward potassium conductance. Both conductances are also activated by serum-derived molecules such as lysophosphatidic acid (Kusaka et al., 1998, 1999). Cultured human Müller cells express calcium-permeable cation channels which are activated by cytosolic calcium; the open time of the channels is increased during administration of bFGF (Puro, 1991a). The opening of these channels provides a pathway for the influx of calcium from the extracellular space at the resting membrane potential, when the cytosolic calcium level is increased after a release of calcium from intracellular stores.

Müller cells have calcium-permeable, store-operated channels (SOCs) which are activated after depletion of internal calcium stores, e.g. upon activation of metabotropic receptors (Moll et al., 2002; Da Silva et al., 2008). Though the molecular identity of SOCs is not well established, several members of the cation-permeable transient receptor potential canonical (TRPC) channel family may be candidate SOCs and may contribute to receptor- and store-operated capacitative calcium entry. Cultured mouse Müller cells express TRPC1 and TRPC6; these channels are activated after stimulation of muscarinic M1 receptors (Da Silva et al., 2008). In chicken retina, TRPC4 was localized to Müller cells and neurons (Crousillac et al., 2003).

Cultured human Müller cells have stretch-activated calcium-permeable cation channels; activation of the channels results in an increased activity of BK channels (Puro, 1991b). The efflux of potassium ions through BK channels (which is associated with an outflow of cell water) was suggested to be a mechanism to decrease the volume of Müller cells after cell swelling (Puro, 1991b).

Cyclic guanosine monophosphate (cGMP) activates cGMP-gated cation channels in bovine and human Müller cells; this results in membrane depolarization and calcium influx, and activation of BK channels (Kusaka et al., 1996). Nitric oxide (NO) donors induce currents that are similar to those activated by cGMP (Kusaka et al., 1996). NO is an activator of the guanylyl cyclase that produces cGMP (Knowles et al., 1989). In situ, NO is derived from retinal neurons and Müller cells (which may constitutively express NO synthetases) (Yamamoto et al., 1993; Liepe et al., 1994; Kurenni et al., 1995; Fischer and Stell, 1999; Ota et al., 1999; Haverkamp et al., 1999; Cao et al., 1999a, b; Kobayashi et al., 2000; Cao and

Eldred, 2001). Under pathological conditions such as inflammation, ischemia, and elevated hydrostatic pressure, Müller cells express inducible NO synthase (Goureau et al., 1994, 1997, 1999; de Kozak et al., 1997; Cotinet et al., 1997a, b; Tezel and Wax, 2000). The presence of calcium-permeable cGMP-gated non-selective cation channels was also described in freshly isolated Müller cells of the bullfrog; these channels open upon activation of the natriuretic peptide receptor-A (Cao and Yang, 2007) which is coupled to guanylyl cyclase. The calcium-binding protein S-100β stimulates a membrane-bound guanylyl cyclase in Müller cells at high calcium concentrations (Rambotti et al., 1999).

2.4.5.5 Chloride Channels

Normally, the chloride conductance of Müller cell membranes is very low (Newman, 1985a). However, pharmacological investigations suggest that Müller cells of the rat express second messenger-gated chloride channels; the opening of the channels and an efflux of chloride ions are implicated in the equalization of the osmotic gradient across Müller cell membranes under hypoosmotic conditions (Fig. 2.75b) (Uckermann et al., 2006; Wurm et al., 2008). These channels are activated after stimulation of adenosine A1 receptors and subsequent activation of the adenylyl cyclase, protein kinase A, and phosphatidylinositol-3 kinase (PI3K). Müller cells of the tiger salamander express calcium-activated chloride channels that are activated upon a depolarization-evoked calcium influx through voltage-gated calcium channels (Welch et al., 2006).

2.5 Retina Metabolism: A Symbiosis Between Neurons and Müller Cells

2.5.1 Energy Metabolism

Müller cells are strikingly resistant to a wide variety of pathogenic conditions, including ischemia, hypoxia, and hypoglycemia (Shay and Ames, 1976; Kitano et al., 1996; Silver et al., 1997; Stone et al., 1999). One reason for this relative insusceptibility to injury is their specialized energy metabolism which depends to 80–90% on glycolysis (aerobically and anaerobically). This enables the Müller cells to reliably switch to anaerobic glycolysis in the presence of insufficent oxygen supply, and to withstand even long-lasting anoxia (Poitry-Yamate et al., 1995; Winkler et al., 2000). As long as oxygen is available, Müller cells are also resistant to the absence of glucose since other substrates such as lactate, pyruvate, glutamate or glutamine can be metabolized to generate energy substrates by the tricarboxylic acid cycle, a pathway that is normally non-dominant in the cells (Tsacopoulos et al., 1998; Winkler et al., 2000). Under these conditions, the carbon skeleton of glutamate enters the tricarboxylic acid cycle as α-ketoglutarate. Short periods of glucose deficiency (45–60 min: Johnson, 1977) can further be compensated by the prominent glycogen deposits in Müller cells (Kuwabara and Cogan, 1961; Reichenbach et al.,

1999; Gohdo et al., 2001). Müller cells are also well endowed with the enzyme, glycogen phosphorylase (Pfeiffer et al., 1994; Pfeiffer-Guiglielmi et al., 2005).

Apparently, the extent of glycolysis and mitochondrial respiration differ in Müller cells of avascular and vascularized retinas. Müller cells of avascular retinas (e.g. of guinea pigs and rabbits) contain only a few mitochondria at their distal-most end, directed towards the choroid as the only oxygen source (Figs. 2.9 and 2.39e) (Sjöstrand and Nilsson, 1964; Magalhães and Coimbra, 1972; Uga and Smelser, 1973; Reichenbach, 1988a, 1989a; Germer et al., 1998a, b; Stone et al., 2008). The mitochondrial energy production of these cells can be blocked over hours without measurable effects on energy-consuming functions such as the maintenance of plasma membrane hyperpolarization (whereas the cells rapidly depolarize when the anaerobic glycolysis is blocked) (Reichenbach et al., 1999). Müller cells from vascularized retinas contain many mitochondria which are distributed along the entire length of the cells, probably due to a sufficent oxygen availability throughout the tissue (Germer et al., 1998a, b). When the mitochondrial energy production of such cells (from rats) is blocked, their plasma membranes slowly depolarize, suggesting that these cells cannot be completely resistant to anoxia (own unpublished results). The plasma membranes of these cells also depolarize more rapidly when anaerobic glycolysis is blocked.

Under normal conditions, the vast majority of glutamate taken up by Müller cells is converted to glutamine, and only a small fraction of glutamate is transported into the mitochondria (Poitry et al., 2000). The expression of the enzyme, aspartate aminotransferase (Gebhard, 1991), of glutamate-aspartate exchangers in mitochondrial membranes, and thus the activity of the malate-aspartate shuttle in Müller cells (Fig. 2.37), are low (LaNoue et al., 2001; Ola et al., 2005; Xu et al., 2007). Therefore, Müller cells are not able to completely oxidize glucose or lactate within the mitochondria. Instead, they display a high rate of aerobic glycolysis resulting in the production of lactate and pyruvate that is released into the extracellular space and taken up by photoreceptors (LaNoue et al., 2001; Xu et al., 2007). The expression level of the glutamate-aspartate exchanger is dependent on the differentiation state of the cells, and is enhanced under pathological or cell culture conditions when the cells dedifferentiate and proliferate. Glucocorticoids inhibit the glutamate-induced increase in mitochondrial NADH (Psarra et al., 2003); hydrocortisone increases the expression of glutamine synthetase in Müller cells, and decreases the level of the glutamate-aspartate exchanger (Ola et al., 2005). When the expression of glutamine synthetase is decreased (as in proliferating cells), more glutamate enters the mitochondria. Since Müller cells lack the phosphoglucose isomerase-1, glycolysis proceeds entirely through the pentose phosphate pathway (Archer et al., 2004).

2.5.1.1 Metabolic Glio-Neuronal Symbiosis

A major function of Müller cells is to nourish retinal neurons and photoreceptors in periods of intense activity. In contrast to the energy metabolism of Müller cells which primarily depends on glycolysis, the energy metabolism of retinal neurons relies on both glycolysis and respiration (Winkler, 1981). All retinal cells use

glucose as primary energy substrate. In periods of intense neuronal activity (as in the dark), photoreceptors and inner retinal neurons utilize monocarboxylates such as lactate and pyruvate as additional fuel for their oxidative energy metabolism. These monocarboxylates are formed in photoreceptors, and additionally are derived from Müller cells (Poitry-Yamate and Tsacopoulos, 1991, 1992; Poitry-Yamate et al., 1995; Tsacopoulos and Magistretti, 1996; Winkler et al., 2000, 2003a, b, 2004a, b; Wood et al., 2005; Xu et al., 2007). (In addition to being an energy substrate, Müller cell-derived lactate has also a functional role in the assembly of photoreceptor outer segment membranes: Jablonski et al., 1999; Jablonski and Iannaccone, 2000; pyruvate and other 2-ketoacids like α-ketoglutarate, but not lactate, act also as free radical scavengers which protect Müller cells from necrosis under nitrosative stress conditions: Frenzel et al., 2005). The neurotransmission in the retina is 80% faster in the dark than in the light; the increased neurotransmission is associated with an ∼40% increase in aerobic glycolysis, and an ∼40% increase in pyruvate consumption (Xu et al., 2007). Half of the metabolic energy consumed in the retina (41% of oxygen uptake and 58% of glycolysis) is utilized to support the activity of the Na, K-ATPase, maintaining the dark current of photoreceptors and other cellular functions such as transmitter uptake (Ames et al., 1992). The metabolic interaction in periods of intense retinal activity has beneficial consequences for both photoreceptors (which survive the periods of metabolic stress associated with dark adaptation) and Müller cells (which are getting rid of the "unwarranted" acidic end product of their metabolism, preventing them from acidotic damage).

The production of lactate in Müller cells is stimulated by glutamate released from activated neurons; thus, glutamate uptake by Müller cells signals the energy requirements of nearby neurons (Poitry-Yamate et al., 1995; Poitry et al., 2000; Voutsinos-Porche et al., 2003). Neuron-derived ammonia participates in the regulation of Müller cell metabolism; it increases the formation of lactate by activating the phosphofructokinase and by inhibiting the α-ketoglutarate dehydrogenase (Marcaggi and Coles, 2001).

The transport of monocarboxylates through cellular membranes is facilitated by transport proteins. Müller cells, neurons and retinal capillaries express different subtypes of monocarboxylate transporters (Bergersen et al., 1999; Gerhart et al., 1999; Chidlow et al., 2005; Martin et al., 2007); loss of the transporters results in abnormal photoreceptor cell function and degeneration (Philp et al., 2003). Under culture conditions, inhibition of glucose transporters causes death of retinal glial cells, while inhibition of monocarboxylate transporters causes death of retinal neurons (Wood et al., 2005).

2.5.1.2 Glucose Metabolism

Glucose is crucial for the function of photoreceptors, retinal neurons, and glial cells. Exogenous glucose can be extracted from the retinal and choroidal circulation, and endogenous glucose may be generated from breakdown of glycogen stores. Photoreceptors, retinal neurons, pigment epithelial cells, glial cells, and vascular endothelium express facilitative glucose transporters (GLUT1-4), suggesting

that they have the capability to transport exogenous glucose from the circulation (Kumagai et al., 1994; Watanabe et al., 1994; Nihira et al., 1995; Hosoya et al., 2008). These transporters also transfer dehydroascorbic acid (vitamin C) across the inner blood-retinal barrier; vitamin C accumulates as reduced ascorbic acid in Müller cells (Woodford et al., 1983; Hosoya et al., 2008). Müller cells may also take up extracellular lactate, transform it to glucose, and release it into the extracellular space, with no incorporation into Müller cell glycogen (Goldman, 1990). Glucagon and VIP, or an increase in cAMP, stimulate gluconeogenesis, while VIP also inhibits the glycolytic flux (Goldman, 1990). Müller cells (in addition to vascular endothelial cells and cone photoreceptors) also take up galactose (Keegan et al., 1985).

2.5.1.3 Glycogen Metabolism

Glycogen is differentially distributed in retinas of various species. In the rabbit retina, glycogen particles are only present in Müller cells; in other species, Müller cells and subclasses of retinal neurons (ganglion cells, rod bipolar and distinct amacrine cells) contain glycogen (Kuwabara and Cogan, 1961; Eichner and Themann, 1962; Schabadasch and Schabadasch, 1972a; Johnson, 1977; Reichenbach et al., 1988a, 1993a, b). Müller cells of the cat (vascularized retina) are filled uniformly with fine-grain glycogen throughout their whole cell bodies (Rungger-Brändle et al., 1996) while rabbit Müller cells (avascular retina) contain glycogen particles mainly in the inner (vitread) part. Short wavelength (blue) cone photoreceptors, distinct retinal neurons, and Müller cells express the brain isoform of glycogen phosphorylase (Reichenbach et al., 1993a, b; Pfeiffer et al., 1994; Nihira et al., 1995; Pfeiffer-Guglielmi et al., 2005; Rothermel et al., 2008). Glycogen is rapidly catabolized and resynthesized when the retina is stimulated by light (Schabadasch and Schabadasch, 1972b) or during retinal ischemia-reperfusion (Johnson, 1977; Gohdo et al., 2001). Müller cells hydrolyze glycogen when they are exposed to elevated extracellular potassium, a signal that is involved in the regulation of neuronal-glial metabolic cooperation (Reichenbach et al., 1993a, b). Insulin increases the glycogen content of Müller cells (Reichenbach et al., 1993a, b). Müller cells may produce insulin (Das et al., 1984, 1987) and have insulin receptors (Naeser, 1997; Gosbell et al., 2002). Insulin may also activate IGF-1 receptors on Müller cells (Layton et al., 2006).

2.5.1.4 Creatine Metabolism

In high-energy consuming, metabolically active tissues like the retina, creatine and phosphocreatine play important roles in energy storage. Müller cells synthesize creatine; the creatine synthetic enzyme is colocalized with glutamine synthetase in the cells (Nakashima et al., 2005). The creatine transporter is localized to various cell types in the retina, including photoreceptors, amacrine, bipolar, and ganglion cells, blood vessels, and perivascular astrocytes, while Müller cells lack this transporter (Acosta et al., 2005).

2.5.2 Lipid Metabolism

The retina has the capacity both to synthesize cholesterol de novo and to take up blood-borne lipids (Fliesler and Keller, 1997). Circulating low-density lipoproteins (LDL) enter the retina through the retinal pigment epithelium and Müller cells via a process mediated by LDL receptors which recognize ApoB (Tserentsoodol et al., 2006a). There is a lipid shuttle from Müller cells to neurons in supplying the needs of neurons for lipids, especially for the maintenance/renewal of the long projection axons of retinal ganglion cells and the photoreceptor outer segments (which consist of ample membraneous disks), as well as for synapse formation (Mauch et al., 2001). This shuttle involves both LDL and high-density lipoproteins (HDL). Müller cells and astrocytes synthesize ApoE and ApoJ which are assembled into cholesterol-rich lipoprotein particles (Boyles et al., 1985; Amaratunga et al., 1996; Shanmugaratnam et al., 1997; Kuhrt et al., 1997; Kurumada et al., 2007). These particles are secreted into the vitreous, and subsequently taken up by retinal ganglion cells and transported centrally within the optic nerve (Amaratunga et al., 1996). Photoreceptor cells have receptors for ApoE (Kurumada et al., 2007); LDL receptors are localized to neurons and Müller cells (Tserentsoodol et al., 2006a). The ABCA1 transporter (which is responsible for the transport of ApoE and ApoA1, the major protein component of HDL) and the scavenger receptors, SR-BI and SR-BII responsible for HDL uptake, are expressed by retinal neurons and photoreceptors (Tserentsoodolet et al., 2006b).

Docosahexaenoic acid (DHA) is a trophic factor required by photoreceptors for their disk membranes. Müller cells take up DHA (Gordon and Bazan, 1990), incorporate it into glial phospholipids, and channel it towards the photoreceptors (Polit et al., 2001). Müller cells express fatty acid-binding and -transfer proteins for the transport of DHA and other fatty acids (Deguchi et al., 1992; Kingma et al., 1998).

2.5.3 Metabolism of Toxic Compounds

Müller cells and photoreceptors express the sterol 27-hydroxylase (Lee et al., 2006) which is a mitochondrial P-450 enzyme that hydroxylates toxic oxysterols formed by photooxidation. Hydroxylation of cholesterol may also promote the efflux of cholesterol from the retina. The peroxisomes of Müller cells (Leuenberger and Novikoff, 1975; Beard et al., 1988; St Jules et al., 1992) may be involved in the metabolism of lipoproteins derived from photoreceptors. Müller cells express glutathione S-transferases (McGuire et al., 1996) which are involved in the detoxication of electrophilic xenobiotics. An increase in the expression of these enzymes may protect retinal neurons from environmental toxicants accumulated in the blood (McGuire et al., 1996, 2000). The immunoreactivity of the glutathione S-transferase, a biomarker of toxicant exposure, increases in Müller cells of mice exposed to aerosolized jet fuel; this finding has relevance for the Air Force personnel that clean and maintain fuel pods (McGuire et al., 2000).

Methanol poisoning results in retinal toxicity in humans and non-human primates (but not rodents) mediated by its metabolite, formate, which is toxic to mitochondria. Formate is detoxified to carbon dioxide by a two-step oxidation process that is ATP- and folate-dependent. The sensitivity of the primate retina to methanol/formate toxicity was ascribed to the limited capacity to oxidize formate due to the low amount of retinal folate (Martinasevic et al., 1996). Because the enzymes for formate detoxification are preferentially localized in Müller cells (Martinasevic et al., 1996), they are the primary target for methanol/formate-induced retinal toxicity (Garner et al., 1995).

2.6 Other Glio-Neuronal Interactions in the Retina

2.6.1 Recycling of Photopigments

Photoreceptors need the support of retinal pigment epithelial and Müller cells to maintain visual sensitivity. Visual pigments in the photoreceptors consist of an opsin and 11-*cis* retinal. Phototransduction is triggered by the photic conversion of 11-*cis* retinal to all-*trans* retinal which is subsequently reduced to all-*trans* retinol in the photoreceptor outer segments (Tsacopoulos et al., 1998). There are two cycles that regenerate 11-*cis* retinal from all-*trans* retinol: the rod and the cone visual cycle (Muniz et al., 2007). Rod-derived all-*trans* retinol is converted to 11-*cis*-retinal in the pigment epithelium while cone-derived all-*trans* retinol is processed in Müller cells. Apparently, Müller cells convert all-*trans* retinol to 11-*cis*-retinol which is subsequently oxidized to 11-*cis* retinal by a retinol dehydrogenase, and released into the extracellular space for uptake by cone photoreceptors (Das et al., 1992; Mata et al., 2002; Muniz et al., 2007). The kinetics of cone pigment regeneration (full recovery within 5 min) is much faster than rod pigment regeneration (∼100 min) (Muniz et al., 2007). Pigment epithelial and Müller cells express RDH10, an all-*trans* retinol dehydrogenase, in the microsomal fraction (Wu et al., 2004). RDH10 generates all-*trans* retinal, which is the substrate for the photoisomerase retinal G protein-coupled receptor (RGR), an opsin found in pigment epithelial and Müller cells (Jiang et al., 1993; Pandey et al., 1994). RGR forms a complex with RDH5 (11-*cis* retinol dehydrogenase) to isomerize all-*trans* retinal to 11-*cis* retinal, thus providing an alternate pathway to obtain *cis* retinoids in the visual cycle. However, the distinct pathways and enzymes implicated in photopigment regeneration in Müller cells remain to be determined (Muniz et al., 2007).

Vitamin A (retinoids) are fat-soluble molecules which need retinol binding proteins to be transfered in aqueous cytosolic and extracellular locations. Müller cells express cellular retinol binding protein (CRBP), that binds all-*trans* retinol, and cellular retinal binding protein (CRALBP) (Fig. 2.48) that binds 11-*cis* retinol and 11-*cis* retinal (Bunt-Milam and Saari, 1983; Bok et al., 1984; Eisenfeld et al., 1985). The interphotoreceptor matrix that surrounds the inner and outer segments of photoreceptors, contains the interphotoreceptor retinoid binding protein (IRBP) which is likely responsible for the transfer of retinoids between cones and Müller

cells. Müller cells are the major source of laminin-ß2 which is a component of the interphotoreceptor matrix (Libby et al., 1997).

In addition to retinal pigment epithelial cells, Müller cells contribute to the assembly of photoreceptor outer segments into stacked discs, in part by the release of lactose and pigment epithelium-derived factor (Wang et al., 2003, 2005b), and may phagocytize and degrade outer-segment discs shed from cone photoreceptors (Long et al., 1986).

It is interesting to note that in respect to photopigment recycling and outer segment renewal, the Müller cells interact with cones but not with rods. It may be speculated that this goes back to very ancestral (pre-)vertebrate retinas which probably contained ~1 cone per Müller cell, but no rods (rods were "invented" later in evolution than cones; for details, see Reichenbach and Robinson, 1995). Whereas the Müller cell metabolism was suffcient to maintain photopigment recycling and outer segment renewal of the cone(s), it might have been overload by the metabolic needs of additional rods (up to >80 per Müller cell in frogs and some fish, cf. Section 2.2.2). This may have then urged the pigment epithelium to overtake of these interactions with the rods.

2.6.1.1 pH Homeostasis and CO_2 Siphoning

Light-evoked neuronal activity generates extracellular alkalinization in the retina of up to 0.1 pH units (Borgula et al., 1989; Oakley and Wen, 1989; Yamamoto et al., 1992) which is caused by activation of neurotransmitter receptors, the release of ammonia from neurons, and the uptake of protons by Müller cells through electrogenic glutamate transporters, for example (Coles et al., 1996; Owe et al., 2006; Beart and O'Shea, 2007). This pH shift is balanced by an efflux of protons, e.g. from the photoreceptor terminals (deVries, 2001), and by the consecutive action of the enzyme carbonic anhydrase and of acid-base transporters of Müller cells (Newman, 1996). Müller cells express a number of acid-base transport systems, including a sodium-bicarbonate cotransporter, a chloride-bicarbonate anion exchanger, and a sodium-proton exchanger (Sarthy and Lam, 1978; Newman, 1991, 1996; Kobayashi et al., 1994). The sodium-bicarbonate cotransporter and the anion exchanger are localized preferentially to the endfeet of the cells (Newman, 1991, 1996). The sodium-bicarbonate carrier transports three bicarbonate molecules along with one sodium ion (Newman, 1991). Because the transporter is electrogenic, cell depolarization evoked by increased extracellular potassium results in an influx of sodium and bicarbonate, resulting in intracellular alkalinization in Müller cells and in an extracellular acidification; the efflux of acid equivalents then buffers the light-evoked extracellular alkalinization (Newman, 1996). Even the small depolarization-induced extracellular acidification generated by Müller cells may have a severe inhibitory effect on synaptic transmission because, for example, an acidification of 0.05 units produces a 24% reduction in the synaptic transmission from photoreceptors to post-receptoral neurons (Barnes et al., 1993). Activity-dependent acid efflux from Müller cells may thus represent a component of a negative feedback system limiting neuronal excitability.

Oxidative degradation of glucose causes the formation of water and carbon dioxide (Fig. 2.66); both metabolic “waste products” are transported out of the retina through Müller cells. The retina is one of the most metabolically active tissues in the body and produces substantial amounts of carbon dioxide which must be removed to prevent tissue acidosis. By the removel of carbon dioxide, Müller cells also regulate retinal pH. Active neurons (particularly photoreceptors in the dark) release metabolic carbon dioxide which is rapidly hydrated to bicarbonate and protons by the enzyme, carbonic anhydrase (Oakley and Wen, 1989). In the retina, carbonic anhydrase II (which constitutes 3% of total retina protein in the chicken) is localized intracellularly in Müller cells and in a subset of amacrine cells, while the membrane-bound carbonic anhydrase XIV is localized extracellularly on Müller cells, astrocytes, and the vascular endothelium (Linser and Moscona, 1981a; Linser et al., 1984; Newman, 1994; Ochrietor et al., 2005; Nagelhus et al., 2005). Bicarbonate is transported to the vitreous humor by sodium-bicarbonate cotransporters localized to the Müller cell endfeet. The preferential localization of acid-base transport systems to Müller cell endfeet leads to a polarized "carbon dioxide siphoning” that augments the carbon dioxide transfer out of the retinal tissue (Newman, 1994). The membrane-bound carbonic anhydrase XIV is suggested to be the target of carbonic anhydrase inhibitors that enhance subretinal fluid absorption in macular edema (Nagelhus et al., 2005). The recovery of intracellular pH following intracellular acidification of Müller cells is dependent on the sodium-proton exchanger.

2.6.1.2 Transcytosis of Retinoschisin

Retinoschisin, a signaling molecule related to neuropilins, is synthesized and secreted by photoreceptor cells in the outer retina; then it interacts with inner retinal cells contributing to synaptic organization and optic nerve fiber integrity. Retinoschisin is taken up by Müller cells from the retinal outer border (the photoreceptor side) and subsequently carried into the inner retina (Reid and Farber, 2005) (cf. also Section 3.2.11).

2.6.1.3 Metal Ion Homeostasis

Müller cells are involved in the iron homeostasis of the retina. The major pathway for iron import occurs via transferrin, the extracellular iron carrier protein; it binds to transferrin receptors on the cell surface, and is endocytozed. Export of iron is achieved by iron transporters, such as ferroportin, while storage of iron is achieved through sequestration by cytosolic ferritin. In the retina, cytosolic ferritins are present predominantly in photoreceptor and bipolar cells (Hahn et al., 2004). Müller cells express transferrin and ferroportin, and store iron mainly in their endfeet (Zeevalk and Hyndman, 1987; Hahn et al., 2004; Chowers et al., 2006). Ferroportin colocalizes with ceruloplasmin and hephaestin to Müller cells, supporting a potential cooperation between these ferroxidases and the iron exporter (Hahn et al., 2004). An elevated expression of transferrin in Müller cells from patients with

age-related macular degeneration may represent a response to the altered retinal iron homeostasis (Chowers et al., 2006). Müller cells express also the zinc transporter protein-3 (ZnT-3), suggesting that they regulate the retinal zinc homeostasis (Redenti and Chappell, 2007). Zinc ions are released from the synaptic terminals of photoreceptor cells (Wu et al., 1993; Qian et al., 1994).

2.7 Mutual Signal Exchange Between Retinal Neurons and Müller Cells

It has already been mentioned at several places that there is a signal exchange between retinal neurons and Müller cells, as well as vice versa. The following sections will compile the hitherto-known facts and some speculations on this mutual signal transfer in normal visual function.

2.7.1 Müller Cells Can Sense – And Respond to – Retinal Neuronal Activity

There are several possible pathways of signal transfer from neurons to Müller cells. For example, the release of neuro- and co-transmitters from active retinal neurons can be "sensed" by the Müller cells by their neurotransmitter receptors (→ Section 2.8); furthermore, an activation of the electrogenic glial neurotransmitter uptake carriers causes a membrane depolarization of the glial cells (→ Section 2.4). Another way how glial cells may perceive neuronal activity is via their K^+ channels; active neurons release K^+ ions into the extracellular space which also causes a membrane depolarization of the Müller cells; vice versa, the decreased K^+ ion release by illuminated photoreceptor cells causes a membrane hyperpolarization of the Müller cells (→ Section 2.5). It has also been speculated that the glial perinodal "fingers" act as ephapses, perceiving the axonal action potentials in the NFL (→ Section 2.1.4, Fig. 2.12). Additional pathways of signal transfer may be provided either directly by hitherto-unknown signal molecules, or indirectly by a decreased extracellular glucose concentration and pO_2 (or increased pCO_2) (→ Section 2.11) or by mechanical stimuli, due to swelling of neuronal cell processes and synapses (→ Section 2.6).

Indeed, it can be demonstrated that Müller cells can sense – and respond to – retinal neuronal activity. In vital rat retinal preparations, light flashes that stimulate neuronal activity evoke rapid calcium transients in Müller cells (Newman, 2005). This neuron-to-glia signaling was suggested to be mediated by a release of ATP from inner retinal neurons and subsequent activation of glial P2Y receptors. Another recent study showed that light stimulation of dark-adapted guinea-pig retina whole-mounts or slices results in two different calcium rises in the Müller cells (Rillich et al., 2009) (Figs. 2.67 and 2.68). Basically, all Müller cells displayed a slow, more or less simultaneous Ca^{2+} rise throughout their cytoplasm when their adjacent (but not distant) photoreceptors were stimulated by flickering light; one may call this

responding Müller cell population a glial macrodomain (Fig. 2.67c). The slow Ca^{2+} rise reached its maximum after 2–3 min and declined thereafter. It is not yet clear which neuronal signal(s) trigger(s) this response; probably, a hyperpolarization of Müller cell membrane (due to the light-induced decrease in subretinal potassium concentration), and a decrease of the electrogenic activity of the glial glutamate and zinc uptake transportes during illumination triggers a Ca^{2+} influx into the cells (Rillich et al., 2009). With a delay of 2–6 min, fast "flickering" Ca^{2+} rises were observed in a subpopulation of the Müller cells (Figs. 2.67a and 2.68a). These Ca^{2+} rises descended from the Müller cell endfeet towards the soma (Fig. 2.68b) and depended on Ca^{2+} release from intracellular stores, probably from abundant smooth ER in the endfeet (cf. Fig. 2.11b). These "fast, flickering" Ca^{2+} responses may be triggered by a suprathreshold slow Ca^{2+} rise in the same cell and/or by (purinergic?) signals from the adjacent neurons.

This raises the question which types of ligand receptors are expressed by Müller cells, as a putative basis for sensing neuronal activity. Generally, there are metabotropic receptors (which are coupled to intracellular second messenger systems) and ionotropic receptors (which represent ligand-gated ion channels). Müller cells express both types of receptors. However, there is a great species-dependent variation in the expression of distinct receptor subtypes. Whereas metabotropic purinergic (P2Y) and metabotropic glutamate receptors are commonly expressed by Müller cells, ionotropic receptors are only expressed in Müller cells of distinct species. Even Müller cells of one animal may vary in their expression of receptors, i.e. receptors may be expressed only in subpopulations of Müller cells from one retina.

Before going into detail, it should be noted that many data regarding receptor expression in Müller cells were obtained in cultured cells. These data must be interpreted with caution, however, because cultured Müller cells are known to differ from cells in situ in important aspects; for example, cultured Müller cells dedifferentiate and lose their Kir channels (Kuhrt et al., 2008), change their receptor expression (Small et al., 1991), undergo a fibroblastic transdifferentiation (Guidry, 1996, 2003, 2005) or even a transdifferentiation into a neuron-like phenotype (Kubrusly et al., 2005). Results obtained in cultured cells may reflect properties of glial dedifferentiation, proliferation, and transdifferentiation in reactive gliosis in situ (Fischer and Reh, 2003; Ooto et al., 2004; Takeda et al., 2008). The following text gives an overview of receptor expression in Müller cells, with the exception of growth factor and cytokine receptors (for these, see Sections 3.1.3 and 3.2.3).

2.7.1.1 Glutamate Receptors

Glutamate is the most important excitatory neurotransmitter in the retina, acting in the vertical axis consisting of photoreceptor, bipolar, and ganglion cells. In addition, glutamate is a gliotransmitter, and may be exocytotically released from Müller cells after activation of receptors that cause intracellular calcium responses (Fig. 2.75b) (Wurm et al., 2008). Excitatory amino acids (glutamate and aspartate) exert their action through the activation of specific ionotropic and metabotropic receptors.

Ionotropic glutamate receptors are ligand-gated cation channels; the direction of the receptor currents reverses at the equilibrium potential of cations (0 mV); thus, activation of the receptors causes a depolarization of the cells. Metabotropic glutamate receptors (mGluRs) are G protein-coupled receptors linked to second messenger systems, for example to phosphoinositide hydrolysis and release of calcium from intracellular stores, inhibition or activation of adenylyl cyclase, or activation of phosphodiesterase.

Ionotropic Glutamate Receptors

There are three major types of ionotropic glutamate receptors called NMDA, AMPA, and kainate receptors. Native receptors of all of these families are tetrameric assemblies comprising more than one type of subunit. NMDA receptors may be composed of NR1, NR2, and possibly NR3 subunits. While NR1 is essential for the formation of functional channels, NR2 and NR3 play a modulatory role. Glutamate binds to the NR2 subunit, while the glycine-binding site is on the NR1 subunit. AMPA receptors are composed of GluR1–4 subunits, and kainate receptors are composed of GluR5–7 and KA-1 and 2 subunits.

The AMPA receptor subunit GluR4 is localized on Müller cells of goldfish and frogs (Yazulla and Studholme, 1999; Vandenbranden et al., 2000b; Vitanova, 2007). Müller cells of the cat express immunoreactivity for the AMPA receptor subunit GluR2 which is increased after retinal detachment (Lewis et al., 1999b). GluR4 was immunohistochemically localized to Müller cells in slices of the rat retina (Peng et al., 1995). Müller cells of the cat express NR2A subunits (Goebel et al., 1998), while Müller cells of the rat display immunoreactivities of NR1, NR2A, and NR2B subunits (Gründer et al., 2000) and express mRNA for NMDA receptor subunits (Pannicke et al., 1999). However, freshly dissociated Müller cells of the rat apparently do not express functional ionotropic glutamate receptors, as indicated by the fact that agonists of the receptors (kainate, NMDA) do not evoke membrane currents when recorded in the whole-cell mode of the patch-clamp technique (Fig. 2.65a) (Felmy et al., 2001; Pannicke et al., 2005a). A lack of alterations in the membrane conductance upon administration of ionotropic glutamate receptor agonists was also observed in whole-cell records of Müller cells from tiger salamanders, mice, guinea pigs, and rabbits (Brew and Attwell, 1987; Schwartz and Tachibana, 1990; Sarantis and Attwell, 1990; Reichenbach et al., 1997; Pannicke et al., 2002; Uckermann et al., 2004a). Acutely dissociated Müller cells of the human retina display NMDA-evoked receptor currents when recorded in the perforated-patch configuration of the patch-clamp technique (Puro et al., 1996b). The reason for the absence of kainate- and NMDA-evoked membrane currents in whole-cell records of freshly isolated rat Müller cells (despite the presence of NMDA subunit mRNA and proteins) is unclear. It could be that in Müller cells (in contrast to neurons) ionotropic glutamate receptors are not activated by agonist binding alone but that a co-activation by distinct intracellular second messengers is required to open the channels. These second messengers may be washed out from the cytosol after establishment of the whole-cell configuration of the patch-clamp technique.

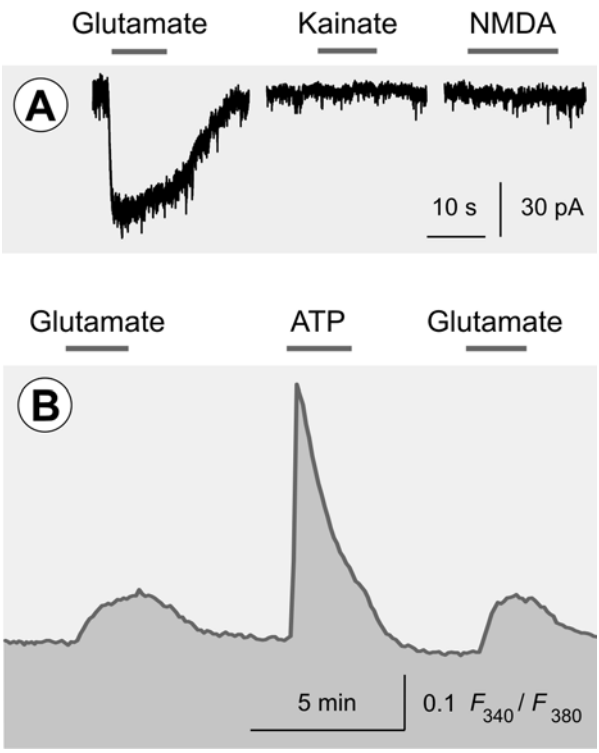

Fig. 2.65 Acutely isolated Müller cells express metabotropic but no functional ionotropic glutamate receptors. (**a**) Administration of glutamate (100 μM) to a rat Müller cell evokes inward currents through electrogenic glutamate transporters, while the glutamate receptor agonists kainate (500 μM) and NMDA (100 μM, in the presence of 10 μM glycine and absence of magnesium) do not evoke membrane currents. The current traces were recorded in whole-cell records at a membrane potential of –80 mV. (**b**) Administration of glutamate (100 μM) and ATP (500 μM) to a human Müller cell evoked intracellular calcium responses, suggesting the presence of metabotropic glutamate receptors. The calcium imaging record was done in an acutely isolated cell from a patient with proliferative vitreoretinopathy. Modified from Bringmann et al. (2002a) and Pannicke et al. (2005a)

Functional ionotropic glutamate receptors are regularly found in cultured Müller cells. Cultured human Müller cells express NMDA receptors and the NR1 subunit (Uchihori and Puro, 1993; Puro et al., 1996b). Activation of NMDA receptors in these cells inhibits the Kir currents by ∼50%; this effect is mediated by an influx of calcium ions (Puro, 1996; Puro et al., 1996b). Cultured Müller cells of young postnatal rats express NMDA receptors (Taylor et al., 2003). Here, glutamate treatment results in a decrease in the NMDA receptor level, an increase in the secretion of neurotrophic factors such as brain-derived neurotrophic factor (BDNF), nerve growth factor (NGF), neurotrophins-3 and -4, and glial cell line-derived neurotrophic factor (GDNF), in sustained activation of the trk tyrosine kinase receptor TrkB by BDNF, and upregulation of the glutamate transporter

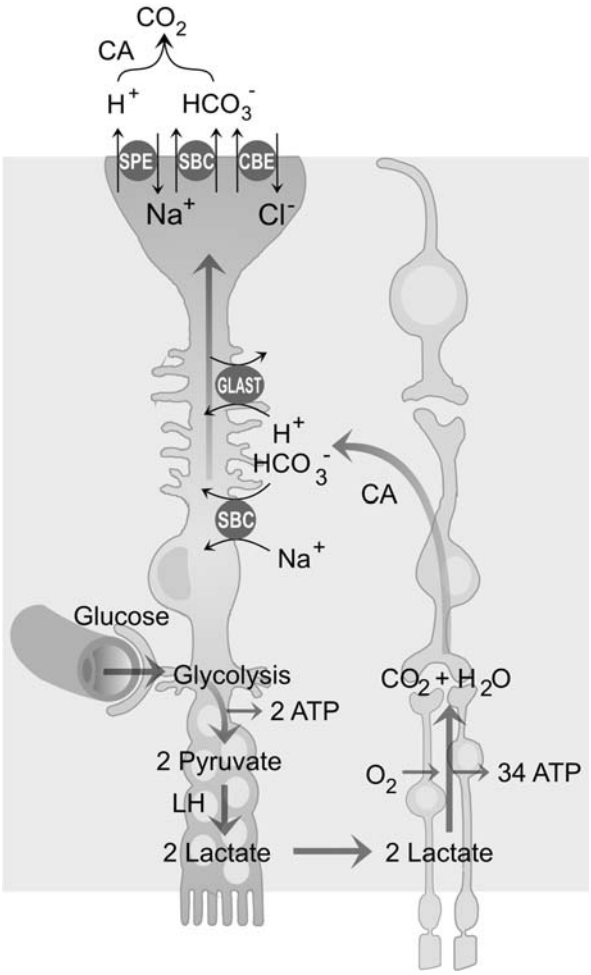

Fig. 2.66 Carbon dioxide siphoning by Müller cells. The oxidative metabolism of retinal neurons and photoreceptors results in the formation of carbon dioxide and water from lactate/pyruvate which are in part produced in Müller cells. The carbonic anhydrase (CA) at the surface of Müller cells converts carbon dioxide and water into bicarbonate and protons which are taken up by the sodium-bicarbonate cotransporter (SBC) and the glutamate transporter GLAST, for example. Bicarbonate and protons are then preferentially released into the blood vessels and the vitreous by the concerted action of SBC, the chloride-bicarbonate exchanger (CBE), and the sodium-proton exchanger (SPE). LH, lactate dehydrogenase

(GLAST) protein (Taylor et al., 2003). It has been suggested that the decrease in the NMDA receptor levels and the sustained activation of TrkB serve as protective mechanisms for Müller cell survival, while the secretion of neurotrophic factors and the upregulation of GLAST may protect retinal neurons from glutamate toxicity (Taylor et al., 2003). Cultured Müller cells of the rabbit express AMPA/kainate receptors that mediate a calcium influx from the extracellular space (Minei, 2002).

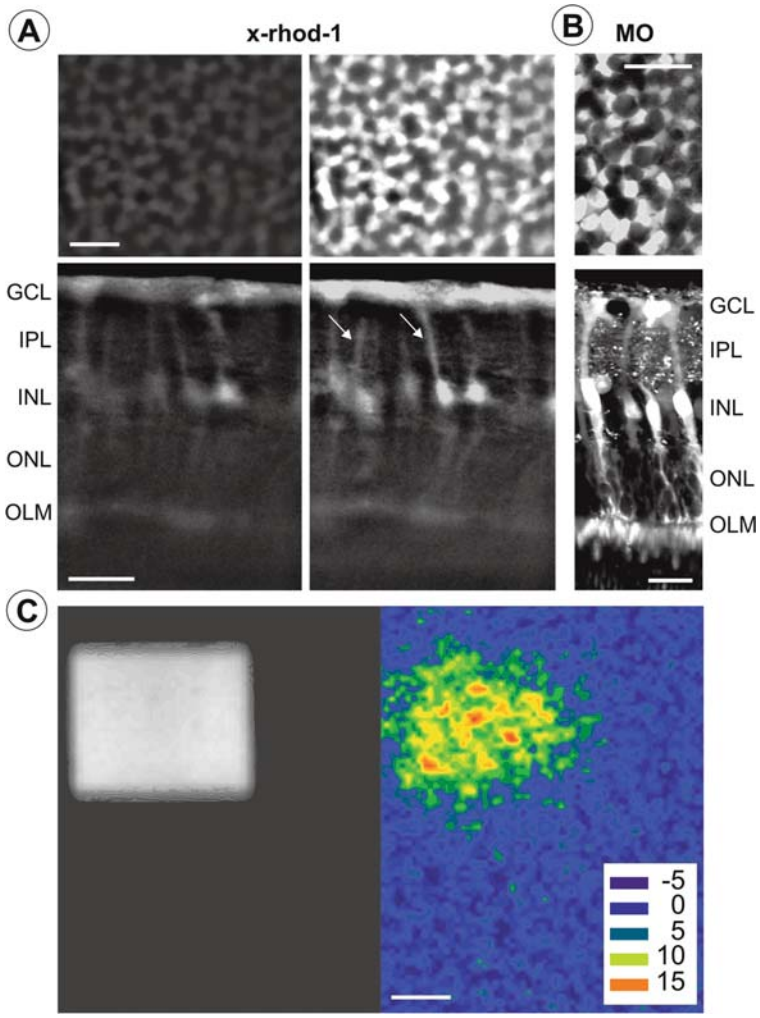

Fig. 2.67 Light stimulation evokes two distinct calcium responses in Müller glial cells of the guinea pig retina. (**a**) Examples of calcium responses in a retinal wholemount (*above*) and a retinal slice (*below*) loaded with x-rhod-1. The focus of the image shown above is in the inner nuclear layer (INL) which contains somata of Müller and neuronal cells. The images were obtained before (*left*) and after (*right*) a 3-min light stimulation. *Arrows* indicate cells that displayed fast calcium rises. (**b**) In a retinal wholemount (*above*: view onto the INL) and slice (*below*), respectively, the vital dye Mitotracker Orange (MO) stained selectively Müller glial cells. In addition, the vital dye stained photoreceptor segments which was not observed after loading of retinal tissues with the calcium dye x-rhod-1. (**c**) Local light stimulation of a retinal wholemount evoked calcium responses in Müller cells of a restricted area. The light stimulus is shown left, and the calcium responses of Müller cell somata in the INL are shown right. The response was recorded after 3 min of stimulation with light of 520 nm. The fluorescence changes of the calcium dye x-rhod-1 are presented in false colors (in percent). *Bars*, 25 μm. GCL, ganglion cell layer; INL, inner nuclear layer; IPL, inner plexiform layer; OLM, outer limiting membrane; ONL, outer nuclear layer. Modified from Rillich et al. (2009)

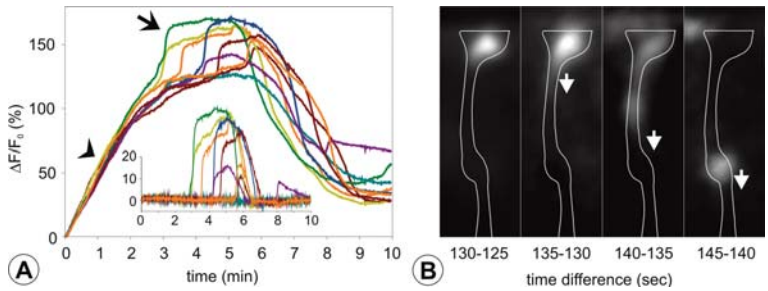

Fig. 2.68 Time course of the light stimulation-evoked calcium responses in Müller glial cells of the guinea pig retina. (**a**) Time-dependent calcium responses in 9 individual Müller cells during light stimulation. The calcium response is composed of a slowly developing calcium rise (*arrowhead*) and (after a delay of ~3 min) fast calcium rises (*arrow*). The inset shows the fast calcium rises after subtraction of the slow responses. (**b**) Example of the intracellular progression of the fast calcium rise in a retinal slice preparation. Shown are calculated differences of two fluorescence images in time intervals of 5 s each (ΔF) during progression of the fast calcium rise in one Müller cell. The time points of the pictures are given as time after onset of stimulation. Modified from Rillich et al. (2009)

Cultured Müller cells are normally resistant to neurotoxic levels of glutamate (up to 1 mM) (Uchihori and Puro, 1993; Kitano et al., 1996; Heidinger et al., 1998); this resistance has been ascribed (at least in part) to a lower affinity of Müller cell AMPA receptors as compared to neuronal receptors (Kawasaki et al., 1996) and the expression of glutamate transporters and glutamine synthetase that rapidly detoxify glutamate.

Cultured chick Müller cells express NMDA (NR1, NR2) and AMPA/kainate receptors (GluR1,4,5) (Lopez-Colome et al., 1993; Lopez et al., 1994, 1997, 1998). Activation of the receptors results in an increase in AP-1 DNA binding activity (Lopez-Colome et al., 1995). The expression of GluR4 is decreased after treatment with glutamate acting at group I mGluRs (Lopez et al., 1998). NMDA receptors are coupled to the phosphoinositide cascade, entry of calcium, and activation of protein kinase C (Lopez-Colome et al., 1993; Lamas et al., 2005, 2007). Activation of AMPA/kainate receptors results in cytosolic calcium responses (Wakakura and Yamamoto, 1994).

Activation of NMDA receptors (for example, by the tripeptide glycine-proline-glutamate which is a cleavage product of IGF-1) stimulates the proliferation of cultured Müller cells (Uchihori and Puro, 1993; Ikeda et al., 1995). In addition to being a mitogen, glutamate also has antiproliferative effects on Müller cells. Activation of mGluRs inhibits the growth factor-induced proliferation of cultured Müller cells (Ikeda and Puro, 1995). Subretinal administration of subtoxic levels of glutamate or α-aminoadipic acid (a glutamate analogue acting selectively in glial cells) in adult mice causes Müller cell dedifferentiation, proliferation, migration, and transdifferentiation into neurons and photoreceptors (Takeda et al., 2008).

Metabotropic Glutamate Receptors

Müller cells may express mGluRs which are coupled to calcium-dependent or calcium-independent intracellular signaling pathways. There is a species variability in the coupling of mGluR activation to intracellular calcium responses in Müller cells. In the absence of external calcium, agonists of group I/III mGluRs evoke calcium waves in Müller cells acutely dissociated from the salamander retina; these waves are mediated by a release of calcium from internal stores (Keirstead and Miller, 1997). The increase in cytosolic calcium frequently begins in the distal (outer) ends of the cells, moves through the cells, and occurs 7–70 s later in the endfeet. Such waves can be also evoked by elevated potassium, ATP, as well as by caffeine or ryanodine (Keirstead and Miller, 1997). While glutamatergic agonists evoke such waves only in a subpopulation of Müller cells, nearly all cells investigated displayed such waves in response to ATP (Keirstead and Miller, 1997). These calcium waves in Müller cells were suggested to provide an extraneuronal pathway for signals to be relayed from the outer to the inner retina (Newman and Reichenbach, 1996). Müller cells of the tiger salamander have calcium-activated potassium channels (Newman, 1985b) and, thus, an increase in cytosolic calcium could enhance the potassium buffering capacity of the cells. The mechanism for the propagation of calcium waves in Müller cells of the tiger salamander is unclear. In salamander and rat Müller cells, antibodies against inositol 1,4,5-triphosphate (IP_3) receptors labels most strongly the distal region of the cells (Peng et al., 1991). Glutamate transporters are localized preferentially to the distal region of salamander Müller cells (Brew and Attwell, 1987), and it is possible that mGluRs are also more densely distributed in this region (Keirstead and Miller, 1997).

In rat Müller cells, glutamate or agonists of group I/II mGluRs are ineffective in evoking cytosolic calcium increases (Newman and Zahs, 1997; Newman, 2005) but potentiate the calcium responses triggered by other stimuli (Newman and Zahs, 1997). However, glutamate evokes a calcium-independent release of ATP from rat Müller cells; this effect is implicated in the autocrine regulation of Müller cell volume (Fig. 2.75b) (Wurm et al., 2008). Pharmacological investigation of the cell volume regulation revealed the presence of the mGlu1 receptor subtype (belonging to the group I mGluRs) and of group II mGluRs in rat Müller cells (Uckermann et al., 2006; Wurm et al., 2008). In retinas of rabbits and guinea pigs, glutamate evokes rises in cytosolic calcium in neurons but not in Müller cells (Fig. 2.69b) (Uckermann et al., 2003, 2004a).

A subpopulation of acutely isolated Müller cells of the human retina (∼30% of cells investigated) respond to extracellular glutamate with transient increases in the intracellular calcium concentration (Fig. 2.65b) and in BK currents (Figs. 2.51 and 2.55b), suggesting the presence of mGluRs (Bringmann et al., 2002a). The BK current responses were always delayed by 10–60 s after beginning of glutamate exposure (similar long latencies of glutamate-evoked calcium responses were described in Müller cells of the tiger salamander: Keirstead and Miller, 1997). These delayed responses are different from the ATP-evoked BK current responses; ATP evokes instantaneous increases in BK currents in virtually all human Müller

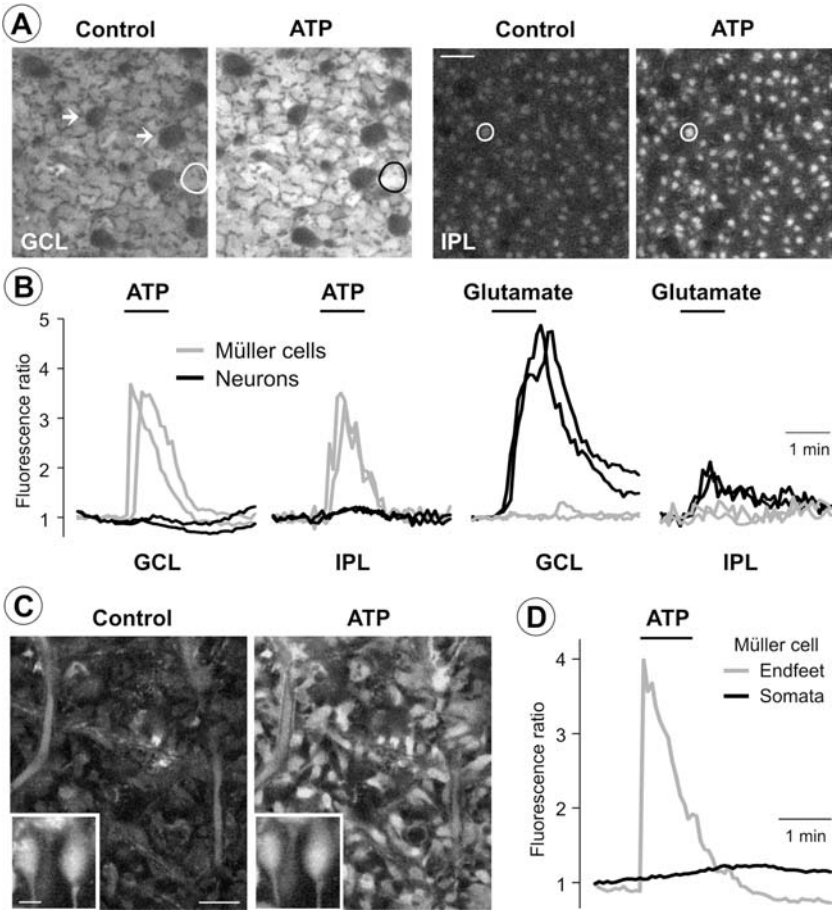

Fig. 2.69 Glutamate and ATP-evoked intracellular calcium responses in tissue preparations of rat and guinea pig retinas. (**a**, **b**) In the guinea pig retina, ATP evokes intracellular calcium responses in Müller cells whereas glutamate induces calcium responses in neurons. (**a**) Views onto the ganglion cell layer (GCL) (*left*) and inner plexiform layer (IPL) (*right*). The images were recorded before (control) and at the peak calcium responses upon application of ATP (200 μM). Examples of Müller cell endfeet (in the GCL) and profiles (in the IPL) are encircled. *Arrows*, ganglion cell bodies. *Bar*, 20 μm. Note that almost all Müller cells respond to exogenous ATP with an increase in intracellular free calcium. (**b**) Time-dependent calcium responses in Müller cell and neuronal cell structures. Upon ATP, Müller cell endfeet in the GCL and Müller cell profiles in the IPL respond with a transient calcium rise (*grey traces*) whereas neuronal cell bodies and synaptic structures in the IPL are non-responsive (*black traces*). Upon administration of glutamate (1 mM), neuronal cell bodies and synaptic structures display calcium responses (*black traces*) whereas Müller cell endfeet and profiles are non-responsive (*grey traces*). A fluorescence ratio of one means no change in the cytosolic free calcium. (**c**, **d**) ATP (200 μM) evokes calcium responses in endfeet but not in somata of Müller cells in tissue preparations of the rat retina. (**c**) View onto the nerve fiber/ganglion cell layers of a retinal wholemount and onto Müller cell somata within the inner nuclear layer of a retinal slice (*insets*). The elongated structures are blood vessels. The images were taken before (control) and during the peak calcium response. *Bars*, 20 and 5 (*insets*) μm. (**d**) Mean calcium responses in Müller cell endfeet and somata. Modified from Uckermann et al. (2004a, 2006)

cells investigated (Fig. 2.55b) (Bringmann et al., 2002a). The increase in BK currents may be associated with a transient activation of a calcium-activated cation conductance (Fig. 2.55b).

Cultured chicken Müller cells express mGluR1 and mGluR5 (Lopez et al., 1998). Activation of the receptors elicit calcium mobilization coupled to the phosphoinositide cascade, activation of protein kinase C and p44/p42 MAPKs (extracellular signal-regulated kinases, ERK1/2) (Lopez-Colome et al., 1993; Lopez et al., 1998; Lopez-Colome and Ortega, 1997).

2.7.1.2 Purinergic Receptors

ATP and adenosine act as neuro- and gliotransmittters in the retina (Perez et al., 1986; Neal and Cunningham, 1994; Peral and Pintor, 1998; Santos et al., 1999; Newman, 2001, 2003b, 2005; Uckermann et al., 2006; Wurm et al., 2008). Müller cells express both adenosine P1 and nucleotide P2 receptors. Adenosine receptors (A1, A2a, A2b, A3) are G protein-coupled receptors that activate intracellular signaling pathways. Nucleotide receptors are either G protein-coupled receptors (metabotropic P2Y receptors) or ligand-gated cation channels (ionotropic P2X receptors). An expression of multiple P2Y receptor subtypes has been described in Müller cells of all animal species investigated so far, while an expression of functional P2X receptors was observed only in human cells. In retinas of most animal species investigated so far, the expression of functional P2X receptors is restricted to neurons.

Adenosine Receptors

In Müller cells of the rat, adenosine evokes calcium responses by activation of A2, but not A1, receptors, via release of calcium from intracellular stores (Li et al., 2001). In another study, adenosine was found to potentiate the light-evoked calcium responses in Müller cells of the rat by activation of A1, A2a, and A2b receptors (Newman, 2005). In Müller cells from tiger salamanders, skates, rabbits, and man, adenosine does not evoke calcium responses (Malchow and Ramsey, 1999; Francke et al., 2002; Bringmann et al., 2002a; Uhlmann et al., 2003). In the rat retina, Müller cells (in addition to neuronal cells in the inner nuclear and ganglion cell layers) express immunoreactivity for A1 receptors (Iandiev et al., 2007c). In these cells, activation of A1 receptors by endogenously released adenosine is implicated in the purinergic signaling cascade that inhibits the osmotic swelling of the cells under hypoosmotic conditions (Fig. 2.75b) (Uckermann et al., 2006; Wurm et al., 2006b, 2008). A1 receptor activation results in the opening of potassium and chloride channels in the Müller cell membrane which is mediated by activation of the adenylyl cyclase, protein kinase A, and PI3K. Though in most cell systems activation of A1 receptors causes a decrease in cAMP, there are also observations that (in dependence on the receptor density) A1 receptors may couple to stimulating G proteins resulting in enhanced formation of cAMP (Cordeaux et al., 2000).

Ionotropic P2X Receptors

Acutely isolated Müller cells from rats, mice, guinea pigs, rabbits, and pigs do not express functional P2X receptors, as indicated by the absence of changes in the membrane conductance upon administration of exogenous ATP (Felmy et al., 2001; Bringmann et al., 2001; Francke et al., 2002). Though gene expression of ionotropic $P2X_{3,4,5}$ receptors has been described in Müller cells of the rat (Jabs et al., 2000), purinergic receptor agonists do not evoke cation currents in the cells (Felmy et al., 2001; Bringmann et al., 2001).

Human Müller cells express (in addition to P2Y receptors) ionotropic $P2X_7$ receptors (Figs. 2.70 and 2.71) (Pannicke et al., 2000b; Bringmann et al., 2001, 2002a, b). In the rodent retina, expression of $P2X_7$ receptor protein is restricted to neuronal and microglial cells (Brändle et al., 1998; Wheeler-Schilling et al., 2001; Innocenti et al., 2004; Franke et al., 2005). In the monkey retina, the expression of $P2X_7$ receptors in a subpopulation of Müller cells has been suggested (Pannicke et al., 2005c), whereas other authors described immunoreactivity for these receptors only in neuronal cells (Ishii et al., 2003a). In human Müller cells, extracellular ATP or BzATP (a more specific agonist of $P2X_7$ receptors) activate $P2X_7$ receptors that are nonselective cation channels which are permeable for sodium, potassium, and calcium ions. Opening of these channels results in activation of a cation conductance (currents at –60 and –100 mV in Fig. 2.70a). The calcium influx through the channels mobilizes calcium from intracellular stores (Fig. 2.70b) and activates BK channels (currents at +120 mV in Fig. 2.70a; Fig. 2.71a) (Pannicke et al., 2000b; Bringmann et al., 2001). The opening of the $P2X_7$ cation channels results in a depolarization of the cells (shift of the membrane potential towards the equilibrium potential of cations at 0 mV) (Fig. 2.71b). The cation currents display a noninactivating kinetics and are increased when the extracellular solution contains low concentrations of divalent cations. The latter fact implies that light-evoked decreases in extracellular calcium will facilitate the gating of $P2X_7$ receptors in Müller cells. In contrast to $P2X_7$ receptors of immune cells such as microglial cells (Innocenti et al., 2004), long-lasting activation of the receptors in Müller cells does not result in the formation of large pores in the plasma membrane (Pannicke et al., 2000b). The influx of sodium ions through open $P2X_7$ receptor channels (resulting in a decrease in the transmembrane sodium gradient and cell depolarization) decreases the efficiency of the electrogenic (sodium-dependent) uptake of neurotransmitters such as glutamate (Fig. 2.71d) (Pannicke et al., 2000b). However, the opening of BK channels (that results in membrane hyperpolarization) may counteract the membrane depolarization (and may serve to enhance the spatial buffering capacity for extracellular potassium). The expression of $P2X_7$ receptor channels in human Müller cells is increased in proliferative retinopathies (Fig. 3.11d); the increase in the amplitude of $P2X_7$ receptor-mediated cation currents correlates with the decrease in the Kir currents and with other features of gliosis (Bringmann et al., 2001). $P2X_7$ receptors are suggested to play a role in induction of proliferative gliosis; both the calcium influx and the activation of BK channels are essential for the BzATP-evoked proliferation of cultured Müller cells (Bringmann et al., 2001).

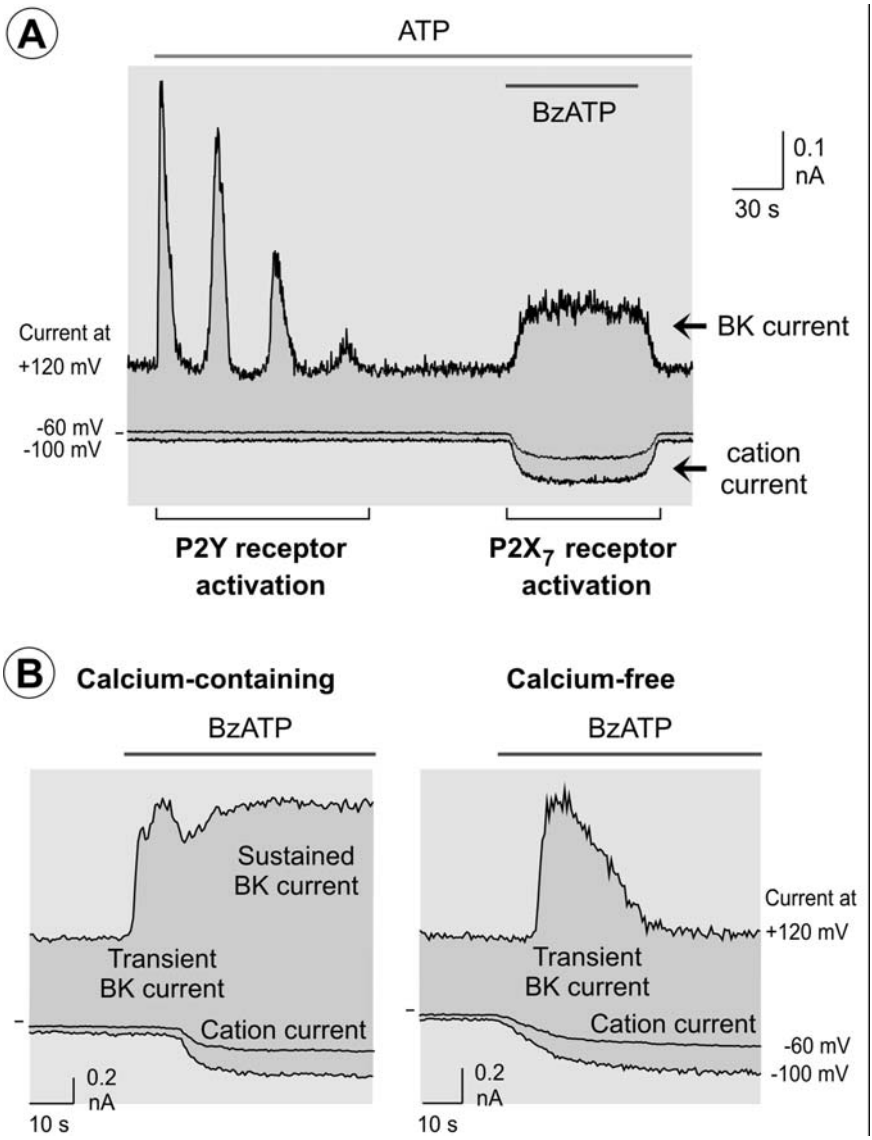

Fig. 2.70 Activation of metabotropic P2Y and ionotropic $P2X_7$ receptors alters the membrane conductance of human Müller cells. (**a**) Activation of P2Y receptors by ATP (100 μM) evokes repetitive transient calcium-evoked activation of BK currents (that were recorded at the potential of +120 mV). Activation of $P2X_7$ receptors by BzATP (50 μM) evokes a sustained calcium-evoked activation of BK currents, as well as cation currents through the $P2X_7$ receptor channels. (**b**) The $P2X_7$ receptor channels are permeable for calcium ions. Administration of BzATP (50 μM) to a human Müller cell evoked a transient increase in BK currents (through stimulation of P2Y receptors and subsequent release of calcium from intracellular stores) followed by a sustained increase in BK currents which is caused by an influx of calcium from the extracellular space through $P2X_7$ receptor channels. Under extracellular calcium-free conditions, the sustained component of the BK current response is absent, whereas the transient BK current increase is virtually independent on extracellular calcium. Modified from Bringmann et al. (2001, 2002a)

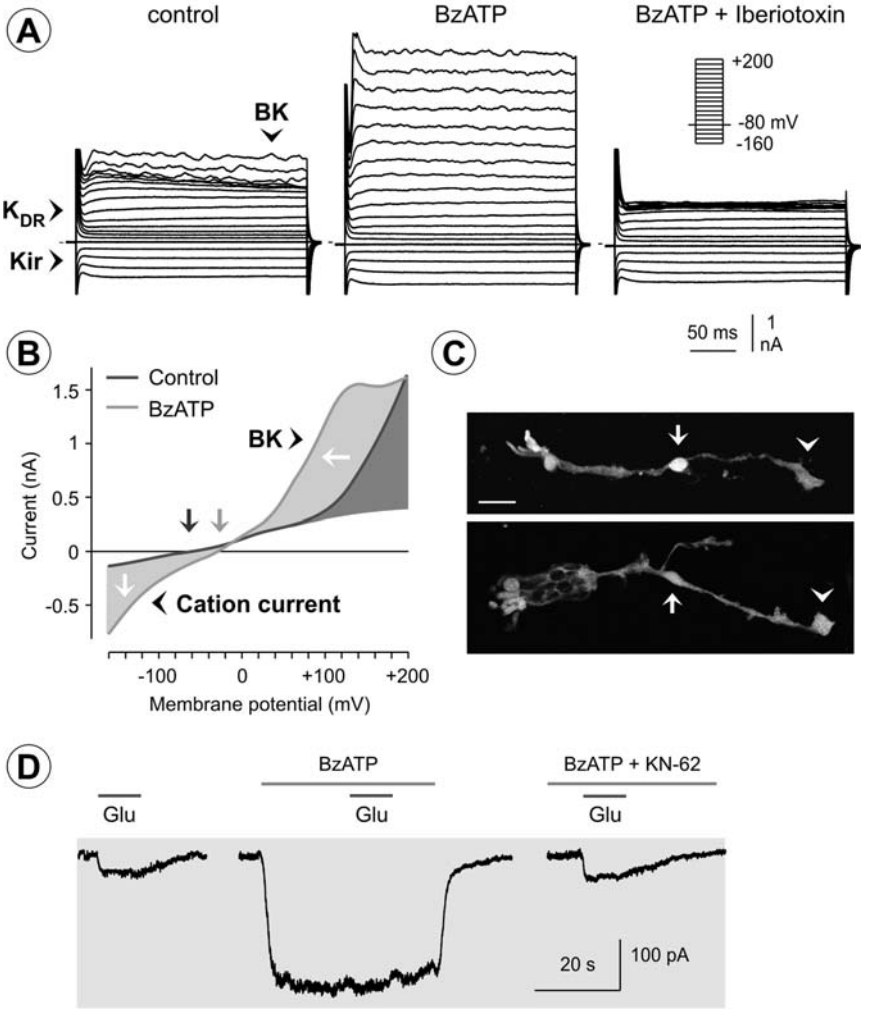

Fig. 2.71 $P2X_7$ receptors of human Müller cells. (**a**) In an acutely isolated cell from a donor eye, activation of $P2X_7$ receptors by BzATP (50 μM) increases the amplitude of BK currents which is inhibited by coadministration of the BK channel blocker iberiotoxin (100 nM). The cell was held at –80 mV, and depolarizing (up to +200 mV) and hyperpolarizing (up to –160 mV) voltage steps were applied with an increment of 20 mV. (**b**) Mean current–voltage relations of Müller cells from patients with proliferative vitreoretinopathy. The currents were recorded before and during activation of $P2X_7$ receptors with BzATP (50 μM). The BzATP-evoked increase of the currents at hyperpolarized (negative) membrane potentials reflects the cation currents flowing through the receptor channels. At positive potentials, a shift in the activation of BK currents towards more negative potentials is apparent which is caused by the calcium influx. Activation of the cation conductance results in a positive shift of the zero-current (0 pA) potential (*dark* and *grey arrows*) that reflects the depolarization of the cells. (**c**) Immunostaining of two acutely isolated human

Metabotropic P2Y Receptors

G protein-coupled P2Y receptors are linked to different intracellular signaling pathways in Müller cells, for example to phosphoinositide hydrolysis and to release of calcium from intracellular stores (which is followed by a second phase of calcium influx from the extracellular space) (e.g. $P2Y_{1,2,4}$) or to a calcium-independent mechanism of transporter-mediated release of adenosine ($P2Y_1$). The former second messenger pathway is involved in the propagation of intra- and intercellular calcium waves (Newman, 2001) and in the purinergic stimulation of Müller cell proliferation (Moll et al., 2002; Milenkovic et al., 2003, 2005), the latter in the autocrine regulation of cellular volume (Fig. 2.75b) (Uckermann et al., 2006; Wurm et al., 2008).

Müller glial cells express various subtypes of P2Y receptors. In cells of the tiger salamander, gene expression of $P2Y_{1,2,4,6,11,13}$ receptors was described (Reifel Saltzberg et al., 2003). P2Y receptor agonists evoke a release of calcium from intracellular stores; the increase in cytosolic calcium in response to P2Y receptor agonists occurs first in the distal (outer) region and later in the endfoot in most salamander Müller cells (Keirstead and Miller, 1997; Reifel Saltzberg et al., 2003). Extracellular ATP may also evoke calcium-independent morphological alterations of salamander Müller cells (Innocenti et al., 2001).

Müller cells of the rat express mRNA for $P2Y_{1,2,4,6}$ receptors (Pannicke et al., 2001; Fries et al., 2004). Calcium responses can be evoked by various P2Y receptor agonists including ATP, ADP (a selective agonist of $P2Y_1$ receptors), uridine 5′-triphosphate (UTP; an agonist of $P2Y_{2,4}$ receptors) and uridine 5′-diphosphate (UDP; an agonist of $P2Y_6$ receptors) (Li et al., 2001). The predominant P2 receptor subtype that evokes calcium responses in rat Müller cells seems to be the $P2Y_1$ receptor (Newman and Zahs, 1997; Li et al., 2001). Similar to rat cells, human Müller cells express mRNA for $P2Y_{1,2,4,6}$ receptors (Fries et al., 2005). A release of calcium from IP_3-gated intracellular stores is evoked by various nucleotides including ATP (Fig. 2.65b), ADP, UTP, UDP, GTP, and inosine 5′-triphosphate (Bringmann et al., 2002a). The increase in cytosolic calcium activates BK channels and cation channels in human Müller cells (Figs. 2.50, 2.55b and 2.72a) (Bringmann et al., 2002a). The cation conductance is likely mediated by calcium-activated cation channels (which were firstly described in cultured human Müller cells: Puro, 1991a),

Fig. 2.71 (continued) Müller cells against the $P2X_7$ receptor protein using two different antibodies. The *arrows* point to the cell somata, and the *arrowheads* to the cell endfeet. Bar, 20 μm. (**d**) Activation of $P2X_7$ receptors by BzATP impairs the electrogenic uptake of glutamate by Müller cells. The uptake currents evoked by glutamate (Glu; 100 μM) are decreased in the presence of BzATP (10 μM). Inhibition of the activation of $P2X_7$ receptors by KN-62 (1 μM) suppressed the BzATP-evoked current, resulting in glutamate uptake currents similar in amplitude as under control conditions. Modified from Pannicke et al. (2000b) and Bringmann et al. (2001)

since clamping the cytosolic calcium at a low level or depletion of intracellular calcium stores by IP_3 before P2Y receptor activation abolish these currents (Bringmann et al., 2002a). In Müller cells of the rabbit, extracellular ATP evokes activation of BK currents but not of cation currents (Fig. 2.72b) (Francke et al., 2003). ATP, ADP, and UTP (but not UDP) evoke intracellular calcium and BK current responses in rabbit Müller cells (Francke et al., 2002; Uhlmann et al., 2003).

There is a species variability in the incidence of Müller cells that respond to P2Y receptor activation with intracellular calcium responses. In mature retinas of rabbits and pigs, only small subpopulations of Müller cells (~10% of the cells) normally respond to exogenous ATP with a transient increase in cytosolic calcium (Figs. 2.45b, c, 2.73a, and 3.8f) (Francke et al., 2002; Uhlmann et al., 2003; Uckermann et al., 2005a; Iandiev et al., 2006b). In the rabbit, the expression of functional P2Y receptors in Müller cells is developmentally regulated. The incidence of immature radial glial/Müller cells that display ATP-evoked calcium responses decrease strongly in the course of the postnatal development; this decrease is inversely related to the increase of the Kir currents (Fig. 2.45b, c) (Uckermann et al., 2002; Iandiev et al., 2006b). Purinergic receptor signaling has been shown to trigger the proliferation of multipotent progenitor cells in the developing retina (Sugioka et al., 1999; Pearson et al., 2002, 2005; Nunes et al., 2007) and is implicated in the regulation of the volume of immature radial glial/Müller cells under anisoosmotic conditions (Fig. 2.45a) (Wurm et al., 2006a). In the developing chicken retina, between embryonic days 3 and 6, activation of $P2Y_{2,4}$ receptors by exogenous ATP or UTP stimulates the proliferation of early retinal progenitors which will become photoreceptors, amacrine, ganglion or horizontal cells (Sugioka et al., 1999; Pearson et al., 2002, 2005). Between embryonic days 6 and 8, activation of $P2Y_1$ receptors by exogenous ATP or ADP stimulates the proliferation of late progenitor cells (Sanches et al., 2002; Franca et al., 2007), a response that is mediated by activation of protein kinase C and MAPKs (Sanches et al., 2002; Nunes et al., 2007).

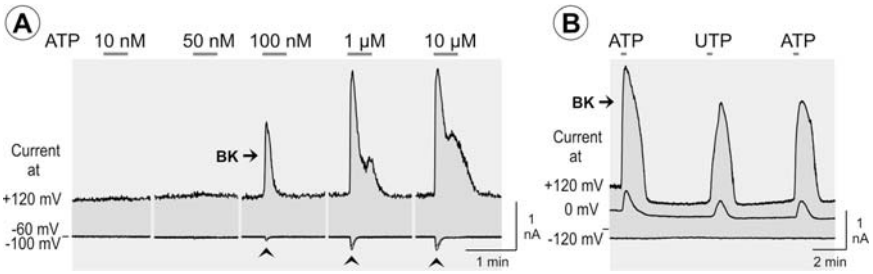

Fig. 2.72 P2Y receptor activation alters the membrane conductance of Müller cells. (**a**) Stimulation of P2Y receptors with increasing ATP concentrations activates BK and cation (*arrowheads*) currents in an acutely isolated human Müller cell from a patient with proliferative vitreoretinopathy. (**b**) Activation of P2Y receptors with ATP (100 µM) or UTP (100 µM) results in an increase in the BK currents in a rabbit Müller cell. Modified from Bringmann et al. (2002a) and Francke et al. (2003)

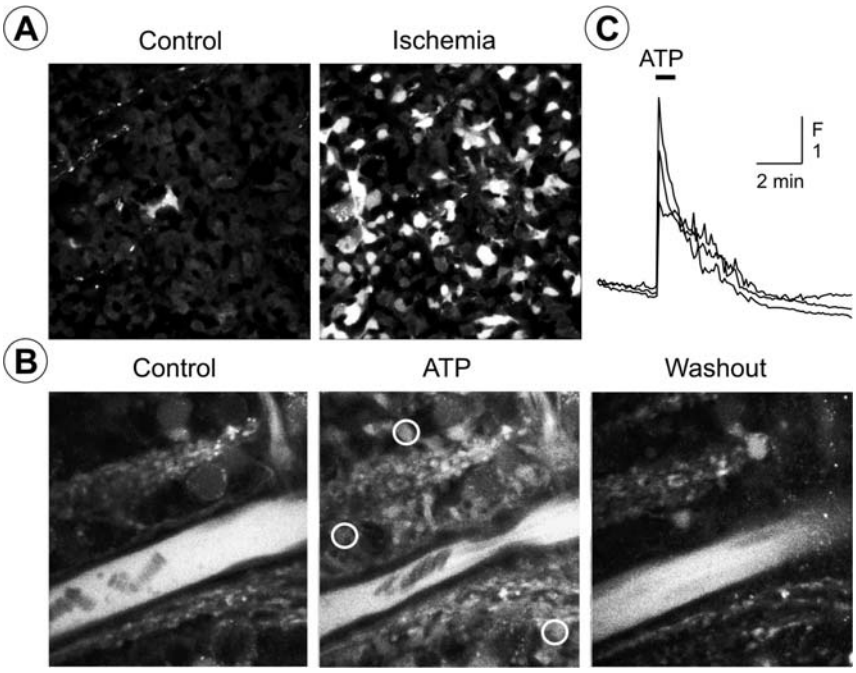

Fig. 2.73 P2Y receptor-evoked calcium responses in Müller cell endfeet. (**a**) The images were taken from a wholemount of a control porcine retina (*left*) and a porcine retina that was isolated three days after a transient retinal ischemia of 1 h (*right*). The tissues were exposed to ATP (200 μM) for 1 min, and the peak calcium responses in Müller cell endfeet within the ganglion cell layer are shown. In the image from the control retinal tissue, only one Müller cell endfoot displayed a calcium response, while numerous endfeet displayed responses in the image from the postischemic retina. (**b**) Intracellular peak calcium responses in Müller cell endfeet on the vitreal surface of a rat retina evoked by ATP (500 μM). Note the constriction of the arteriole in response to ATP. (**c**) Time dependence of the calcium responses in the Müller cell endfeet indicated by the circles in (**b**)

In retinas of rabbits and pigs, the purinergic calcium responsiveness of Müller cells increases under pathological conditions. The incidence of Müller cells that display P2Y receptor-evoked calcium and BK current responses is elevated after transient retinal ischemia (Fig. 2.73a) (Uckermann et al., 2005a), retinal detachment (Fig. 3.8f) (Uckermann et al., 2003; Uhlmann et al., 2003; Iandiev et al., 2006b), and in proliferative retinopathies (Fig. 2.45b, c) (Francke et al., 2002). The increase in purinergic calcium responsiveness is inversely related to the decrease in Kir currents (Fig. 2.45b) and, thus, depends upon the strength of gliosis. Since the expression level of Kir channels is a major indicator of the differentiation state of Müller cells (Bringmann et al., 2000a), both the decrease in Kir currents and the increase in P2Y receptor-evoked calcium responsiveness indicate a dedifferentiation of the cells under pathological conditions, supporting the proliferation and other gliotic alterations of the cells. The mechanism of the increase in glial calcium responsiveness

under pathological conditions is unclear; it may involve increased expression of $P2Y_{1,2}$ receptor proteins (Iandiev et al., 2006b), an increase in the activity of BK channels (Bringmann et al., 1999b, 2007) resulting in prolongation of the calcium responses (Fig. 3.4b) (Moll et al., 2002), and a resensitization of P2Y receptors by the action of growth factors. Growth factors such as PDGF, epidermal growth factor (EGF), and NGF are capable to resensitize P2Y receptors which are depressed in their function by extracellular ATP; this effect is mediated by activation of PI3K (Weick et al., 2005). Müller cells of patients with proliferative retinopathies display an elevation in the calcium-activated cation currents evoked upon activation of P2Y receptors (Bringmann et al., 2002a). Stimulation of cellular proliferation represents one effect of increased P2Y receptor responsiveness in Müller cells of the diseased retina (Bringmann et al., 2003b). In cultured Müller cells, activation of P2Y receptors increases cellular proliferation, via a signaling cascade that involves an increase in the cytosolic calcium level, activation of BK currents and MMPs, the autocrine release of growth factors, transactivation of growth factor receptor tyrosine kinases, and activation of ERK1/2 and PI3K (Fig. 3.3) (Moll et al., 2002; Milenkovic et al., 2003, 2005). The increased P2Y receptor responsiveness may be also involved in the regulation of cell shape and volume (Uckermann et al., 2006) associated with cellular migration (Wu et al., 2007) and proliferation, and in the induction of other markers of gliosis such as upregulation of GFAP. Whether purinergic receptor signaling is also involved in a transdifferentiation of Müller cells into neuron-like cells under pathological conditions in the mature retina (cf. Section 3.1.4), remains to be determined.

In contrast to Müller cells of the rabbit and pig, nearly every Müller cell examined from tiger salamanders, rats, guinea pigs, and man display intracellular calcium responses (or an increase in BK currents) upon activation of P2Y receptors by ATP (Li et al., 2001; Bringmann et al., 2002a; Reifel Saltzberg et al., 2003; Uckermann et al., 2004a). In tissue preparations of the guinea pig retina, exogenous ATP evokes calcium responses in Müller cells but not in neuronal cells whereas glutamate induces calcium responses in neurons but not in Müller cells (Fig. 2.69a, b) (Uckermann et al., 2004a). A similar absence of ATP-evoked calcium responses in neurons, and its presence in Müller cells, was found in the rabbit retina (Uckermann et al., 2003). In tissue preparations of the rat retina, ATP-evoked calcium responses are restricted to the inner half of Müller cells, i.e. to the processes which traverse the inner plexiform layer, and to the cell endfeet in the ganglion cell/nerve fiber layers; ATP-evoked calcium responses are not observed in the somata and outer processes of the cells (Fig. 2.69c, d) (Newman, 2005; Uckermann et al., 2006).

In the rat retina, a long-range intercellular calcium signaling within the network of glial cells can be triggered by various stimuli such as electrical or mechanical stimulation and focal application of neurotransmitters (Newman and Zahs, 1997, 1998). The waves propagate at 20–30 μm/s and up to 180 μm from the site of initiation through the processes and endfeet of astrocytes and Müller cells within the ganglion cell and inner plexiform layers. These waves were suggested to underlie an extraneuronal long-range signaling system that modulates neuronal activity. The propagation of the calcium waves from astrocytes to Müller cells, and between

Müller cells, depends upon the release and extracellular diffusion of ATP, activation of P2Y receptors, and release of calcium from internal stores (Newman and Zahs, 1997; Newman, 2001). Between astrocytes, the waves propagate by the spread of an internal messenger via gap junctions. Interestingly, the release of ATP precedes the calcium waves in Müller cells (Newman, 2001), suggesting that the release of ATP is independent on calcium. Glial calcium waves are associated with a modulation of the firing rate of neighboring neurons, leading to enhancement and depression of the light-evoked spike activity of ganglion cells (Newman and Zahs, 1998) (see also Section 2.7.2).

Under constant illumination conditions (i.e. in the absence of neuronal stimulation), Müller cells in tissue preparations of the rat retina generate spontaneous calcium transients by the release of calcium from internal stores (Newman, 2005). These calcium transients occur at a frequency of 4.6 per cell per 1,000 s, and range from 2.5 to 6 s in duration. The transients start within the inner and middle portions of the inner plexiform layer, and propagate into the outer portion of the inner plexiform layer and into the endfeet of Müller cells. Stimulation of the retina with flickering light, administration of ATP or adenosine, or antidromic stimulation of ganglion cells increase the frequency of the calcium transients in Müller cells (Newman, 2005). The effect of flickering light was found to be mediated by a release of ATP from retinal neurons and activation of glial P2Y receptors (Newman, 2005). The increase in the frequency of light-evoked calcium transients is potentiated by adenosine, suggesting that this effect is augmented under pathological conditions such as ischemia and hypoxia when adenosine is rapidly released in the retina (Roth et al., 1997; Ribelayga and Mangel, 2005). Light-evoked calcium responses are not observed in the somata or outer processes of Müller cells, nor in astrocytes (Newman, 2005). Amacrine cells are believed to release ATP (Santos et al., 1999). The cholinergic starburst amacrine cell is a likely candidate that mediates purinergic neuron-to-glia signaling, because it may corelease ATP along with acetylcholine (Neal and Cunningham, 1994). The effect of antidromic activation of ganglion cells can be explained with a release of ATP from ganglion cell axons, that have contact to other retinal neurons, or from ganglion cell dendrites (Newman, 2005). The purinergic neuron-to-glia signaling is involved in the light-evoked dilation and constriction of retinal arterioles (Metea and Newman, 2006), suggesting that calcium waves in rat Müller cells may serve to regulate the blood flow rate in the superficial vascular plexus, in dependence on the synaptic activity in the inner plexiform layer (neurovascular coupling). Furthermore, these calcium waves may transmit volume-regulatory signals over long distances which prevent (via autocrine release of glutamate and purinergic receptors agonists) the swelling of the inner Müller cell processes and endfeet (Fig. 2.75b) when ganglion cell synapses and bodies enlarge their volume upon activation of AMPA/kainate receptors (Fig. 2.59).

In addition to vascular innervation by specific neurons, glial cells were suggested to mediate an activity-dependent regulation of the local blood flow (termed neurovascular coupling or functional hyperemia), owing to their capability to release vasoactive factors in response to neuronal activity. Glial cells induce vessel relaxation or constriction via multiple mechanisms, e.g. by release of ATP (Burnstock,

1989) and adenosine (Anderson and Nedergaard, 2003), and by a pathway that involves synaptic release of glutamate and stimulation of glial mGluRs, resulting in intracellular calcium responses and the release of arachidonic acid metabolites (Harder et al., 1998; Zonta et al., 2003; Mulligan and MacVicar, 2004). In the retina, both constriction and dilation of arterioles in response to light exposure were suggested to be mediated by a purinergic neuron-to-glia signaling that triggers calcium waves in glial cells, and subsequent activation of the calcium-dependent phospholipase A_2 (Metea and Newman, 2006). Activation of this enzyme results in the production of arachidonic acid, followed by a production and release from glial cells of arachidonic acid metabolites (epoxyeicosatrienoic acids that cause vasodilation, and 20-hydroxyeicosatetraenoic acid that triggers vasoconstriction) (Metea and Newman, 2006). NO determines whether vasodilating or vasoconstricting responses are produced by glial cells, possibly by modulating the production of distinct arachidonic acid metabolites (Metea and Newman, 2006). Superfusion of tissue preparations of the rat retina with ATP evokes simultaneous calcium responses in Müller cell endfeet and constrictions of retinal arterioles (Fig. 2.73b, c); the latter are likely mediated by constriction of pericytes (Peppiatt et al., 2006). The constriction of pericytes is apparently not evoked by ATP released from glial cells, but rather by a direct signaling from neurons to pericytes (Peppiatt et al., 2006).

Activation of P2Y receptors has at least two functional roles in Müller cells of the rat: (i) triggering of intracellular calcium responses that mediate long-range calcium signaling in the glial cell network implicated in neurovascular coupling, for example (Newman and Zahs, 1997; Metea and Newman, 2006), and (ii) a calcium-independent release of adenosine that is involved in the regulation of Müller cell volume (Uckermann et al., 2006; Wurm et al., 2008). Apparently, there is a spatial difference in P2Y receptor-evoked calcium signaling and calcium-independent stimulation of adenosine release. Whereas ATP-evoked calcium responses are restricted to the inner processes and the endfeet of rat Müller cells (Fig. 2.69c, d) (Newman, 2005; Uckermann et al., 2006), the calcium-independent release of adenosine involved in the regulation of cellular volume can be observed also in the somata of the cells (Fig. 2.75a). The data suggest that the functional coupling of $P2Y_1$ receptors to calcium-dependent and -independent intracellular effector molecules differs in dependence on the subcellular region of rat Müller cells.

2.7.1.3 GABAergic Receptors

Ionotropic $GABA_A$ and $GABA_C$ receptors are ligand-gated chloride channels, while $GABA_B$ receptors are metabotropic, G protein-coupled receptors. Using electrophysiological recordings of whole-cell membrane currents, the expression of ionotropic GABA receptors in Müller cells was found to be strikingly species-dependent. Müller cells derived from rather different species, such as the skate, salamander, baboon, and man, express neuronal-like $GABA_A$ receptors (Malchow et al., 1989; Qian et al., 1993, 1994; Reichelt et al., 1996, 1997a, b; Bringmann et al., 2002a; Zhang et al., 2003b; Biedermann et al., 2004). By contrast, exogenous GABA does not induce membrane currents in Müller cells of the goldfish,

mouse, rat, guinea pig, rabbit, pig, and the cynomolgus monkey *Macaca fascicularis*, suggesting the absence of functional ionotropic GABA receptors in cells from these species (Malchow et al., 1989; Reichelt et al., 1996; Biedermann et al., 2002; Pannicke et al., 2005c). At the resting membrane potential, GABA evokes two types of inward currents in a subpopulation of enzymatically isolated human Müller cells: a fast, transient $GABA_A$ receptor current (Fig. 2.74a), and a sustained current mediated by electrogenic (sodium-dependent) GABA transporters (Fig. 2.74b) (Reichelt et al., 1997a; Bringmann et al., 2002a; Biedermann et al., 2004). The direction of the currents through $GABA_A$ receptor channels reverses at the equilibrium potential of chloride ions (approximately –30 mV: Fig. 2.74c) (Biedermann et al., 2004); therefore, opening of the receptor channels results in a depolarization of the cells (Malchow et al., 1989). The current–voltage relation of perforated-patch $GABA_A$ receptor currents (Fig. 2.74c) suggests that acutely isolated human Müller cells have a mean intracellular chloride concentration of 37 mM (Biedermann et al., 2004). The receptor currents are increased by known modulators of $GABA_A$ receptor channels such as pentobarbital, diazepam, and zinc ions (Qian et al., 1996; Reichelt et al., 1997b; Biedermann et al., 2004). Zinc ions are released from the synaptic terminals of photoreceptor cells (Wu et al., 1993; Qian et al., 1994), and are also found in high concentrations in fish Müller cells (Wietsma et al., 1992). $GABA_A$ receptors are localized across the entire plasma membrane of human Müller cells. The GABA-evoked chloride currents in human Müller cells are totally suppressed in the presence of bicuculline, excluding the possibility that the cells express functional $GABA_C$ receptors (Biedermann et al., 2004). Similarly, Müller cells of the skate do not express functional $GABA_C$ receptors (Qian et al., 1996). $GABA_A$ receptors may have different functional roles: they may be involved in the buffering of changes in the extracellular pH (since the receptor channels are also permeable for bicarbonate), a chloride efflux through the receptor channels may stimulate the GABA uptake by the cells (which is driven by a cotransport of sodium and chloride ions) and may compensate the decrease in the extracellular chloride concentration caused by the chloride influx into activated neurons. The depolarization of the cells may activate voltage-gated potassium, sodium, and calcium channels, resulting in an activation of Müller cells and in the release of gliotransmitters. However, the precise functional roles of $GABA_A$ receptors in Müller cells remain to be determined.

Müller cells of the bullfrog retina express immunoreactivity for metabotropic $GABA_B$ receptors (Zhang and Yang, 1999). Müller cells of the guinea pig have no functional $GABA_B$ receptors (Biedermann et al., 1994).

2.7.1.4 Glycinergic Receptors

Glycine receptors (GlyRs) are ligand-gated chloride channels. Müller cells of the bullfrog retina express functional GlyRs (Du et al., 2002a); the subunits GlyRα1 and GlyRß were identified by immunohistochemistry (Lee et al., 2005). GlyRs were not found in Müller cells from rats, mice, and primates (Greferath et al., 1994; Wässle et al., 1998; Haverkamp and Wässle, 2000; Lin et al., 2000; Haverkamp et al., 2003). In enzymatically dissociated human Müller cells, glycine does not evoke alterations

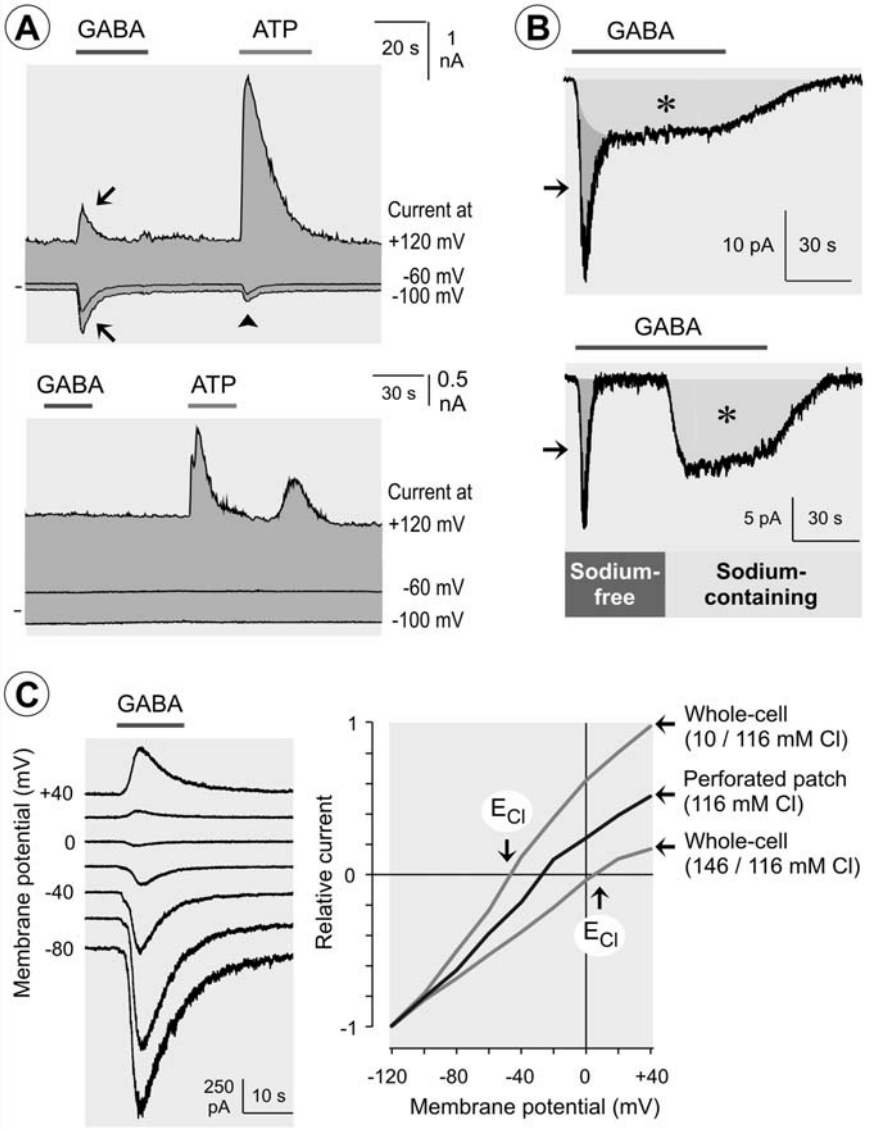

Fig. 2.74 $GABA_A$ receptor currents in human Müller cells. Plasma membrane currents were recorded in enzymatically dissociated cells. (**a**) Subpopulations of human Müller cells express $GABA_A$ receptors. Extracellular administration of GABA (500 μM) evoked a transient increase in the inward and outward membrane currents (*arrows*) in the record of one of the two cells shown. Administration of ATP (500 μM) evoked a transient increase in the BK channel-mediated outward potassium currents (at +120 mV) in nearly all Müller cells investigated. In the record shown above, ATP evoked also transient cation currents (*arrowhead*).(**b**) Under potassium-free recording conditions, extracellular administration of GABA (100 μM) evokes two kinds of inwardly

in the membrane conductance (Bringmann et al., 2002a), suggesting the absence of glycine receptors and transporters.

2.7.1.5 Cholinergic Receptors

Focal administration of carbachol onto astrocyte somata initiates calcium waves in the network of astrocytes and Müller cells of the rat retina (Newman and Zahs, 1997). In a small subpopulation of acutely dissociated human Müller cells, acetylcholine causes delayed and very small BK current increases, suggesting the expression of acetylcholine receptors coupled to a release of calcium from internal stores (Bringmann et al., 2002a). Acetylcholine (but not nicotine) evokes calcium responses in a subpopulation of cultured rabbit Müller cells, via activation of muscarinic M1 receptors (Wakakura et al., 1998). Acetylcholine also evokes calcium responses in a subpopulation of Müller cells from the tiger salamander but not from the skate (Malchow and Ramsey, 1999). Cultured chicken Müller cells express muscarinic and nicotinic receptors, and the ß2-nicotinic receptor subunit, but not choline acetyltransferase (Kubrusly et al., 2005). Cultured murine Müller cells express M1 and M4 receptors; M1 receptor activation results in a release of calcium from internal stores and subsequent calcium influx from the extracellular space through transient receptor potential canonical (TRPC) channels (Da Silva et al., 2008).

2.7.1.6 Catecholaminergic Receptors

Epinephrine and norepinephrine evoke inward currents, and an increase of the input resistance, in dissociated Müller cells of the tiger salamander (Henshel and Miller, 1992). In human Müller cells, epinephrine and serotonin do not evoke alterations in the membrane conductance (Bringmann et al., 2002a). Systemic or intravitreal administration of α2-adrenergic agonists in rats elicits phosphorylation of ERK1/2 and an increase in GFAP in Müller cells (Peng et al., 1998). In tissue preparations of the rat retina, norepinephrine evokes calcium responses in a small fraction of Müller cells (Li et al., 2001), and focal administration of phenylephrine onto

Fig. 2.74 (continued) directed currents: a transient, rapidly inactivating current mediated by $GABA_A$ receptors (*arrows*), and a sustained current (*asterisks*). The sustained current is depressed under extracellular sodium-free conditions (*below*), indicating that this current is mediated by electrogenic (sodium-dependent) GABA transporters. (**c**) Voltage dependency of the $GABA_A$ receptor currents. For the current–voltage relations of the receptor currents shown at right, the currents were recorded in the whole-cell mode (with 116 mM chloride in the extracellular solution and 10 or 146 mM chloride in the intracellular solution), and in the perforated-patch mode (with 116 mM extracellular chloride). In the whole-cell records, the receptor currents reverse from inward to outward currents near the equilibrium potentials of chloride ions (E_{Cl}). The example of whole-cell current records shown at left was made with 146/116 mM chloride. Modified from Bringmann et al. (2002a) and Biedermann et al. (2004)

astrocyte somata initiates calcium waves in the network of astrocytes and Müller cells (Newman and Zahs, 1997). Norepinephrine stimulates the production and release of BDNF by cultured rat Müller cells (Seki et al., 2005). Activation of ß-adrenergic receptors in rat Müller cells cultured under hyperglycemic conditions leads to a decrease in the expression and formation, respectively, of prostaglandin E_2, tumor necrosis factor (TNF), interleukin (IL)-1ß, and inducible NO synthase (Walker and Steinle, 2007). Müller cells in the bullfrog but not rat retina express 5-hydroxytryptamine 2A receptors (Han et al., 2007).

2.7.1.7 Dopaminergic Receptors

Müller cells of amphibians, rats, and guinea pigs express dopamine D_2 receptors (Muresan and Besharse, 1993; Biedermann et al., 1995). Dissociated Müller cells of the tiger salamander respond to dopamine with the activation of an inward current and an increase in the input resistance (Henshel and Miller, 1992). In Müller cells of the guinea pig, activation of D_2 receptors results in a closure of Kir channels (Biedermann et al., 1995). In human Müller cells, dopamine does not evoke alterations in the membrane conductance (Bringmann et al., 2002a). In tissue preparations of the rat retina, focal ejection of dopamine to glial cells triggers calcium responses in Müller cells, resulting in a release of ATP from the cells (Newman, 2003b). Müller cells of the goldfish display immunolabeling for D_1 receptors (Mora-Ferrer et al., 1999). Cultured Müller cells express D_1 receptors; activation of the receptors stimulates the adenylyl cyclase activity (Kubrusly et al., 2005). In addition, cultured Müller cells can express the machinery required for dopamine synthesis and release (Kubrusly et al., 2008).

2.7.1.8 VEGF Receptors

VEGF primarily operates through two tyrosine kinase receptors, the type 1 receptor (fms-like tyrosine kinase-1, flt-1) and the type 2 receptor (kinase insert domain-containing receptor/fetal liver kinase-1, KDR/flk-1) (Ferrara et al., 2003). In the human retina, immunoreactivity for VEGF is expressed, in addition to vascular endothelial cells, by all major classes of neurons and Müller cells (Amin et al., 1997; Famiglietti et al., 2003). In the neuroretina, flt-1 is localized to pericytes (Witmer et al., 2002), while KDR/flk-1 is expressed by blood vessels, astrocytes, Müller cells, and ganglion cells (Stone et al., 1995a, b; Stitt et al., 1998).

In Müller cells of the rat, activation of KDR/flk-1 by VEGF results in exocytotic release of glutamate that is involved in the autocrine regulation of cell volume (Fig. 2.75) (Wurm et al., 2008). This effect is dependent on activation of the phospholipase C, a release of calcium from intracellular stores, an influx of calcium from the extracellular space, and activation of the protein kinase C and Src tyrosine kinases. In addition, activation of voltage-gated sodium channels (that causes rapid fluctuations of the membrane potential necessary for the activation of voltage-dependent calcium channels) is likely implicated in the VEGF-evoked exocytotic

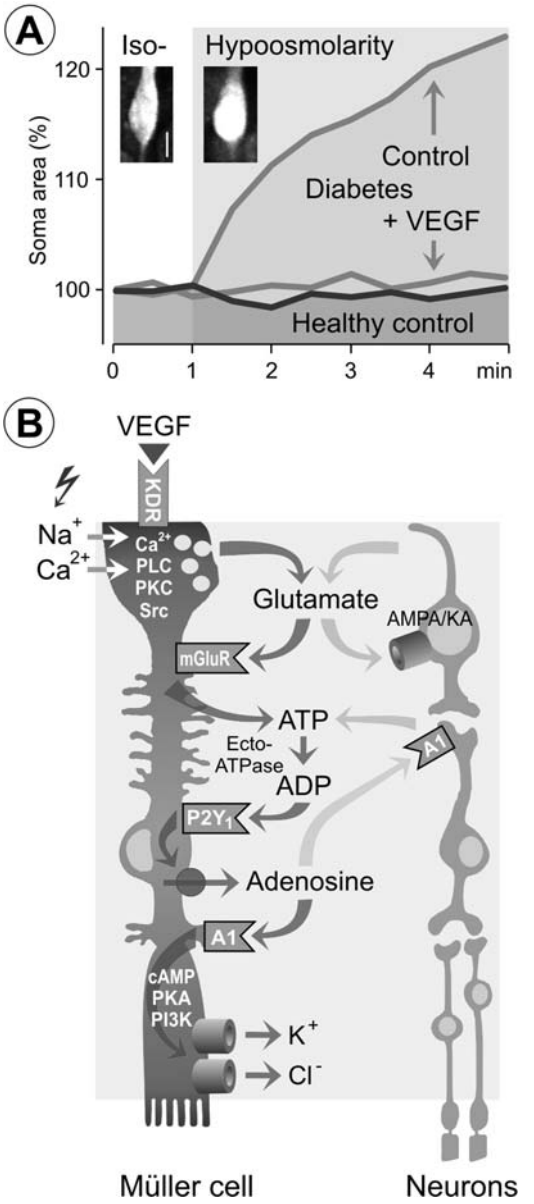

Fig. 2.75 The release of the gliotransmitters glutamate, ATP, and adenosine is involved in the autocrine prevention of osmotic Müller cell swelling by VEGF. (**a**) Under hypoosmotic conditions, Müller cells in retinas of diabetic rats display a time-dependent swelling of their somata, a response not observed in Müller cells of control retinas. The osmotic Müller cell swelling is prevented by VEGF (10 ng/ml). Insets, soma of a Müller cell before (*left*) and during (*right*) hypotonic exposure. (**b**) The autocrine glutamatergic-purinergic signaling cascade involved in the VEGF-evoked inhibition of Müller cell swelling. Activation of KDR/flk-1 receptors by VEGF evokes a calcium-, phospholipase C (PLC)-, protein kinase C (PKC)-, and Src kinase-dependent

release of glutamate, as suggested by the inhibitory effect of the sodium channel blockers tetrodotoxin and saxitoxin.

Glial cells in epiretinal membranes from patients with proliferative retinopathies, and cultured human Müller cells, express KDR/flk-1 and flt-1 (Chen et al., 1997; Eichler et al., 2004b). Activation of the receptors by VEGF suppresses the release of the pigment epithelium-derived factor (PEDF) from the cells (Eichler et al., 2004b). Hypoxia increases the expression of both VEGF receptors in Müller cells.

2.7.1.9 Thrombin Receptors

In tissue preparations of the rat retina, thrombin evokes calcium responses in Müller cells, resulting in a release of ATP from the cells (Newman, 2003b). Thrombin inhibits the Kir currents and stimulates the proliferation of cultured human Müller cells (Puro et al., 1990; Puro and Stuenkel, 1995). The inhibition of the Kir currents is mediated by a release of calcium from intracellular stores (Puro and Stuenkel, 1995). In whole-cell records of freshly isolated human Müller cells, thrombin does not evoke alterations in the membrane conductance (Bringmann et al., 2002a).

2.7.1.10 Peptidergic Receptors

The retinal content of natriuretic peptides (NPs) such as atrial natriuretic peptide (ANP) is increased after transient ischemia-reperfusion (Kalisch et al., 2006). Müller cells and neurons of the rat retina express ANP, brain NP (BNP), and C-type NP (CNP) (Cao et al., 2004). Freshly isolated Müller cells of the bullfrog have NP receptor-A; activation of the receptor causes the opening of a non-selective cation conductance in the plasma membrane, likely mediated by calcium-permeable cyclic nucleotide-gated cation channels (Cao and Yang, 2007). In rat Müller cells, ANP evokes a glutamatergic-purinergic signaling cascade of autocrine regulation of

Fig. 2.75 (continued) exocytotic release of glutamate from Müller cells. Voltage-gated sodium channels mediate rapid fluctuations of the membrane potential necessary for the activation of depolarization-activated calcium channels implicated in the exocytosis of glutamate-containing vesicles. Glutamate activates metabotropic glutamate receptors (mGluRs) resulting in a calcium-independent release of ATP from Müller cells. ATP is extracellularly converted to ADP that activates $P2Y_1$ receptors, resulting in transporter-mediated release of adenosine. Activation of A1 receptors by adenosine causes a cAMP-, protein kinase A (PKA)-, and phosphatidylinositol-3 kinase (PI3K)-dependent opening of potassium and chloride channels; the ion efflux equalizes the osmotic gradient across the plasma membrane and thus prevents water influx and cellular swelling under hypoosmotic stress conditions. In swollen cells, the ion efflux is associated with a water flow out of the cells, resulting in a decrease in the cell volume. While the release of glutamate from Müller cells is calcium-dependent, all steps of the cascade after activation of the mGluRs are calcium-independent. Neuron-derived glutamate and ATP may activate the volume-regulatory signaling cascade in dependence on the neuronal activity. Müller cell-derived glutamate and adenosine may activate neuronal AMPA/kainate and A1 receptors, resulting in stimulation and inhibition, respectively, of neuronal activity. Modified from Wurm et al. (2008)

Müller cell volume which is mediated by the activation of different subtypes of NP receptors (Kalisch et al., 2006). The effects of NP receptor activation are mediated by the actions of phospholipase C and protein kinase C, and an influx of calcium from the extracellular space; the intracellular calcium responses are likely evoked by cGMP (Kalisch et al., 2006).

Neuropeptide Y (NPY) is expressed in the rat retina by neuronal, vascular, microglial and Müller cells, and in the toad retina by amacrine and Müller cells (Zhu and Gibbins, 1996; Alvaro et al., 2007). NPY is released in the retina in response to light (Bruun and Ehinger, 1993) and increasingly expressed under hypoxic and oxidative stress conditions (Yoon et al., 2002). In cultured Müller cells of the guinea pig, NPY has both antiproliferative (at low concentrations) and proliferative effects (at higher concentrations) (Milenkovic et al., 2004). The proliferative effect is mediated by activation of Y_1 receptors, ERK1/2, and partially of the p38 MAPK, PI3K, and PDGF and EGF receptor tyrosine kinases (Milenkovic et al., 2004). Y_1 and P2Y receptors partially share common signal transduction pathways in cultured Müller cells. NPY inhibits the osmotic swelling of Müller cells observed under osmotic stress conditions (Uckermann et al., 2006). This effect is mediated by an activation of Y_1 receptors that evokes a glutamatergic-purinergic signaling cascade which is also evoked by activation of KDR/flk-1 with VEGF (Fig. 2.75b). Müller cells in retinas from patients with proliferative vitreoretinopathy, and glial cells in epiretinal fibroproliferative membranes, express Y_1 receptors; this is not the case in control retinas (Cantó Soler et al., 2002a, b).

Cultured Müller cells of chicks and rats have receptors for vasoactive intestinal peptide (VIP) and glucagon that, upon activation, induce an increase in cAMP (Koh et al., 1984; Koh and Roberge, 1989). In amphibian Müller cells, VIP and glucagon stimulate gluconeogenesis; VIP also inhibits glycolysis (Goldman, 1990). Cultured rat and chicken Müller cells have PAC1 receptors for the pituitary adenylyl cyclase activating polypeptide (PACAP) (Kubrusly et al., 2005; Seki et al., 2006). PACAP stimulates the production of cAMP and IL-6 in the cells (Nakatani et al., 2006; Seki et al., 2006). Arginine-vasopressin (AVP) increases the protein synthesis in cultured Müller cells (Reichelt et al., 1989). Müller cells express angiotensin II type 1 and 2 receptors, and angiotensin II and its bioactive metabolite Ang-(1–7) (Kurihara et al., 2006; Senanayake et al., 2007). Under inflammatory conditions, endogenous angiotensin II induces GFAP in Müller cells through STAT3 activation.

Rat and human Müller cells express the somatostatin receptors sst1 and sst2 (Helboe and Møller, 1999, 2000). Müller cells have insulin receptors which may play roles in metabolic and regulatory mechanisms; the expression of insulin receptors is decreased in diabetes (Naeser, 1997; Gosbell et al., 2002). Insulin may also activate IGF-1 receptors expressed by Müller cells (Charkrabarti et al., 1991; Layton et al., 2006). Müller cells express endothelin-B receptors (Iandiev et al., 2005b) and the receptor Gnai2 (Roesch et al., 2008) mediates signaling from the endothelin-B receptor. Retinal light damage and inherited photoreceptor degeneration increases the expression of these receptors in Müller cells; endothelin-2 released from photoreceptors may function as a stress signal that activates Müller cells in situ (Rattner and Nathans, 2005).

2.7.1.11 Receptors for Neurotrophic Factors

Müller cells have high (Trk) and low-affinity ($p75^{NTR}$) receptors for neurotrophic factors such as GDNF, NGF, neurturin, neurotrophin-3, and ciliary neurotrophic factor (CNTF) (Schatteman et al., 1988; Yan and Johnson, 1988; Chakrabarti et al., 1990; Hopkins et al., 1992; Radeke et al., 1993; Hu et al., 1998; Harada et al., 2000a, b, 2002a, 2003; García et al., 2003; Valter et al., 2003; Sarup et al., 2004). $p75^{NTR}$ binds all neurotrophins with similar affinity and is thought to help to ensure the specificity of each neurotrophin. In the rat retina, $p75^{NTR}$ is expressed by Müller cells but not ganglion or bipolar cells (Hu et al., 1998; Wexler et al., 1998). In the human and monkey retina, $p75^{NTR}$ appears confined to Müller cells (Schatteman et al., 1988; Hopkins et al., 1992) while TrkA is expressed by ganglion and Müller cells (Carmignoto et al., 1991). Retinal ischemia and light-induced or inherited retinal degeneration are associated with an increase in Müller cell expression of $p75^{NTR}$ and of the high-affinity neurotrophin receptor TrkC (Tomita et al., 1998; Harada et al., 2000a, b; Nakamura et al., 2005). Neurotrophin-3 induces an increase in the production of bFGF in Müller cells, resulting in a rescue of photoreceptor cells from light-evoked apoptosis, while NGF decreases the production of bFGF (Harada et al., 2000a, b).

In the rat retina, GDNF is localized to photoreceptor cells while neurturin is localized to second- and third-order neurons (Harada et al., 2003). In the normal retina, the receptors for GDNF and neurturin, GFRα1 and 2, are mainly expressed in the photoreceptor cell layer (Harada et al., 2002b, 2003; Koeberle and Ball, 2002). Light-evoked photoreceptor degeneration results in an upregulation of GFRα2 in Müller cells throughout all retinal layers (Harada et al., 2003). In cultured Müller cells (that express both GFRα1 and GFRα2), GDNF increases the gene expression of BDNF, bFGF, and GDNF, while neurturin increases the gene expression of neurturin (Harada et al., 2003).

2.7.1.12 Steroid Hormone Receptors

Müller cells express progesterone receptors (Li et al., 1997). In cultured porcine Müller cells, the membrane-associated progesterone receptor component 1 is localized to plasma membranes and microsomes (Swiatek-De Lange et al., 2007). Progesterone induces alterations in the morphology of the cells, calcium influx and subsequent PI3K-mediated phosphorylation of protein kinase C and ERK1/2, as well as a protein kinase C-dependent activation of VEGF expression and secretion. 17ß-Estradiol protects cultured Müller cells from oxidative stress-induced apoptosis via alterations in gene expression (Li et al., 2006).

In the chicken retina, glucocorticoid receptors are selectively localized to Müller cells (Gorovits et al., 1994). In Müller cells of salamanders, these receptors colocalize with glutamine synthetase in the cytoplasm of the cells, and are also present in the mitochondria (Psarra et al., 2003). The selective localization of glucocorticoid receptors in Müller cells is responsible for the cell-specific expression of proteins like glutamine synthetase and the glutamate transporter, GLAST (Grossman et al.,

1994). Steroid hormones also regulate the mitochondrial metabolism such as the glutamate-induced increase in mitochondrial NADH (Psarra et al., 2003). Müller cells in the rat retina express mineralocorticoid receptors (Mirshahi et al., 1997). Activation of these receptors by aldosterone increases the expression of epithelial sodium channels (Golestaneh et al., 2001).

2.7.1.13 Receptors for Extracellular Matrix Components

Müller cells express various receptors for extracellular matrix components, including the integrin subunits α1, α2, α3, and ß1 (integrins are collagen-binding receptors) and α-dystroglycan, a central member of the membrane-associated dystrophin-glycoprotein complex (Schmitz and Drenckhahn, 1997; Hering et al., 2000; Moukhles et al., 2000; Guidry et al., 2003; Méhes et al., 2005). This complex forms a bridge between the extracellular matrix and the cytoskeleton; dystrophin binds to subplasmalemmal actin filaments as well as to a plasma membrane anchor, ß-dystroglycan, which is associated on the external side with the extracellular matrix receptor, α-dystroglycan, that binds to the basal lamina proteins, laminin and agrin (Schmitz and Drenckhahn, 1997). Müller cells express distinct glycosylated isoforms of α-dystroglycan in apposition to the basal lamina of the inner limiting membrane and around blood vessels, and in their processes that enwrap the synapses in the ganglion cell and inner plexiform layers (Moukhles et al., 2000). In addition, ß-dystroglycan and dystrobrevin are expressed in membrane domains that contact basement membranes (Blank et al., 1997; Koulen et al., 1998; Ueda et al., 1998, 2000). Dystroglycans of Müller cells may participate in organizing the synapses, and may be important for the adhesion of Müller cells to the extracellular matrix molecule laminin as a component of the basement membranes around the vessels and at the inner limiting membrane (Fig. 2.49). Laminin induces a clustering of α-dystroglycan and of intracellular protein components of the dystroglycan-containing complex, such as syntrophin, in the Müller cell membrane (Noel et al., 2005). Given that syntrophin binds utrophin and Dp71 which in turn bind to the actin cytoskeleton in Müller cells (Claudepierre et al., 2000), the interaction of laminin with the dystroglycan-containing complex may have also roles in the stabilization of their radial architecture, and in the transduction of signals from the extracellular matrix into Müller cells. For example, this complex appears to be involved in the laminin-evoked stimulation of Müller cell migration (Méhes et al., 2005).

Müller cells express various other cell surface adhesion/receptor molecules such as N-cadherin, cadherin-11, NCAM, CD44, and CD81 (Bartsch et al., 1990; Duguid et al., 1991; Kuppner et al., 1993; Chaitin et al., 1994; Rich et al., 1995; Nishina et al., 1997; Kuhrt et al., 1997; Clarke and Geisert, 1998; Chaitin and Brun-Zinkernagel, 1998; Krishnamoorthy et al. 2000; Honjo et al., 2000b). The transmembrane adhesion molecule, CD44, is supposed to mediate neuro-glial interactions; it binds hyaluronic acid, chondroitin sulfates, and other extracellular matrix components such as fibronectin, laminin and collagen types I and VI, as well as various cytokines and growth factors. The cytoplasmic domain of CD44 is linked

to the actin cytoskeleton. Müller cells in vitro express the neural cell recognition molecule F11 (Willbold et al., 1997a) which is a multifunctional protein interacting with L1/Ng-CAM, Nr-CAM, tenascin-C, tenascin-R (restrictin) and receptor protein tyrosine phosphatase-ß.

2.7.1.14 Other Receptors

Müller cells of the goldfish express cannabinoid 1 receptors (Yazulla et al., 2000). In cultured Müller cells of mice (but not in murine Müller cells in situ), type 1 sigma receptors are localized to the nuclear and endoplasmic reticulum membranes (Ola et al., 2001; Jiang et al., 2006). The binding activity of the receptors is increased under oxidative and nitrosative stress. Salamander Müller cells express the multifunctional ectoenzyme CD38 which converts NAD^+ into the intracellular calcium-mobilizing second-messenger cyclic ADP-ribose. NAD^+ triggers intracellular calcium waves, a mechanism which depends on the activation of ryanodine receptors (Esguerra and Miller, 2002).

Lysophosphatidic acid (LPA), acting at G protein-coupled receptors, activates a nonspecific, calcium-permable cation conductance in cultured bovine and human Müller cells (Kusaka et al., 1998). In enzymatically dissociated human Müller cells, LPA does not evoke changes in the membrane conductance (Bringmann et al., 2002a). In the rat retina, LPA induces calcium responses in Müller cells, resulting in a release of ATP from the cells (Newman, 2003b). In cultured Müller cells, LPA stimulates actin polymerization and cell spreading (Santos-Bredariol et al., 2006).

Patched (ptc), a component of the sonic hedgehog (Shh) receptor complex, is expressed in Müller cells (Jensen and Wallace, 1997). Shh is a soluble signaling protein and a potent mitogen for rat Müller cells (Wan et al., 2007). Shh also induces Müller cells to dedifferentiate and adopt the phenotype of rod photoreceptors (Wan et al., 2007) (cf. Section 3.1.4).

Müller cells express receptors for advanced glycation end products (AGEs) (Hammes et al., 1999; Barile et al., 2005; Tezel et al., 2007b). AGEs are formed during oxidative stress and hyperglycemia; the levels of AGEs and AGE receptors in the retina increase with age, in diabetic retinopathy, and in the course of glaucoma (Hammes et al., 1999; Barile et al., 2005; Tezel et al., 2007b).

Müller cells express the low-density lipoprotein-related protein (LRP1; CD91) (Birkenmeier et al., 1996; Sánchez et al., 2006) which is a multifunctional receptor for α2-macroglobulin and ApoE. Since α2-macroglobulin can bind growth factors and proteinases, LRP1-mediated clearance of these factors is involved in the regulation of cellular proliferation and migration evoked, for example, by agonists of G protein-coupled receptors (Milenkovic et al., 2005). In retinal neovascularization, Müller cells upregulate LRP1 (Sánchez et al., 2006). LRP1 is also involved in the lipid shuttle from Müller cells to neurons.

As pigment epithelial cells, Müller cells express a retina-specific nuclear receptor which interacts with the promoter of the CRALBP gene in the presence of retinoic acid receptor (RAR) and/or retinoid X receptor (RXR) (Chen et al., 1999).

Finally, Müller cells (as well as photoreceptors and retinal neurons) express the EP3 receptor for prostaglandin E_2 (Zhao and Shichi, 1995).

2.7.2 Müller Cells May Modulate Retinal Neuronal Activity

Once the Müller cells detect (increased) neuronal activity, their intracellular signaling pathways (e.g., Ca^{2+} rises) may trigger a variety of cellular reactions which, in turn, may modulate the activity of the neurons. Obviously, any variation of their many homeostatic and/or neuro-supportive functions (→ Sections 2.3–2.8) must affect neuronal functioning, as well. Müller cells may modulate neuronal activity by regulating the extracellular concentration of neuroactive substances, including potassium and neurotransmitters which are taken up by channel- and transporter-mediated mechanisms, and by the regulation of the extracellular acid-base homeostasis. In addition, Müller cells play a more active role in the control of the neuronal activity and synaptic transmission (Newman, 2003a). By release of so-called gliotransmitters, particularly glutamate and ATP, activated Müller cells provide excitatory and inhibitory effects on neighbouring neurons. Excitation is mediated predominantly by glutamate whereas ATP, after extracellular conversion to adenosine, causes neuronal suppression (Newman, 2003a; 2004). This type of glia-to-neuron signaling has been called "gliotransmitter release" (Grandes et al., 1991; Araque, 2008). In the following, some examples of this "novel" glial function will be presented.

2.7.2.1 Release of Glutamate

Under pathological conditions, when the cells are severely depolarized, a release of glutamate from Müller cells into the extracellular space might occur via reversal of the electrogenic glutamate transporters; this non-vesicular release of glutamate may contribute to excitotoxic damage of neurons (Szatkowski et al., 1990; Billups and Attwell, 1996; Maguire et al., 1998; Marcaggi et al., 2005). In addition, Müller cells may also release glutamate under normal conditions, via a vesicular mechanism. By measuring the cell volume regulation of acutely isolated Müller cells of the rat, it has been demonstrated pharmacologically that Müller cells are capable to release glutamate; this release is part of an autocrine glutamatergic-purinergic signaling cascade that prevents osmotic swelling of Müller cells (Fig. 2.75b) (Wurm et al., 2008). Secretion of glutamate from isolated Müller cells can be evoked by activation of KDR/flk-1 receptors with VEGF, and is likely mediated by calcium-dependent exocytosis of glutamate-containing secretory vesicles. The latter assumption is supported by the observation that an inhibitor of the vesicle-membrane V-type ATPase (which is required to load glutamate into secretory vesicles) prevents the effect of VEGF on the regulation of Müller cell volume (Wurm et al., 2008). Activation of phospholipase C (resulting in a release of calcium from intracellular stores), influx of calcium from the extracellular space, and activation of protein kinase C and Src tyrosine kinases are involved in the triggering of glutamate release from

Müller cells by VEGF (Wurm et al., 2008). The VEGF-evoked release of glutamate from isolated Müller cells is inhibited in the presence of blockers of voltage-gated sodium and calcium channels (such as tetrodotoxin and kurtoxin), suggesting that activation of voltage-gated sodium channels causes rapid fluctuations of the membrane potential required for the activation of voltage-gated calcium channels that mediate the influx of calcium from the extracellular space. The VEGF-evoked release of glutamate is not mediated through a reversal of glutamate transporters (Wurm et al., 2008). These data suggest that glutamate is secreted from Müller cells through a mechanism very similar to neuronal vesicle release. This finding is important for the interpretation of data obtained in tissue preparations; for instance, blockers of voltage-dependent sodium channels can not be used to distinguish between neuronal and glial contributions to a glutamatergic response. In addition to VEGF, agonists of various other receptors (such as the EGF receptor, P2Y, NP, and Y_1 receptors) inhibit the osmotic swelling of rat Müller cells (Uckermann et al., 2006, Kalisch et al., 2006, Weuste et al., 2006). Probably, every stimulus that triggers a cytosolic calcium rise (such as activation of ligand receptors, or electrical and mechanical stimuli) evokes an exocytotic release of glutamate from Müller cells.

Glutamate released from Müller cells may modulate neuronal activity. In eyecup preparations of the rat, calcium waves evoked in retinal glial cells by mechanical stimulation cause a release of glutamate that activates inhibitory interneurons (presumably GABA- and glycinergic amacrine cells) via activation of AMPA/kainate and mGluRs; this results in inhibition of the light-evoked spike activity of a subpopulation of neurons in the ganglion cell layer (Newman and Zahs, 1998). Furthermore, glutamate released from Müller cells upon exposure to VEGF may directly activate AMPA/kainate receptors in neurons of the ganglion cell layer, resulting in a swelling of neuronal cell bodies (Fig. 2.76) (Wurm et al., 2008). The calcium-dependent release of glutamate from Müller cells may have functional impact also under pathological conditions when the calcium responsiveness upon P2Y receptor activation is increased, e.g. after retinal detachment and in proliferative retinopathies (Figs. 2.45b, c, 2.73a, and 3.8f). However, whether an increase in ATP-evoked calcium responses, and the resulting glutamate release from Müller cells, contributes to excitotoxic damage of the retina under pathological conditions remains to be determined.

2.7.2.2 Release of D-Serine

Müller cells may be involved in setting the sensitivity of retinal ganglion and amacrine cells to light stimuli through a potentiation of synaptic currents after the release of D-serine (Miller, 2004). D-Serine is an endogenous ligand of the glycine modulatory binding site of the NMDA receptor that must be occupied before glutamate can open the receptor channel. D-Serine activates the glycine binding site with a potency three-fold higher than that of glycine, and (since this site is normally not saturated) is required for the full activity of NMDA receptors in retinal ganglion cells (Stevens et al., 2003). NMDA receptors are important

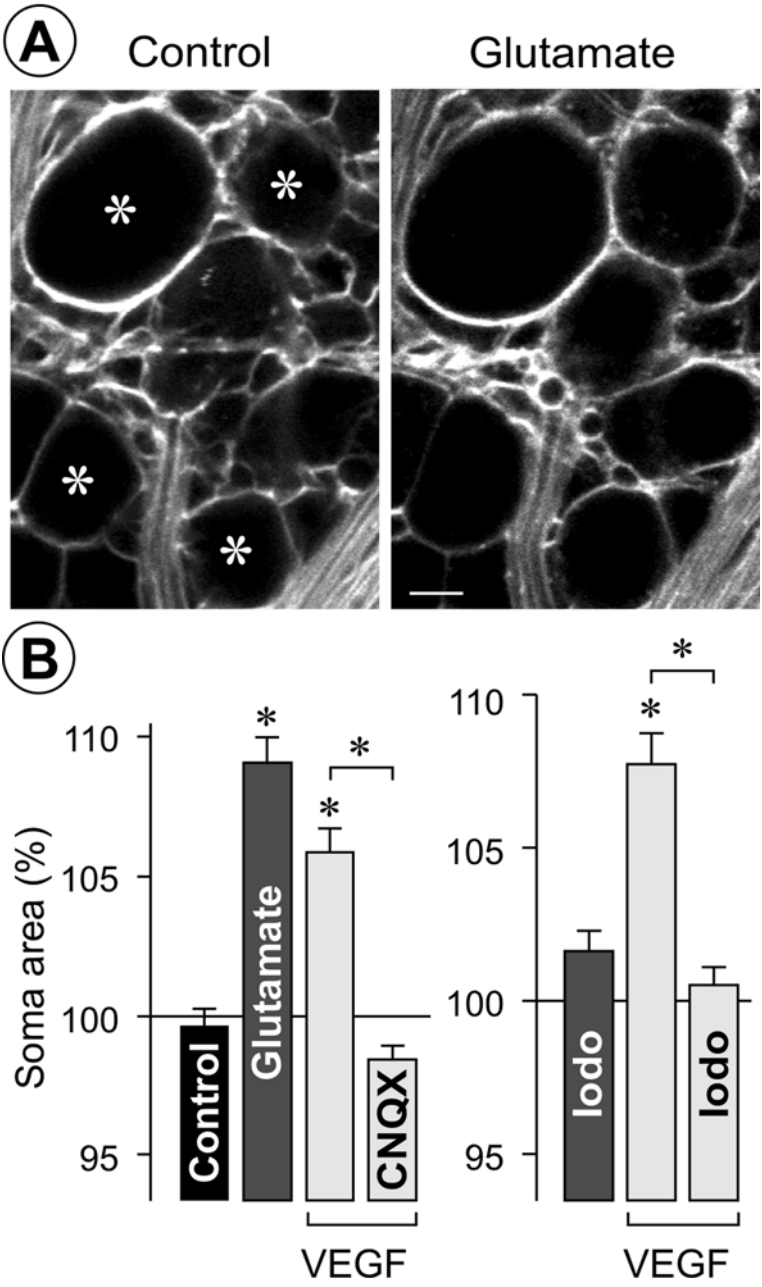

Fig. 2.76 Müller cell-derived glutamate may induce swelling of neuronal cell somata in the ganglion cell layer of the rat retina. The plasma membranes in retinal wholemounts were stained with a FM dye. (**a**) The size of neuronal cell bodies (∗) in the ganglion cell layer of retinal wholemounts increases upon administration of glutamate (1 mM, 15 min). Bar, 5 μm. (**b**) The cross-sectional area of neuronal somata shows an increase upon administration of glutamate and

synaptic receptors that are intrinsic to all ganglion cells and most amacrine cells as well as horizontal cells in some species (O'Dell and Christensen, 1989; Dixon and Copenhagen, 1992). D-serine is synthesized from L-serine by serine racemase that is present in retinal ganglion cells, astrocytes, and Müller cells (Stevens et al., 2003; O'Brien et al., 2005; Dun et al., 2008). The D-serine degrading enzyme, D-amino acid oxidase, has been localized to Müller cells and rods in the frog retina (Beard et al., 1988). The uptake (and possibly the efflux) of D-serine from Müller cells is likely mediated by the sodium-dependent neutral amino acid exchanger ASCT2 (O'Brien et al., 2005; Dun et al., 2007), coupled to a counter-movement of L-serine or L-glutamine (Ribeiro et al., 2002); the release of D-serine from Müller cells can be evoked by activation of glutamate receptors (Oliet and Mothet, 2006). The coupling of glutamine efflux to D-serine uptake might regulate the extracellular D-serine concentration, in dependence on the strength of neuronal activity (Ribeiro et al., 2002). It can not be ruled out that D-serine is released from Müller cells via exocytosis of secretory vesicles. D-serine is localized to synaptic vesicle-like structures in glial cells (Williams et al., 2005). In the developing human retina, D-serine is localized to punctate inclusions in Müller cells (Diaz et al., 2007). The NMDA receptors of cultured chick Müller cells and retinal neurons are structurally different, resulting in a 30-fold lower affinity for D-serine of Müller cell receptors as compared to neuronal receptors (Lamas et al., 2005). In the human fetal retina, Müller cells express D-serine immunoreactivity shortly before the development of first functional synapses at 12 weeks of gestation, suggesting a role of Müller cell-derived D-serine in shaping synaptogenesis (Diaz et al., 2007). In cultured Müller cells, D-serine acting on NMDA receptors regulates gene expression, cAMP-responsive element-binding protein (CREB) phosphorylation, and expression of the immediate-early gene, c-fos (Lamas et al., 2007).

In addition to retinal ganglion cells, Müller cell endfeet express kynurenine aminotransferase (Rejdak et al., 2001, 2004, 2007) that is pivotal to the synthesis of kynurenic acid, an antagonist of the coagonist site of the NMDA receptor. This suggests that Müller cells may inhibit glutamatergic neurotransmission via the release of kynurenic acid.

2.7.2.3 Release of Purinergic Receptor Agonists

Upon stimulation with receptor agonists such as glutamate, ATP, dopamine, and thrombin, and after electrical or mechanical stimulation, Müller cells of the rat

Fig. 2.76 (continued) VEGF (10 ng/ml, 15 min), respectively. The effect of VEGF is prevented by the competitive inhibitor of AMPA/kainate receptors, cyanonitroquinoxalinedione (CNQX; 50 μM), suggesting that VEGF evokes a release of endogenous glutamate that subsequently activates ionotropic glutamate receptors expressed by retinal neurons. (**c**) The VEGF-evoked swelling of retinal neurons is prevented in the presence of the gliotoxin iodoacetate (iodo; 1 mM), suggesting that Müller cell-derived glutamate contributes to neuronal cell swelling. $*P<0.001$. Bar, 5 μm. Modified from Wurm et al. (2008)

release purinergic receptor agonists including ATP and adenosine (Newman, 2001, 2003b; Uckermann et al., 2006; Wurm et al., 2008). Glutamate, which is released from Müller cells in a calcium-dependent manner, activates group I/II mGluRs on Müller cells, resulting in a release of ATP from the cells. ATP is extracellularly converted to ADP that activates purinergic $P2Y_1$ receptors; activation of these receptors triggers the release of adenosine from the cells via nucleoside transporters (Fig. 2.75b) (Uckermann et al., 2006; Wurm et al., 2008). The mechanisms of the glutamate-evoked release of ATP from Müller cells, and of the activation of adenosine transporters, remain to be determined. In contrast to the secretion of glutamate, the release of ATP and adenosine from rat Müller cells is a calcium-independent, non-exocytotic process, and does not depend on activation of phospholipase C, protein kinase C, or Src tyrosine kinases (Uckermann et al., 2006; Weuste et al., 2006; Kalisch et al., 2006; Wurm et al., 2008). The observation of a calcium-independent release of purinergic receptor agonists is in agreement with studies showing (i) that glutamate does not evoke calcium responses in rat Müller cells (Fig. 2.69b) (Newman and Zahs, 1997; Uckermann et al., 2004a; Newman, 2005), (ii) that ATP is released from cultured astrocytes in a calcium-independent manner (Wang et al., 2000), and (iii) that the release of ATP from retinal glial cells may actually precede the glial calcium responses (Newman, 2001). It is likely that, in addition to Müller cell-derived glutamate, also neuron-derived glutamate evokes a release of ATP and adenosine from Müller cells; this signaling may represent a part of the neuron-to-glia signaling in the retina (cf. Section 2.7.1).

The release of ATP from Müller cells has been implicated in a signaling pathway from Müller cells to retinal neurons. In tissue preparations of the rat retina, selective activation of glial cells results in a release of ATP from Müller cells into the inner plexiform layer (Newman, 2003b). Müller cell-derived ATP was suggested to be converted extracellularly to adenosine that activates A1 receptors in a subset of retinal ganglion cells, resulting in the activation of a potassium conductance, cellular hyperpolarization, and a decrease in the spontaneous spike activity (Newman, 2003b, 2004). Müller cell-derived adenosine may act as a negative feedback regulator of the glutamatergic "forward" neurotransmission. In the retina, ganglion and amacrine cells express purinergic P2 receptors (Greenwood et al., 1997; Santos et al., 1998; Taschenberger et al., 1999) and, thus, may respond directly to ATP released from Müller cells. In addition, Müller cell-derived ATP may be implicated in the protection of photoreceptor cells under dark-adapted conditions which are associated with hypoxic stress, as extracellular degradation of ATP generates the neuroprotectant, adenosine (Ribelayga and Mangel, 2005).

In addition to the involvement in glia-to-neuron signaling, Müller cell-derived ATP and adenosine have autocrine effects. ATP and adenosine released from Müller cells inhibit the swelling of the cells under conditions of osmotic stress (Fig. 2.75b) (Uckermann et al., 2006; Wurm et al., 2008) (cf. Section 2.4.4). Moreover, ATP released from retinal glial cells and subsequent activation of purinergic receptors evoke long-range calcium waves that propagate in the glial cell network of the rat retina (Newman, 2001). The waves propagate through the network of astrocytes by diffusion of an internal messenger (presumably IP_3) through gap junctions, whereas

the waves are propagated from astrocytes to Müller cells, and among Müller cells, by the release of ATP (Newman and Zahs, 1997; Newman, 2001). These glial calcium waves are associated with a modulation of the firing rate of neighboring neurons; the light-evoked spike activity of ∼50% of the neurons within the ganglion cell layer is decreased when the calcium waves reach the neurons while other neurons display excitation (Newman and Zahs, 1998). In tissue preparations of the rat retina, ATP released from glial cells upon mechanical stimulation propagated outward from the stimulation site with a velocity of 41 μm/s, somewhat faster than the 28 μm/s velocity of glial calcium waves; at 100 μm from the stimulation site, the ATP concentration reached 6.8 μM (Newman, 2001). Based on data obtained in tissue preparations of the rat retina, it was suggested that light flashes evoke a release of ATP from retinal neurons that enhances the frequency of spontaneous calcium transients in Müller cells; the light-evoked calcium transients begin in Müller cells processes within the inner plexiform (synaptic) layer and spread into cell endfeet at the inner retinal surface (Newman, 2005). Adenosine greatly potentiates the calcium responses of Müller cells to light (Newman, 2005). However, it is likely that a light-evoked release of glutamate and of other transmitters from retinal neurons also results in a release of ATP from Müller cells that evokes intracellular calcium waves in an autocrine manner.

Though the inhibition of osmotic glial cell swelling (Uckermann et al., 2006; Wurm et al., 2008) and the inhibition of ganglion cell activity (Newman, 2003b) are both mediated by release of ATP from Müller cells and subsequent activation of A1 receptors by adenosine, there is a difference between the two signaling cascades. Adenosine that activates neuronal A1 receptors has been suggested to be extracellularly formed from ATP by the consecutive action of ecto-ATPases and ecto-apyrases (Newman, 2003b). In contrast, adenosine that activates glial A1 receptors is released via nucleoside transporters, and only the action of ecto-ATPases (but not of ecto-apyrases) is involved in the signaling cascade (Fig. 2.75b). The retinal parenchyma of the rat lacks immunoreactivity for the ATP-degrading ectoenzyme, NTPDase1 (ecto-apyrase) (Iandiev et al., 2007c) that produces sufficent amounts of AMP as the substrate for enzymatic adenosine formation (Failer et al., 2003). It can not be ruled out that pharmacological modulation of the glial purinergic signaling pathway also indirectly modifies the neuronal activity, via alterations of the glial cell volume and thus of the extracellular space volume.

The receptor-mediated sensing of the neuronal activity by Müller cells, the ATP-mediated calcium waves, and subsequent release of glutamate and purinergic receptor agonists are especially important under conditions when the neurons are intensely activated, and may have at least three functional roles, (i) facilitation of the glial cell-mediated neurovascular coupling (i.e. the regulation of local blood flow in regions of high neuronal activity), since glial calcium waves may transmit blood flow-regulatory signals from the inner plexiform (synaptic) layer to the arterioles localized at the inner surface of the retina; (ii) protection of photoreceptors from hypoxic damage and limitation of neuronal hyper-excitation which may overburden the homeostatic functions of Müller cells (activation of neuronal A1 receptors by glia-derived adenosine depresses transmitter release); and (iii) autocrine cell

volume regulation under conditions when activated neurons swell (Fig. 2.59) and the extracellular hypoosmotic conditions favor Müller cell swelling. Glial calcium waves may transmit such volume-redulatory signals through the retinal tissue both tangentially (i.e., among neighboring columnar units) and radially (within the layers of a given columnar unit). Thus, they may traverse the boundaries between the hierarchical levels of functional domains (cf. Section 2.2.3)

2.7.2.4 Release of GABA

Based on observations obtained in tissue preparations of rat and primate retinas, it has been suggested that Müller cells are capable to release GABA (Neal and Bowery, 1979; Sarthy, 1983; Andrade da Costa et al., 2000). In tissues of the rat retina, depolarizing stimuli cause a release of GABA from Müller cells which is largely calcium-dependent, and is inhibited by the blocker of voltage-gate sodium channels, tetrodotoxin (Sarthy, 1983; but see Moran et al., 1986). However, the release of GABA evoked by a GABA mimetic is independent on calcium but dependent on sodium, and is likely mediated by a carrier-mediated exchange mechanism (Sarthy, 1983).

2.7.2.5 Release of Acyl-CoA-Binding Protein

In the retina, acyl coenzyme A-binding protein (ACBP; also known as "diazepam binding inhibitor") is expressed in Müller cells (Yanase et al., 2002). ACBP interacts with the α1-subunit of the $GABA_A$ receptor, resulting in a reduction of the receptor currents. GABAergic synaptic transmission is critical for the direction-selectivity of ganglion cells. Horizontal optokinetic stimulation of the rabbit retina in vivo evokes increased expression and phosphorylation of ACBP in Müller cells (Barmack et al., 2004; Qian et al., 2008). It has been suggested that Müller cells, depolarized by the discharge of GABAergic amacrine cells, secrete ACBP into the inner plexiform layer, resulting in a decreased sensitivity of $GABA_A$ receptors located on ganglion cell dendrites that receive a GABAergic direction-selective signal from starburst amacrine cell axon terminals (Barmack et al., 2004). Thus, Müller cells may be implicated in the horizontal optokinetic reflex by providing a local negative feedback loop on the GABAergic transmission in neighboring retinal neurons. Upon membrane depolarization or activation of protein kinase C, cultured rabbit Müller cells secrete phosphorylated ACBP (Qian et al., 2008). In addition to modifying GABAergic transmission, ACBP (which has the ability to bind long chain acyl-CoA esters) may have a functional role in lipid/energy metabolism, as suggested by the colocalization of ACBP and brain-type fatty acid binding protein in Müller cells (Yanase et al., 2002).

2.7.2.6 Release of Retinoic Acid

Müller cells are a source of all-*trans* retinoic acid (which does not participate in the visual cycle). In addition to being a morphogenetic factor, retinoic acid also

acts as a neuromodulator, via regulation of gap junctional conductances and of the synaptic transfer between photoreceptors and horizontal cells (Weiler et al., 2001; Dirks et al., 2004). Müller cells contain cellular retinol-binding protein (Eisenfeld et al., 1985), and synthesize retinaldehyde and retinoic acid from retinol; retinoic acid is subsequently released into the extracellular space (Edwards et al., 1992). The presence of cellular retinoic acid-binding protein in distinct amacrine neurons (and, in some species, Müller cells) (De Leeuw et al., 1990; Milam et al., 1990), as well as of retinoic acid receptors in inner retinal neurons (Fischer et al., 1999), suggest a role of retinoic acid in glia-to-neuron signaling. Müller cells also express aldehyde dehydrogenase-2 which oxidizes retinaldehyde to retinoic acid. This varies with the retina topography; the number of aldehyde dehydrogenase-expressing Müller cells is higher in the dorsal than in the ventral retina (McCaffery et al., 1991).

2.7.2.7 Production of Nitric Oxide

Not only retinal neurons but also Müller cells were shown to express constitutive NO synthetases (Liepe et al., 1994; Huxlin, 1995; Kurenni et al., 1995; Djamgoz et al., 1996; López-Costa et al., 1997; Fischer and Stell, 1999; Ota et al., 1999; Haverkamp et al., 1999; Cao et al., 1999b; Kobayashi et al., 2000; Cao and Eldred, 2001). Under pathological conditions, Müller cells also express inducible NO synthase (Dighiero et al., 1994; Goureau et al., 1994, 1997, 1999; Goldstein et al., 1996; de Kozak et al., 1997; Cotinet et al., 1997a, b; Tezel and Wax, 2000). NO is an activator of the guanylyl cyclase which produces cGMP (Knowles et al., 1989). In addition to photoreceptors, bipolar cells, and some amacrine and ganglion cells (Gotzes et al., 1998), guanylyl cyclases are expressed by Müller cells (Rambotti et al., 1999). NO can readily diffuse out of Müller cells and may activate neuronal guanylyl cyclases, close NMDA receptor channels (Kashii et al., 1996), and increase calcium channel currents (Goldstein et al., 1996). NO activates cGMP-gated conductances in ganglion cells and photoreceptors (resulting in increased phototransduction), closes gap junctions in horizontal cells, and enhances the light-evoked response of cholinergic amacrine cells (Koch et al., 1994; Ahmad et al., 1994; Goldstein et al., 1996; Pottek et al., 1997; Neal et al., 1997). The NO production by Müller cells is strongly enhanced during dark adaptation (Ye and Yang, 1996; Zemel et al., 1996). NO is implicated in the glial cell-mediated neurovascular coupling in the retina; it determines whether glial cells release vasoconstricting or -dilating arachidonic acid metabolites upon light stimulation of the retina (Metea and Newman, 2006). In addition, NO affects the contractile tone of Müller cells (Kawasaki et al., 1999).

In the retina, glial cells are the major source of NO under hypoxic conditions (Kashiwagi et al., 2003). In response to ischemia and inflammation, early in diabetic retinopathy, and after excitotoxic damage to the retina, Müller cells increase the expression of inducible NO synthetase (Goureau et al., 1994; Jacquemin et al., 1996; Kobayashi et al., 2000; Abu-El-Asrar et al., 2001, 2004a, b; Nakamichi et al., 2003). Most likely, this response is effective to increase local retinal blood flow, to prevent platelet aggregation, and to protect neurons from apoptosis by closure of

NMDA receptors and through a mechanism mediated by the cGMP to protein kinase G pathway (Goldstein et al., 1996). Higher concentrations of NO and subsequent formation of free nitrogen radicals are cytotoxic for neurons, and are involved in the development of diabetic retinopathy, for example (Goureau et al., 1999; Koeberle and Ball, 1999). Cultured Müller cells express neuronal, endothelial, and inducible NO synthases and produce NO in response to cytokines and inflammatory factors, hypoxia or elevated hydrostatic pressure; the inflammatory NO production is blocked by transforming growth factor (TGF)-ß (Liepe et al., 1994; Goureau et al., 1994, 1997, 1999; de Kozak et al., 1997; Cotinet et al., 1997b; Haverkamp et al., 1999; Kim et al., 1999; Cao et al., 1999a, b; Tezel and Wax, 2000; Kashiwagi et al., 2003). In vitro, excess production of NO by Müller cells causes apoptotic death of cocultured neurons (Goureau et al., 1999; Tezel and Wax, 2000). In vivo, the susceptibility to develop endotoxin-induced uveitis is correlated with the extent of the production of TNF and nitrite by Müller cells, suggesting that Müller cell-derived NO is a causative factor of ocular inflammation (de Kozak et al., 1994; Cotinet et al., 1997b). Moreover, the inherited retinal dystrophy observed in RCS rats was suggested to be caused by an abnormal release of TNF and NO from microglial and Müller cells in response to inflammatory stimulants (de Kozak et al., 1997).

Production of Hydrogen Sulfide

Hydrogen sulfide (H_2S) is a gaseous neuromodulator that can be synthesized by transsulfuration enzymes such as cystathionine γ-lyase. In salamander retinas, this enzyme is localized to Müller cells, suggesting that Müller cells produce H_2S (Pong et al., 2007). The presence of the enzyme may also reflect a requirement for cysteine and glutathione synthesis via the transsulfuration pathway, as a defense against oxidative stress.

2.8 Physiological Müller Cell-Neuron Interactions: A Short Summary

In the preceeding Sections 2.1, 2.2, 2.3, 2.4, 2.5, 2.6, and 2.7, many data were given about the ontogenetic development and the (comparative) mature structure and function of Müller cells. The presentation of a wealth of data, including many details and species-specific peculiarities, is always accompanied by the danger that the overburdened reader can't see the wood for the trees, anymore. . . Thus, the following short text tries to summarize the take-home messages.

- Every Müller cell aligns together with its neuronal siblings within an ontogenetically, structurally, and functionally defined columnar unit (Figs. 2.15 and 2.16) which is the principal site of Müller cell-neuron interactions.
- During phylogenesis, glial cells and neurons arise from common ancestral neural cells (Fig. 1.2); accordingly, there occurs a sharing of labor between neurons (information processing) and glial cells (homeostasis). This co-operation is based

upon a partial division/sharing out (and further specialization) of the ancestral neural genes among neurons and glial cells. Many molecules are expressed only by neurons (e.g., the molecules of visual transduction by the photoreceptors) or by glial cells, respectively (e.g., glutamine synthetase, carbonic anhydrase etc by the Müller cells); this necessitates – and allows – the metabolic and functional "symbiosis" between neurons and glial cells. Other molecules, such as many ion channels and ligand receptors, are expressed by both neurons and glial cells (although often at different levels); this provides the basis for a lively signal exchange between neurons and Müller cells, and vice versa.

- Generally, Müller cells are physically softer and functionally more compliant than neurons. Thus, their shape depends on the presence and shape of adjacent neuronal elements, and their metabolism depends on the momentary neuronal activity. Moreover, the vast evolutionary diversity and specialization of vertebrate retinas (leading to striking differences in the neuronal constituents and circuits, as exemplified in Fig. 1.13) is accompanied by a diversity of Müller cell shapes (e.g., Fig. 3.1) and functions. The latter adaptation may be the cause for the confusing variety in species-specific patterns of the expression of certain ligand receptors, ion channels, and transmembrane carriers by vertebrate Müller cells.
- Despite of the above-mentioned variability, virtually all Müller cells studied so far are characterized by common properties such as a high potasssium conductance of their membrane (accompanied by a very negative resting membrane potential), expression of the molecular machinery required for transmitter recycling (uptake carriers and enzymes), and by their ability to respond to a variety of stimuli by intracellular calcium rises or even by transcellular calcium waves.

Considering these basics, it becomes clear that any disturbance in Müller cell functions must have deleterious consequences for the functioning and even survival of retinal neurons. Moreover, Müller cells may change their properties in the course of retinal injuries. Several instances of pathological mechanisms have already been mentioned when the individual normal properties of Müller cells were presented in the preceeding chapter. The following chapter is devoted to a more systematic treatise of the contribution of Müller cells to retinal diseases and injuries.